Research and development of a new biocontrol agent against the foliar diseases downy and powdery mildews in cucurbit crops

Maria Barceló Genestar

Research and development of a new biocontrol agent against the foliar diseases downy and powdery mildews in cucurbit crops

Maria Barceló Genestar

Evolutive Biology, Ecology and Environmental Sciences Department

Plant Physiology Section

Universitat de Barcelona

Barcelona, 2024

Faculty of Biology
Department of Evolutionary Biology, Ecology, and Environmental Sciences
Doctoral program in Ecology, Environmental Sciences, and Plant Physiology

Research and development of a new biocontrol agent against the foliar diseases downy and powdery mildews in cucurbit crops

Recerca i desenvolupament d'un nou agent de biocontrol contra les malalties foliars del míldiu i l'oïdi en cultius de cucurbitàcies

Thesis submitted by

Maria Barceló Genestar

to qualify for the

Doctorate degree by the Universitat de Barcelona

Doctorate candidate

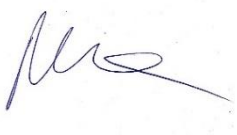

Maria Barceló Genestar

Barcelona, 18 November 2024

Directors

Mª Isabel Trillas Gay & Guillem Segarra

Tutor

Mª Isabel Trillas Gay

Agraïments

M’agradaria expressar el meu més profund agraïment a totes les persones que han estat essencials en la realització d’aquesta tesi doctoral.

En primer lloc, vull agrair sincerament a la meva tutora i directora de tesi, la Dra. Maria Isabel Trillas, i al Dr. Guillem Segarra Braunstein, per la seva gran implicació i ajuda en tot moment. Gràcies per totes les ensenyances i per compartir la vostra experiència i coneixement amb tanta generositat. La vostra guia ha estat essencial en cada etapa d'aquest treball, i aquest no hauria estat possible sense la vostra dedicació i paciència.

També vull expressar el meu agraïment a les meves companyes de laboratori, Patricia Gjakoni i Rosa Maria Noguera, així com a Javier Méndez Viera, del Departament de Genètica, Microbiologia i Estadística, i al Servei de Camps Experimentals de la Universitat de Barcelona, per la seva dedicació, cura i col·laboració en els experiments realitzats durant aquests anys.

Així mateix, vull agrair també a l'empresa Biocontrol Technologies S.L. pel seu suport, acompanyament i esforç econòmic al llarg d’aquest projecte. Valoro profundament la confiança que han dipositat en mi.

També voldria dedicar un reconeixement especial a l’Eva Prats Miralles, cap de la Unitat de Microscòpia Electrònica (TEM/SEM), i a l’Olga Jáuregui, dels Serveis Cromatogràfics dels Centres Científics i Tecnològics de la Universitat de Barcelona (CCiTUB), pel seu suport i assessorament en les tècniques de microscòpia electrònica i en l'anàlisi dels metabòlits.

Finalment, dedico aquesta tesi a la meva família i amigues, que han estat un pilar imprescindible al llarg d’aquest camí. En particular, a la meva mare, la meva germana Nina i la meva tieta Tita, per la seva il·lusió i confiança dipositada en mi, pel seu suport moral incondicional i els ànims constants. Gràcies per ser un exemple de dones fortes i valentes, que sempre tiren endavant. La seva companyia i afecte m'han sostingut en els moments difícils i m'han donat la força necessària per seguir endavant.

A tots vosaltres, gràcies de tot cor.

This work was supported by an industrial PhD scholarship (2020 DI 04) for the period 2020-2024, awarded through a collaboration between the University of Barcelona and Biocontrol Technologies S.L.

The scholarship was granted by AGAUR (Agència de Gestió d'Ajuts Universitaris i de Recerca), Generalitat de Catalunya.

Summary

This PhD thesis explores the initial stages of developing a new Plant Protection Product aimed at combating the fungal diseases downy mildew (*Pseudoperonospora cubensis*) and powdery mildew (*Podosphaera fusca*) in cucurbit plants. According to FAOSTAT, cucurbits are the fourth most-produced primary crop in the European Union, highlighting their economic significance as staple foods and vital contributors to global food production and agricultural economies. The research focuses on the isolation, identification, characterization, efficacy evaluation, study of the mode of action, and safety assessment of various microbial strains, particularly within the [redacted] genus. The study began by isolating and pre-screening microbial species from different locations and types of plants affected by either of these two diseases. This phase yielded 724 microbial isolates, comprising 491 bacterial and 233 fungal strains. [redacted] group strains were predominantly found on plants from the Solanaceae and Cucurbitaceae families, especially in powdery mildew-infected tissues. Fungal species, including [redacted], [redacted], and [redacted], were primarily isolated from woody plants, using malt extract agar with antibiotics to optimize yeast-like fungal isolation. The selected strains underwent molecular screening for initial taxonomic classification, including the [redacted] gene to exclude pathogenic species, along with further sequencing of the 16S rRNA gene for bacteria and ITS regions for fungi. This process led to the identification of 128 strains from the [redacted] group and 11 strains from desired yeast-like fungal species.

The efficacy trials against both pathogens, conducted under controlled conditions in cucumbers, showed that several isolates significantly reduced disease severity (between [redacted] disease reduction). Notably, the strains most effective against one disease also showed high efficacy against the other. Among these, [redacted] stood out for their strong preventive efficacy in both pathosystems. Additionally, these bacterial treatments demonstrated efficacy comparable to the standard biological product strain QST 713, even surpassing it with a prototype formulation. In contrast, yeasts proved to be more effective as curative treatments for powdery mildew.

Safety assessments of the five most effective strains from previous trials were conducted based on the bioinformatic study of the Whole Genome Sequencing in accordance with EU regulatory requirements. Ultimately, only [redacted] and [redacted] were selected for further analysis as the most promising candidates that met both efficacy and regulatory standards. Their safety profiles were confirmed based on their classification within well-established non-pathogenic [redacted] species, the absence of plasmids or mobile genetic elements associated with antimicrobial resistance, the lack of toxin or

virulence factor genes, and the absence of metabolites of concern. Furthermore, the genes involved in the synthesis of beneficial secondary metabolites, such as surfactin and fengycin, which are critical for biocontrol effectiveness, were found in their genomes. The production of these lipopeptides, along with other important secondary metabolites, was further validated through LC-QTOF-MS/MS analysis. Additionally, in evaluating biofilm formation and environmental resilience, strain [redacted] exhibited superior biofilm-forming ability and environmental adaptability, especially in outdoor conditions with UV exposure, suggesting it may have greater field application potential. Scanning Electron Microscopy further confirmed that strain [redacted] formed more homogeneous, mucus-like biofilms than strain [redacted], improving its capacity to prevent pathogen colonization on plant surfaces. This biofilm resilience under varied environmental stresses highlights strain [redacted]'s suitability for long-term effectiveness as a biocontrol agent.

In sum, all these studies underscore the potential of [redacted] as a strong candidate for the final development of this strain in a microbial Plant Protection Product aimed at managing downy and powdery mildews in cucurbits and potentially other crops. A patent application for strain [redacted] is underway, with further studies planned to validate its large-scale agricultural application and regulatory compliance.

Key words: [redacted], [redacted], biofilm, biological control, cucurbits, disease development, efficacy trials, environmental adaptability, fengycin, infection, iturin, LC-QTOF-MS/MS, lipopeptides, microbial isolates, *Podosphaera fusca*, plant protection, *Pseudoperonospora cubensis*, regulatory compliance, secondary metabolites, surfactin, safety assessment, whole genome sequencing.

Resum

Aquesta tesi doctoral explora les fases inicials del desenvolupament d'un nou producte fitosanitari destinat a combatre les malalties fúngiques míldiu (*Pseudoperonospora cubensis*) i oïdi (*Podosphaera fusca*) en cultius de cucurbitàcies. Segons la FAOSTAT, les cucurbitàcies són el quart cultiu primari més produït a la Unió Europea, destacant la seva importància econòmica com a aliments bàsics i contribuint de manera significativa a la producció alimentària global.

L'estudi va començar amb l'aïllament i la preselecció d'espècies microbianes de diferents llocs i tipus de plantes afectades per una d'aquestes dues malalties. Aquesta fase va concloure amb 724 aïllats microbians, incloent 491 bacteris i 233 fongs. Les soques del gènere [redacted] es van trobar sobretot en plantes de les famílies Solanaceae i Cucurbitaceae, especialment en teixits infectats per oïdi. Les espècies fúngiques, incloent [redacted], [redacted] i [redacted], es van aïllar principalment de plantes llenyoses també infectades per oïdi. Les soques seleccionades es van sotmetre a un cribratge molecular per a la classificació taxonòmica mitjançant la seqüenciació del gen 16S rRNA en bacteris i de la regió ITS en fongs. Aquest procés va conduir a la identificació de 128 soques del grup [redacted] i 11 soques de les espècies fúngiques desitjades.

Els assaigs d'eficàcia contra ambdós patògens, realitzats en condicions controlades en cogombres, van mostrar que diversos aïllats reduïen significativament la gravetat de la malaltia (amb una reducció de malaltia entre el [redacted]). Les soques més efectives contra una malaltia també van mostrar una alta eficàcia contra l'altra. Entre aquestes, les soques de [redacted] van obtenir la millor eficàcia preventiva en ambdós patosistemes. A més, aquests tractaments bacterians van demostrar una eficàcia comparable a la de la soca QST 713 del producte biològic de referència, fins i tot superant-la amb la formulació prototip. En canvi, els llevats van demostrar ser més efectius com a tractaments curatius per a l'oïdi.

Les avaluacions de seguretat de les cinc soques més efectives es van dur a terme basant-se en l'estudi bioinformàtic de la seqüenciació del genoma d'acord amb els requisits normatius de la UE. Finalment, només el [redacted] i el [redacted] van ser seleccionats per a una anàlisi posterior com els candidats més prometedors. Els seus perfils de seguretat es van confirmar basant-se en la seva classificació dins d'espècies de [redacted] no patògenes, l'absència de plasmidis o elements genètics de mobilitat associats a resistències antimicrobianes, la manca de gens de toxines o factors de virulència i l'absència de metabòlits perillosos. A més, es van trobar en els seus genomes gens implicats en la síntesi

de metabòlits secundaris beneficiosos, com la surfactina i la fengicina, que són molt importants per a l'eficàcia del biocontrol. La producció d'aquests lipopèptids, juntament amb altres metabòlits secundaris, es va validar posteriorment mitjançant una anàlisi LC-QTOF-MS/MS. A més, en l'avaluació de la formació de biofilm i la permanència en fulla, la soca [redacted] va mostrar una capacitat superior de formació de biofilm i adaptabilitat ambiental, especialment en condicions a l'exterior, cosa que suggereix un major potencial d'aplicació en camp. La microscòpia electrònica d'escaneig va confirmar a més que la soca [redacted] formava biofilms més homogenis i de textura mucosa que la soca [redacted].

En resum, aquest treball subratlla el potencial dels agents de biocontrol en l'agricultura sostenible, presentant la soca [redacted] com un candidat destacat per a productes de biocontrol destinats al maneig del míldiu i l'oïdi en cucurbitàcies i possiblement en altres cultius. Actualment, s'està tramitant una sol·licitud de patent per a la soca [redacted], i es planifiquen futurs estudis per validar la seva aplicació a gran escala en l'agricultura i el seu compliment normatiu.

Paraules clau: adaptabilitat ambiental, aïllats microbians, anàlisi LC-QTOF-MS/MS, avaluació de seguretat, [redacted], [redacted], biofilm, compliment normatiu, control biològic, cucurbitàcies, desenvolupament de malalties, fengicina, infecció, iturina, lipopeptids, metabòlits secundaris, *Podosphaera fusca*, proves d'eficàcia, *Pseudoperonospora cubensis*, seqüenciació del genoma complet (WGS), surfactina.

Table of contents

GENERAL INTRODUCTION AND MAIN OBJECTIVES

GENERAL INTRODUCTION

1. The Cucurbitaceae family

Botanical classification. The Cucurbitaceae, or cucurbit family, represents a medium-sized plant family characterized by a diverse array of species thriving in warmer regions worldwide. This family holds significant economic importance, particularly for species bearing edible fruits, serving as a staple starch source in many regional diets. Thus, this family includes some of the world's most valuable crops such as cucumber, melon, watermelon, squash, zucchini, and pumpkin (Chomicki et al., 2019; Zhang et al., 2022). All of them play a crucial role in global food production and agricultural economies (Romero et al., 2007; Bellón-Gómez et al., 2014).

The Cucurbitaceae family consists of more than 800 species distributed among more than 100 genera (Zhang et al., 2022; Alhomaidi, 2024). Major characters such as androecium and gynoecium morphology, tendril branching, pollen structure, and seed coat patterns have helped establish and clarify the intricate taxonomy within the Cucurbitaceae family (Ali et al., 2013). However, the family's taxonomic classification has been refined in recent years through molecular and morphological data, leading to a more natural classification that elucidates the relationships between tribes and genera within Cucurbitaceae (Schaefer & Renner, 2011; Zhang et al., 2022). This taxonomic richness, coupled with the economic and medicinal importance of various species, underscores the family's pivotal role in botanical research and agricultural practices. Cucurbit production often faces significant challenges from a wide range of pathogenic infections, with over 200 documented diseases caused by diverse factors (Zitter et al., 1996).

The economic importance of cucumbers, according to the data extracted from FAOSTAT (https://www.fao.org/faostat/en/#data/QV), can be summarized by their Gross Production Value (GPV) over the years, with an average GPV from 2016 to 2022 of approximately 41,495,240 thousand International dollars (Int$). This data indicates that cucumbers are a significant crop in terms of economic value, with production values consistently in the tens of billions of Int$ annually.

Additionally, only referring to the most recent information (specific values for the year 2022) and according to the FAOSTAT data, the comparison of some primary crops in the European Union, based on the area harvested and production quantities, reveals the following position of cucumbers presented in Table 0.1.

Table 0.1. Comparison of the area harvested and production quantities of some primary crops in the European Union in 2022, according to FAOSTAT (https://www.fao.org/faostat/en/#data/QCL).

Primary crops	Area Harvested	Production
Wheat	24,217,040 hectares	134,326,040 tons
Barley	10,300,100 hectares	52,033,580 tons
Almonds	905,430 hectares	410,820 tons
Apples	477,980 hectares	12,559,280 tons
Cherries	124,980 hectares	614,860 tons
Cabbages	124,160 hectares	3,658,570 tons
Carrots and turnips	96,760 hectares	4,412,420 tons
Apricots	72,070 hectares	637,400 tons
Cantaloupes and other melons	62,950 hectares	1,626,920 tons
Asparagus	58,390 hectares	298,440 tons
Artichokes	58,000 hectares	609,880 tons
Watermelons	56,960 hectares	2,685,740 tons
Cucumbers and Gherkins	31,200 hectares	2,694,420 tons
Blueberries	29,582 hectares	202,821 tons
Avocados	25,050 hectares	148,060 tons
Bananas	21,260 hectares	613,040 tons

It is highlighted in yellow the significant area devoted to the cultivation of cucurbits and the substantial production quantities achieved.

As it is shown, referring to the cultivation of cucurbits in global, the total amount of area harvested reach up to 151,110 hectares, achieving a position just below the apple crop and above the cherry cultivation. Moreover, when taking cucurbits all together, the production adds up to a total of 7,007,080 tonnes, the fourth position in the table only preceded by the cultivation of wheat, barley and apples. Focusing on cucumbers (in darker yellow), its cultivation has a relatively smaller area harvested compared to the crops in the previous positions on the Table 0.1. However, it is worth notice that cucumbers have substantial production quantities much higher than some other high-value crops like almonds, cherries and apricots, with larger harvested areas. This means that its yield, in terms of tons produced per hectare, is much higher than in most of the crops presented. Thus, cucumbers are a key crop in terms of both harvested area and production volume within the dataset. This comparison underscores the importance of cucumbers in terms of production efficiency, achieving high yields from a relatively smaller area.

2. The diseases: cucurbit downy and powdery mildews

Downy mildew diseases. Downy mildew diseases are a group of closely related microorganisms belonging to Oomycetes. The foliar disease they cause, represents a significant threat to agricultural and horticultural systems globally, as it causes significant losses in crop yield and quality. Notably, grapevine (*Vitis vinifera*) is severely affected by downy

mildew caused by *Plasmopara viticola*, which poses a major challenge for grape production globally, particularly in humid conditions (Júnior et al., 2020; Giacomelli, 2023; Hernández et al., 2022). Similarly, maize (*Zea mays*) and sorghum (*Sorghum bicolor*) are also highly susceptible to downy mildew, with reports indicating losses of up to 100% in some regions due to pathogens like *Peronosclerospora sorghi* (Yeturi & Velazhahan, 2016). Cucurbit crops are also critically affected by downy mildew, with the disease being recognized as one of the most damaging in these categories (Neufeld et al., 2013; Montazar et al., 2019).

Oomycetes, also known as water Molds, are a group of eukaryotic microorganisms that were historically classified as fungi due to their filamentous morphology and parasitic ecological niches (Elsherbiny et al., 2020). Despite their fungal-like appearance, oomycetes are truly classified as Stramenopiles, also called Heterokonts, along with brown algae and diatoms. Oomycetes are characterized by filamentous growth and osmotrophic feeding, and often by having flagellated cells with two flagella of different types (Gijzen, 2009). Unlike typical fungi, oomycetes exhibit diploidy, possess cell walls primarily composed of cellulose and β-glucans rather than chitin, develop aseptate hyphae, undergo oogamous reproduction and produce few secondary metabolites (Fawke et al., 2015).

Pseudoperonospora cubensis. *P. cubensis* ranks among the most economically significant and widespread plant pathogens (Lebeda & Choen, 2011). The disease occurs across different geographic regions, warm, temperate, subtropical and tropical regions, both in open field cultures and protected environments such as greenhouses (Palti and Cohen, 1980; Cohen, 1981; Lebeda, 1990; Thakur and Mathur, 2002). Its prevalence is notably higher in areas receiving high annual precipitation, i.e., > 300 mm^3 (Lebeda, 1990). Moreover, the survival and spread of *P. cubensis* are influenced by factors such as solar radiation, with studies showing the effects of sunlight exposure on the viability of *P. cubensis* sporangia (Kanetis et al., 2010). Favorable conditions, including high relative humidity (above 80%) and moderate to cool temperatures (ranging from 17–20ºC), promote pathogen growth and dissemination, facilitating rapid disease spread.

In this context, the severity of cucurbit downy mildew is highlighted by its damaging levels in greenhouse-grown cucurbits, with winter and spring production potentially serving as a source of inoculum (Ojwang et al., 2021). The enclosed nature of these environments also allows sporangia produced by the pathogen to remain inside, increasing the likelihood of infection. Additionally, the formation of guttation droplets along leaf boundaries, resulting from reduced water potential in the xylem vessels at night, further exacerbates the frequency of infection. However, these same enclosed conditions can sometimes work against pathogen progression.

For instance, under sunny skies and inadequate ventilation, temperatures within greenhouses can soar to 45°C or higher—lethal levels for the pathogen.

P. cubensis manifests through distinctive symptoms of infection, characterized by pale-yellow lesions on leaf surfaces, which may evolve into larger, necrotic areas under conducive environmental conditions. However, these symptoms vary among cucurbit species and even genotypes (Lebeda, 1990). For example, it causes irregular, localized, yellow lesions in some species like cucumber and luffa, while lesions in cantaloupe and watermelon are circular and irregular (Lebeda and Schwinn, 1994). Genetically resistant cultivars may show minimal symptoms under controlled conditions, producing small water-soaked lesions (Thomas et al., 1987; Zitter, Hopkins & Thomas, 1996).

P. cubensis stands as one of the most studied biotrophic parasites -i.e., pathogens that feed on living host cells- within the Peronosporomycetes group (Zitter, Hopkins & Thomas 1996; Dick 2001; Göker et al. 2007; Voglmayr 2008). Historically, the taxonomy and nomenclature of *P. cubensis* have undergone refinements and clarifications. It was first described by Berkeley in 1868 from herbarium specimens originating from Cuba. Over time, various synonyms have been attributed to *Pseudoperonospora cubensis*, including *Peronospora cubensis* and *Plasmopara cubensis*, reflecting the complexity of taxonomic classification within the Peronosporaceae family (Lebeda & Choen, 2011). Recent taxonomic classification places *Pseudoperonospora cubensis* within the kingdom Chromista, subdivision Peronosporomycotina, class Peronosporomycetes (originally described as Oomycetes), order Peronosporales, and family Peronosporaceae (Lebeda & Choen, 2011). This family comprises at least 17 genera (Göker et al., 2007; Voglmayr 2008), with *Bremia, Peronospora, Hyaloperonospora*, and *Plasmopara* being among the most widespread genera in Europe and North America, responsible for causing serious diseases in cultivated plants (Lebeda and Schwinn 1994; Voglmayr 2008). These genera are distinguished by the shape and branching patterns of their sporophores/sporangiophores and their ability to release zoospores (Dick, 2002; Voglmayr, 2003; Choi et al., 2005; Göker et al., 2007). Thus, the genus *Pseudoperonospora* occupies an intermediate position between *Plasmopara* and *Peronospora* in these terms, exhibiting characteristics between zoospore-producing genera such as *Pythium* and those that do not, such as *Peronospora* (Göker et al., 2007). For instance, *Pseudoperonospora cubensis* produces zoospores but its sporophores resemble those of *Peronospora* spp., with which it shares a close affinity evidenced by similar haustoria, conidiosporangiophore morphology, and conidiosporangial coloration. (Lébeda and Cohen, 2011). However, Riethmüller et al. (2002) state that the genus *Pseudoperonospora* is monophyletic.

Powdery mildew diseases. Another common foliar disease caused by biotrophic parasite fungi that affects a wide range of crops is powdery mildew. These diseases cause a significant threat to agriculture, impacting economically crucial crops which play a vital role in global food production and agricultural economies (Feng et al., 2021; Franke & Menz, 2007). Among these, grapevines (*Vitis vinifera*) are notably affected by *Erysiphe necator*, which can cause severe economic losses in viticulture globally (Asci et al., 2021; Kunova et al., 2021). Tomatoes (*Solanum lycopersicum*) also suffer from powdery mildew, with resistance linked to specific genes that have been targeted for genetic modification to enhance disease resistance (Pramanik et al., 2021; Zhang et al., 2013). Additionally, cucurbits, particularly pumpkins (*Cucurbita pepo*), are susceptible to powdery mildew, which can be mitigated through soil amendments like wollastonite that enhance plant resilience (Li et al., 2019).

Powdery mildew is caused by various pathogens belonging to the true ascomycete fungi, which constitute the order Erysiphales, characterized by the sole family, Erysiphaceae. Referring to the principal characteristics of powdery mildew fungi, they are obligate biotrophic pathogens, with asexual reproduction, sexual or both (depending on the species and the environmental conditions), and they grow well in humid environments with moderate temperatures (like greenhouses). Powdery mildew cells and spores exhibit similarities to those of other filamentous ascomycetes, comprising cell walls, nuclei, vacuoles, Woronin bodies, and various organelles (Akai, 1968; Martin & Gay, 1983; Mims et al., 1995; Roberts et al., 1996; Rohringer et al., 1982).

Podosphaera fusca. *P. fusca* is the causal agent of powdery mildew on cucurbits and its impact on these crops is particularly severe, with the disease causing significant reductions in fruit quality and crop yields (Bellón-Gómez et al., 2014). Thus, powdery mildew stands out as one of the most prevalent, conspicuous, and easily identifiable diseases affecting cucurbits. In fact, it is one of the most limiting factors for cucurbit production in many countries, including Spain (Pérez-García et al., 2009).

Characterized by a whitish, talcum-like fungal growth on leaf surfaces, petioles, and stems (Sitterly, 1978; Zitter et al., 1996), powdery mildew rarely affects fruits. This disease manifests as a white powdery fungal growth on various parts of the plant, including leaves, stems, and petioles (Angelini et al., 2019). This disease can be attributed to either *Golovinomyces cichoracearum* or *Podosphaera fusca*, both obligate biotrophic ectoparasites inducing similar symptoms. In Spain, as in many other regions globally, *P. fusca* is recognized as the primary causal agent and a major constraint on cucurbit production (Fernández-Ortuño et al., 2006; del Pino et al., 2002).

P. fusca belongs to the Kingdom Fungi; Phylum Ascomycota; Subdivision Pezizomycotina; Class Leotiomycetes; Order Erysiphales; Family Erysiphaceae, which is known for causing powdery mildew diseases in a wide range of cultivated plants (Kim et al., 2019). Its genus is *Podosphaera*, and the specie is *fusca* (Pérez-García et al., 2009). However, the nomenclature of this pathogen remains somewhat inconsistent in the literature. Various designations have been used, including *Sphaerotheca fuliginea, Sphaerotheca fusca, Podosphaera fusca*, or *Podosphaera xanthii*. Advances in scanning electron microscopy and molecular analyses have led to widespread acceptance of merging the genus *Sphaerotheca* with *Podosphaera* (Braun et al., 2002) and finally, in recent years, *Podosphaera fusca* was identified as probably being *Podosphaera xanthii* according to the current taxonomy, highlighting the ongoing refinement and classification of powdery mildew pathogens (Park et al., 2023).

Control of downy and powdery mildews. These diseases are typically controlled through chemical treatments, planting resistant varieties, or biocontrol methods. Moreover, efforts to manage these infections in protected environments have included the development of early warning models for predicting the occurrence greenhouses, utilizing disease records and microclimatic parameter analysis (Yang et al., 2007).

Referring to the chemical or conventional pesticides, the most used in agriculture are the copper-based fungicides. These fungicides have been a traditional and effective method, known since 1885, to suppress many pathogens and are still widely used due to their effectiveness (Koledenkova et al., 2022). However, these fungicides have been associated with several negative environmental impacts, highlighting soil contamination, with drastic adverse effects on soil organisms, and potential ecological harm, with significantly high risks to beneficial insects and mammals (Pietrzak & McPhail, 2004; Bünemann et al., 2006; Lamichhane et al., 2018; Burandt, 2023).

Many other kinds of synthetic fungicides have been extensively used against downy mildew diseases with significant disease reductions (Adhikari et al., 2012; Yang et al., 2022; Li et al., 2023). However, the widespread use of pesticides in agriculture raises concerns about their potential impact on soil life and the environment (Słomnicka et al., 2017). Therefore, the EU has been actively seeking to reduce its reliance on conventional pesticides and has limited the availability of pesticide active substances used in effective plant protection products (Khudhair, 2023). In this context, the EU has adopted a "hazard-based" approach for the approval of active substances, emphasizing the need for safer and more environmentally friendly methods.

Furthermore, the generation of resistance hosts, such as cisgenic melons overexpressing specific genes for resistance, have shown promise in conferring resistance to downy mildew

(Benjamin et al., 2009). However, despite the efforts to breed resistant cultivars, the emergence of new pathogenic strains presents ongoing challenges to mitigation strategies, and it seems that host resistance alone may not be effective due to the pathogen's diversity and virulence complexity.

Taking all into account, the application of biocontrol agents (BCAs) can offer sustainable disease management solutions (Nuñez-Palenius et al., 2022). Nevertheless, the slow implementation of microbial biological control of pests indicates the challenges in reaching the EU market, despite the huge potential of these biocontrol agents (Marine et al., 2016). Overall, the focus on BCAs underscores the shift towards more sustainable and environmentally friendly disease management practices (Romero et al., 2007), where the integration of BCAs with chemical fungicides is being explored as a way to reduce fungicide doses and residues on harvested crops, highlighting the potential for a holistic approach to disease control (Pintye et al., 2012).

3. Biocontrol agents and Plant Protection Products

Bacillus spp., *Pseudozyma* spp., *Ampelomyces* spp. and *Trichoderma* spp. have demonstrated efficacy in controlling downy and powdery mildews across various crops, offering environmentally friendly alternatives to chemical fungicides and promoting sustainable agricultural practices (Legler et al., 2015; Hashem & Tabassum, 2019; Bovolini et al., 2018; Ons et al., 2020; Nuñez-Palenius et al., 2022).

Referring to powdery mildews, today there are some BCAs to effectively treat them, highlighgting *Bacillus subtilis* QST 713 (Serenade®), *Bacillus amyloliquefaciens* MBI 600 (Serifel®), *Ampelomyces quisqualis* M-10/AQ-10 (AQ-10®) and *B. amyloliquefaciens* subsp. *plantarum* D747 (Amylo-x® WG), which are employed in grapes against *Botrytis cinerea* and *Uncinula necator*; or *Bacillus pumilus* QST 2808 (Sonata® ASO) and *B. subtilis* IAB/BS03 (Aviv®), which are specific for cucurbits, against *Podosphaera fusca* and *Golovinomyce cichoracearum*. On the other hand, *Pseudozyma aphidis* has demonstrated parasitic activity against cucurbit powdery mildew (Gafni et al., 2015). Furthermore, the production of antifungal glycolipids by biocontrol agents like *Pseudozyma flocculosa* has been implicated in their biocontrol activity against powdery mildew fungi (Hammami et al., 2011).

In contrast, the biological control of downy mildews is harder, but Serenade® Max has also been widely used in the United States to combat the disease in cucurbits, according to the United States Environmental Protection Agency (Washington D.C., 2015). Moreover, *Trichoderma harzianum* T39 has been studied for inducing downy mildew resistance in grapevines, showcasing a potential alternative to chemical treatments (Perazzolli et al., 2012).

Regulatory framework of EU disease control. The directive 2009/128/EC (http://data.europa.eu/eli/dir/2009/128/oj), implemented in 2014, established the framework for Community action to achieve a sustainable use of pesticides, promoting the use of integrated pest management and of alternative approaches or techniques such as non-chemical alternatives to pesticides. The Directive applies to pesticides that are Plant Protection Products (PPP) as defined in Regulation (EC) No. 1107/2009. The Biological control of plant disease using microbial PPP or Biocontrol agents (BCAs) offers a promising approach for managing plant diseases while reducing the environmental and health risks associated with conventional chemical fungicides. This strategy is aligned with the Farm to Fork strategy of the Green Deal (https://food.ec.europa.eu/horizontal-topics/farm-fork-strategy_en) and with the reduction on the use of the most hazardous chemical products.

However, the successful utilization of BCAs necessitates thorough evaluation across various domains to ensure human and environmental safety, ecological compatibility and efficacy (Vurukonda et al., 2018). Exclusion criteria encompass evaluating pathogenicity, virulence, allergenicity, and toxicity towards humans, animals, and plants (Vurukonda et al., 2018). According to the European Commission exposed in the “Guidance on the approval and low-risk criteria linked to "antimicrobial resistance" applicable to microorganisms used for plant protection in accordance with Regulation (EC) No 1107/2009”, fungi producing antibiotic substances and bacteria harbouring antibiotic resistance genes are to be excluded. In addition, the bacteria must be sensitive to at least two antibiotics from different families to be used to treat a patient in case of an infection.

4. Role of bacteria and fungi in the biocontrol of the diseases

The control of mildews presents an important challenge due to their biotrophic nature, targeting the aerial parts of host plants. Therefore, BCAs must act within the phyllosphere, which is a more dynamic environment where biological control against various plant pathogenic fungi tend to be less successful than in the rhizosphere, due to the traditional modes of microbial competition for nutrients and space are not that effective (Andrews, 1992; Fokkema, 1996). Moreover, the intense sporulation and rapid spread characteristic of these diseases make their control exceptionally challenging, even with chemical fungicides.

Bacteria: the genus *Bacillus*. Research into the biocontrol potential of *Bacillus* began with the discovery of the insecticidal activity of Cry proteins produced by *B. thuringiensis*. The utilization of bacteria as potential biocontrol agents (BCAs) has seen a notable increase in recent years, with the genus *Bacillus* emerging as a prominent candidate. *Bacillus* species belong to the Bacteria Kingdom; Firmicutes Phylum; Bacilli Class; Bacillales Order; and

Bacillaceae Family (Maughan & van der Auwera, 2011). Presently, numerous *Bacillus* species (*B. subtilis, B. pumilus, B. amyloliquefaciens*, and *B. licheniformis*) are extensively studied to mitigate the incidence of agriculturally significant diseases (Raaijmakers & Mazzola, 2012), where *Bacillus* species has demonstrated antagonistic activity against various phytopathogenic microorganisms affecting agricultural crops such as maize, rice, and fruits (Zeriouh et al., 2011; García-Gutiérrez et al., 2013; Wang et al., 2014; Li et al., 2015; Bovolini et al., 2018). These *Bacillus* strains have been found to produce antifungal compounds, such as surfactin and fengycin, which directly inhibit the growth of mildew pathogens and stimulate plant defence mechanisms (Li et al., 2015; Tanaka et al., 2017; Li et al., 2019).

Fungi: yeast-like fungi species. Several fungal species have been extensively studied for their potential of being effective biocontrol agents against powdery mildews, including *Ampelomyces* spp., *Pseudozyma* spp., *Verticillium lecanii*, *Tilletiopsis* spp., and *Acremonium alternatum* (Kiss, 2003). Two examples are the biofungicides AQ10 Biofungicide® and Sporodex®, containing *Ampelomyces quisqualis* and *Pseudozyma flocculosa*, respectively.

Pseudozyma spp., belonging to the Basidiomycota phylum; Ustilaginomycetes Class; Ustilaginaceae family, secrete antifungal compounds and enzymes that target powdery mildew fungi (Hammami et al., 2011) and act swiftly through antibiosis, collapsing powdery mildew colonies by altering cell membrane fluidity with identified fatty acids and antifungal metabolites (Choudhury et al., 1994; Hajlaou et al., 1994; Benyagoub et al., 1996). On the other hand, *Aureobasidium* spp., belonging to the Ascomycota phylum; Dothideomycetes class; Aureobasidiaceae family, also produce antifungal compounds and enzymes targeting plant pathogens (Zhang et al., 2010) and compete with them for nutrients, inhibit spore germination, and reduce the incidence of fungal diseases on various crops (Zhang et al., 2010). Additionally, the biocontrol activity of *Aureobasidium pullulans* has been attributed to its ability to produce volatile organic compounds and induce oxidative stress in pathogens, thereby suppressing their growth and virulence (Al-Qaysi et al., 2021).

MAIN OBJECTIVES OF THE PhD THESIS

The general aim of this PhD thesis is to isolate, identify, characterize, evaluate the efficacy, mode of action and safety of microbial strains, particularly [redacted] species, as biocontrol agents against key plant pathogens, such as those causing cucurbit downy mildew (*Pseudoperonospora cubensis*) and cucurbit powdery mildew (*Podosphaera fusca*), in order to develop a Plant Protection Product as a sustainable and effective alternative to chemical pesticides for plant disease management in agriculture.

The main objectives from each PhD chapter are the ones as follows:

1. **Isolation and screening of microbial species.** The main objective of the first chapter was to generate a large collection of isolates obtained from various plant sources, and to characterize and classify the isolated strains to identify the most promising candidates for use as biocontrol agents, based on relevant literature and their taxonomic classifications.
2. **Efficacy trials of selected isolates.** The second chapter aimed to explore the effectiveness of a large collection of different microorganisms and isolates in the control of downy and powdery mildew diseases in cucumber and select the best five candidate strains in order to further develop one of them as a Plant Protection Product.
3. **Safety assessment of the selected isolates.** The main objective of the third chapter was to conduct a WGS data analysis to stablish the safety profiles of the [redacted] and the [redacted], with focus on the detection of antimicrobial resistance genes, toxin producing regions or virulence factors and the secondary metabolites producing regions, with the corresponding identification and quantification of metabolites in the growth medium.
4. **Characterization of the selected isolates: biofilm formation.** The main objective of this chapter was to investigate and characterize the biofilm formation capabilities of selected [redacted] strains, particularly strains [redacted] and [redacted], and to evaluate the role of biofilms in enhancing the colonization and persistence on plant leaves, in order to promote overall efficacy of these strains as biocontrol agents against downy and powdery mildews.

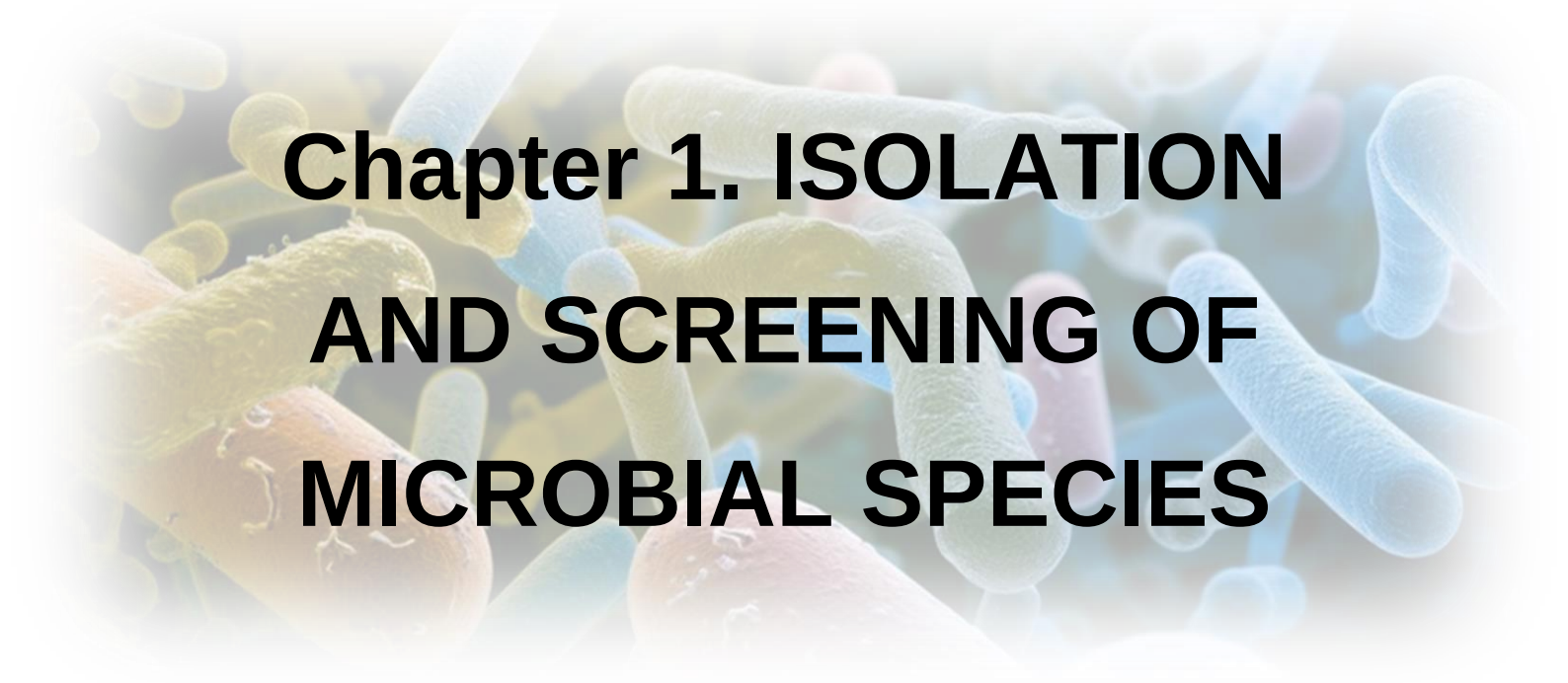

Chapter 1. ISOLATION AND SCREENING OF MICROBIAL SPECIES

ABSTRACT

This chapter focuses on the isolation and pre-screening of microbial species for their potential use as biocontrol agents in agricultural settings. The isolation of bacterial and fungal strains is fundamental in microbiological research, facilitating the study of their characteristics, interactions, and potential applications in fields such as agriculture. For bacterial isolation, protocols typically involve sampling from environments such as soil, plant tissues, or water, particularly targeting the endosphere, phyllosphere, or rhizosphere. Methods like surface sterilization of plant material followed by homogenization and serial dilution plating on selective media are commonly used. Fungal isolation begins with sampling from soil, plant tissues, or air, often collecting spores or mycelium for DNA extraction and identification using ITS sequencing.

This study specifically aimed to generate a large collection of isolates from various plant sources, characterizing and preclassifying them to identify the most promising candidates for use as biocontrol agents. The primary bacterial genus targeted was [redacted], while the fungal genera included [redacted], [redacted] and [redacted]. The main results drawn from this chapter included a total of 724 microbial strains were isolated, comprising 491 bacterial species and 233 fungal species. Regarding the best sources, the majority of [redacted] group species were isolated from Solanaceae and Cucurbitaceae families, particularly from plants infected with powdery mildew, with endophytic bacteria being more prevalent. Moreover, the "Plant endophyte" technique was the most effective for isolating [redacted] group species. Regarding the fungal isolation protocols, the use of malt extract agar (MEA) amended with antibiotics was more successful for isolating desired yeast-like fungi than corn meal agar (CMA).

A molecular screening was conducted, where the [redacted] gene was effective in quickly detecting strains belonging to the [redacted] group, allowing for the exclusion of potentially pathogenic [redacted] species. Finally, the 16S rRNA gene of the bacterial selected candidates and the ITS region of the fungal candidates were sequenced to taxonomically classify them. The isolated strains displayed high diversity, with significant differences in colony morphology and genetic profiles.

This chapter underscores the importance of detailed isolation protocols and advanced molecular techniques in identifying and characterizing microbial strains with potential biocontrol applications, contributing to sustainable agriculture and environmental management.

INTRODUCTION

1. Microbial isolation protocols

The isolation of bacterial and fungal strains is a fundamental process in microbiological research, facilitating the study of their characteristics, interactions, and potential applications in fields such as agriculture and medicine. Different isolation protocols are employed to ensure the successful extraction and purification of these strains for further analysis and experimentation. The choice of isolation method can significantly impact the purity, viability, and characteristics of the isolated strains (Rijavec et al., 2007). Researchers have developed and optimized various protocols to isolate specific bacterial and fungal strains efficiently, considering factors such as the source of the strains, the intended downstream applications, and the environmental conditions in which the strains are found (Paudel et al., 2015).

This PhD thesis outlines the diverse isolation protocols used for bacteria and fungi to be employed as biocontrol agents, based on current methodologies and recent advancements highlighted in key research studies.

Bacterial Isolation Protocols. Isolation of bacteria typically involves sampling from various environments, such as soil, plant tissues, or water. When dealing with biocontrol agents, they are typically isolated from the endosphere, phyllosphere or rhizosphere (O'Brien, 2017). In agricultural studies, bacterial isolation from plants often starts with surface sterilization of the plant material followed by homogenization and serial dilution plating on selective media. For instance, Yang et al. (2008) describe the process of isolating bacteria from cucumber microenvironments using nutrient-rich R2A agar to cultivate the bacteria from serially diluted samples.

A critical step in bacterial isolation is the use of selective media and conditions to ensure the growth of the target bacteria while suppressing contaminants. The production of extracellular hydrolytic enzymes and siderophores can also be used as selection criteria to identify bacteria with biocontrol potential. This was demonstrated by Zheng et al. (2018), who examined 163 bacterial isolates for their ability to produce protease, chitinase, cellulase, and siderophores.

Fungal Isolation Protocols. On the fungal front, researchers have explored the isolation of fungal strains from various sources, such as marine environments and agricultural lands, for their enzymatic activities and biodegradation capabilities (Miao & Qian, 2005; Jayadev, 2017). Fungal isolation protocols similarly begin with sampling, which may include soil, plant tissues, or air. In the study of fungal communities associated with plants, spores or mycelium from

fungal colonies are often collected for DNA extraction and identification using ITS and EF1-α sequencing. This approach was detailed by Khol et al. (2019), who used ITS1/ITS4 and EF1-728F/EF2 primers for the molecular identification of fungal isolates from various environmental samples.

Risk assessment is a crucial component of fungal isolation, particularly for potential biocontrol agents. This includes evaluating the ability of the isolates to grow at different temperatures and assessing their pathogenicity towards non-target organisms. For example, isolates unable to grow at human body temperature (36°C) are preferred for safety reasons in biocontrol applications.

Advanced Techniques and Applications. Recent advancements in isolation techniques involve the use of molecular tools and genomic fingerprinting to ensure accurate identification and characterization of microbial strains. BOX-PCR fingerprinting, for instance, has been employed to differentiate bacterial isolates based on their genetic profiles, ensuring the selection of genetically diverse and potentially effective biocontrol agents (Zheng et al., 2018). Furthermore, the integration of plant growth-promoting assays and biocontrol efficacy tests in both greenhouse and field conditions has enhanced the practical applications of these isolated strains.

In conclusion, the isolation of bacterial and fungal strains involves a series of meticulous steps, from sampling and cultivation to molecular identification and functional assays. These protocols not only facilitate the discovery and characterization of microbial diversity but also pave the way for their application in sustainable agriculture and environmental management.

2. The chosen microbial species

Selected bacteria: *Bacillus*. The genus *Bacillus* is characterized by aerobic or facultative anaerobic growth, Gram-positive staining, bacillary morphology (rod-shaped bacterium), often flagellar motility, and variable size (0.5 to 10 µm). Optimal growth occurs at neutral pH, with a wide temperature growth range, although most species are mesophilic (temperature between 30 and 45 °C). Their metabolic diversity associated with promoting plant growth and controlling pathogens is noteworthy (Tejera-Hernández et al., 2011). Additionally, they can form highly resilient dormant endospores, which can remain viable in the environment until conditions become favourable for initiating their metabolic processes and generating a vegetative cell (Errigton, 2003; Tejera-Hernández et al., 2011). Therefore, the formation of heat and desiccation-resistant endospores is a crucial feature for formulating biotechnological products based on strains of this bacterial genus (Pérez-García et al., 2011).

Selected fungal genera. The fungal genera [redacted] spp., [redacted] spp., and [redacted] spp. were specifically chosen in this PhD thesis for their demonstrated efficacy as biocontrol agents against plant diseases, according to literature (Andrews, 1992; Bélanger & Labbé, 2002). [redacted] and [redacted] belongs to the Basidiomycota phylum (Sipiczki & Kajdácsi, 2009). Both species are known to produce hydrolytic enzymes and antifungal compounds effective against powdery mildew fungi (Hammami et al., 2011; Zhang et al., 2019), within other plant pathogens. Another fungal genus recognized for its significant role as a biocontrol agent is [redacted], which belongs to the Ascomycota phylum. They compete with plant pathogens for nutrients, inhibit spore germination, produce volatile organic compounds and induce oxidative stress in pathogens, thereby suppressing their growth and virulence (Zhang et al., 2010; Al-Qaysi et al., 2021).

3. Species assignation by morphological determination

[redacted] **group.** Macroscopic identification of species within the *Bacillus* genus involves considering several morphological traits. Common characteristics aiding in identification include colony appearance, texture, colour or pigmentation presence, and growth patterns. Additionally, variations in colony morphology, such as the presence of mucoid or dry colonies, play a crucial role in distinguishing between different species within the *Bacillus* genus (Makky et al., 2008). These macroscopic features offer valuable information for accurate *Bacillus* species differentiation from other bacterial groups without microscope assistance. Moreover, since *Bacillus* genus are Gram-positive bacteria, the rapid and cost-effective KOH test can be performed to quickly determining the Gram characteristics of bacteria (Halebian et al., 1981; Ahmed et al., 2013) by assessing the viscosity of a bacterial colony treated with a 3% KOH solution. Gram-negative bacteria exhibit a viscous consistency due to cell wall lysis, while Gram-positive bacteria do not (Rinihapsari, 2021; Rohayati et al., 2023). The KOH test is considered a valuable supplement or substitute to Gram staining and antibiotic susceptibility testing for the initial classification of bacteria since it is much simpler, faster and less toxic (Johnson et al., 1995). In cases where Gram staining results are ambiguous, the KOH test can provide a quick confirmation of the true Gram reaction of the bacteria.

On the other hand, identification of species within the *Bacillus* genus relies also on specific morphological traits observed using an optical microscope. These characteristics include cell shape, size, arrangement, and the presence of endospores. Typically, *Bacillus* species (focusing on [redacted] group) exhibit rod-shaped cells, form endospores, and may occur singly, in pairs, or in chains (Bhandari et al., 2013).

To differentiate species within the [redacted] group from those in the *Bacillus cereus* group, additional morphological traits come into play. [redacted] typically measures approximately [redacted] µm in width and [redacted] µm in length, whereas *Bacillus cereus* is larger, ranging from 1.0-1.2 µm in width and 3-5 µm in length (Latif et al., 2020). Moreover, [redacted] is renowned for its motility, while *Bacillus cereus* also exhibits motility albeit to a lesser degree (Latif et al., 2020). Furthermore, [redacted] demonstrates a more efficient biofilm formation compared to *Bacillus cereus* (Bottone, 2010). These disparities in motility and biofilm formation are observable under the microscope, facilitating their differentiation. Finally, while both groups share similarities in sporulation processes and certain protein families, differences in fatty acid composition and genetic variances -identified through DNA-DNA hybridization tests- exist between them and contribute to distinguishing species within the [redacted] group from those in the *Bacillus cereus* group (Borriss et al., 2011; Gastélum et al., 2020).

Fungal candidates. On a macroscopic scale, several morphological traits aid in identifying [redacted] spp., [redacted] spp. and [redacted] spp. from others. Common characteristics facilitating species identification include colony appearance, texture, colour, growth rate, and pigmentation. For instance, [redacted] (mostly for [redacted]) typically appears on a Petri dish as white to cream-colored colonies with a fluffy or floccose texture. The colonies of [redacted] are often described as having a powdery or velvety appearance. The growth pattern of this yeast-like fungus on agar plates is characterized by its fluffy, cotton-like texture, which distinguishes it from other microbial colonies. Additionally, [redacted] colonies may exhibit a circular or irregular shape, depending on the growth conditions and medium used (Avis et al., 2001). On the contrary, [redacted] spp. typically appear on a Petri dish as dark-coloured colonies with a velvety or suede-like texture. These colonies can range in colour from dark brown to black (due to their dark pigmentation), and they often have a powdery appearance or velvety surface. However, in fresh colonies, other colours in a whiter to pink range may appear. The colonies of [redacted] spp. may exhibit a circular or irregular shape, depending on the growth conditions and medium used.

On the other hand, to identify fungal species using an optical microscope, key morphological traits to consider include: the size and shape of cells, the presence of budding, the formation of pseudohyphae, and the arrangement of cells in culture. Additionally, the observation of any distinctive structures such as spore-like cells or budding patterns can aid in the accurate identification of different species (Avis et al., 2001). Thus, [redacted] spp. are characterized by their yeast-like appearance, often appearing as small, spherical cells, with some species showing elongated or oval forms. These cells may be observed singly or in clusters (Avis et al., 2001; Hammami et al., 2011). [redacted] spp. are visualized as dark-coloured, yeast-

like cells. These cells often appear as elongated or oval-shaped structures, and they may be observed singly or in clusters. Chlamydospores of [redacted] spp. are described as dark brown, smooth to lightly rough-walled, globose to ellipsoidal, and septate. In contrast, conidia are often yeast-like, appearing hyaline, aseptate, smooth-walled, ellipsoidal to lemon-shaped, and variable in size (Campana et al., 2022).

4. Molecular classification for the taxonomical identification

The classification and identification of microorganisms, particularly bacteria and fungi, have historically been challenging due to their diverse morphological characteristics and phenotypic plasticity. Traditional methods relying solely on phenotypic traits often face limitations, such as ambiguity in species delineation and misclassification (Woese et al., 1990). However, the introduction of molecular techniques has revolutionized microbial taxonomy, offering unprecedented insights into microbial diversity, evolutionary relationships, and ecological functions (Theron & Cloete, 2000).

Molecular approaches provide a more reliable means of species identification by delving into the genetic makeup of organisms, revealing evolutionary relationships and genetic divergence (Theron & Cloete, 2000). By focusing on conserved genetic markers such as the 16S rRNA gene in bacteria and the ITS region in fungi, researchers can infer phylogenetic relationships and classify microorganisms into distinct lineages (Theron & Cloete, 2000). Therefore, in this PhD thesis, the 16S rRNA gene was used to classify the bacteria. This gene, which typically consists of around 1,500 base pairs of nucleotides, has been extensively used for bacterial identification and classification due to its conserved nature across bacterial species (Johnson et al., 2019).

However, due to the number of bacterial strains isolated in this work was too large to sequence them all, a faster molecular pre-screening was required. The genetic region employed for this purpose was an internal region of the 16S rRNA gene (named as [redacted]), where specific primers were used. This pre-screening enabled the selection of only [redacted] group species, or very close to this group. The [redacted] gene of *Bacillus* strains, specifically [redacted], is known to amplify at 595 base pairs of DNA fragments ([redacted]; [redacted]). This gene is part of the core genes of *Bacillus* strains and has been utilized in various studies for genetic diversity analysis and phylogenomics (Mullins et al., 2020; Liu et al., 2020). The [redacted] group, to which the [redacted] gene belongs, has been extensively studied for its genomic and specialized metabolite diversity (Mullins et al., 2020).

In the case of fungal candidates, the Internal Transcribed Spacer (ITS) gene was used for the taxonomical classification, and only the information from the sequencing of this gene was

enough to determine their specie. The ITS gene of fungal strains typically ranges between 580 to 800 base pairs in length (Ogbuji et al., 2021) and has been widely recognized as a universal DNA barcode marker for fungi due to its high variability and suitability for fungal identification (Schoch et al., 2012; Raja et al., 2017).

OBJECTIVES

The main objective of this chapter was to generate a large collection of isolates obtained from various plant sources, and to characterize and preclassify the isolated strains to identify the most promising candidates for use as biocontrol agents, based on relevant literature and their taxonomic classifications.

Achieving this goal necessitated the development of a standardized model for searching, isolating, cultivating, and preserving microorganisms, adapting it to the specific characteristics of each taxonomic group of interest. Moreover, it was essential to establish and implement various protocols for the rapid and large-scale selection or elimination of isolated strains.

More specifically, the objectives proposed in this chapter were:

1. To determine the best plant source for the isolation of *Bacillus* species, including different types of plants infected with either downy mildew or powdery mildew, healthy plants and seeds.
2. To determine the best bacterial isolation protocol to obtain the *Bacillus* species, found naturally in the environment.
3. To quickly discard strains with a high potential to be pathogenic (such as bacteria from the *Bacillus cereus* group).
4. To determine the best plant source for the isolation of the desired yeast-like fungi species, including different types of plants infected with powdery mildew or healthy plants.
5. To determine the best fungal isolation protocol to obtain the desired yeast-like fungi species. specifically belonging to the genera [redacted], [redacted] and [redacted], found naturally in the environment.
6. To morphologically characterize and be able to recognize all the preselected isolates, both bacteria and yeasts.
7. To molecularly determine the taxonomic identity of the most promising strains, both bacterial and fungal.

MATERIALS AND METHODS

Plant sample collection

Leaves of infected plants with powdery mildew or downy mildew were collected from Autumn 2020 since Autumn 2021. A great collection of potential antagonists for both diseases was obtained from various infected cultivars with either downy or powdery mildew diseases, including [redacted]. Moreover, all the plant samples were collected from different locations at different times, including [redacted] and [redacted]. Additionally, some bacteria were isolated from [redacted] seeds from [redacted], including [redacted]. Samples were collected and stored in plastic bags in the fridge to be processed within one to three days.

1. Isolation, growth and storage of the selected species

Bacterial species with potential for being BCAs. For the isolation of [redacted] group strains, leaf samples were cut under sterile conditions into small pieces (approx. 0.5 cm2), which were put in 0.9% saline solution. After vortexing for 1.5 min, samples were kept at 80 ºC for 15 min. Then, the bacterial solutions were diluted, plated on Trypticasein Soy Agar (TSA, from Condalab, Spain) and incubated at 30 ºC for 2 days. On the other hand, leaf endophytes were also isolated. The procedure consisted of cutting the leaf samples into small pieces (approx. 1 cm^2), sterilizing with 70% ethanol and washing with sterilized distilled water. The samples were finally air dried and put on TSA Petri dishes for 2 days at 30ºC, allowing endophytes to come out the leaves.

Additionally, between 5 to 10 seeds of different cucurbit species were sterilized twice with sodic hypochlorite (3%) for 5 min. Then, seeds were washed with sterilized distilled water and were submerged in 95% ethanol for 5 min, also twice. Surfaced-sterilized seeds were finally washed with sterile distilled water and cut in small pieces. The pieces were directly put onto a TSA plate to let the endophytes go out and, additionally, the pieces were put into sterilized distilled water and diluted 1/10. Both solutions were finally seeded on a TSA plate and incubated at 32°C for 2 days.

In the 3 different bacterial isolation protocols, after the incubation, the TSA Petri dishes were full of different bacteria. About 5 single colonies per plate were selected based on their

morphology characteristics and appearance, which were transferred on new TSA Petri dishes to obtain pure cultures. After being incubated at 32 ºC for 24 h, the isolated bacteria were re-plated on TSA to ensure the purity of the cultures. Finally, the strains were inoculated into 5 mL of sterile Luria Bertani (LB) broth (from Condalab, Spain) and incubated at 30 ºC with agitation (150 rpm) for 24 h. The bacterial solutions were stored in cryotubes with 15% glycerol at -80 ºC and plates were stored at 4 ºC for further experiments.

Yeast-like fungi species with potential as BCAs. For the isolation of yeast-like fungi clumps of powdery mildew conidia from different leaf samples were transferred on malt extract agar (MEA, from Condalab, Spain) or MEA at 1/10 strength, both amended with 100 mg/L streptomycin and 15 mg/L tetracycline, according to Köhl et al. (2019). The plates were incubated for 7 to 14 days at 19 °C in the dark. On the other hand, according to Urquhart et al. (1994), leaf sections (approx. 5 cm^2) with powdery mildew were attached with adhesive tape (sporulating surface down) were transfer to Petri dishes with corn meal agar (CMA, from Condalab, Spain) amended with 10 µg/mL of Dichloran and 100 µg/mL of ampicillin. The leaf samples were removed after 6 h, 24 h and 48 h and replaced by a new lid. The plates were then incubated at 19 ºC for 7 - 10 days. About 5 different strains per plate were selected, spread on PDA and incubated at 19 ºC and dark for 7 - 10 days. After that, isolated colonies were transferred to new PDA and incubated again to ensure their purity.

To store the yeast-like fungi strains, the pure colonies obtained were grown in a liquid homemade medium rich in glucose (10 g peptone, 25 g glucose and 1 g Microbiological yeast extract per 1 L of distilled water) and incubated at 20 ºC with agitation (150 rpm) for 24h. The resulting liquid cultures were finally frozen in cryotubes with a final concentration of glycerol of 15%. Plates were stored at 4 ºC for further experiments.

2. Morphological characterization of the isolated microbials

Bacterial candidates. Bacterial characterization was performed first by an optical microscope morphology determination to discard cocci species and looking for short and not very thin bacilli, characteristics of the [redacted] group according to literature.

Afterwards, a KOH+/- test was performed in all the species that met the above characteristics. The analysis consisted of the addition of 1 – 2 drops of a 3% KOH solution on a microscope slide and mixing well with a loop of the bacteria during 1 min. After this time, if the consistency of the mixture had become viscous/mucus-like, the result was that the treated bacterium was KOH+, indicating it was a Gram-negative strain. On the other hand, if the mixture remained totally liquid with a strong surface tension, it indicated that the bacterium was Gram-positive.

Additionally, in this study, two distinct selective media were employed to facilitate the screening and identification of *Bacillus* spp. strains. Firstly, following the protocol outlined by Knight and Proom (1950), we utilized an ammonia basal medium supplemented with glucose to a final concentration of 3%. The composition of this medium per litter included: KH_2PO_4 (1.5 g), $(NH_4)_2HPO_4$ (7 g), $MgSO_4.7H_2O$ (0.5 g), $CaCl_2.2H_2O$ (0.3 g), $MnSO_4.4H_2O$ (40 mg), $FeSO_4.7H_2O$ (2.5 mg), ammonium molybdate (2 mg), glucose (30 g), and agar (15 g). These constituents were dissolved in distilled water (1 L), and the pH was adjusted to 7.0 before autoclaving for 20 minutes. Incubation at 37°C for 2 days was found to promote the growth of [redacted] on this medium. On the other hand, another selecting medium was prepared incorporating phenol red (also phenolsulfonphthalein or PSP) as the selective reagent. This medium, per litter, comprised: peptone (10 g), meat extract (1 g), D-mannitol (10 g), sodium chloride (10 g), phenol red (0.025 g), and agar (15 g). The pH was adjusted to 7.1.

Fungal candidates. Regarding to fungal candidates, the different species were classified according to the appearance of the colonies. Macroscopically, desirable colony traits included colours ranging from various shades of white and yellow, as well as softer shades of orange, brown, and pink. Additionally, colonies with both smooth and rough growth edges, exhibiting textures from watery and less dense to more mucous, were considered favourable. Furthermore, the presence of micellar growth combined with yeast growth was also identified as a highly desirable characteristic. Also, the presence of yeast-type cells and mycelium fragments were determined with optical microscopy.

3. Molecular classification

DNA extraction. For DNA extraction, the different strains were cultivated overnight in LB medium, in case of bacteria, or TII medium, in case of yeast-like fungi. Microbial solutions were then centrifugated at 4000g for 10 min. The pellets were resuspended in 200 µL of TE buffer, prepared with 10mM Tris-HCl containing 1mM EDTA•Na_2. DNAs were extracted by E.Z.N.A.® Bacterial DNA Kit (Omega Bio-tek), following the fabricant instructions. Alternatively, a simple extraction was performed by boiling the microbial solutions at 100 ºC for 15 min and immediately nailing in ice for another 15 min, followed by a centrifugation to remove cell debris. The quality and concentration of DNA were determined on a nanodrop spectrophotometer: the NanoPhotometerTM from BioNova cientifica S.L.

Pre-screening using specific gene group identification for bacteria. For a pre-taxonomical identification of the bacterial strains, PCRs were performed using the 96-well T100™ Thermal Cycler (BioRad). The DreamTaq DNA polymerase (Thermo Scientific™) and the primers [redacted] and [redacted]

[redacted], purchased from Life Sciences, were used for the PCR amplification of a 595-bp fragment, corresponding to an internal portion of the [redacted] group 16S rRNA, according to [redacted]. The protocol for the PCR was: initial denaturation set at 95 ºC for 2 min, 30 cycles of denaturation at 95 ºC for 30 s, annealing at 59 ºC for 30 s and extension at 72 ºC for 60 s, followed by a final elongation step at 72ºC for 5 min. The protocol was adapted from [redacted]

Finally, electrophoresis in 1% agarose gel were performed using GeneRuler 100 bp Plus (Thermo Scientific) using Syber-safe staining (Thermo Fisher Scientific) and visualized on a UV transilluminator, the Molecular Imager® Gel Doc™ XR System, and using the Image Lab™ Softward Version 4.0 (BioRad Laboratories, Inc.).

Sequencing conserved genes for specie determination. For all the most promising candidates, both bacterial and yeast-like fungi strains, the sequencing of widespread used genes to determine their genera and specie was performed using the Phusion High-Fidelity DNA polymerase (Thermo Scientific).

For bacterial strains, the 16S rRNA gene region was amplified by using the universal primers 27F (5′-AGAGTTTGATCCTGGCTCAG-3′) and 1492R (5′-GTTTACCTTGTTACGACTT-3′), according to Bahuguna *et al.* (2020), which were also purchased from Life Sciences. The PCR protocol consist of an initial denaturation at 98 ºC for 30 s, 30 cycles of denaturation at 98 ºC for 10 s, annealing at 56 ºC for 20 s and extension at 72 ºC for 20 s, followed by a final elongation step at 72ºC for 7 min and finally hold at 4 ºC.

In the case of fungi and yeast-like fungi, and the universal primers ITS1 (5'-TCCGTAGGTGAACCTGCGG-3') and ITS4 (5'-TCCTCCGCTTATTGATATGC-3'), according to White *et al.* (1990) and purchased from Life Sciences, were used to amplify the ITS region through PCR following the PCR conditions: initial denaturation set at 98 ºC for 30 s, 30 cycles of denaturation at 98 ºC for 10 s, annealing at 60.4 ºC for 20 s and extension at 72 ºC for 40 s, followed by a final elongation step at 72ºC for 7 min and finally hold at 4 ºC.

The resulting amplicons were purified by peqGOLD® Gel Extraction Kit (avantorTM), following the fabricant instructions, and the concentration of purified DNA was quantified with the nanodrop spectrophotometer. Finally, the purified amplicons were sent to the sequencing services of the Parc Científic de Barcelona for Sanger sequencing (both forward and reverse sequencing). Afterwards, the obtained sequences were visualized and forward and reverse sequences were aligned by using the BioEdit software 7.2.5 (Hall, 1999). Consensus sequences were analysed using the BLAST software on the NCBI (National Center

Biotechnology Information, https://blast.ncbi.nlm.nih.gov), where the filter “Sequences from type material” was applied.

RESULTS

1. The final collection of isolated microbial strains

A large collection (724 strains) of potential antagonists, belonging to a wide group of different microorganisms, was generated for one year, from Autum 2020 to Autum 2021. The sources of microorganisms were different plant species distributed throughout various provinces of Spain. The number of isolated strains from each province and type of cultivars is shown in Figure 1.1.

Figure 1.1. Total numbers of strains isolated from different plant species obtained from different Spanish provinces, collected during an entire year. The numbers refer to both species of bacteria and fungi.

As a summary, most microorganisms were extracted from [redacted], where a total of [redacted] strains over 724 in total were obtained, which represent [redacted]. This source of microorganisms is closely followed by the [redacted], from which [redacted] strains were isolated ([redacted]). [redacted] strains were obtained from the [redacted], [redacted] strains from different [redacted] and finally a group of [redacted] were isolated from a wide variety of plant sources. Moreover, [redacted] more bacterial strains ([redacted]) were isolated from different varieties of [redacted].

From the total of 724 strains, 491 bacterial species and 233 fungal species were isolated. In the following graphic (Figure 1.2) the exact number of bacteria and fungi extracted from the specific kind of plants are shown.

Figure 1.2. Final collection of potential antagonists. It is shown the total of the microbial strains isolated from different cultivars and plants infected with **A. powdery mildew**, with a total of 234 bacterial isolates and 233 fungal isolates, or with **B. downy mildew**, with a total of 224 bacterial isolates. The number of bacterial strains is shown in black, whereas the number of fungal strains is represented in grey.

A great variety of different plants were used as sources of strains with potential as biocontrol agents against downy and/or powdery mildew, including

2. Morphological characterization of the microbial strains

Preselection of the bacterial species. Over the 491 bacterial strains in total, the first step for the screening was the morphological characterization of the isolates based on their macroscopical traits, such as their colour and colony appearance. Examples are shown in Figure 1.3.

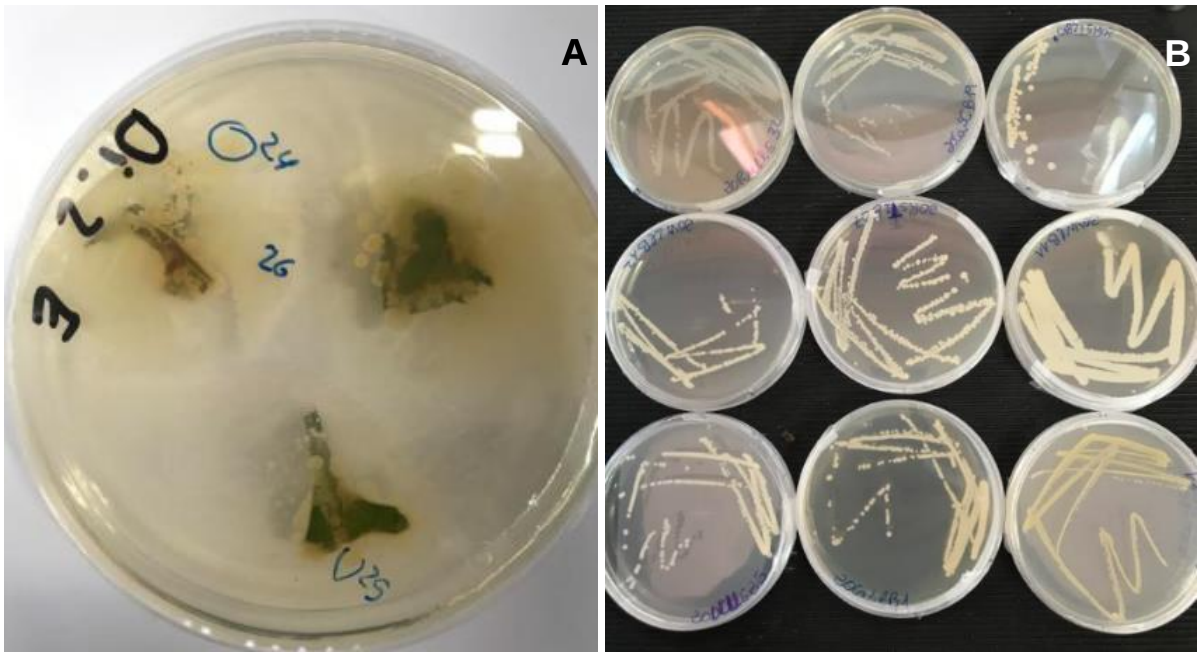

Figure 1.3. Different images of isolated bacterial strains obtained through **A.** disinfecting the leaf surfaces to extract endophytes and **B.** boiling the plant samples to extract only *Bacillus* species.

Once discarded the first most strange colonies, based on colours and textures, the KOH+/- analysis was performed in the rest of the strains, as *Bacillus* species belong to the wide group of Gram+ bacilli. From a total of 491 bacterial strains tested, 274 strains were KOH+ (Gram-) and 217 were KOH- (Gram+). However, some strains with morphological characteristics very similar to those of the [redacted] group were selected for the subsequent experiments, despite their responses to the KOH method, due to the previously mentioned factors. Then, after selecting at a macroscopic level, an analysis of the morphology at a cell level was conducted. An initial overview was performed by an optical microscope to determine the cell morphology, only looking for whether the cells were bacilli or cocci. From the 491 bacterial strains in total, 152 cocci and 339 bacilli were identified, from which 153 bacilli were also KOH- (Gram+). All cocci were directly discarded (both KOH+/-). Results are shown in Table 1.1.

Table 1.1. Summary of the first pre-screening based on strain morphology at a cellular level. It was considered first the KOH+/- determination and then the cell type: bacilli or cocci.

Source	Morphology	KOH+ (Gram-)	KOH- (Gram+)
[redacted]	Bacilli	94	63
	Cocci	35	31
[redacted]	Bacilli	84	71
	Cocci	48	32
[redacted]	Bacilli	8	19
	Cocci	5	1

A more detailed morphological determination was conducted again with the optical microscope to differentiate strains close or belonging to [redacted] group from ones close or belonging to *Bacillus cereus* group. The images shown in Figure 1.4 correspond to strains which belong to the [redacted] group, i.e., [redacted]. In this case, despite belonging to the same species, the strains showed very different macroscopic and microscopic morphologies. It can be easily appreciated that the bacterial cells corresponding to [redacted] were slightly larger than in the case of [redacted]. Moreover, since all strains were grown in the same conditions, it was observed that the growth (in terms of cell density) of strain [redacted] was higher than in the case of strain [redacted].

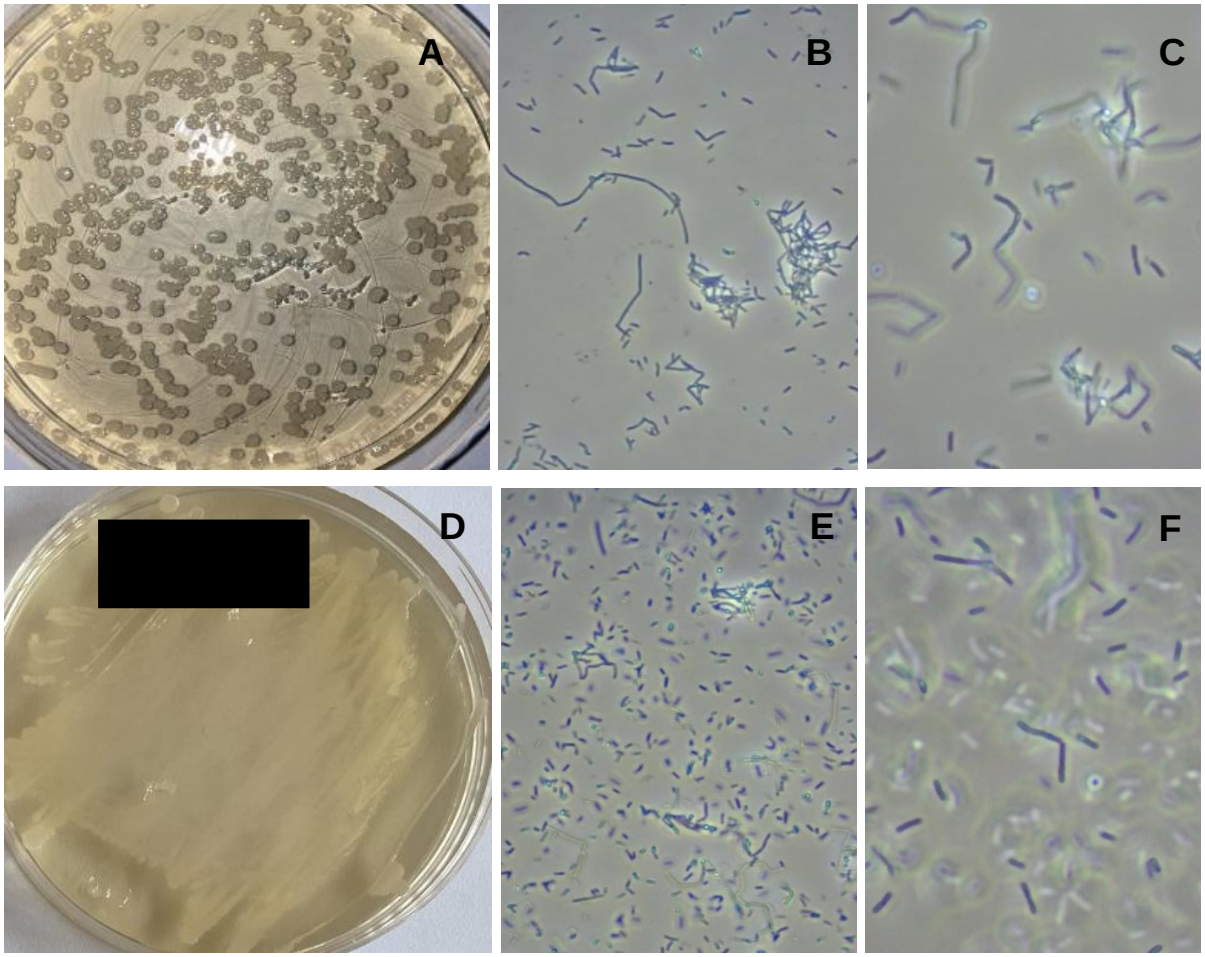

Figure 1.4. Comparison between different morphological shapes of the KOH+ bacilli selected strains [redacted] (above) and [redacted] (below). The images correspond to the macroscopical appearance (**A** & **D**) and microscopical morphology at 40x (**B** & **E**) and at 100x (**C** & **F**), respectively.

In addition, the best potential candidates based on these characteristics (bacilli KOH-) were further analysed macroscopically by culturing them on selective media for *Bacillus* spp. and by scrutinizing colony morphology using a magnifying glass. These two analyses were performed to gather more information about the preselected strains and be able to recognize them easily rather than to continue with the preselection. For example, at a first look on the Petri dishes of

strains [redacted] the bacterial growth appeared to be very similar. However, as it is shown in Figure 1.5, when using a magnifying glass, differences in colony appearance could be observed. The colonies of strain [redacted] had very smooth edges and grew with round morphologies. The colonies seemed to have a very homogeneous texture. Strain [redacted] seemed also quite homogeneous and with more whitish edges than the inside and quite rough. On the other hand, strain [redacted] had a little rough edge and a kind of striations could be seen inside the colonies.

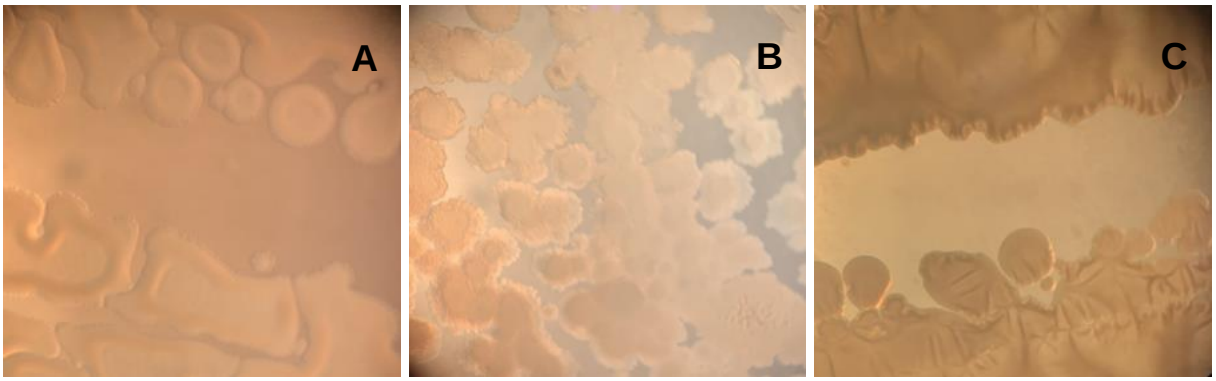

Figure 1.5. Images taken with a magnifying glass of the bacterial strains [redacted] (**A**), [redacted] (**B**) and [redacted] (**C**), respectively. The differences in colony morphology can be easily appreciated.

Preselection of yeast-like fungi species. Out of a total of 233 fungal strains, 103 yeast-like fungi strains were initially selected for sharing common characteristics with the desired groups, including [redacted] and [redacted].
In the case of yeast-like fungi species, all the 103 strains were sent to the sequencing services of PCB and only some images of the finally selected candidates are shown below. For instance, as it is shown in Figure 1.6, the mycelium of strain [redacted] is very dense, with a cream-white colour, forming yeast-like growth colonies in some areas. When the plate becomes old (1 week), green edges appear. It must produce some kind of pigment and, as it was previously mentioned, the presence of grey to black aerial mycelium and pigmentation visible on the reverse side of cultures on petri plates can also be indicative of [redacted] species (Darge & Woldemariam, 2021). Another [redacted] identified was strain [redacted], in which no visible pigmentation was observed.

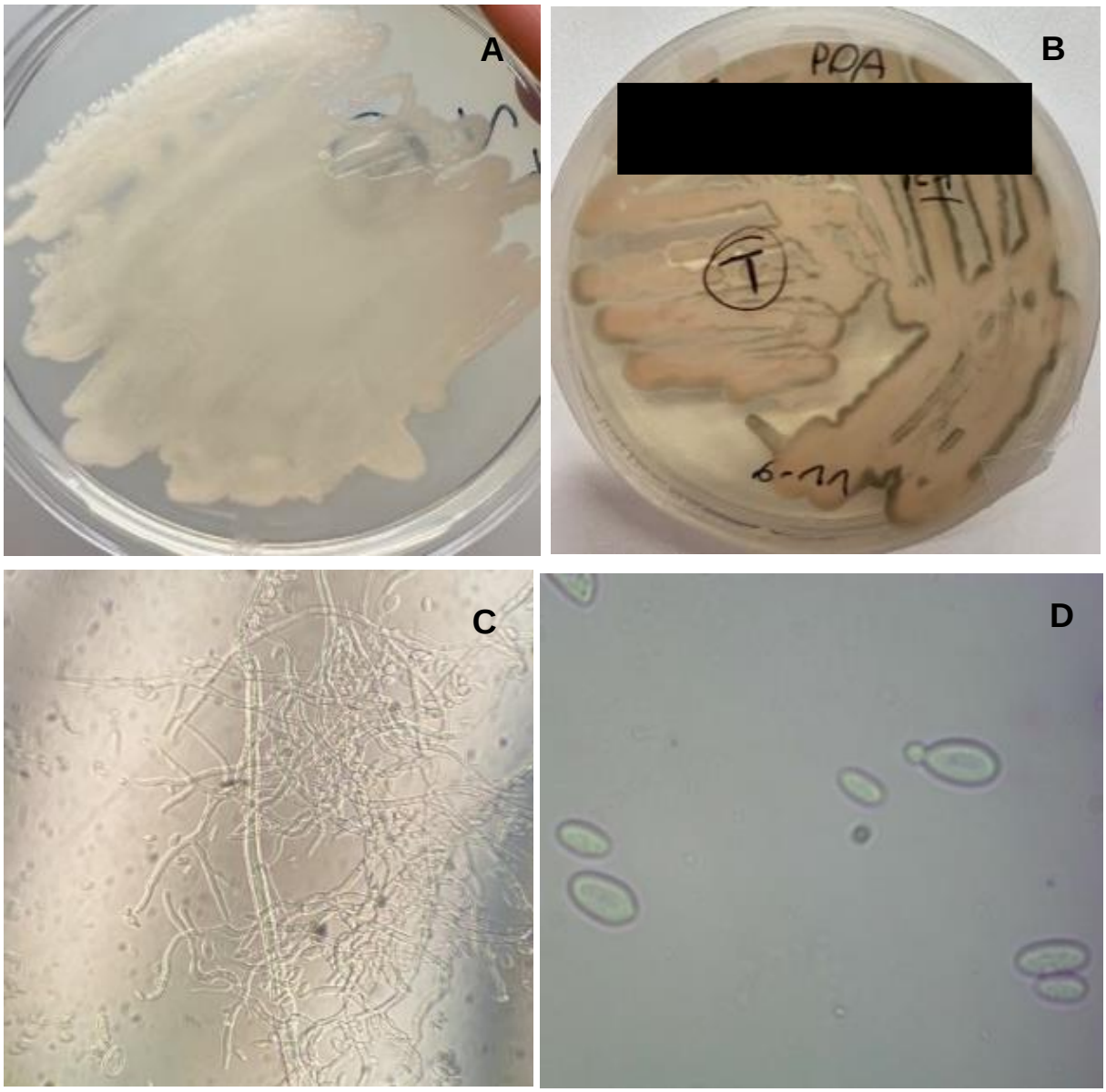

Figure 1.6. Macroscopical and microscopical appearance of [redacted]. **A.** Fresh culture of strain [redacted], showing a whitish mycelium with a slightly creamy and dense texture. **B.** 2-week culture of the same strain which has evolved to a much darker green colour and a more compact texture. **C.** Micellar growth of strain [redacted] seen under a microscope at 10x. **D.** Yeast type cells of this same strain visualized at 40x.

Referring to the morphology of [redacted], an example can be observed in strain [redacted] (Figure 1.7A & 1.7B). As shown, the cells were much smaller than in previous cases and, similar to [redacted], green edges appeared surrounding the growth of the microorganism. On the other hand, [redacted] (1.7C & 1.7D) exhibited well-defined mycelium, with small villi observed along the edges. On the surface, it appeared as a dense, white-to-pink liquid resembling yeast itself. In comparison, [redacted] shared similarities with [redacted], albeit with larger villi along its edges. Its colour was pinker, leaning towards a creamy white hue, with tiny star-like formations of villi in areas of lesser growth.

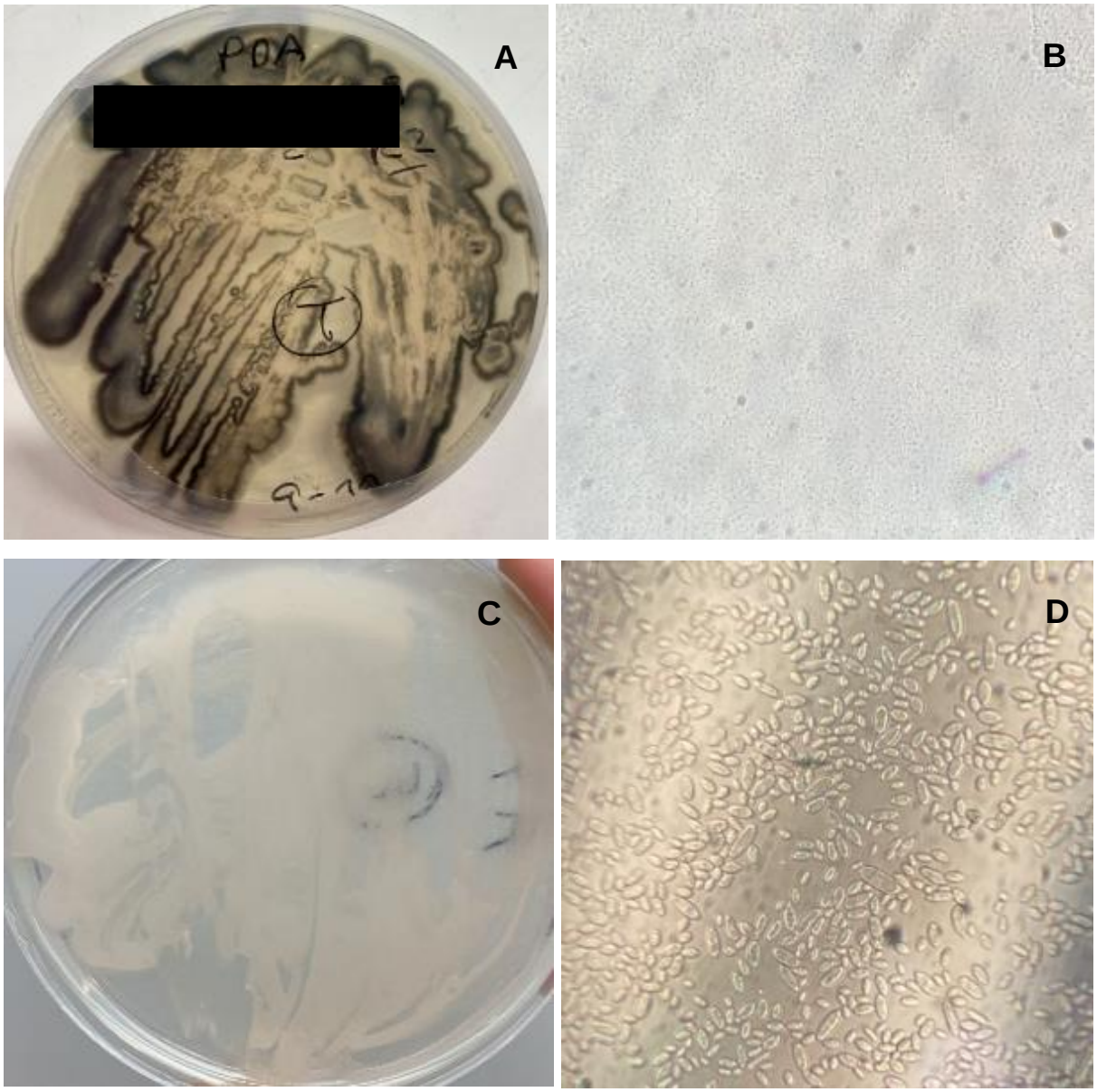

Figure 1.7. Macro and microscopical morphology of [redacted] (**A** & **B,** respectively). It has a very dry and compact appearance. Its micellar growth is floury white, with very dark green edges a week after sowing. Macro and microscopical morphology of [redacted] (**C** & **D,** respectively). It manifested as a dense, white-to-pink liquid mycelium with little villi along the edges.

3. Molecular identification of the selected strains

Molecular characterisation of bacterial strains. Primers [redacted] were used for the PCR amplification of the internal portion of the 16S rRNA gene shared within the [redacted] group species. This means that the presence of a band in the 1%-agarose electrophoresis gel (Figure 1.8) indicated that the tested strains had high probability of belonging to this group. All the bands were detected within 500 and 600 bp. Moreover, this genetic detection allows the discard of other *Bacillus* species which could potentially belong to *Bacillus cereus* or close species.

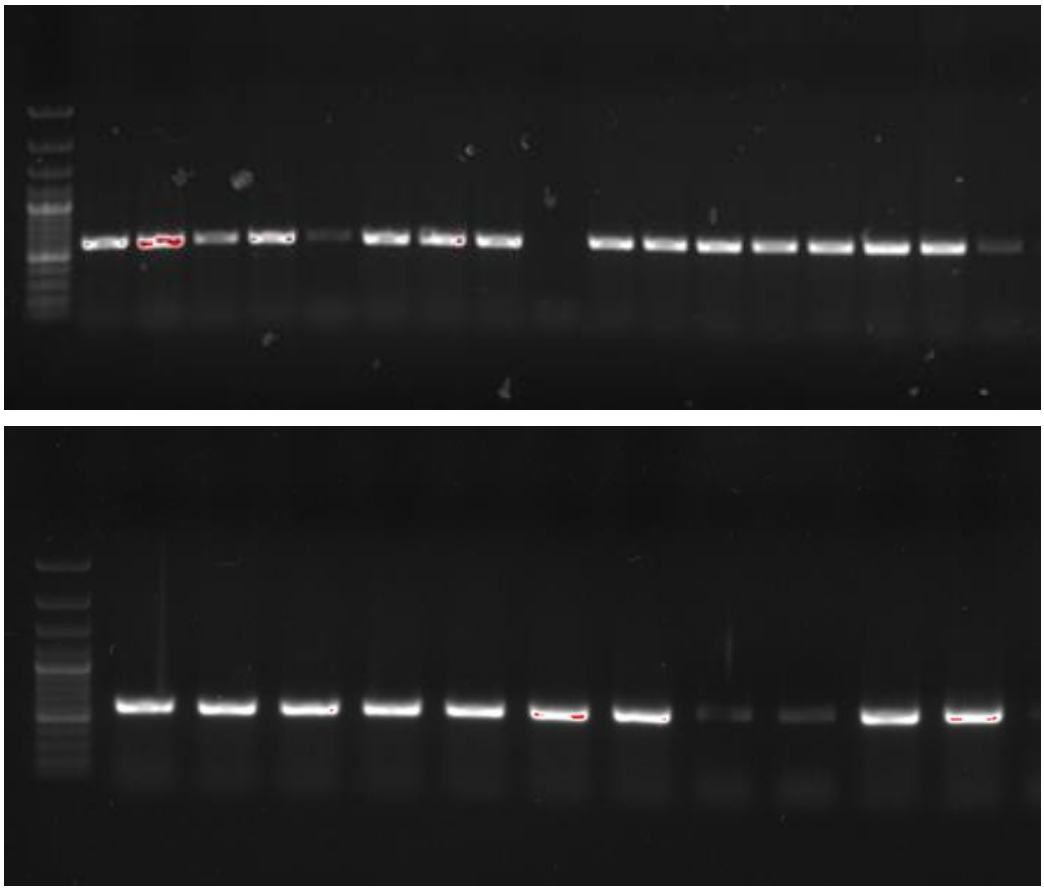

Figure 1.8. 1%-agarose electrophoresis gel of the PCR amplification of an internal portion of the [redacted] group 16S rRNA, with a band length of 595 bp, from a collection of KOH- bacilli to detect strains belonging to the [redacted] group, according to Wattiau et al. (2001). The primers [redacted] were used to perform the PCR. The presence of a band indicated high probability for the tested strain to belong to the mentioned group.

Most of the strains shown an amplification of the shared portion of the 16S rRNA gene, since a preselection of all bacterial strains was previously performed to direct the analysis by testing only the strains with the highest probability of success, i.e., only the KOH- (Gram+) bacilli were tested for the genetic detection.

In Table 1.2, it is shown the total of bacterial strains that formed the whole collection of possible candidates to be biocontrol agents, divided by the type of plants from which they were isolated. When referring to the total number of microbes found, [redacted] were the best source of [redacted] group species, with [redacted] of the strains belonging to the [redacted] group out of the total bacteria. This was closely followed by the [redacted] and [redacted].

However, when focusing only on the detection of the desired species within the preselected KOH- bacilli, the best sources were the [redacted] of the strains belonging to the [redacted] group among the KOH- bacilli) and the [redacted], closely followed by [redacted]. In contrast, no strains belonging to the [redacted]

[redacted] group were isolated from [redacted]. From various other sources, categorized as "Others," numerous bacterial strains ([redacted]) were isolated; however, only [redacted] strains) were identified as species of the [redacted] group. Most of the strains were KOH+ and were discarded in the initial selection process. However, when focusing solely on the KOH- bacilli, the percentage of desired strains was high ([redacted]).

Table 1.2. The percentage of success referring to how many strains from the total isolated from each plant sources were potential candidates as antagonists against downy and/or powdery mildews, meaning if they belong to a taxonomical group with potential as biocontrol according to the literature.

Sources	Total of microbes	KOH- Bacilli	[redacted] group	% success over the total	% success over KOH+ bacilli
[redacted]					
[redacted]					
[redacted]					
[redacted]					
[redacted]					
[redacted]					
Totals	**491**	**153**	**128**		

A total of 128 species belonging to the [redacted] group were obtained. The strains were classified from three different perspectives in order stablish the best source and technique to obtain the desired *Bacillus* species with more potential as biocontrol agents for downy and powdery mildews.

In the first graphic (Figure 1.9A), the obtained *Bacillus* strains were classified by plant source: [redacted]. In the second graphic (Figure 1.9B), the obtained *Bacillus* strains were classified by the disease source: [redacted].

Finally, the third graphic (Figure 1.9C) show these same strains classified by the technique performed to isolate the desired strains: [redacted]

In summary, the majority of [redacted] group species came from [redacted].

Figure 1.9. An schematic overview of the number of bacteria belonging to the [redacted] group, divided by **A.** Type of plant from where they were obtained; **B.** Disease pustules from where they were isolated and **C.** Technique used to perform the isolations: "*Bacillus* group", which consisted of boiling the bacterial solutions at 80 ºC for 15 min, and Plant and Seed endophytes, which consisted of disinfecting the surface of the leaf or seed, respectively. The results are given in percentages.

Molecular classification of the *Bacillus* species by sequencing. Of the 128 [redacted]-positive strains, the 16S rRNA gene was sequenced for those that also showed high efficacy in parallel efficacy trials (presented in the next chapter). The results obtained from sequencing and performing a BLAST search in the NCBI database are shown in Table 1.3. The mean length of the 16S rRNA gene region was 1387 bp.

Table 1.3. Taxonomical identification at species level, using the BLAST tool of the NCBI (https://blast.ncbi.nlm.nih.gov), of the *Bacillus* strains selected based on their taxonomical and efficacy profiles as potential biocontrol agents. The "Sequences from type material" filter was applied for the search.

Strain	Sequence assignation	Query covery	E-value	Percent identity	GenBank acc. numb.
[redacted]					

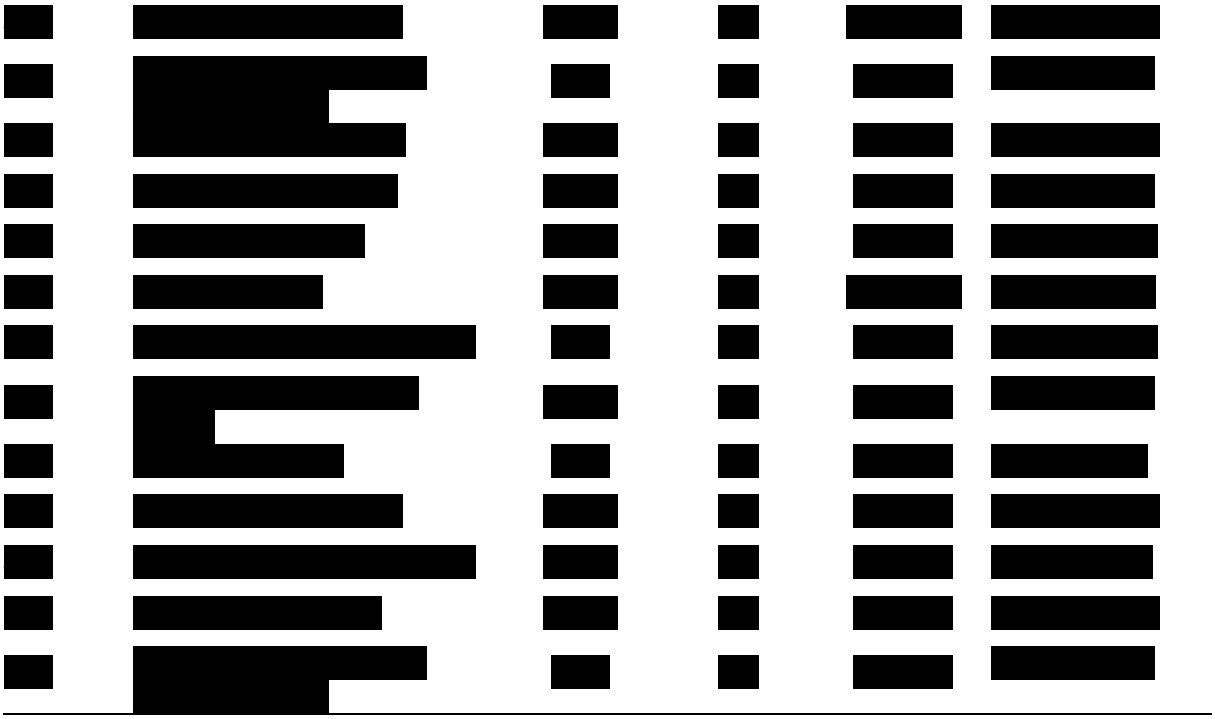

GenBank acc. numb. = GenBank accession number.

Following the initial taxonomic identification, certain strains were excluded from further consideration. For example, strain [redacted] (*B. cereus*) was removed from the list of promising candidates due to its pathogenic potential associated with its classification. Similarly, strains [redacted] were also discarded. These strains either belong to undesirable *Bacillus* species with potential opportunistic pathogenicity or lack scientific evidence supporting their efficacy in targeted biocontrol applications. Table 1.4 shows the sources of origin from which the desired strains were isolated.

Table 1.4. Source of origin from which the desired bacterial strains were isolated from. The location, the type of plant, the disease with which the corresponding plant was infected (or none) and the isolation protocol used to obtain the strains are presented.

Strain	Location	Plant source	Plant disease	Isolation protocol
[redacted]				

Molecular classification of the yeast-like fungal species. As it is shown in the following images from Figure 1.10, the lengths of the bands obtained from the PCR amplicons were slightly different between the fungal strains, with values from 500 to 600 bp approximately.

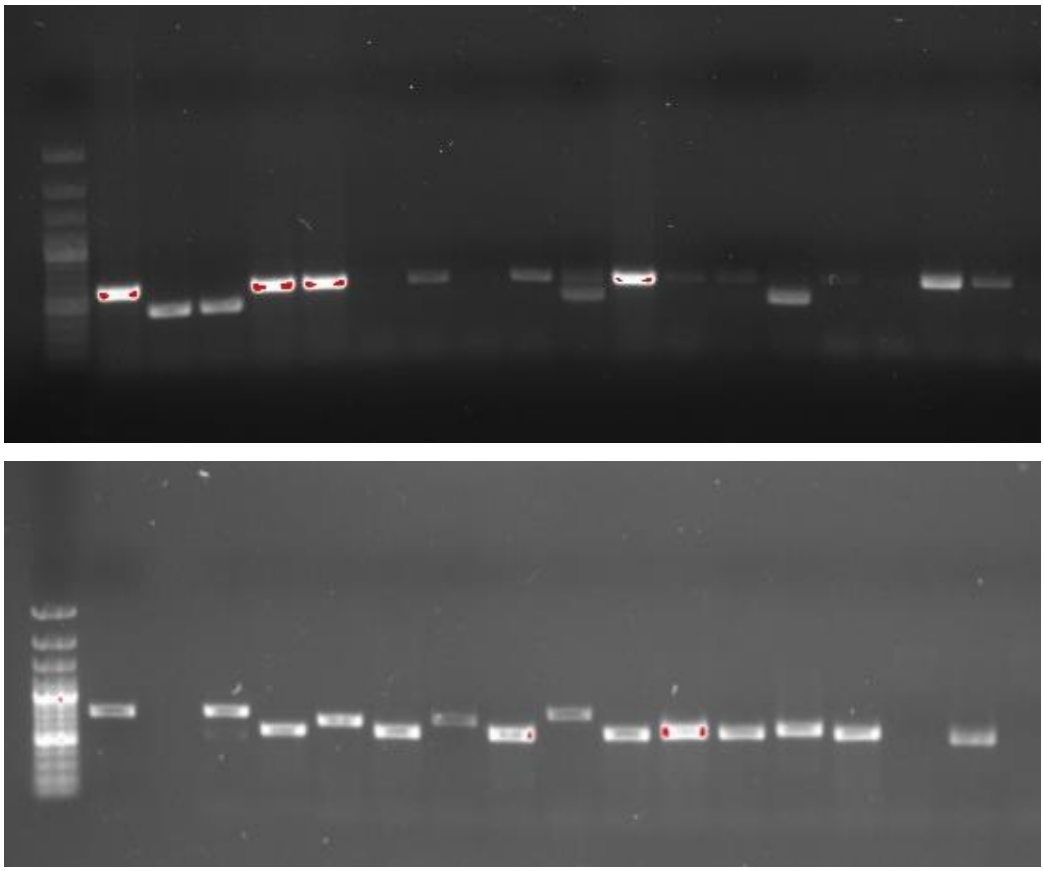

Figure 1.10. 1%-agarose electrophoresis gel of the PCR amplification of the Internal Transcribed Spacer (ITS) gene region from a collection of yeast-like fungi to sequence and identify fungal strains belonging to different taxonomical groups which, according to literature, have the potential to perform as biocontrol agents against powdery mildews. The ITS gene has a length that ranges between 580 to 800 base pairs. The primers ITS1 (forward) and ITS4 (reverse) were used to perform the PCR.

A total of 103 different fungal strains (morphologically selected from the 233 fungal strains isolated in total) was sequenced. Despite high diversity among the 103 assessed isolates, the dominant genus was *Sporobolomyces,* representing more than the 60% of the isolates. Notably, only 11% of the identified isolates belonged to known powdery mildew antagonists,

including [redacted] strains.

Results are shown in the following table (Table 1.5).

Table 1.5. Taxonomical identification at species level of the resulting interesting yeast-like fungi strains based on literature for as being capable to perform as potential biocontrol agents. The sequences of the ITS region were used to determine the species by the BLAST software on the NCBI (https://blast.ncbi.nlm.nih.gov).

Strain	Specie determination	Query covery	E-value	Percentage identity	GenBank acc. numb.
[redacted]					

GenBank acc. numb. = GenBank accession number.

In the following table (Table 1.6), the sources of origin from which these desired strains were isolated from are shown.

Table 1.6. Source of origin from which the desired yeast-like fungi strains were isolated from. The location, the type of plant, the disease with which the corresponding plant was infected (or none) and the isolation protocol used to obtain the fungal strains are presented.

Strain	Location	Plant source	Plant disease	Isolation protocol
[redacted]				

DISCUSSION

The isolation of microbial biocontrol agents is a crucial step in developing sustainable agricultural practices, offering an environmentally friendly alternative to chemical pesticides. This discussion synthesizes findings from the PhD thesis and from recent studies to identify the most effective isolation protocols for bacterial and fungal strains, particularly those with biocontrol potential against plant pathogens. The most effective isolation protocols are those that integrate multiple steps and selection criteria to ensure the recovery of diverse and potent microbial strains. According to Zheng et al. (2018), protocols that combine selective media, enzyme and metabolite production assays, and molecular fingerprinting are particularly successful. These protocols not only ensure the recovery of biocontrol agents with multiple modes of action but also enhance the reliability and reproducibility of the process.

Thus, the protocols for **the isolation** of the desired bacteria were focused on the obtention of species belonging to the [redacted] group, since studies have shown that they can be useful to fight against both diseases. In fact, many *Bacillus* species are registered as PPPs against these and other plant diseases (https://www.mapa.gob.es/es/agricultura/temas/sanidad-vegetal/listasustanciasactivasaceptadasexcluidas_tcm30-618972.pdf). Some examples successfully employed are *B. amyliliquefaciens* strain MBI 600 (Serifel®), *B. subtilis* strain QST 713 (Serenade®), *B. subtilis* strain IAB/BS03 (Aviv®), *B. pumilus* strain QST2808 (Sonata® ASO), *B. amyloliquefaciens* AH2 (Botrybel®) and *B. amyloliquefaciens* IT-45 (Cilus Plus®), within others.

Biocontrol agents are typically sourced from the endosphere, phyllosphere or rhizosphere, where they exhibit antagonistic properties against plant pathogens (Valle et al., 2015). Therefore, to focus the search and selection strategy of strains belonging to the [redacted] group and, given that the resulting biological product is intended to be applied to the leaves of the plants, the phyllosphere was chosen as a source of isolates. More specifically, the aim was to isolate bacteria that naturally lived in the diseased leaves so that their optimal habitat for growth and colonization was the same as where the resulting biocontrol product would later be applied.

The phyllosphere harbours a rich diversity of bacteria that interact with plant leaves, influencing plant health, growth, and ecosystem processes. The most prevalent bacteria found in or on plant leaves include a diverse range of species that play crucial roles in plant health and growth. These bacteria colonize the leaf surfaces, forming communities that contribute to various processes important for both global ecosystems and individual plant behaviour (Lindow & Brandl, 2003). Among these bacteria, endophytic bacteria are ubiquitous in plants and can

be isolated from various plant parts, including stems, leaves, roots, fruits, tubers, and nodules (Toubal et al., 2018). Studies have shown that the bacterial communities on plant leaves differ from those on other plant parts like petals, with specific families such as Pseudomonadaceae and Microbacteriaceae being more abundant on leaves (Junker et al., 2011). Furthermore, *Bacillus* species are commonly found colonizing plant surfaces, including the phylloplane (Kim et al., 2012; Sun et al., 2022). Additionally, other bacterial strains were isolated from different varieties of cucurbit seeds, because according to Khalaf and Raizada (2018), some strains of bacterial seed endophytes can antagonize fungal and oomycete pathogens, including downy and powdery mildews.

In this PhD thesis, 491 bacterial strains were isolated from a great variety of locations and type of plant sources, infected or not with downy and powdery mildew. In comparison to other studies, the number of isolated strains was quite large. For example, Zheng et al. (2018) collected a total of 163 bacterial isolates only from different microenvironments of field-grown cucumber plants. Therefore, the diversity of characteristics and the number of species found in this work was higher.

Regarding the **screening of desired strains**, the first steps of this work aimed at identifying *Bacillus*, i.e., Gram-positive bacilli. The cell morphology was easy to determine by optical microscopy, and the Gram characteristics were determined by the KOH test. However, performing the KOH test on *Bacillus* species can yield varying results leading to inconsistencies with traditional Gram staining results (Halebian et al., 1981). It has been found that some strains of *Bacillus*, such as *Bacillus cereus*, may show a positive reaction in the KOH test, indicating Gram-negative characteristics (Carlone et al., 1982). However, this false positive response to the KOH test is useful to directly discard some of them. Additionally, some *Bacillus* species outside the cereus group may not be accurately detected using the KOH test (Cayer et al., 2020). Since some Gram-positive species like [redacted] can produce a viscous substance as their natural grow, this appearance can resemble the DNA release from Gram-negatives bacteria in KOH solution. Therefore, it is important to determine before the KOH test whether the strain already had viscous texture. It is essential to consider the limitations of the KOH test when dealing with *Bacillus* species. Although this technique is not as much accurate as the Gram staining, it is good enough to perform a general first screening when the number of strains is too large.

As a summary of all the screening steps to identify desired bacterial species with high potential for being biocontrol agents against downy and powdery mildew, from the total of 491 isolated bacterial strains, 339 bacilli were obtained, within which only 153 of them were Gram-positive.

Afterwards, the [redacted] gene, an internal portion of the 16S rRNA gene extracted from [redacted], was very useful in this work to rapidly detect strains belonging to the [redacted] group. This gene (595 bp) is part of the core genes of *Bacillus* strains and has been successfully utilized in various studies for genetic diversity analysis and phylogenomics (Wang et al., 2019; Mullins et al., 2020; Liu et al., 2020). Most of the preselected strains analysed showed an amplification of this shared portion of the 16S rRNA gene, meaning that the great majority of *Bacillus* (Gram-positive bacilli) found naturally living on or in plant leaves belong to this group, which is according to the literature. Moreover, the [redacted] region was used mostly to discard pathogenic *Bacillus* species far from the [redacted] group, such as *Bacillus cereus* or *Bacillus thuringensis*. Of the total selected and sequenced *Bacillus* strains (<128), only one—*B. cereus* strain [redacted]—belonged to a potentially pathogenic species.

When referring to the total number of microbes found, the best source of [redacted] group species was the [redacted]. However, when we focus only the detection of the desired species to the preselected KOH- bacilli, the best sources were [redacted] In summary, the majority of [redacted]. Additionally, the best protocol used to isolate them was the [redacted] technique, meaning that more desired species were found [redacted].

At this point, a further taxonomical characterization of the *Bacillus* species was required. Therefore, the 16S rRNA gene of all the finally selected species was sequenced. However, the information from this gene was not enough to clarify the taxonomy at a species level in the case of a few strains due to the low interspecific variability and high similarity of this gene between very close species within the [redacted] group (Zhao et al., 2020). Thus, although the 16S rRNA gene is widely used for bacterial community analyses, it falls short in offering detailed diversity insights beyond the genus level (Fox et al., 1992).

On the other hand, regarding to the yeast-like fungi strains, literature revealed that specific species of basidiomycetes, like [redacted] spp., shown to be promising biocontrol agents against powdery mildew disease, since they can hyperparasite these pathogens. Moreover, other species like [redacted] spp. and [redacted], are today registered in different countries as PPPs. Sporodex®, for example, is a fungal biocontrol product for powdery mildew in greenhouse crops which contains *P. flocculosa* strain PF-A22 as its active substance. It was registered as a biofungicide in Canada in 2002 and in the USA in 2003 (Jarvis et al., 2007). In

contrast, no fungi have been demonstrated to be a very good biocontrol agent against downy mildew. Therefore, yeast-like fungi species were only isolated from powdery mildew pustules.

Fungal isolation protocols for the search of biocontrol agents often begin with the collection of spores or mycelium from environmental samples, as described by Khol et al. (2019). Ballistospore-forming yeasts, like [redacted] spp., occur naturally on powdery mildew infected leaves of numerous plant species (Urquhart et al., 1994) and, in fact, [redacted] spp. have been consistently isolated from plants worldwide infected with powdery mildew (Klecan et al., 1990; Knudsen & Skou, 1993; Urquhart et al., 1994). In contrast, although [redacted] is recognized as one of the most effective fungal biocontrol agents against powdery mildews, only few isolates of this species have been identified worldwide (Avis et al., 2001; Paulitz & Bélanger, 2001).

Therefore, fungal isolates were obtained from powdery mildew pustules on leaves with low disease severity and incubated under moist conditions to facilitate the development of potential antagonists. This selection of powdery mildew pustules as a source aimed to increase the likelihood of identifying powdery mildew-specific antagonists adapted to the ecological niche, as isolating from symptom-free leaf surfaces might lead to most isolates from common phyllosphere inhabitants not antagonistic to powdery mildews, potentially outcompeting powdery mildew antagonists in a pathogen-free environment (Köhl et al., 2019).

Over 230 fungal isolates distinct from powdery mildew fungi were obtained from many leaf samples, indicating the presence of hyphomycetes and yeast species in powdery mildew pustules. Sequence information from ITS region was used for identification, revealing high taxonomic diversity among the isolates. Identification at the species level was crucial for assessing risks and excluding potential pathogens, with preliminary risk assessments conducted based on available literature data (Zinniel et al., 2002).

In Khöl et al (2019), for instance, a total of 1,237 fungal isolates were obtained from over 500 leaves with powdery mildew pustules, from which 850 were tested. Only 3% belonged to species that have been reported in literature as antagonistic to powdery mildews. In contrast, in this PhD thesis a total of 233 fungal candidates were isolated, from which 103 were sequenced and 11% of them resulted to belong to a desired fungal species. It is worth notice that, in the case of the fungi, the molecular screening was much more complicated than in the case of bacteria because of two reasons: the specific yeast-like species we were looking for are not that abundant on leaves in natural habitats as *Bacillus* spp., and because we could not perform a first morphological screening homologous to the KOH- and bacilli determination

previous to the selection by sequencing. Therefore, the percentages of “success” in this case were much lower, being the [redacted] the best plant source for these mentioned species.

These 11 desired species came from [redacted]. Moreover, 8 of them were extracted with the isolation protocol proposed by [redacted], in comparison to only 3 desired isolates extracted according to [redacted], meaning that, at least in this work, the use of [redacted] was more successful to isolate the desired species than the [redacted].

CONCLUSIONS

The principal outcome from this chapter has been the large collection of a total of 724 isolated microbial strains, from which 128 *Bacillus* strains and 11 yeast-like fungi strains were selected as potential candidates for being biocontrol agents.

The specific conclusions extracted were:

1. The majority of [redacted] group species came from [redacted]. Moreover, plants [redacted] were a better source of isolates than plants [redacted]. Additionally, a relatively high number of efficient strains against both diseases was obtained from [redacted].
2. The best protocol used to isolate [redacted] group species was the [redacted] technique, meaning that more desired species were found [redacted].
3. The selection / discard process of bacterial candidates based on the internal portion of the 16S rRNA gene ([redacted]) was successful, as only one strain (*B. cereus* strain [redacted]) out of 128 was found to belong to an undesired *Bacillus* species.
4. The best plant source for these fungal species were diverse [redacted]. Only 1 or 2 strains were found on other type of plant leaves, including [redacted].
5. The best protocol to isolate antagonistic fungal strains for powdery mildew was the method employed by [redacted], with which 8 desired strains were extracted in

comparison to only 3 isolates extracted according to [redacted]. This meant that the use of [redacted] was more successful to isolate the desired species.

6. The morphology profile of the finally selected species was well documented and registered by macroscopical and microscopical analyses in order to be able to easily recognize the desired species.
7. All the finally selected candidate strains were molecularly classified according to the sequencing of high conserved genomic regions, being the 16S rRNA gene for bacterial strains and the ITS1/ITS4 region for the yeast-like fungi strains.

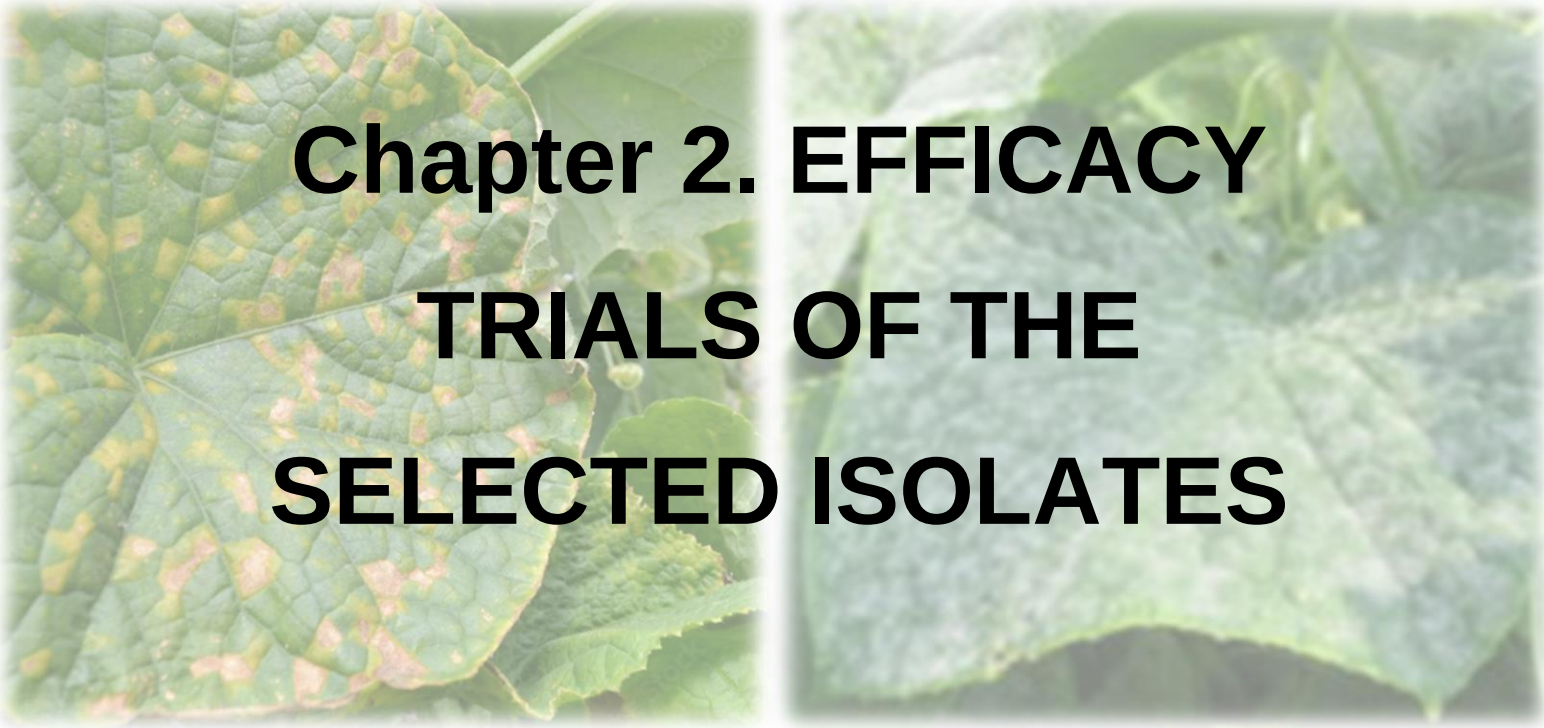

Chapter 2. EFFICACY TRIALS OF THE SELECTED ISOLATES

ABSTRACT

This chapter of the PhD thesis focuses on the efficacy trials of selected isolates against two major fungal diseases affecting cucurbits: downy mildew and powdery mildew. The family Cucurbitaceae, encompassing economically significant crops such as cucumbers, melons, and squashes, suffers extensively from downy mildew, caused by *Pseudoperonospora cubensis*, and powdery mildew, caused by *Podosphaera fusca*. These pathogens are obligate parasites, and both diseases have significant economic impacts on global food production. In this context, the primary objective of this work was to explore the effectiveness of a large collection of isolates, including bacterial and fungal strains, in controlling these diseases in cucumbers, aiming to identify the most promising candidates for development as microbial PPPs.

The trials were conducted under controlled growth chamber conditions to evaluate the efficacy of these isolates against both pathogens. The experiments included both preventive and curative treatments. Key factors like bacterial application dose, pathogen inoculum concentration and environmental conditions were standardized to ensure reliable and reproducible results. From a total of 128 *Bacillus* spp. isolates and 11 yeast-like fungi isolates, 67 different strains were tested against downy mildew, with [redacted] showing significant disease reduction ([redacted]), highlighting strains [redacted]. For powdery mildew, 41 isolates were screened, with [redacted] bacterial strains ([redacted]) and [redacted] fungal strain ([redacted]) demonstrating high efficacy ([redacted]). It was also investigated the role of metabolites produced by the bacterial isolates in the disease reduction of cucurbit downy mildew, where the metabolites of the selected strains [redacted] were particularly effective. In contrast, for strains [redacted], the presence of bacterial cells was crucial for efficacy, indicating a limited effect of their metabolites alone. Moreover, comparisons between bacterial and fungal isolates revealed that bacterial treatments often outperformed fungal treatments in preventive applications, while fungal strains performed better as curative treatments. Finally, the prototype bacterial formulations demonstrated slightly higher efficacy than the bacterial solutions when applied preventively and even exceeded the efficacy achieved with Serenade® Max in curative applications.

The chapter concludes with the identification of 5 promising bacterial strains as biocontrol agents against cucurbit downy and powdery mildew. These agents demonstrated significant disease reduction in controlled conditions, providing a foundation for further development and potential field application as microbial PPPs.

INTRODUCTION

1. Cucurbits and the impact of downy and powdery mildews

The botanical family Cucurbitaceae, commonly referred to as cucurbits, encompasses a variety of cultivated species with significant global or local economic importance. Among these, the cucumber (*Cucumis sativus* L.) stands out as one of the most widely cultivated members of the family (Lv et al., 2012). The main characteristics of *Cucumis sativus* encompass its vining growth habit, lobed leaves, and tendrils that aid in climbing and support. Cucumber plants produce yellow flowers that develop into cylindrical fruits with a waxy green skin, reflecting their rapid growth and prolific fruiting capabilities. Cucumbers are valued for their culinary versatility, nutritional benefits, and commercial importance in global agriculture.

Cucurbits (Cucurbitaceae family) are one of the most seriously affected crops by downy mildew, afflicting plants such as cucumbers, melons, squash and watermelon, in which substantial agricultural losses are inflicted (Lebeda & Cohen, 2010; Naegele et al., 2016). Cucurbit downy mildew is caused by the oomycete *Pseudoperonospora cubensis*. Furthermore, powdery mildew stands out as one of the most prevalent, conspicuous, and easily identifiable diseases affecting cucurbits, playing a crucial role in global food production and agricultural economies, including Spain and leading to substantial yield reductions and economic impacts globally (Pérez-García et al., 2009; Chiniquy et al., 2019; Romero et al., 2007; Bellón-Gómez et al., 2014). Cucurbit powdery mildew is caused by the ascomycete fungi *Podosphaera xanthii* or *Podosphaera fusca*. The nomenclature of the primary causal agent was somewhat inconsistent in the literature (Taylor et al., 2000; Braun et al., 2002; Park et al., 2023). Both pathogens have an obligate parasitic nature, meaning that they have specialized nutrition requirements that makes it difficult to grow in culture in the laboratory. As biotrophic microorganisms, these pathogens feed on living host cells, forming a relationship that helps them evade the host's immune system while still causing disease (Christita et al., 2021; Nguyen et al., 2020).

1. Downy mildew pathogen: *Pseudoperonospora cubensis*

Pseudoperonospora cubensis exhibits a specialized host range within the Cucurbitaceae family, affecting cultivated, semi-cultivated, weedy, and wild genera and species (Palti and Cohen, 1980; Cohen, 1981; Lebeda and Widrlechner, 2003). The pathogen's host specificity varies, with around 60 species and 20 genera identified as hosts, and pathotypes defined to distinguish host preferences (Ojiambo et al., 2015; Lebeda, 1992b). The pathogen constantly expands its host range, posing a significant threat to cucurbit cultivation globally (Rsaliyev et

al., 2018). In interactions with *Cucumis sativus* (cucumber), a susceptible host to *P. cubensis*, minimal variability has been observed due to the genetic uniformity of cucumber and therefore *C. sativus* primarily serves as a susceptible control for differentiating pathotypes and races of *P. cubensis* (Lebeda and Widrlechner, 2003). While some cucumber cultivars with field resistance have been identified, available genotypes lack reliable resistance sources (Lebeda et al., 1991; Lebeda and Widrlechner, 2003).

Life cycle and parasitism mechanisms of *P. cubensis* are showed on Figure 2.1. The asexual reproduction in *P. cubensis* primarily involves the dispersal and germination of asexual spores, such as conidiosporangia and zoosporangia. Sporangia, which are ovoid or elliptic in shape, mature to a light grey to deep-purple coloration (Zitter et al., 1996). These sporangia dislodge easily from sporangiophores and are distributed by wind, water splash or human activity (Polesani et al., 2010). Upon landing on a host plant's leaf surface and under suitable environmental conditions of high humidity and moderate temperatures (sporangia require contact with water, such as rain or dew) the spores germinate and form a germ tube (Polesani et al., 2010). The germination process is indirect, where the multinucleate protoplast differentiates into 5 to 15 biflagellate zoospores, emerging through a papilum (Palti and Cohen, 1980). The zoospores exhibit active swimming towards stomatal apertures, where they settle, shed their flagella, and encyst (Cohen 1981). Subsequently, a germ tube emerges from the cyst, producing an appressorium that leads to the development of a penetration hypha. This hypha breaches the stomatal aperture and enters the substomatal cavity of the leaf tissue (Cohen 1981). Stomatal penetration is the predominant mechanism of *P. cubensis* entry, although direct (epidermal) penetration is observed rarely (Lebeda, 1990). Enzymes secreted by the pathogen assist in breaking down the plant cell wall, allowing the fungus to enter the leaf (Polesani et al., 2010).

Under favourable environmental conditions of high humidity (above 94%), leaf wetness and moderate temperatures around 20 ºC (Haggag, 2002; Ghosh et al., 2015; Zheng et al., 2018), and in a susceptible host, the colonization of the parasite in tissue proceeds relatively quickly, potentially leading to systemic infection and damage to various parts of the plant beyond the initial infection site (Polesani et al., 2010). Sporangiophores emerge from stomata within 5 to 7 days, primarily on the lower side of the leaves where stomata are more frequent (Cohen, 1981). A new infection cycle typically initiates every 7 to 14 days on susceptible hosts, depending on environmental conditions. The disease cycle of *P. cubensis* is polycyclic, emphasizing the continuous nature of its reproductive and infective processes (Kranz, 2003).

Sexual reproduction in *P. cubensis* is a rare occurrence and has not been definitively confirmed in most regions where the pathogen is prevalent. It involves the production of oospores, a

process typical of species within the Peronosporaceae family (Michelmore, 1981). This reproductive phase occurs towards the end of the season when infected tissues undergo necrosis (Bedlan, 1989; Lebeda, 1990). Unambiguous observations of oospores have been reported in countries like Austria (Bedlan, 1989), Israel (Cohen et al. 2004), India (Mahrisi and Siradhana, 1984; Singh and Sokhi, 1989), Iran (Zaker and Ommati, 1991) and China (Zhang et al., 2006). However, attempts to detect oospores in cucurbit plants in regions such as Central Europe and the USA have been largely unsuccessful. Therefore, the survival mechanisms of *P. cubensis* still remains unclear in these regions, particularly by oospores (Lebeda, 1986a; Lebeda and Schwinn, 1994; Lebeda and Urban, 2004a).

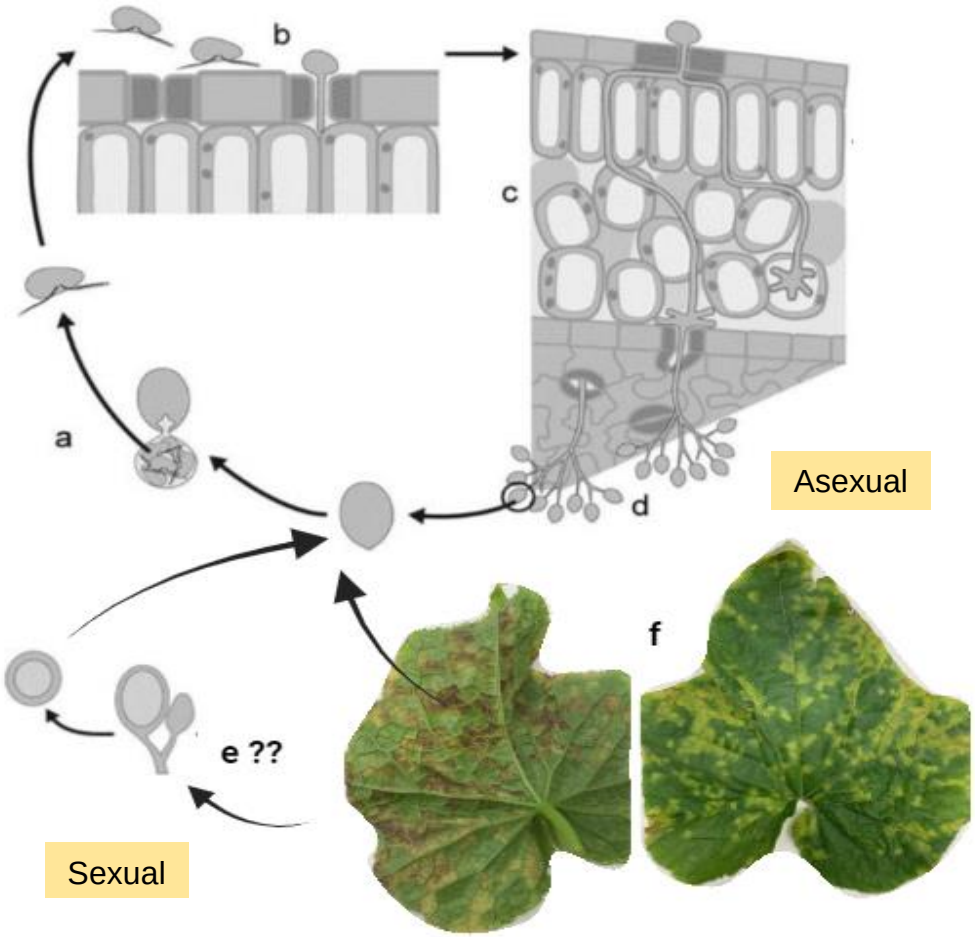

Figure 2.1. The life cycle of *Pseudoperonospora cubensis*: (a) Grey lemon-shaped sporangia, dispersed through the air, land on leaf surfaces and, in the presence of moisture, germinate to release biflagellate zoospores. (b) These zoospores navigate to stomata, where they encyst before penetrating the leaf surface through a germ tube. (c) Hyphae then infiltrate the mesophyll layer, establishing clavate-branched haustoria within plant cells. (d) Then, sporulation occurs, with up to 6 sporangiophores emerging through each stomate, each bearing sporangia at their tips. These sporangia are dislodged by changes in hydrostatic pressure and carried by wind currents to infect new hosts. (e) The function of the sexual stage of *P. cubensis* remains elusive. (f) Symptoms of *P. cubensis* infection. Image extracted and modified from Savory et al. (2011).

The biology of *P. cubensis* manifests through distinctive symptoms of infection, characterized by pale-yellow lesions that may evolve into larger necrotic areas on leaf surfaces, wilting, and the appearance of greyish-white fungal growth on the leaf undersides (Polesani et al., 2010). However, symptoms of infections vary among cucurbit species and even genotypes, influenced by environmental factors such as humidity and temperature (Lebeda, 1990). For example, it causes irregular, localized, yellow lesions in some species like cucumber and luffa, while lesions in cantaloupe and watermelon are circular and irregular (Lebeda and Schwinn, 1994). Genetically resistant cultivars may show minimal symptoms under controlled conditions, producing small water-soaked lesions (Thomas et al., 1987; Zitter, Hopkins & Thomas, 1996). *P. cubensis* targets specifically the leaves of cucurbitaceous plants (Cohen, 1981; Zitter, Hopkins & Thomas, 1996). Although sporangiophores have been observed on stems, leaf petioles, tendrils, and peduncles of heavily infected melons (Palti and Cohen, 1980). Fruit watery spots followed by pathogen sporulation have been recorded on cucumbers (Palti and Cohen, 1980). Infections may occur at all stages of plant development, although symptoms on young leaves are infrequent, with cotyledons being more susceptible (Lebeda, 1990).

2. Powdery mildew pathogen: *Podosphaera fusca*

Podosphaera fusca has been identified as a fungus with a broad host range, infecting various plant species. Research has shown its presence on different hosts across regions (Yeh et al., 2020; Kiss & Vaghefi, 2021). The pathogen has been found in cucurbits, composites, legumes, and other plant families, demonstrating its ability to infect a wide range of hosts (Kiss et al., 2020). Studies have emphasized the significant impact of *P. fusca* as a major limiting factor for cucurbit production globally (Martínez-Cruz et al., 2016; Polonio et al., 2019; Polonio et al., 2021). The pathogen's effect on crop productivity highlights the importance of understanding its host range and specificity (Martínez-Cruz et al., 2022; Polonio et al., 2021).

The life cycle of *P. fusca* (Figure 2.2) involves several key stages that contribute to its reproduction and spread. Like all powdery mildew fungi, *P. fusca* exhibit its biotrophic lifestyle, exclusively invading epidermal cells of their host plants. Thus, it is dependent on living plant cells to complete its asexual life cycle (Polonio et al., 2021). The infection of the host plant typically begins with asexual conidia germinating on the surface of the plant leaf or stem, resulting in a septate mycelium of uninucleate cells. Thus, this monokaryotic mycelium cannot reproduce sexually. Upon landing on the host surface, a conidial spore must attach and penetrate the host cuticle and cell wall. Employing a combination of enzymatic and mechanical mechanisms, the fungus penetrates the host cell wall (Green et al., 2002). Subsequently, the fungus develops a haustorium, which invaginates the host plasma membrane, facilitating

nutrient acquisition while preserving the integrity of the invaded cell (Polonio et al., 2019; Weßling et al., 2012). The process consists of two stages: first, the hyphae secrete enzymes on or into the food source, which break down biological polymers into smaller units, such as monomers. Second, these monomers are then absorbed into the mycelium by facilitated diffusion and active transport. The external mycelium gives rise to short, erect conidiophores, each of which carries a single row of barrel-shaped spores (the affected parts are thus covered by a forest of conidiophores that take on a white powdery appearance). The mature spores break off and are easily dispersed by the wind, leading to the spread of the disease to other parts of the plant and neighbouring plants (Hafez et al., 2018; Zhao et al., 2022).

The asexual reproduction is much more frequent than the sexual reproduction in the normal life cycle of this pathogen. However, in autumn, sexual chasmothecia can be produced, which represent the resting stage (hibernation) of the pathogen. When two compatible monokaryotic mycelia join, a dikaryotic mycelium is formed (fruiting bodies), which produces ascospores. These ascospores remain dormant throughout the winter to germinate in spring. When the asci expand, they break the wall of the chasmothecia, launching the ascospores into the air.

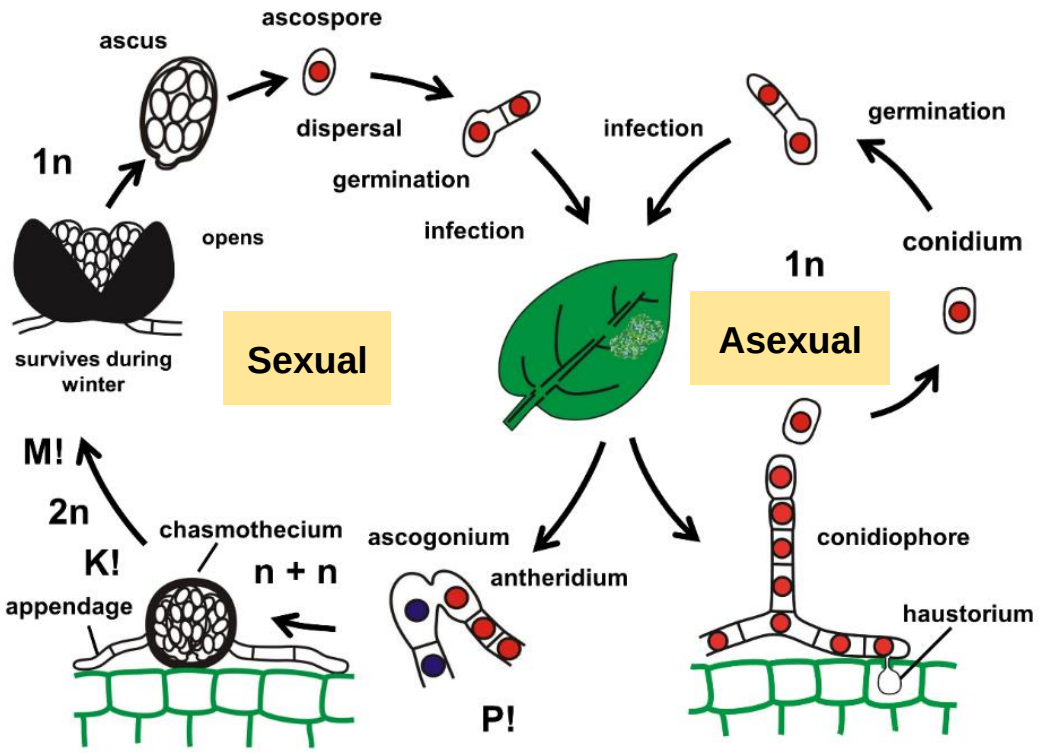

Figure 2.2. Typical life cycle of Erysiphales, Ascomycota. Image extracted from Wikimedia Commons, the free media repository (File:04 03 19 life cycle, Erysiphales, Ascomycota (M. Piepenbring).png).

The development of powdery mildew on plants is influenced by various factors, including environmental conditions -relative high humidity of 65-80% and moderate temperatures, around 25ºC (Romero et al., 2004; Tesfagiorgis & Laing, 2010; Khalaf and Raizada, 2018)-

host susceptibility, and the presence of fungal spores. The disease can progress rapidly under favourable conditions, leading to the formation of characteristic white powdery patches on the plant surface. As the infection advances, the fungus continues to produce conidia, which can be dispersed by wind, water, or other means to initiate new infections on healthy plant tissues (Alavilli et al., 2022).

The main symptoms of cucurbit powdery mildew include the characteristic whitish, talcum-like fungal growth on leaf surfaces, petioles, and stems (Sitterly, 1978; Zitter et al., 1996). This powdery appearance is due to the fungal mycelium and conidia that cover the plant, leading to a dusty or flour-like texture (Zhao et al., 2022). As the disease progresses, the affected plant tissues may become distorted, stunted, or chlorotic, even causing necrosis, and premature leaf drop (García-Gutiérrez et al., 2012). These effects reduce the photosynthetic capacity of the plant and compromise the overall plant's health, growth and development (Romero et al., 2003). Thus, severe infections can lead to reduced fruit quality, yield losses, and overall economic impacts on cucurbit crops (Lebeda et al., 2011).

3. Importance of efficacy assays under controlled conditions

The importance of *in vivo* or *ad planta* analyses in evaluating biocontrol agents, as efficacy in *in vitro* tests may not directly correspond to effectiveness on plants (Drenker et al., 2023). Growth chambers provide a transitional environment between laboratory settings and field conditions, allowing researchers to bridge the gap between controlled experiments and real-world applications (Drenker et al., 2023).

Growth chamber experiments are essential for evaluating the efficacy of biocontrol agents, providing a controlled setting to assess their performance against specific pathogens (Law et al., 2017). In a growth chamber, factors like pathogen inoculum concentration, plant growth stage, and environmental conditions can be standardized, reducing variability and allowing for a more focused evaluation of biocontrol efficacy (Law et al., 2017). Thus, conducting efficacy assays of biocontrol agents against pathogens in growth chambers rather than in open fields offers several advantages. This controlled environment allows for precise monitoring of variables that can influence the efficacy of biocontrol agents, such as temperature, humidity, and light exposure, ensuring more accurate and reproducible results (Godebo et al., 2022). However, research studies highlight that, in some cases, biocontrol agents demonstrate better consistency and greater efficacy against various plant pathogens in controlled growth chamber conditions compared to field trials (Godebo et al., 2022).

The temperature range in a greenhouse for optimal plant growth varies based on the plant varieties, the season, different locations and different studies. Referring to the case concerning to this work, the optimal temperature for growing cucumbers in greenhouses typically ranges between 25°C and 30°C. Studies have indicated that cucumber plants thrive best within this temperature range for optimal growth and development (Ding et al. 2022). Maintaining temperatures within this range provides an ideal environment for cucumber cultivation, ensuring healthy plant growth and maximizing yield potential. In addition to temperature, relative humidity is another crucial factor for successful cucumber growth in greenhouses. It is generally recommended to maintain relative humidity levels between 60% and 80% for cucumbers to thrive in greenhouse conditions. Adequate humidity levels help support plant transpiration, nutrient uptake, and overall plant health. On the other hand, the optimal temperature for the growth of *Bacillus* species, particularly [redacted], is crucial for their survival and productivity. Studies have shown that the optimal growth temperature for *Bacillus* species to be around 30°C (Droffner & Yamamoto, 1985; Leguérinel et al., 2006). These temperatures are considered ideal for the growth and metabolic activities of *Bacillus* species, ensuring their efficient functioning in various applications.

In this context, the environmental conditions established in the growth chambers for the efficacy trials were highly favourable for the progression and survival of the pathogens (85 - 95% RH and 19 - 25ºC), to the detriment of the most optimal conditions for the progression of the *Bacillus* strains (60 – 80% RH and 30 ºC). It is therefore worth mentioning that bacteria could be expected to be even more efficient under real conditions, as their growth would likely be enhanced precisely by these environmental conditions more similar to their optimal growth conditions.

OBJECTIVES

This work aimed to explore the effectiveness of a large collection of different microorganisms and isolates in the control of downy and powdery mildew diseases in cucumber and select the best five candidate strains to further develop one of them as a Plant Protection Product.

Specific objectives of this chapter were:

1. To conduct a large screening of a collection of preselected isolates (both bacteria and fungi) based on their efficacy against downy, as preventive treatments, and powdery mildew, as preventive and curative treatments, in cucurbits in the growth chamber.
2. To validate, at least 3 times, the efficacy results obtained with the strains that were able to significantly reduce the disease severity to stablish a ranking of the most promising

candidates in the two tested pathosystems, and including the best strains selected in the University of Sevilla with the same purposes.

3. To test the effects on the disease severity -in the cucurbit downy mildew pathosystem- of the presumably produced metabolites by the selected bacterial strains, to verify whether the effectiveness of these strains is due to the performance of the bacterial cells themselves or because of the metabolites produced during growing.
4. To compare the efficacies of the isolated strains with the biological reference product Serenade® Max in both pathosystems, either by using it or only its strain *B. subtilis* QST 713, and with preventive and curative applications (in powdery mildew). Moreover, to compare the efficacies of the isolates with the chemical reference product Enervin® Duo against cucurbit downy mildew.
5. To compare the efficacies obtained with the bacteria and the fungi candidates against cucurbit downy mildew, as preventive treatments, and against cucurbit powdery mildew, both preventively and curatively.
6. To test the selected bacteria as prototype formulated products on both pathosystems and as preventive and curative treatments, to have a preliminary idea about the growing times, spores' survival during drying process as well as the conservation (wettable powder).
7. To determine the minimum effective dose of the formulated bacteria to obtain the maximum effectiveness with the minimum amount of powder, to make it easier to produce on a large scale and without the coformulation leaving traces on the leaves.

MATERIALS AND METHODS

Plant material and growth conditions

The seeds of *Cucumis sativus* var. “Marketer” were provided by Semillas Fitó S.A. The plants were grown in a IBERCEX growth chamber (Ibercex-ASL. S.A., Madrid, Spain) during 3 weeks at 25ºC and 65% RH, with 16 h of light (white cool lamps with a mean PAR of 221 µmol m-2 s-1) and 8 h of darkness. The growing substrate was composed of 25% perlite, plus 25% vermiculite and 50% coconut fibber; and the nutrient solution used was the Peters Professional Foliar Feed: 27:15:12 TE. (ICL growing solutions, UK) supplemented with CaCl2 + MgSO4. In the cucurbit downy mildew efficacy trials, 3-weeks old plants were used, while in the cucurbit powdery mildew assays the plants used were 2 weeks old.

1. Efficacy trials on cucurbit plants against downy mildew

The *P. cubensis*, used in the cucumber downy mildew studies, was collected from infected cucumber plants grown in commercial greenhouses of Almería, between 2020 to 2023. In addition, samples of frozen infected leaves from the Agronomy Department, Escuela Técnica Superior de Ingeniería Agronómica (ETSIA), University of Sevilla were also used. The pathogen inoculum was renewed approximately every 3 months. To maintain the pathogen alive, a reservoir of infected plants was maintained in a tunnel (covered with plastic to maintain a RH of 80 - 90%).

The bioassays were performed in a walking chamber maintained at 19 ºC during the day and 16ºC at night and a cycle of 10 h darkness and 14 h of light (led grow lights Heliospectra with an HelioCONNECT program of intensities: 300 for 450 nm; 300 for 660 nm; 70 for 735 nm and 800 for 570 nm). Three plastic tunnels (100 cm long, by 68 cm wide by 64 cm high) were specially prepared to efficiently retain high levels of relative humidity (RH) (80 to 90%), but also let enough light get in, with a mean PAR of 180 µmol m^{-2} s^{-1} inside the tunnels. An average of 16 3-week-old plants were placed in each tunnel so that the leaves of different treatments were not in contact with each other.

Figure 2.3. Assembly of the cucurbit downy mildew bioassay in a culture chamber with controlled conditions of light and temperature. Plastic tunnels and humidifiers were used to increment and control the relative humidity of the assays, which were conducted on *Cucumis sativus* var. Marketer artificially inoculated with the pathogen *Pseudoperonospora cubensis*.

Pathogen inoculation. Sporangia from *P. cubensis* were detached from infected leaves by submerging them in cold sterile water and gently scratching with a brush. The purity of the suspension was checked using an optical microscope and the concentration of sporangia was measured by a Neubauer chamber. The pathogen suspension was finally adjusted to the optimal concentration, which was previously determined to be 1 x 10^4 sporangia/mL to obtain a disease severity in the range between 65 and 85%. Then, it was finally sprayed on the lower surface of the first and second fully developed leaves. After inoculation, the tunnels were kept closed covered with plastic sheets and plants were left in the darkness for 24 h. Humidifiers were used for about 6 h to increase the relative humidity up to 90% inside the tunnels.

Disease evaluation. Disease evaluation was performed at 5 days after pathogen inoculation (dpi), according to literature (Michereff *et al.,* 2009; Neufeld et al., 2017), and following the diagrammatic scale shown in Figure 2.4. The disease severity (or % of disease) per plant was calculated as the average affected leaf area (ALA) between leaves 1 and 2. The percentage of disease reduction (%DR) was calculated as the reduction of disease severity relative to the untreated control plants, i. e., %DR = ((ALA of control plants – ALA of treated plants) / ALA of control plants) x 100.

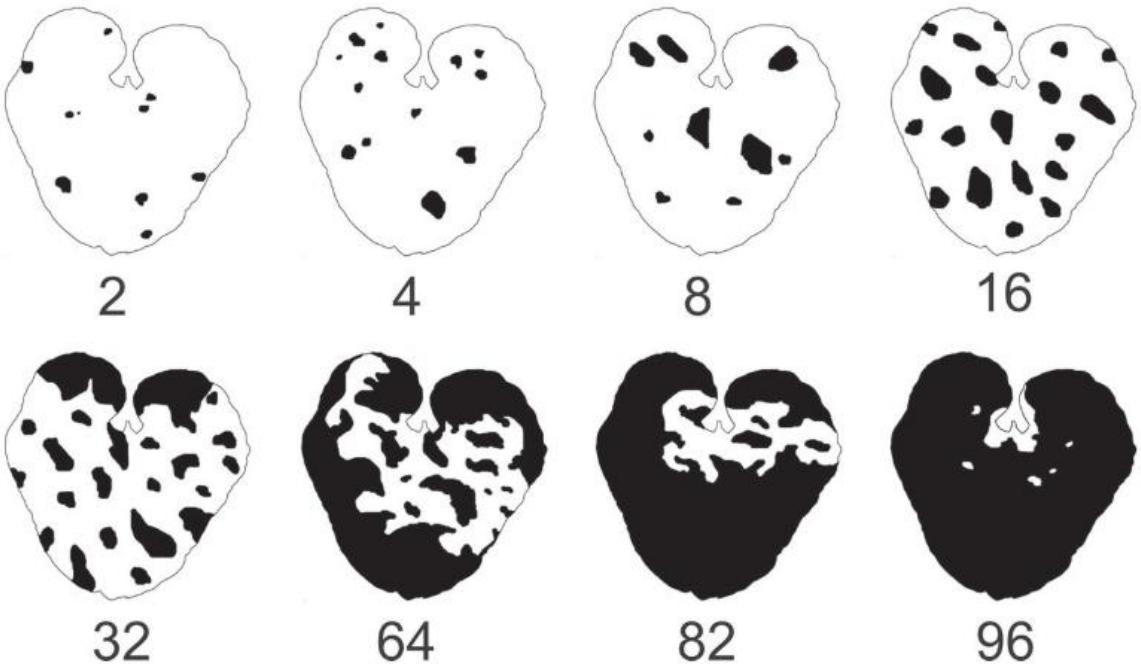

Figure 2.4. Diagrammatic scale of melon downy mildew showing increasing percentages of affected leaf area-severity (Michereff *et al.,* 2009).

2. Efficacy trials on cucurbit plants against powdery mildew

The *P. fusca*, used in the cucumber powdery mildew studies, was collected from infected cucumber plants grown in greenhouses of Almería, between 2020 to 2023.

The bioassays were performed in a CONVIRON E-15 growth chamber with controlled conditions maintained at 25ºC and a cycle of 16 h of light and 8 h darkness per day. Six plastic tunnels (56 cm long, by 40 cm wide by 35 cm high) were specially prepared in order to efficiently retain high levels of relative humidity (RH) (80 to 90%), but also let enough light get in, with a mean PAR of 205 µmol m^{-2} s^{-1} inside the tunnels. An average of 12 2-week-old plants were placed in each tunnel so that the leaves of different treatments did not touch.

To conserve the pathogen alive, a reservoir of infected plants was maintained in two other tunnels. Additionally, *Cucurbita pepo* plants (Zucchini Black Beauty variety) were used to multiply the pathogen as they resulted highly sensitive.

Figure 2.5. Assembly of the cucurbit powdery mildew bioassay in a culture chamber with controlled conditions of light and temperature. Plastic tunnels were used to increment and control the relative humidity of the assays, which were conducted on *Cucumis sativus* var. marketer artificially inoculated with the pathogen *Podosphaera fusca.*

Pathogen inoculation. Conidia from *P. fusca* were detached from infected leaves by submerging them in sterile distilled water and gently scratching with a brush. The purity of the suspension was checked using an optical (stereo) microscope and the concentration of conidia

was measured by a Neubauer chamber. The pathogen solution was finally adjusted to the optimal concentration, which was also previously determined at 1 x 10^4 conidia/mL for a disease severity between 65 and 85%. Then, it was finally sprayed on the top surface of the cotyledons and leaves 1 and 2. After inoculation, plastic tunnels were gently closed to reach high humidity inside.

Disease evaluation. Disease evaluation was performed at 12 dpi, according to literature (Romero et al., 2004; Tesfagiorgis & Laing, 2010) and following an adaptation for cucurbit powdery mildew of the diagrammatic scale from Michereff *et al.* (2009) presented in Figure 2.6. The disease severity (or % of disease) per plant was calculated as the average affected leaf area between leaves 1 and 2. The percentage of disease reduction was calculated as the reduction of disease severity relative to the untreated control plants, explained above.

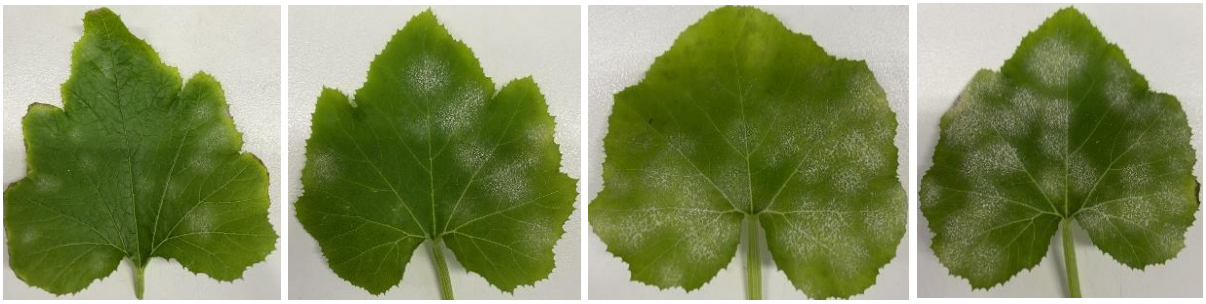

Figure 2.6. Severity scale of the cucurbit powdery mildew *Podosphaera fusca* showing increasing percentages of affected leaf area, corresponding to 16% - 32% - 64% - 82% of severity, respectively from left to right zucchini leaves. This scale was constructed as an adaptation of the diagrammatic scale from Michereff *et al.* (2009) for cucurbit powdery mildew.

3. Preparation of the antagonists for efficacy evaluation

A total of 108 different species of both bacteria and yeast-like fungi were tested in one or both cucurbit pathosystems (downy and powdery mildew) in growth chamber conditions.

Moreover, some of the isolated and pre-selected 128 *Bacillus* strains from the previous chapter were sent to E.T.S. de Ingeniería Agronómica, University of Sevilla, to be tested against the downy mildew of Solanaceae (tomato plants), *Phytophthora infestans*, in tomato plants, and against the strawberry powdery mildew, *Podosphaera aphanis*. After that, the most efficient isolates from the University of Sevilla were later sent back to be tested again in the University of Barcelona against the two pathosystems in cucumber plants, and vice versa. These additional studies could be performed thanks to the granting of the Project *PLEC 2021-007686 convocatòria "Proyectos de I+D+I en líneas estratégicas"*, leaded by Biocontrol Technologies, S.L, and in collaboration with the University of Barcelona and the University of Sevilla.

Bacterial antagonists. The potential antagonists, belonging to the [redacted] group, were defrosted from -80 ºC and plated on Trypticasein Soy Agar (TSA, from Condalab, Spain) Petri dishes. After 24h, a loop of bacteria was inoculated in Luria Bertani (LB) broth (from Condalab, Spain) and the bacterial solutions were incubated at 30 ºC and 150 rpm. Then, bacterial solutions were centrifuged at 4,000 g for 10 min and the pellets were resuspended in the same volume of sterile distilled water. The bacterial solutions were diluted 1/10 and OD_{600} were read to determine the bacterial concentration according to the correlation of OD_{600} and Colony Forming Units per mL (CFU/mL), set up for each one of the strains. Then, concentrations of the inoculum solutions were adjusted to 1 x 10^8 CFU/mL.

Cucumber plants were treated with the selected bacterial strains ([redacted] group) as a foliar spray (FS) with a low pressure hand sprayer as follows: leaves 1 and 2 of each plant were sprayed on the lower surface with about 1 mL (10 sprays of 100 µL) of the bacterial suspension 1 x 10^8 CFU/mL or distilled water (the non-treated control). The biological reference product Serenade® Max (*B. subtilis* (*amyloliquefaciens*), strain QST713, from Bayer) and the chemical reference product Enervin® Duo (active substances: Initium®, Ametoctradin and Dimetomorf, from BASF) were used as positive controls, which were prepared following the fabricant instructions; Serenade® Max was applied at 2.0 g/L and Enervin® Duo was applied at 1.0 mL/L, both as foliar sprays. Also, strain QST 713 was applied as a bacterium (at 1 x 10^8 CFU/mL as explained above) only with research purposes.

Metabolite assays in cucurbit downy mildew. The five bacterial isolates that performed better in terms of disease reduction were subjected to further assays to measure their potential effectiveness of their metabolites against *P. cubensis*. The effect on the disease severity of each treatment was measured and compared with the other treatments of the same strain, and with another strain each time.

Different treatments were prepared for each strain. First, bacterial solutions were prepared and adjusted to 1 x 10^8 CFU/mL according to the OD_{600} measures, as explained previously. The first treatment, which included bacterial cells plus metabolites, was obtained directly from the growth broth of LB and diluted in sterile distilled water as corresponded according to the OD_{600} value. Another treatment was prepared with the metabolite solution alone, by using the resulting supernatant from the centrifuged bacterial solutions. They were collected, passed through a 0.22 µm filters and diluted in sterile distilled water according to the OD_{600} outcome. Finally, a set of plants were inoculated only with LB medium (diluted as corresponded) to discard its effects on the disease reduction.

Fungal antagonists. The potential fungal antagonists were treated as yeasts, and so they were grown in a liquid homemade medium rich in glucose (10 g peptone, 25 g glucose and 1 g Microbiological yeast extract per 1 L of distilled water) for 24 h and at 150 rpm in ambient conditions. The solutions were centrifuged at 4000 g for 10 min and the pellets were resuspended in the same volume of sterile distilled water. A sample of the fungal solutions (1mL) were diluted several times with distilled water for quantification, by using the Neubauer chamber, and adjust the concentration to 1 x 10^7 spores/mL, the optimal concentration according to the literature (Urquhart & Punja, 1997; Nofal & Haggag, 2005; Laur *et al*., 2018).

Experimental design. The different treatments were arranged in a randomized complete block design consisting of 6 plant replicates, divided in different plastic tunnels: in three large tunnels in the case of cucurbit downy mildew and in six short tunnels in the case of cucurbit powdery mildew. Each bacterial treatment was tested at least 3 times in each of the different efficacy trials performed, including screening and efficacies validation as preventive treatments in cucurbit downy mildew and in cucurbit powdery mildew (also as curative treatments in this case), the comparisons with the other strains tested first and selected in the University of Sevilla, the metabolite's effect assays in cucurbit downy mildew, and the comparisons with the fungal strains, as preventive and curative treatments, only in the cucurbit powdery mildew pathosystem.

In the preventive studies, cucumber plants were treated 24 h before the pathogen inoculation with the selected microbial strains (*B. subtilis* group or yeasts). In the curative trials conducted only in the cucumber powdery mildew pathosystem, the isolated strains were applied 5 days after the pathogen inoculation. For each plant, both leaves 1 and 2 were sprayed with about 1 mL (10 sprays of 100 µl) of the bacterial suspension -or the pathogen inoculum-, on the underside of the leaf in the case of downy mildew, and on the upper side of the leaf in the case of powdery mildew. Sterile distilled water was used to set the non-treated control plants.

4. Efficacy trials of the selected bacteria as wettable powder

Bacterial formulation as wettable powder. The media used to produce the maximum number of viable spores in the formulated product was the [redacted] The pH was adjusted to [redacted] with addition of 1 M NaOH. 50 mL of the solution were put in a 250 mL Erlenmeyer and closed with a cellulose plug. After autoclaving them and let cool down to 55ºC, filter-sterilized salt solutions were added: [redacted].

After adding the coformulant, the bacterial solution become very thick in texture and were centrifuged in 50 mL falcon tubes at 9,000 g for 10 min. The supernatant was discarded. The pellets were collected and were spread out in a Petri dish overnight, under the laminar flow cabin, to dry them. The resulting products were put in paper envelopes and allowed to dry at room temperature till constant weight. The water content was measured by drying a 0.1 g sample at 60ºC for 24h. Dilutions were made to quantify the survival of the spores once the process had finished. Finally, the resulting powder was passed through the double electric strainer (MICROCOMPUTER SCREENER FT-91) with an opening diameter of 425 and 75 µm respectively for 15 min. The powder was stored at 4ºC in the fridge for further experiments. The viability of the spores was analysed at least for 40 days.

Efficacy trials with the prototype formulation. Once the wettable powder of the desired strains was obtained, the efficacy trials in both downy and powdery mildew were performed as explained in the respective material and method section. The experiments were conducted analysing 3 different concentrations of wettable powder: [redacted] of powder dissolved in sterile distilled water. The coformulant alone in the same concentrations was used in parallel as controls to measure the effects of the coformulant alone on both studied diseases. The viability and efficacy of the wettable powder was measured for at least 3 months.

5. Statistical Analysis

The data were subjected to statistical analysis using the Statistical Package for the Social Sciences (IBM SPSS Statistics 25; SPSS Inc., Chicago, IL, United States). The mean values among the measurements in each treatment were determined and compared within them and with the reference products (Serenade® MAX and Enervin® Duo) and with the untreated control plants. Statistical analysis of the collected data was performed using ANOVA test (p-value < 0.05) followed by a Tukey's test when significant differences were found.

The Biological Control Index (BCI) was calculated according to Byrne et al. (2005) to evaluate the performance of one strain along different experiments. The BCI was applied to combine the efficacy with the consistency of the disease reduction, according to: BCI = Efficacy/Consistency, where the efficacy is the percentage of the mean disease reduction, and the consistency is the standard deviation of those means.

Finally, the correlation between the disease severity of the untreated control plants with the disease reduction obtained in each different efficacy trial by applying one bacterial strain as a preventive treatment on cucumber plants artificially inoculated with the pathogens was measured by a Simple scatter – Linear Regression of the jamovi software version 1.6.15.0, with a 95% confidential interval.

RESULTS

1. Efficacy trials against cucurbit downy mildew

Screening for the best antagonists. A total of 67 preselected microorganisms, based on their taxonomical group, were evaluated as preventive treatments in the pathosystem of cucurbit downy mildew, i.e., their efficacy in disease reduction was tested against *P. cubensis*. From all the strains tested, [redacted] of them showed disease severities significantly lower than the untreated control plants and therefore were selected for further evaluation. These strains were: [redacted]. The rest of them were discarded. In this pathosystem, the performance of the yeast-like fungi strains was very poor. Results are shown in the following table (Table 2.1).

Table 2.1. Summary of the efficacy results, in terms of % Disease Reduction (% DR), obtained in the screening of the large collection of antagonists tested as preventive treatments against the cucurbit downy mildew pathogen *Pseudoperonospora cubensis.*

Strain	Trial	Affected leaf area (%)		% DR	Strain	Trial	Affected leaf area (%)		% DR
		Contr.	Treated				Contr.	Treated	
[redacted]									

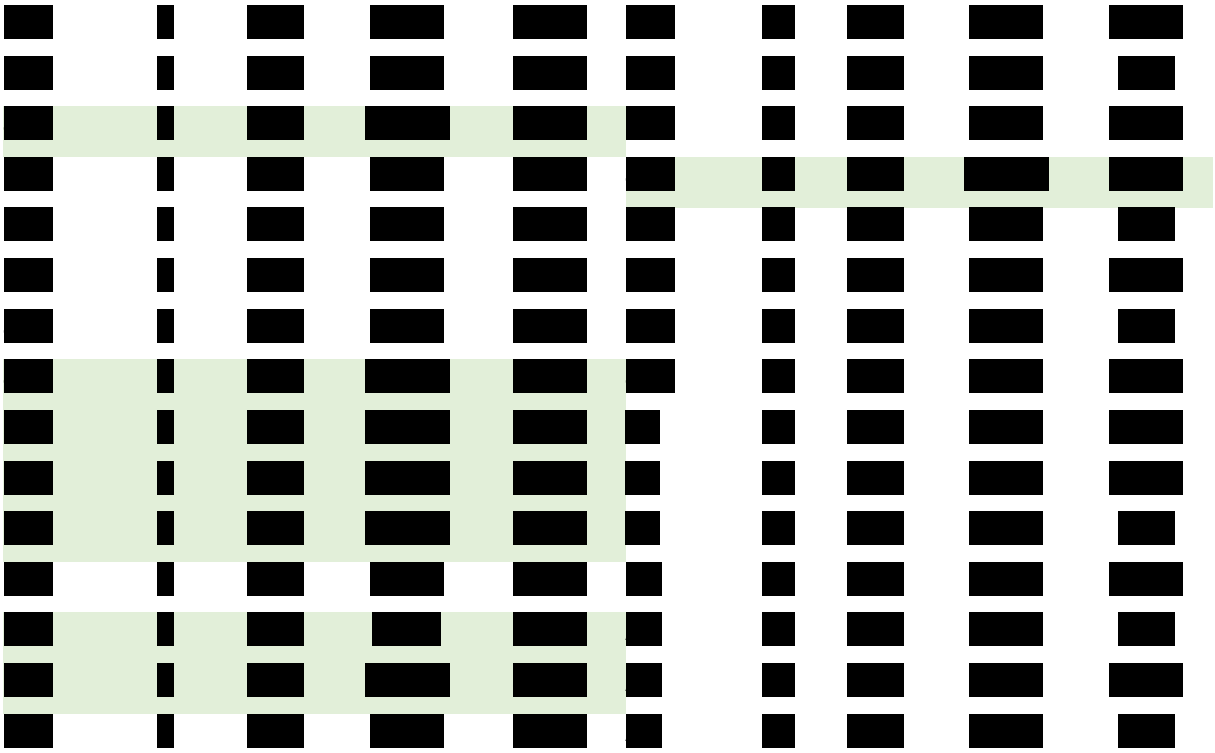

A total of 67 species were tested comprising both bacteria (only numbers) and yeast-like fungi (capital letters plus numbers) previously selected based on their taxonomical group. Bacterial isolates were applied at 1 x 10^8 CFU/mL, while fungal isolates were applied at 1 x 10^7 CFU/mL. The number of the bioassay (trial) and the affected area of the corresponding untreated control plants are also shown (Contr.). The affected leaf area and the efficacies obtain with each strain are represented in percentages. Data was collected at 5 dpi and analysed by averaging the disease per plant, with 6 replicates per treatment. Within each different bioassay, the statistical analysis was performed using AVOVA and Tukey's test (p-value < 0.05), and the data with significant differences compared to the untreated control are market with an asterisk (*). The rows marked in green correspond to the selected strains. The row in yellow mark the performance of the chemical reference product Enervin® Duo (Ch. Std. = Chemical standard*)*, applied at 1.0 mL/L.

In the following images from Figure 2.7, the severity of cucurbit downy mildew of different bacterial treatments (, respectively) applied preventively are shown in comparison with the untreated controls (only inoculated with *P. cubensis*). The bacterial strains were tested in a bioassay, in which the untreated control pants had an average affected leaf area of . The bacterial strains showed disease reductions of , respectively. The bacterial strains were also tested in the same efficacy trial, in which the untreated control plants had an average affected leaf area of . The bacterial treatments showed a disease reduction of respectively.

Figure 2.7. Images of the affected leaf areas of cucumber plants infected with the cucurbit downy mildew pathogen *Pseudoperonospora cubensis* and treated 24h before with a bacterial strain (plant above) and compared to the untreated controls (plant below). **A., B.** & **C.** The affected leaf area of plants treated with the bacterial strains [redacted], showing [redacted] of disease severity, respectively, compared to a control plant with an average affected leaf area of [redacted] **D.** & **E.** Bacterial strains [redacted], showing a disease severity of [redacted] respectively, compared to an untreated control plant (plants below), with an average affected leaf area of [redacted].

Validation assays at different times for the best antagonists against cucurbit downy mildew. The [redacted] most effective strains selected in the initial screening were tested again to have at least three efficacy results in different bioassays. The group of tested strains in each assay was different to compare their real efficacies and reduce the little effects of non-controllable parameters intrinsic to a bioassay, i.e., with living beings. The reference chemical product Enervin® Duo and the biological reference product Serenade® Max were used for comparisons. A summary of the efficacy results obtained in these different assays with the selected strains as preventive treatments against cucurbit downy mildew is presented in the following table (Table 2.2).

In the first validation assay, strains [redacted] were tested again against *P. cubensis*. All the bacterial treatments got a disease severity significantly lower than the untreated control plants, except strain [redacted]. The disease severity ranged from [redacted], which correspond to disease reductions from [redacted]. The disease severity of the untreated control plants was [redacted].

In the second validation assay, strains [redacted] and *B. subtilis* strain QST 713 (from Serenade® Max) used as a bacterium itself were tested again against *P. cubensis*. Only strain [redacted] got an affected leaf area significantly lower from the untreated control plants. The affected leaf areas ranged from [redacted], while the untreated control plants showed a disease severity of [redacted]. These data, in terms of disease reduction, ranged from [redacted], while *B. subtilis* strain QST 713 showed a disease reduction of [redacted], a very similar performance compared with the ones of the strains from our own collection.

In the third validation assay, strains [redacted], and the *B. subtilis* strain QST 713 used as a bacterium itself were tested again against *P. cubensis*. In this case, only strain QST713 got an affected leaf area significantly lower from the untreated control plants, corresponding to a [redacted]. In contrast, the bacterial treatments showed disease severities from [redacted] which were equivalent to disease reductions from [redacted], while *B. subtilis* strain QST 713 obtained [redacted].

After discarding strain [redacted] due to its taxonomical classification (it was a [redacted], see Chapter 1) and also having discarded strain [redacted] for poor efficacy, a final wide experiment was conducted with the [redacted] most effective strains analysed together in order to compare the efficacies of the different strains without any possible variation in the assay conditions due to the intrinsic nature of the bioassay. All the selected bacterial strains ([redacted]) were tested together with the formulated biological reference product Serenade® Max. In this final case, only the formulated product got a disease severity significantly lower than the untreated control plants, which corresponded to a [redacted] of disease reduction. However, strains [redacted] also achieved quite good performance, showing disease severities ranging from of [redacted] which corresponded to disease reductions from [redacted].

Finally, the selected strains were the [redacted], which achieved an average disease severity significantly lower than the untreated control plants, indicating high disease reduction values, i.e., good efficacies.

Table 2.2. Summary of the efficacy results, in terms of % Disease Reduction (% DR), of the final selected [redacted] tested at least 3 times on cucumber plants (*Cucumis sativus*) cv. Marketer artificially inoculated with *Pseudoperonospora cubensis.*

Strain	Validation I & II	Validation III	Final assay	Mean (% DR)
[redacted]				

Data was collected at 5 dpi, and values are means of 6 plants per treatment, including leaves 1 and 2. The asterisks (*) mark statistical significance of the bacterial treatment (at 1 x 10^8 CFU/mL) on the disease severity respectively to the untreated control plants, according to ANOVA and Tukey's tests (p-value < 0.05). Ser.B. = Strain QST 713 (from Serenade® Max) applied as a bacterial treatment (at 1 x 10^8 CFU/mL), and Ser.F. = Serenade® Max formulated (at 2.0 g/L), both marked in grey. The finally selected strains are marked in bold.

Comparison of the most effective agents selected against the downy mildew pathogens *Pseudoperonospora cubensis* (cucumber) and *Phytophtora infestans* (tomato). Among the other strains sent to the University of Sevilla, some were there selected because of their high efficacy in the pathosystem of downy mildew (*P. infestans*) in tomato plants. These new strains were: [redacted]. Referring to the strains previously selected against cucurbit downy mildew, their efficacy was also tested against *P. infestans*. Only the bacterial strains [redacted] achieved good efficacies against this pathogen, so the other strains ([redacted]) were discarded. Four assays were performed to test the strains together and compare between them and with the biological product Serenade® Max on cucumber plants artificially inoculated with *P. cubensis.* The values obtained in each assay are presented in the Table 2.3.

In the first comparison assay (DMa29), although strain [redacted] and the formulated Serenade® Max show efficacies, in terms of disease reduction, around [redacted] in both cases, no significant differences were found between treatments and with the untreated control plants. In the second comparison assay (DMa30). Only the formulated Serenade® Max treatment show a good disease reduction of [redacted]. In these two bioassays, the inoculum of *P. cubensis* was very old and the efficacy results of these trials were not good enough.

For the second assay (DMa31), fresh pathogen samples were collected from greenhouses with cucumber plants naturally infected by *P. cubensis* to proceed with the tests. The bacterial strains tested included strains [redacted], along with the biological product Serenade® Max and the reference chemical product Enervin® Duo for comparison. All treatments showed significant differences compared to the untreated control plants, as well as within treatments. The highest efficacy was observed with Enervin® Duo, as expected, achieving a disease reduction of [redacted] followed closely by strains [redacted], with disease reductions of [redacted] respectively. Strains [redacted] also demonstrated strong efficacy, with disease reductions [redacted]. In this assay, the Serenade® Max formulation showed the lowest efficacy, with a disease reduction of [redacted]. A final comparison trial (DMa32) was conducted, where almost all treatments showed significant differences compared to the untreated control plants, and within treatments. The highest efficacy was achieved with strain [redacted], resulting in a disease reduction of [redacted].

Table 2.3. Summary of the comparison trials about the preventive effects of the best BCAs, in terms of % Disease Reduction (% DR), selected against *Pseudoperonospora cubensis* and *Phytophtora infestans,* on disease severity on cucumber plants (*Cucumis sativus*) cv. Marketer artificially inoculated with *P. cubensis* 24h after antagonist applications.

Strain	*DMa29-30*	*DMa31*	*DMa32*	Mean (% DR)
[redacted]				

Data was collected at 5 dpi, and values are means of 6 plants per treatment, including leaves 1 and 2. The asterisks (*) mark statistical significance of the bacterial treatment (at 1 x 10^8 CFU/mL) on the disease severity respectively to the untreated control plants, according to ANOVA and Tukey's tests (p-

value < 0.05). *DMa* = *Downy Mildew assay*, followed by the corresponding assay number. Ser.B. = Strain QST 713 (from Serenade® Max) applied as a bacterial treatment (at 1 x 10^8 CFU/mL), and Ser.F. = Serenade® Max formulated (at 2.0 g/L), both marked in grey. The selected strains are marked in bold.

Strains [redacted] were selected as the final candidates as biocontrol agents, with an average disease reduction of [redacted], respectively. All the other strains were discarded. Here, it is important to mention that, since efficacy trials in other pathosystems (mentioned above) were conduct in parallel, the mean efficacies against all the tested pathogens were considered to select the 5 best antagonists. Therefore, not all the strains with the higher efficacies in the cucurbit downy mildew correspond to the ones selected at this point. For example, strain [redacted] had a very good performance against *P. cubensis*, but it did not show good efficacy in other pathosystems, so it was discarded in favour of other strains with a broader spectrum of action and more stable efficacies, such as strain [redacted]. The other exception is with strain [redacted], which did not reach a very high average efficacy against *P. cubensis*, but it was a very good antagonist against *P. infestans* in tomato plants, and the average efficacy was very high considering the other pathosystems.

Preventive effects of the metabolites produced by the five best BCAs. The average values from the 3 efficacy trials evaluating the effects of the metabolites produced by the best BCAs on the disease severity of cucurbit downy mildew are presented in Figure 2.8, in terms of % disease reduction.

In the case of strain [redacted], the effects of the treatment with the bacterial cells plus metabolites achieved a disease reduction significantly different from the treatment where only LB medium was applied, corresponding to [redacted] of disease reduction compared to a [redacted]. The treatment of the metabolites alone also showed significant differences, but only achieving a [redacted] of disease reduction. Similar outcomes were obtained when evaluating strains [redacted] of disease reductions were obtained, respectively, in the treatments of bacterial cells with metabolites; [redacted] with the treatments of metabolites alone, and disease reductions of [redacted] when applying the LB medium alone. In contrast, in the cases of strains [redacted], only significant differences respect to the treatment of LB medium alone were obtained with the treatment of bacterial cells together with the metabolites produced during bacterial growth. These average values correspond to disease reductions of [redacted] with the treatments of bacterial cells plus metabolites (respectively for strains [redacted]) compared to [redacted] in the treatment of medium alone. The metabolites alone only achieved disease reductions of [redacted] respectively.

Figure 2.8. Preventive effect of the metabolites produced by the five selected BCAs on disease severity on cucumber plants (*Cucumis sativus*) cv. Marketer artificially inoculated with *Pseudoperonospora cubensis*. Data were collected at 5 dpi. Values correspond to the average disease reductions from 3 different bioassays, each value stablished as the mean ± standard error of 6 plants per treatment. Different letters show significant differences according to Tukey's test ($p < 0.05$). Bact.+Met. = bacterial cells plus metabolites produced. Met. = only the metabolites produced during the growth process. medium = control plants only sprayed with the LB medium.

As a summary of the data obtained in the efficacy trials evaluating the effects of the metabolites on the disease severity, it can be noted that all the strains achieved higher efficacies when the treatment included living cells with metabolites produced during the growth process. The metabolites produced by strains [redacted] were the most effective ones. In the cases of strains [redacted], it was clear that the effects on the reduction of the cucurbit downy mildew disease were because of the bacterial cells themselves, with a very poor performance of the metabolites. Moreover, it should be noted that, although the LB medium had little effects on the disease severity caused by *P. cubensis*, no significant differences were found compared to the untreated control plants.

Summary of the 5 most effective antagonist against downy mildew. All the efficacy data in the cucurbit downy mildew pathosystem were pooled together in order to stablish a ranking between the last selected bacterial strains as the best antagonists against *P. cubensis*. As it is shown in Table 2.4, the most effective strain was the [redacted], with an average disease reduction of [redacted] The next best strain in this pathosystem was strain [redacted]

[redacted] respectively. Finally, strain [redacted] only achieved a [redacted] of disease reduction. However, these data were not the only one considered to select the final candidate as the most promising BCAs, since the efficacy results from the cucurbit powdery mildew, presented in the following experiments, also had considerable weight in the decision-making process (see next section). Also, the efficacy data on the pathosystems studied at the University of Seville (tomato downy mildew and strawberry powdery mildew) were considered. Another very important pillar considered, studied in parallel, was the taxonomic characterization of the strains and their study of Whole Genome Sequencing (WGS), which will be presented in the next chapter.

Table 2.4. Summary of all the efficacy results, in terms of % Disease Reduction (%DR), obtained in the different experiments analysing the preventive effect of the best BCAs on the disease severity on cucumber plants (*Cucumis sativus*) cv. Marketer artificially inoculated with *Pseudoperonospora cubensis* 24 h after antagonists' application.

Strain	Screening	Validations	Comparisons	Mean (% DR)
[redacted]				
[redacted]				
[redacted]				
[redacted]				
[redacted]				
[redacted]				
[redacted]				

The %DR shown in “Validation” and Comparison” assays are the average values obtained from 3 different bioassays. Bacterial solutions were applied at 1 x 10^8 CFU/mL. Ser.B. = Strain QST 713 (fom Serenade® Max) applied as a bacterial treatment (at 1 x 10^8 CFU/mL), and Ser.F. = Serenade® Max formulated (at 2.0 g/L), both marked in grey.

Since the % of disease reductions obtained in each experiment were different with the same bacterial strain, the BCI was applied to combine the efficacy consistency of the disease reduction. As it is shown in Table 2.5, the more stable effects were the ones with strains [redacted], respectively), although all of them showed a similar BCI. When focusing on the standard deviation within the efficacy trials, strain [redacted] seemed to be the most stable one, but less assays were conduct with this strain and the lowest efficacy results were obtained.

Table 2.5. Biological Control Index (BCI) of the 5 best strains obtained as preventive treatments from all the bioassays conducted on cucumber plants (*Cucumis sativus*) cv. Marketer artificially inoculated with *Pseudoperonospora cubensis*.

Strain	Sd	Mean (% DR)	BCI
[redacted]	[redacted]	[redacted]	[redacted]
[redacted]	[redacted]	[redacted]	[redacted]
[redacted]	[redacted]	[redacted]	[redacted]
[redacted]	[redacted]	[redacted]	[redacted]
[redacted]	[redacted]	[redacted]	[redacted]

BCI was calculated as the Efficacy (% of Disease Reduction, %DR) divided by the Consistency (standard deviation, Sd) obtained on the disease severity of all the bioassays conducted.

Moreover, the disease reduction obtained by using the 5 best strains as preventive treatments in the cucurbit downy mildew were correlated with the corresponding % of affected leaf area of the untreated control plants to observe how much disease control was achieved depending on how severe the disease was. As shown in Figure 2.9, when the disease severity of the untreated control plants was high ([redacted]), the disease reductions were significantly lower than when it was in a range that more closely resembles normal field and greenhouse conditions (between [redacted] of disease severity). In this more real range, it is clearly seen that strains [redacted], for example, achieved % disease reductions between [redacted].

Figure 2.9. Correlation between the affected leaf area of control plants, i.e., the percentage of disease severity, obtained in each different efficacy trial, with the % of disease reduction obtained by applying each one of the 5 best bacterial strains as preventive treatments on cucumber plants (*Cucumis sativus*) cv. Marketer artificially inoculated with *Pseudoperonospora cubensis*. [redacted].
Multiple Spline curve lines & Scatter. P-value < 0.001.

Summarizing, it was observed a clear indirect correlation between the increasing affected leaf areas of the untreated control plants with decreasing disease reductions achieved as the preventive actions of the strains. The regression followed a trendline of [redacted].

2. Efficacy trials against cucurbit powdery mildew

Screening for the most effective antagonists. A total of 41 preselected microorganisms, based on their taxonomical group, were evaluated in the pathosystem of cucurbit powdery mildew, i.e., their efficacy in disease reduction was tested against *Podosphaera fusca*.

Only the strains showing a disease severity significantly lower than the untreated control plants from the corresponding bioassay were selected to continue with the following tests, and the rest of them were discarded. These selected bacterial strains were [redacted], as it is shown in Table 2.6. In fact, the best strains coincided with the best strains from the previous screening in the cucurbit downy mildew. No new strains with high efficiency were detected in this screening.

However, in this pathosystem, it is worth mentioning that the yeast-like fungi species were more effective than in the previous one, as all the efficacy results were higher. In fact, strain [redacted] shown significant differences compared to the untreated control plants. Therefore, they were reevaluated in the validation assays.

Table 2.6. Summary of the efficacy results, in terms of % Disease Reduction (% DR), obtained in the screening of the large collection of antagonists tested as preventive treatments against the cucurbit powdery mildew pathogen *Podosphaera fusca.*

Strain	Trial	Affected leaf area (%)		% DR	Strain	Trial	Affected leaf area (%)		% DR
		Contr.	Treated				Contr.	Treated	
[redacted]									

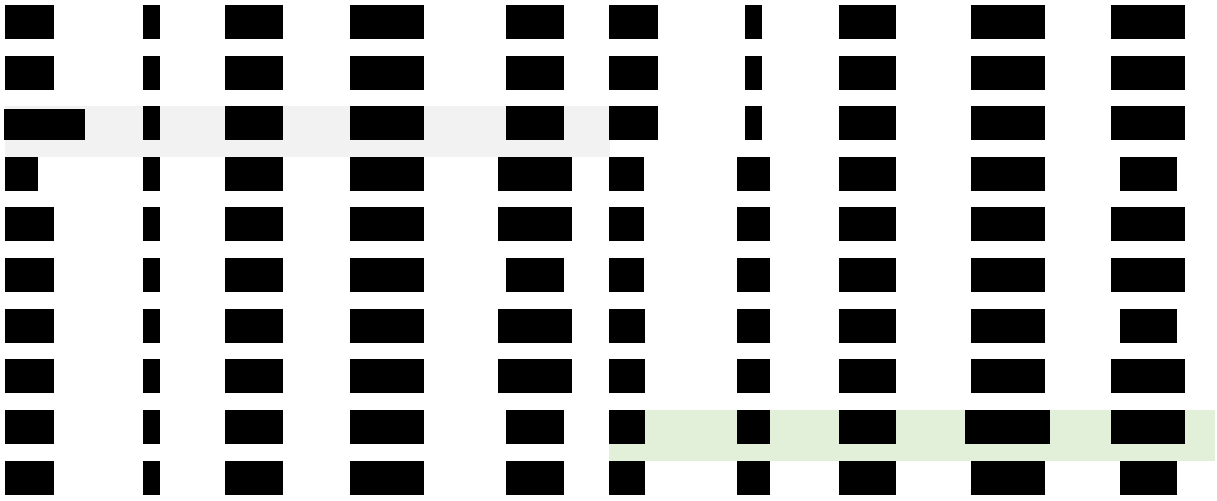

A total of 41 species were tested comprising both bacteria (only numbers) and yeast-like fungi (capital letters plus numbers) previously selected based on their taxonomical group. Bacterial isolates were applied at 1 x 10^8 CFU/mL, while fungal isolates were applied at 1 x 10^7 CFU/mL. The number of the bioassay (trial) the affected leaf area of the corresponding untreated control plants is also shown (Contr.). The affected leaf area and the efficacies obtain with each strain are represented in percentages. Data were collected at 12 dpi and analysed by averaging the disease per plant, with 6 replicates per treatment. The statistical analysis was performed using AVOVA and Tukey's test, and the data with significant differences are market with an asterisk (*). The rows marked in green correspond to the selected strains. The row in grey mark the performance of *B. subtilis* strain QST 713 from the biological reference product Serenade® Max, applied as a bacterium at 1 x 10^8 CFU/mL.

Figure 2.10. Images of the disease severity obtained on *Cucumis sativus* var. "Marketer" plants artificially inoculated with *Podosphaera fusca* 12 days after applying different bacterial strains as preventive treatments. The percentages of affected leaf area (the one above) correspond, approximately, to 8%, 16%, 32% and 64%, from left to right.

Validation assays for the best antagonists against cucurbit powdery mildew. Since the efficacy assays were performed almost in parallel, the 13 most effective strains selected in the cucurbit downy mildew trials were also tested and validated in cucurbit powdery mildew pathosystem. Results are summarized in Table 2.7.

In the first validation assay, strains [redacted] were tested against *P. fusca.* None of the bacterial treatments got an affected leaf area significantly lower than the one obtained in the untreated control plants, due to a high variability in the data collected. However, high disease reductions were obtained, corresponding to [redacted]. In the second validation assay, strains [redacted] were tested together with the biological reference product Serenade® Max against *P. fusca.* Significant differences in terms of disease severity were achieved only in the treatment with strain [redacted] of the untreated control plants, which correspond to a disease reduction of [redacted]). No disease reductions were obtained with the other strains or with the biological reference product, which performed very poorly (only a [redacted] of disease reduction).

In the third validation assay, strains [redacted] were tested against *P. fusca.* Significant differences in terms of % disease severity were only achieved in the treatments with strains [redacted] of affected leaf area, respectively, compared to a [redacted] in the untreated control plants. In terms of disease reduction, the treatments with strains [redacted] almost achieved significant differences in the % of affected leaf area, which were [redacted]. These values correspond to a disease reduction of [redacted].

In the final validation assay, strains [redacted], and the biological reference product Serenade® Max were tested against *P. fusca.* None of the bacterial treatments got a disease severity significantly lower than the untreated control plants, due to a high variability in the data collected. However, high disease reductions were obtained with [redacted].
The treatment with Serenade® Max did not show any disease reduction at all.

Table 2.7. Summary of the efficacy results, in terms of % Disease Reduction (% DR), of the final selected 13 strains tested on cucumber plants (*Cucumis sativus*) cv. Marketer artificially inoculated with *Podosphaera fusca* 24h after antagonist applications.

Strain	Validation I	Validation II	Validation III	Validation IV	Mean (% DR)
[redacted]					

Data was collected at 12 dpi, and values are means of 6 plants per treatment, including leaves 1 and 2. The asterisks (*) mark statistical significance of the bacterial treatment (at 1 x 10^8 CFU/mL) on the disease severity respectively to the untreated control plants, according to ANOVA and Tukey's tests (p-value < 0.05). Ser.F. = Serenade® Max formulated (at 2.0 g/L), marked in grey. The finally selected strains are marked in bold.

Comparison between the most effective bacterial and fungal BCAs. The most effective bacterial strains against cucurbit powdery mildew (and against downy mildew) were tested both as preventive (24 h before pathogen inoculation) and curative (5 days post pathogen inoculation) treatments and compared with the most effective yeast-like fungi strains which, according to literature, may be good antagonists as curative biocontrol agents against powdery mildews. All the efficacy results obtained both as preventive and as curative treatments of the bacterial and fungal strains tested and compared are shown in the next table (Table 2.8).

Comparison of the strains as **preventive treatments.** In the first efficacy assay, bacterial strains [redacted] were compared with yeast-like fungi strains [redacted]. No significant differences were observed between the treatments and the untreated control plants [redacted]. Notably, the fungal strain [redacted] achieved a substantial disease reduction of [redacted], while the best-performing bacterial strain, [redacted] reduction. Among the bacterial strains, strain [redacted] showed higher preventive effects than most fungal strains, with strain [redacted] exhibiting no disease reduction (Table 8).

In the second efficacy assay, bacterial strains [redacted] were tested alongside yeast-like fungi strains [redacted], and compared with the biological reference product Serenade® Max. No significant differences were observed between the fungal treatments and the untreated control plants ([redacted] disease severity). However, strains [redacted] showed disease reductions of [redacted] respectively. All bacterial treatments demonstrated significant reductions in affected leaf area compared to the untreated control plants: [redacted], with this last one being the most effective treatment. It is important to note that Serenade® Max was a formulated product, while the bacterial treatments utilized fresh cells (Table 8).

In the third assay, the preventive effects of bacterial strains [redacted] were compared with yeast-like fungi strains [redacted]. Significant differences were only observed with strain [redacted] affected leaf area) compared to the untreated control plants ([redacted] disease severity), corresponding to a disease reduction of [redacted]. Generally, the bacterial strains exhibited higher preventive effects than the fungal strains. In the final assay, the preventive effects of bacterial strains [redacted] were compared with yeast-like fungi strains [redacted]. No significant differences were observed between the treatments and the untreated control plants. Nonetheless, the fungal strain [redacted] again demonstrated the highest preventive effect, with a disease reduction of [redacted] (Table 8).

Comparison of the strains as **curative treatments.** In the first curative assay, bacterial strains [redacted] were compared with yeast-like fungi strains [redacted]. No significant differences were observed between the treatments and the untreated control plants. The fungal strain [redacted] was the most effective, with a disease reduction [redacted] followed by strains [redacted]. In the second assay, only fungal strains were tested, including [redacted] showed significantly lower affected leaf areas [redacted], respectively) compared to the untreated control plants ([redacted]), corresponding to disease reductions of [redacted]. Strains [redacted] also achieved high disease reductions of [redacted] respectively, leading to the discard of strain [redacted] (Table 8).

In the third assay, bacterial strains [redacted] were tested alongside yeast-like fungi strains [redacted], and the biological reference product Serenade® Max. Only fungal strain [redacted] and bacterial strains [redacted] showed significantly reduced affected leaf areas compared to the untreated control plants ([redacted]). Disease reductions for these strains were [redacted]. Serenade® Max achieved a disease reduction of [redacted] and strain [redacted] was discarded. Finally, in the last curative assay, bacterial strains [redacted] were compared with yeast-like fungi strains [redacted]

[redacted]. No significant differences were found between the disease severities of the treatments and the untreated control plants ([redacted] affected leaf area). Despite the lack of significant differences, notable disease reductions were observed: [redacted] (Table 8).

Table 2.8. Summary of the effects (in terms of % of Disease Reduction) obtained with the bacterial and fungal strains on the disease severity of cucumber plants (Cucumis *sativus*) cv. Marketer artificially inoculated with *Podosphaera fusca,* when applied as preventive treatment (24h before pathogen inoculation) and as curative treatments (5 days post pathogen inoculation).

Strain	Preventive treatments			Mean (%)	Curative treatments			Mean (%)
[redacted]								

Data was collected at 12 dpi, and values are means of 6 plants per treatment, including leaves 1 and 2. The asterisks (*) mark statistical significance of the bacterial treatments (at 1 x 10^8 CFU/mL) or the fungal treatments (at 1 x 10^7 CFU/mL) on the disease severity respectively to the untreated control plants, according to ANOVA and Tukey's tests (p-value < 0.05). Ser.F. = Serenade® Max formulated (at 2.0 g/L), marked in grey. Fungal strains are named with a letter and a number, while bacterial strains only consist of a number. The finally selected strains are marked in bold.

In general terms, the bacterial strains showed higher effects on disease severity when applied as preventive treatments, while the fungal strains performed better as antagonists against *P. fusca* when applied as curative treatments. Finally, only the bacterial strains [redacted] were selected to proceed with the following experiments, since the mean efficacies from both tests as preventive and curative treatments were the highest. Referring to the fungal isolates, strains [redacted] were selected and conserved for future experiments considering their use as curative treatments against powdery mildew.

Summary of the 5 most effective antagonists as preventive treatments. The summary of the efficacies of the 5 best antagonists, only as preventive treatments, are presented below in Table 2.9, including the efficacy validation assays (from Table 2.7) and the comparison assays with the yeast-like fungi strains (from Table 2.8). Once discarded strain [redacted] (see Discussion),

the most effective strain was the [redacted], with a mean preventive efficacy against the cucurbit powdery mildew *P. fusca* of [redacted]. The other selected strains, the [redacted] obtained a mean efficacy of [redacted]. Thus, the other three strains were finally discarded, but well stored.

Table 2.9. Summary of the efficacies, in terms of % of Disease Reduction (% DR) of the 5 best biocontrol agents as preventive treatments against the cucurbit powdery mildew (CMP) *Podosphaera fusca* on cucumber plants (*Cucumis sativus*) cv. Marketer.

Strain	CPM1	CMP2	CMP3	CMP4	CMP5	Mean (% DR)
[redacted]						
[redacted]						
[redacted]						
[redacted]						
[redacted]						
[redacted]						

Data was collected at 12 dpi, and values are means of 6 plants per treatment, including leaves 1 and 2. The asterisks (*) mark statistical significance of the bacterial treatment (at 1 x 10^8 CFU/mL) on the disease severity respectively to the untreated control plants, according to ANOVA and Tukey's tests (p-value < 0.05). CMP = Cucurbit powdery mildew, followed by the number of the assay. Ser.F. = Serenade® Max formulated (at 2.0 g/L), marked in grey.

Since the % of disease reductions obtained in each experiment were different with the same bacterial strain, the BCI was applied to combine the efficacy consistency of the disease reduction. As it is shown in Table 2.10, the more stable effects of the strains were the ones with [redacted]. When focusing on the standard deviation within the efficacy trials, the most variable strain was the [redacted]. These results coincided quite closely with those obtained in the pathosystem of cucurbit downy mildew.

Table 2.10. Biological Control Index (BCI) of the 5 best strains obtained as preventive treatments from all the bioassays conducted on cucumber plants (*Cucumis sativus*) cv. Marketer artificially inoculated with *Podosphaera fusca.*

Strain	Sd	Mean (% DR)	BCI
[redacted]			
[redacted]			
[redacted]			
[redacted]			
[redacted]			

BCI was calculated as the Efficacy (% of Disease Reduction, %DR) divided by the Consistency (standard deviation, Sd) obtained on the disease severity of all the bioassays conducted.

The % of disease reduction obtained by using the 5 best strains as preventive treatments in the cucurbit powdery mildew were correlated with the corresponding % of affected leaf area of the untreated control plants in order to observe how much disease control was achieved depending on how severe the disease was. As it is shown in Figure 2.11, strain [redacted] was the one with more stable effects on disease control independently from the severity of the disease: in the disease severity range between [redacted], all the disease reductions achieved were between [redacted]. In contrast, the effects on the disease reduction of strains [redacted] were more variable along different disease severities. As it was shown previously, the disease reductions achieved with strains [redacted] were stable, but the lowest ones.

Figure 2.11. Correlation between the affected leaf area of control plants, i.e., the percentage of disease severity, obtained in each different efficacy trial, with the % of disease reduction obtained by applying each one of the 5 best bacterial strains as preventive treatments on cucumber plants (*Cucumis sativus*) cv. Marketer artificially inoculated with *Podosphaera fusca*. [redacted] Multiple Spline curve lines & Scatter. P-value = 0.004.

It can be observed that there was a little direct correlation between the increasing % of affected leaf areas of the untreated control plants with the % of disease reductions achieved as the preventive actions of the strains. The regression followed a trendline of [redacted].

3. Efficacy trials of the selected bacteria as wettable powder

Viability of the formulated products along the time. The [redacted] and the [redacted] were formulated four different times as wettable powder and the viability of the resulting powders was measured along 40 days. Similar viable spore concentrations were

obtained in the different formulations, with no significant differences observed between the formulated bacterial products. During the studied period, the survival of the spores in the wettable powder did not vary significantly. In the next table (Table 2.11), the average number of colonies forming units counted on TSA Petri dishes of the four formulated powdery of each strain are shown. In general terms, the concentration of viable spores obtained in the powder with strain [redacted] were slightly higher than the ones with strain [redacted]. However, for practical purposes the concentrations obtained are almost equal. A drop in the spore viability was observed at day 40 in both cases but, as mentioned above, it was not much important in this case, and it was being improved in parallel experiments.

Table 2.11. Spore survival (in CFU/g) of the bacterial formulations of the [redacted] and [redacted] for a period of 40 days.

Strain	***Day 0***	***Day 7***	***Day 14***	***Day 40***
[redacted]	[redacted]	[redacted]	[redacted]	[redacted]
[redacted]	[redacted]	[redacted]	[redacted]	[redacted]
[redacted]	[redacted]	[redacted]	[redacted]	[redacted]
[redacted]	[redacted]	[redacted]	[redacted]	[redacted]

The given values represent the average spore survival of the four formulated products of the bacterial strains [redacted], at different times during a period of 40 days, in which they were stored at 4 ºC in the fridge.

The 3rd and 4th prototypes of formulated bacteria ([redacted]) were used in the efficacy trials on cucumber plants, where the following doses of the formulated powders dissolved in water equal to the given number of bacterial spores per mL, approximately. Considering that only 1 mL of the bacterial formulation was applied on each cucumber leaf, in the following table (Table 2.12) an approximation of the number of spores per leaf (or spores/mL) is shown.

Table 2.12. Equivalence of the number of spores applied as foliar sprays of the 3rd and 4th formulated products of the bacterial strains [redacted] with the three different doses analysed in the cucurbit downy and powdery mildew pathosystems.

Dose applied	**Strain** [redacted] (spores/mL)	**Strain** [redacted] (spores/mL)
[redacted]	[redacted]	[redacted]
[redacted]	[redacted]	[redacted]
[redacted]	[redacted]	[redacted]

Values correspond to the average number of spores in the powder approximately at 40 days since it was produced (stored at 4 ºC), when the concentration of the formulations was more stable.

Efficacy of the formulated bacteria against downy and powdery mildews. In all the efficacy trials on cucurbit plants in which the formulated bacteria were evaluated, similar outcomes were obtained. Results are shown in Table 2.13. The disease severities obtained in the three efficacy trials of each pathosystem (cucurbit downy or powdery mildews) and mode of application of the formulations (i.e., either preventive or curative treatments) were significantly lower than the untreated control plants and the plants treated only with the coformulant. Remarkably, no differences were found within the three doses for the same formulated bacterial strain, neither between the two formulated bacteria. However, it is worth notice that strain [redacted] performed better than strain [redacted] in the cucurbit downy mildew pathosystem as a preventive treatment and, in contrast, strains [redacted] performed better than strain [redacted] in the cucurbit powdery mildew pathosystem in all the efficacy trials, both as a preventive treatment and as a curative treatment.

Table 2.13. Summary of the preventive and curative effects on disease severity of the formulated strains [redacted] on cucumber plants (*Cucumis sativus*) cv. Marketer artificially inoculated with cucurbit downy mildew (CDM) *Pseudoperonospora cubensis* or with cucurbit powdery mildew (CPM) *Podosphaera fusca*.

Strain	CDM-Preventive	CPM-Preventive	CPM-Curative
[redacted]	[redacted]	[redacted]	[redacted]
[redacted]	[redacted]	[redacted]	[redacted]
[redacted]	[redacted]	[redacted]	[redacted]
[redacted]	[redacted]	[redacted]	[redacted]
[redacted]	[redacted]	[redacted]	[redacted]
[redacted]	[redacted]	[redacted]	[redacted]

The values shown represent the average disease reduction (%DR) obtained in three different efficacy trials of each pathosystem and mode of application of the formulations (i.e., either preventive or curative treatments).

DISCUSSION

The principal outcome of this PhD thesis was that, in general terms, when a strain was efficient against one disease, it was also efficient against the other one. However, it is worth notice that, according to the initial idea of testing the microbial strains only against the same disease from which they were isolated, such as in Köhl et al. (2019), was partially fulfilled with some strains. For instance, strain [redacted] was isolated [redacted] and turned out to be more effective in combating this disease than in combating [redacted]. Overall, isolating microbial strains from infected tissues for biocontrol is effective, as these microbes can inhibit pathogens and support plant health (Maldonado-González et al., 2015; O'Brien, 2017; Araujo et al., 2020).

Chapter 2. EFFICACY TRIALS OF THE SELECTED ISOLATES

Considering the information from the Chapter 1 and after performing the efficacy trials against the two studied pathosystems, some conclusions about the best disease and plant sources for the isolation of potential efficient antagonists were extracted. Most of the best selected strains in this work came from [redacted], as presented in the previous chapter. In contrast, although almost the half of bacterial isolates ([redacted]) were obtained from [redacted], only [redacted] efficient strains were obtained from this disease: strain [redacted].

Additionally, the [redacted] were remarkably considered as promising antagonists because, according to Khalaf and Raizada (2018), one strain can be efficient against both diseases at the same time. Unlike [redacted] residing in other plant organs, [redacted] have the unique ability to [redacted] and play a crucial role in establishing the [redacted] (Johnston-Monje and Raizada, 2011; Truyens et al., 2015; Huang et al., 2016; Johnston-Monje et al., 2016; Mitter et al., 2016). In fact, a relatively high number of efficient strains was obtained from [redacted] considering that only [redacted] strains were isolated from this source, coinciding with Khalaf and Raizada (2018). [redacted]

Therefore, our results are like those in previous research, where a significant proportion of [redacted] exhibit antagonistic activity against plant pathogens, underscoring their potential in biocontrol strategies (Berg, 2009; Khalaf and Raizada, 2018). Indeed, studies have demonstrated that [redacted] express traits beneficial for plant growth, such as nutrient acquisition and phytohormone biosynthesis (Khalaf and Raizada, 2016), and antipathogenic characteristics (Glawe, 2008; Khalaf and Raizada, 2018; Nelson, 2017).

Cucumis sativus (cucumber) was chosen for efficacy experiments due to its economic importance, adaptability, and widespread greenhouse cultivation, which makes it vulnerable to fungal pathogens (Pessarakli, 2016; Sebastian et al., 2010; Paris, 2016b; Pető et al., 2016; Kates et al., 2017). The efficacy trials on cucurbit downy mildew and cucurbit powdery mildew revealed significant insights into the performance of various *Bacillus* strains and their formulations. Our results underscore the differential efficacy of these strains, which varied across pathosystems and treatment conditions.

In the **cucurbit downy mildew pathosystem**, [redacted] different species were evaluated against the cucurbit downy mildew (*Pseudoperonospora cubensis*), [redacted] of the total species

tested) showed efficacies above [redacted] in the first trial, in terms of disease reduction. However, the great majority of species tested ([redacted] of the total) did not achieve the [redacted] of disease reduction. [redacted] of the total) achieved efficacies between [redacted], and finally a group of [redacted] of the total) showed efficacies comprised between [redacted] Most microorganisms from this last group managed to significantly reduce the disease severity and, in general, these most effective strains as antagonists -including strains [redacted], turned out to be the same ones in the two pathosystems where they were tested.

The performance of the yeast-like fungi strains against cucurbit downy mildew, as preventive treatments, was very poor. However, these results were expected since, according to literature, these species may be efficient in reducing the disease severity in superficial leaf diseases like powdery mildew and as curative treatments, but not under these conditions in which oomycetes colonize the inside of the leaves.

On the other hand, considering the comparisons of the isolates tested and selected at the University of Barcelona and those tested and selected at the University of Sevilla, it is worth noting that, in most cases, when a particular strain was effective in reducing disease severity in one pathosystem, it was also effective in the other pathosystems. In this regard, two new effective strains against the downy mildew of Solanaceae (*P. infestans*) and the strawberry powdery mildew (*P. aphanis*) were selected from the University of Sevilla: [redacted]. Both strains achieved high disease reductions in cucurbit downy and powdery mildew when tested at the University of Barcelona. Conversely, the strains that were effective and selected from the cucurbit pathosystems were then tested at the University of Sevilla, where they also showed high disease reduction against *P. infestans* and *P. aphanis*. These most effective strains were the [redacted].

As a summary, the [redacted] emerged as the most effective in reducing cucurbit downy mildew. The next most effective strain was [redacted]. This is in line with recent studies that have highlighted the potential of *Bacillus* strains, mostly [redacted], in biocontrol (Chowdhury et al., 2015; Rabbee et al., 2019). Here, it is worth notice that strain QST 713 (from Serenade® Max) showed lower efficacy than the selected strains in this work. In contrast, when applied as the commercialised formulated product, almost the highest disease reduction was observed. Thus, it must be considered that, when comparing the percentages of disease reduction of the bacteria alone with formulated products, it is expected to have quite large differences in the results obtained, given that the commercialized products may carry metabolites and other compounds that would help in the control the disease.

Referring to the **metabolite effects on disease reduction**, the trials demonstrated that the presence of both bacterial cells and their metabolites improved their efficacy, particularly for strains [redacted]. The effects of the treatments including the bacterial cells plus metabolites and also the treatments with the metabolites alone achieved higher disease reductions compared to the treatment where only LB medium was applied. This aligns with previous research suggesting that bacterial metabolites can significantly enhance disease suppression (Ongena and Jacques, 2008).

In contrast, in the cases of strains [redacted], only significant differences respect to the treatment of LB medium alone were obtained with the treatment of bacterial cells together with the metabolites produced during bacterial growth. These results indicated that their efficacies appeared to be primarily due to the bacterial cells themselves, with metabolites showing minimal effect. This could be due to specific traits of strains, such as the production of antimicrobial peptides, which require direct bacterial presence for optimal activity (Koumoutsi et al., 2004). Overall, these findings suggest that the strain-specific production of secondary metabolites plays a crucial role in their biocontrol efficacy (Rabbee et al., 2019).

Our results also indicated that under high disease severities ([redacted]), the efficacy of the strains decreased. This indirect correlation between increasing disease severity and decreasing control efficacy highlights the challenges in managing severe infections. Strains [redacted], for instance, demonstrated better performance under moderate disease severity ([redacted]), achieving reductions between [redacted]. This suggests their potential suitability for real-field conditions where disease severity is generally moderate. In fact, research supports that controlling diseases at moderate severities is more effective than at very high severities because biocontrol agents are more successful in managing diseases when applied preventatively or at early stages (Compant et al., 2005; Thambugala et al., 2020).

On the other hand, in the **cucurbit powdery mildew pathosystem**, the principal outcome extracted from this work was that the bacterial strains exhibited higher efficacy when applied preventively than the fungal strains, whereas curative applications were less effective. This is consistent with findings by Han et al. (2015), which demonstrated the preventive superiority of *Bacillus*-based treatments against powdery mildew. In this pathosystem, [redacted] different species were evaluated, within which only [redacted] bacterial strains ([redacted] of the total) obtained efficacies [redacted] Most strains ([redacted] of the total) didn't achieved efficacies up [redacted]) achieved efficacies between [redacted] and finally a group of [redacted] of the total) showed efficacies comprised between [redacted], also in terms of disease reduction.

Considering the final two selected strains, [redacted] showed the highest overall efficacy as a preventive treatment, surpassing [redacted]. In contrast, when applied as curative treatments strain [redacted] was slightly better than strain [redacted]. Moreover, stability in disease control was a notable attribute of strains [redacted], which maintained consistent disease reductions (between [redacted]) across varying disease severities, from [redacted], suggesting robustness in diverse conditions.

Here, it should be mentioned that, although strain [redacted] achieved the best efficacy results when applied as a preventive treatment, it did not work well curatively. Additionally, WGS studies indicated potential regulatory challenges under EFSA guidelines for PPP registration, limiting its practical application despite its preventive efficacy (see next chapter). Also, it belongs to [redacted], which is a *Bacillus* species more far from the desired [redacted] group than other strains. For all these reasons, this strain was discarded. Additionally, it is also worth notice that the yeast-like fungal isolates [redacted] showed the highest efficacies as curative treatments, although they had a poor performance as preventive treatments in this disease.

Referring to the **formulated strains and dose-response studies**, when comparing the formulated strains [redacted] and [redacted] across both pathosystems, strain [redacted] was more effective against cucurbit downy mildew, particularly as a preventive treatment. Conversely, strain [redacted] showed superior efficacy against cucurbit powdery mildew in both preventive and curative applications. These results coincided with the ones obtained when testing these bacterial strains just as bacterial solutions. Moreover, the dose-response analysis indicated that the efficacy did not vary significantly across different concentrations ([redacted]). This suggests that a lower dose could be sufficient for effective disease control, providing a cost-effective solution for growers. Moreover, this stability in performance, especially for strain [redacted], highlights its potential for broader application with minimal dose adjustments.

Therefore, since no significant differences were found between the efficacy of the formulation doses applied on the cucumber leaves, an average concentration of [redacted] spores/mL with the formulated strain [redacted] and [redacted] spores/mL with the formulated strain [redacted] can be considered and compared with the stable concentration of [redacted] cells/mL for both strains when applied as bacterial solutions. In these conditions, the efficacies obtained as preventive treatments in the cucurbit downy and powdery mildews were slightly higher when the formulations were applied. In contrast, when used as curative treatments against powdery mildew, only in the case of strain [redacted], the performance of the bacterial solution was better than

the formulated bacteria ([redacted] of disease reduction). However, the differences observed within the efficacies were not significant in any case.

Additionally, it must be considered that the formulas produced here were only a merely indicative model. In parallel, the concentration of viable spores in the dust, drying conditions, etc. have been improved. They were stored in the fridge, with a quite stable spore viability.

These results underscore the potential of these *Bacillus* strains as biocontrol agents, providing an environmentally friendly alternative to chemical fungicides. Future studies should focus on optimizing formulation techniques and exploring synergistic effects with other biocontrol agents, like *Trichoderma asperellum* strain T34, to enhance efficacy further.

CONCLUSIONS

In conclusion, the study's findings elucidate the varying efficacies of different *Bacillus* strains in controlling cucurbit downy mildew and powdery mildew diseases, highlighting that, in general terms, when a strain was efficient against one disease, it was also efficient against the other one. The research supports the critical roles of strain selection, application timing, and disease severity in determining the success of biocontrol strategies.

1. From a total of [redacted] isolates evaluated against cucurbit downy mildew and [redacted] isolates evaluated against cucurbit powdery mildew, including bacterial and fungal strains, [redacted] of them (strains [redacted]) showed significant reductions on the disease severity in the first pathosystem, while only [redacted] strains ([redacted]) showed significant reductions in the second pathosystem. The effective bacterial strains coincided in both.
2. All the [redacted] selected bacterial strains were validated at least three times in both pathosystems. In CDM, the most effective strain was the [redacted], with an average disease reduction of [redacted]. The next best strain in this pathosystem was strain [redacted], with average disease reductions of [redacted], respectively. In CPM, strain [redacted] achieved the best efficacy results when applied as a preventive treatment, but it did not work well curatively. Thus, strain [redacted] showed the highest overall efficacy with a mean preventive efficacy of [redacted]. In contrast, when applied as curative treatments, strain [redacted] was slightly better than strain [redacted], showing efficacies of [redacted] respectively.

3. In the efficacy trials assessing the impact of metabolites on disease severity, all strains demonstrated improved effectiveness when treatments included both living bacterial cells and the metabolites produced during their growth. However, the metabolites from strains [redacted] exhibited significantly greater effects compared to those from strains [redacted]. Notably, for strain [redacted], the reduction in cucurbit downy mildew disease was primarily attributed to the bacterial cells themselves, as the metabolites alone showed very limited efficacy.
4. When comparing the efficacies obtained with the final selected strains from this chapter with the biological reference product Serenade® Max, no significant differences were found in any of the studied pathosystems with preventively applications, while the isolated strains in this work performed even better that it when applied curatively. Referring to the chemical reference product Enervin® Duo, it got the highest disease reduction in against *Pseudoperonospora cubensis*, as expected.
5. In general terms, the bacterial strains showed higher effects on disease severity when applied as preventive treatments, while the fungal strains performed better as antagonists against *P. fusca* when applied as curative treatments.
6. In all experiments with formulations of the selected strains, strain [redacted] achieved the highest efficacy against CDM as a preventive treatment, reducing disease by more than [redacted]. Strain [redacted] showed greater efficacy against CPM, achieving around [redacted]. Overall, the efficacy of the formulated products was slightly higher than that of the bacterial solutions and very similar to the efficacy of Serenade® Max as a preventive treatment. Notably, when applied curatively, the prototype formulations developed in this study outperformed Serenade® Max.
7. The dose of the formulated powder did not influence very much on the effects achieved on the disease control in any pathosystem, being these ones even more stable with strain [redacted]. Thus, the minimum effective dose was stablished at [redacted].

Chapter 3. SAFETY ASSESSMENT OF THE SELECTED ISOLATES

ABSTRACT

Whole Genome Sequencing (WGS) has emerged as a crucial technique for evaluating the safety and efficacy of bacterial strains used as PPPs. The comprehensive genetic information obtained from WGS enables detailed analysis of potential pathogenicity, virulence factors, metabolites of concern for human health and antibiotic resistance genes, which are critical for ensuring that these strains do not pose risks to human health, non-target organisms, or the environment. This chapter focuses on the application of WGS in assessing the safety profile of [redacted] and [redacted] for use as biocontrol agents in agriculture.

WGS data were obtained from Macrogen Inc. and assembled using Unicycler. The genomes were annotated with Prokka and analysed for antibiotic resistance genes using ResFinder and the Comprehensive Antibiotic Resistance Database (CARD). Secondary metabolite gene clusters were identified using antiSMASH 7.0. Phenotypic analysis of metabolite production was performed via LC-QTOF-MS/MS, with cultivation in Landy medium and subsequent extraction and quantification of secondary metabolites.

The *de novo* assemblies revealed single circular chromosomes for both strains, with no plasmids detected. Phylogenetic analysis confirmed the taxonomic identity of strains [redacted], respectively, with ANI values exceeding 98%. [redacted] potential antimicrobial resistance genes (AMR) were identified in strain [redacted], considered intrinsic to [redacted] genomes, while [redacted] AMR genes were detected in strain [redacted], none associated with mobile genetic elements. Both strains exhibited genomic potential to produce several secondary metabolites, including [redacted], with similarity values ranging from [redacted] The quantitative LC-QTOF-MS/MS analysis detected high amounts of [redacted] in the culture medium of both strains, as expected. In the qualitative LC-QTOF-MS/MS analysis, the detection of [redacted] matched the genomic predictions. Despite the presence of gene regions for [redacted], no amount of this compound was detected in the growth medium.

The comprehensive genetic analysis and phenotypic confirmation performed in this work support the safe use of [redacted] as PPPs in agriculture.

INTRODUCTION

1. Whole Genome Sequencing (WGS)

Whole Genome Sequencing. WGS is increasingly recognized as a vital tool for assessing the safety profile of bacteria intended for use as PPPs. The comprehensive nature of WGS allows for detailed analysis of genetic content, providing critical insights into the presence of undesirable traits that could pose risks to human health, non-target organisms, or the environment. In this context, one of the most significant applications of WGS is in the detection of pathogenicity and virulence factors. By comparing the genome of a candidate strain with known pathogenic strains, researchers can identify genetic elements that may contribute to harmful effects. Moreover, WGS can identify genes responsible for antibiotic resistance, which is also crucial in determining the safety of biocontrol agents (Wang et al., 2022; Ladner, 2023). Antibiotic resistance genes in bacteria can be transmitted to other microorganisms within the environment through horizontal gene transfer (HGT). This process facilitates the dissemination of resistance traits, resulting in the development of multi-drug resistant (MDR) strains, which complicates infection treatment. HGT has been observed in genes related not only to antibiotic resistance but also to virulence and metabolic functions (Juhas et al., 2008; Brito, 2021). The spread of resistance genes via HGT is a significant public health threat, as it contributes to the emergence of resistant bacterial strains and diminishes the effectiveness of current antibiotics used to combat infections (Zhang et al., 2011; McInnes et al., 2020; Lin et al., 2021). Moreover, according to the European Food Safety Authority (EFSA), in cases where someone is infected with such bacteria, i. e., with a biocontrol agent, it is essential that the bacteria remain susceptible to at least two of the major antibiotic families that are crucial for human and animal health (Mombert et al., 2020). This ensures that there are still effective treatment options available to combat infections. Thus, accurately predicting antimicrobial resistance and associated Mobile Genetic Elements (MGEs) from sequence data highlights the critical role of genomic analysis in assessing the safety profile of bacteria for PPPs (Punina et al., 2015; Daehre et al., 2018; Ladner, 2023).

On the other hand, microorganisms produce two types of metabolites: primary and secondary. Primary metabolites are involved in essential processes like growth and reproduction and are not usually of concern (Mombert et al., 2020). However, secondary metabolites, derived from primary ones, serve ecological roles such as competition and parasitism, and some may pose risks to human, animal, or environmental health (OECD, 2018). In this context, the detection of secondary metabolites or toxin producing genes is also critical for ensuring the safety and efficacy of the product, as identifying these genes helps to prevent the unintended release of

harmful strains into the environment. Furthermore, it also ensures compliance with regulatory standards, as products containing bacteria with toxin production potential might be restricted or require additional testing (European Commission, 2011; 2013). This screening contributes to minimizing ecological risks and enhancing public trust in biological control agents.

Additionally, WGS allows for a thorough examination of the genetic composition of bacterial strains, offering insights into their potential interactions with plants, pathogens, and the environment (Wang, 2024). Therefore, by sequencing the complete genome of bacteria, the key genetic factors linked to plant growth promotion, biocontrol activities, and the production of essential secondary metabolites for plant health can be identified (Qiao et al., 2014; Iqbal et al., 2021; Petrillo et al., 2021; Wang, 2024). Moreover, the genetic foundation of bacterial traits contributing to their beneficial effects on plants, such as siderophore production, antibiosis, and colonization mechanisms can be uncovered (Okungbowa et al., 2019).

Regulatory Implications. Regulatory bodies require robust evidence to approve the use of bacterial strains as PPPs. The ability of WGS to provide comprehensive genetic information supports the development of a thorough safety dossier. For example, WGS data can demonstrate the absence of genes associated with pathogenicity and confirm the presence of beneficial traits such as biocontrol efficacy and plant growth promotion (Rabha et al., 2023). In this context, according to the European Commission in Guidance on the approval and low-risk criteria linked to “Antimicrobial Resistance” applicable to microorganisms used for plant protection in accordance with the Regulation (EC) No 1107/2009 (SANTE/2020/12260), two requirements are essential for the safety profile of bacterial strains as PPPs, which can be extracted from the WGS information:

- *Overall, the micro-organisms shall not be infective or pathogenic to humans.*
- *Antimicrobial resistance: The Uniform Principles outline that it should be demonstrated that, if the microorganisms are resistant to antimicrobial(s), this resistance or its possible transfer does not interfere with the effectiveness of antimicrobials used in human and animal health care or that this possible transfer does not lead to adverse effects on human and animal health. When the resistance can be transferred, the microorganism should not be approved.*

Regarding to the potential risks of secondary metabolites, their production must be evaluated as part of risk assessments for their approval as PPPs (Mombert et al., 2020). The EU has established specific data requirements and principles for these evaluations (European Commission, 2013; 2011). To clarify these processes, a guidance document was finalized in 2020, outlining a stepwise approach to assess risks, starting with identifying metabolites of potential concern through data collection and culminating in a quantitative risk assessment for those identified as posing a threat (European Commission, 2020a).

2. *Bacillus* spp.

The genus *Bacillus* comprises Gram-positive, low (G+C) content, endospore-forming rod-shaped bacteria, with [redacted] as the type species (http://www.bacterio.net/bacillus.html). *Bacillus* species are widely dispersed across various environments such as soil, plants, animals, food, and extreme environments (Ventosa et al., 1989; Maugeri et al., 2002; Krishnamurthi et al., 2009; Suárez-Contreras & Yañez-Meneses, 2020). This versatility highlights the adaptability of *Bacillus* species to different ecological niches. Therefore, these ubiquitous bacteria are widely utilized as biocontrol agents due to their capability to antagonize crop pathogens and the potential for developing stable spore-based commercial products (Borriss, 2015). In this line, some *Bacillus* species can secrete a diverse array of secondary metabolites that exhibit antibacterial, antifungal, or both properties (Stein, 2005; Ongena and Jacques, 2008; Chen et al., 2009; Zhao and Kuipers, 2016).

Furthermore, the taxonomic classification within the genus *Bacillus* has been subject to refinement over the years. Studies have led to the reclassification of certain *Bacillus* species into new genera based on phylogenetic analyses and distinctive characteristics (Feng et al., 2016). Currently, the genus comprises over 300 species (and some subspecies), although some of these have been reassigned to other genera. In recent years, there has been significant taxonomic development in two selected groups of the genus *Bacillus*: *B. subtilis* group and *B. cereus* group (Fritze, 2004; Qin & Driks, 2013) (Figure 3.1A). *B. cereus* group includes some species known to cause infections in humans (Koneman et al., 1997; Euzéby, 2009). Therefore, these species are medically significant, including *B. cereus*, which causes a foodborne illness, and *B. anthracis*, which causes anthrax.

In this context, accurate classification and identification are crucial for the safe use of *Bacillus* strains in agriculture. Phylogenetic analyses based on 16S rRNA gene sequences are commonly used for bacterial identification, especially for species and taxa above the species level (Figure 3.1B). A 97% similarity level is typically used for species delineation (Stackebrandt and Goebel, 1994), with a 98.7% threshold also applied for species differentiation (Kim et al., 2014). However, this cut-off value may not be applicable for *Bacillus* species, which often exhibit very high 16S rRNA gene sequence similarities (>99%) (Ash et al., 1991; Fan et al., 2017). Therefore, recently, the average nucleotide identity (ANI) and digital DNA-DNA hybridization, based on genome sequence data, have been employed for accurate bacterial taxonomic identification (Richter and Rosselló-Móra, 2009; Rooney et al., 2009; Meier-Kolthoff et al., 2013; Chun et al., 2019).

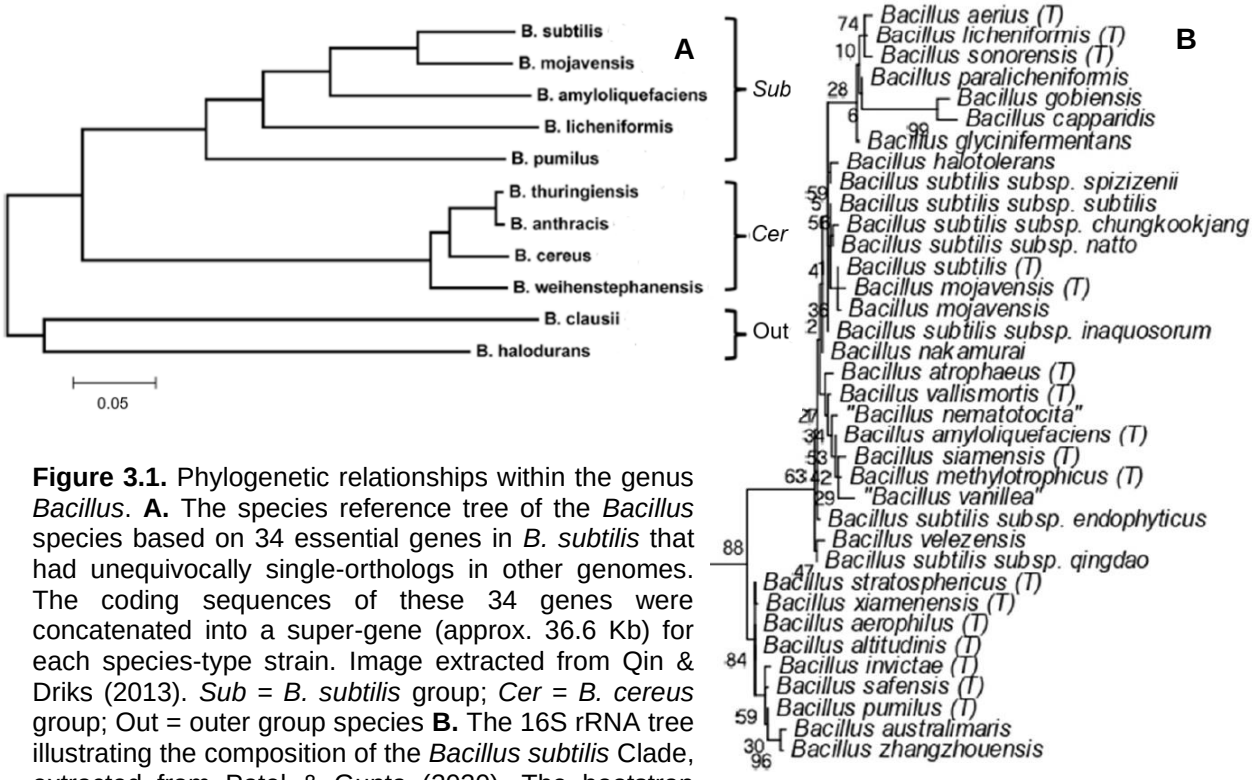

Figure 3.1. Phylogenetic relationships within the genus *Bacillus*. **A.** The species reference tree of the *Bacillus* species based on 34 essential genes in *B. subtilis* that had unequivocally single-orthologs in other genomes. The coding sequences of these 34 genes were concatenated into a super-gene (approx. 36.6 Kb) for each species-type strain. Image extracted from Qin & Driks (2013). *Sub* = *B. subtilis* group; *Cer* = *B. cereus* group; Out = outer group species **B.** The 16S rRNA tree illustrating the composition of the *Bacillus subtilis* Clade, extracted from Patel & Gupta (2020). The bootstrap scores are shown at each branch node.

***Bacillus subtilis* group.** *Bacillus subtilis* is designated as Qualified Presumption of Safety (QPS) by the European Food Safety Authority (EFSA) and as Generally Recognized As Safe (GRAS) by the United States Food and Drug Administration (FDA) (de Boer et al., 1991). These designations indicate that experts consider the organism safe for its intended use, including as a substance added to food. Thus, *B. subtilis* has been extensively studied and serves as a model Gram-positive bacterium. It has been researched in plant rhizosphere colonization, biofilm formation, antibiotic synthesis, bioengineering, and fermented food production (Morikawa, 2006; Earl et al., 2008; Kamada et al., 2015).

The *B. subtilis* group species, comprising phylogenetically homogenous bacteria, is a significant cluster within the genus *Bacillus* (Hong et al., 2022). The *B. subtilis* group, which includes the subspecies *B. subtilis* subsp. *subtilis*, *B. subtilis* subsp. *stercoris*, *B. subtilis* subsp. *inaquosorum*, and *B. subtilis* subsp. *spizizenii*, along with closely related species such as *B. tequilensis, B. velezensis, B. nakamurai, B. vallismortis, B. siamensis,* [redacted]*, B. mojavensis, B. amyloliquefaciens,* and *B. atrophaeus*, form a phyletic group with high 16S rRNA gene sequence similarity (>98.7%) (Heo et al., 2019). This makes it challenging to identify these species only through 16S rRNA gene sequence phylogenetic analysis (Rooney et al., 2009; Adelskov and Patel, 2016; Fan et al., 2017). The taxonomic reassessment of *Bacillus* species, which has resulted in the proposal of new subspecies and species within the

B. subtilis group, highlights the need for a polyphasic approach to ensure accurate classification (Guerra-Cantera & Raymundo, 2005; Ruiz-García et al., 2005). This approach combines multiple methods, including phenotypic, genotypic, and chemotaxonomic analyses, for a more comprehensive and reliable understanding of organisms. In microbial taxonomy, this comprehensive strategy integrates traditional techniques like morphology and biochemical tests with modern tools such as DNA sequencing, phylogenetics, and the analysis of cellular components (e.g., fatty acids and proteins).

[redacted] is a notable species known for its ability to thrive in [redacted] and its efficacy as a biocontrol agent against plant pathogens, particularly *Fusarium* and *Rhizoctonia solani* ([redacted]), highlighting their ecological importance and potential in sustainable agriculture (Sagredo-Beltrán et al., 2018). Moreover, [redacted] reported that *B.* [redacted] exhibited strong activities against other major phytopathogens: *Botrytis cinerea, Alternaria alternata, Phytophthora infestans,* and *Rhizoctonia bataticola*.

[redacted] is distinguished by its genomic composition, which includes genes responsible for producing secondary metabolites. These include non-ribosomal peptide synthases (NRPSs) that synthesize non-ribosomal peptides such as surfactin, fengycin, iturin, and bacilysin, as well as polyketide synthases (PKSs) that generate compounds like bacillaene. Together, these metabolites contribute to its biocontrol capabilities and highlight its potential for novel compound synthesis (Feng et al., 2022). Additionally, strains of [redacted] have been found to produce extracellular lipases, alkaline proteases, and biosurfactants, showcasing their diverse enzymatic capabilities with potential industrial applications (Gharbi et al., 2018; Mahnashi et al., 2022; Karnwal et al., 2023). Moreover, [redacted] exhibits plant growth-promoting traits such as nitrogen fixation, phosphate solubilization, and indole acetic acid production, making it beneficial for enhancing crop productivity under stressful conditions (El-Akhdar et al., 2020). Moreover, studies have demonstrated its ability to alleviate salt stress in wheat, promote lily growth, and induce systemic resistance against root-knot nematodes in tomato plants (Xia et al., 2019; El-Akhdar et al., 2020; Gao et al., 2022).

Regarding to the taxonomical classification of [redacted], different names have been used to identify strains belonging to the now known as [redacted]. These synonymous are extracted from the List of Prokaryotic names with Standing in Nomenclature ([redacted]). The parent taxon, *Bacillus*, was established by Cohn in 1872, while the basonym or original name, [redacted], was first proposed by [redacted]. The species was later renamed [redacted], who also noted that it is an earlier heterotypic

synonym of [redacted], species originally described by [redacted]

Etymologically, [redacted]. The type strain is registered in different data base as [redacted]; while the 16S rRNA gene is registered in GenBank under [redacted]. The risk-group classification for [redacted] was assigned as Risk Group 1 by the LPSN (Parte et al., 2020), based on the German TRBA 466 "Classification of Prokaryotes (Bacteria and Archaea) into Risk Groups". These risk-group 1 organisms are unlikely to cause disease in a healthy individual but could cause disease in someone who is susceptible, according to the Approved List of Biological Agents produced by the Advisory Committee on Dangerous Pathogens (ACDP).

3. Secondary metabolites production

Production of lipopeptides: surfactins, iturins and fengycins. Surfactins, iturins, and fengycins are three major classes of lipopeptides (molecules composed of a lipid linked to a peptide) produced by various strains of *Bacillus* species, known for their diverse biological activities and potential applications in different fields. These lipopeptides are cyclic substances characterized by containing seven or ten α-amino acids linked to a chain of fatty acids. These fatty acid chains vary in length, ranging from C_{13} to C_{16} for surfactin, C_{14} to C_{17} for iturin, and C_{14} to C_{18} for fengycin (Souza et al., 2018). The diversity in the number of carbon atoms in the fatty acid chains and amino acid composition leads to the formation of various isoforms, which can be further subdivided into homologous series differing in the aliphatic chain length (Behary et al., 2012). Regarding to the biocontrol of plant diseases, these same three families are most-studied lipopeptides for their antagonistic action against a variety of fungal phytopathogens, such as *Rhizoctonia solani* (Yu et al., 2002; Guo et al., 2014), *Pythium ultimum, Botrytis cinerea* (Ongena et al., 2005), *Podosphaera fusca* (Romero et al., 2007), *Fusarium graminearum* (Zhao et al., 2014; Gong et al., 2015), and *Sclerotinia sclerotiorum* (Alvarez et al., 2012).

Surfactins, the main representative of this family, are composed of a seven-peptide ring and a fatty acid tail chain, exhibiting powerful biosurfactant properties (Zhou et al., 2023). These molecules are amphiphilic, allowing them to reduce surface tension and form micelles, making them effective in various applications such as environmental remediation and heavy oil transportation (Zhou et al., 2023). Surfactins have been shown to possess antibacterial, antifungal, antiviral, antitumor, hemolytic activities, and a toxin inhibitor action, highlighting their broad spectrum of biological effects (Seydlová & Svobodová, 2008; Meena et al., 2015).

Iturins are characterized by their antifungal properties and are known for their ability to inhibit the growth of various fungal pathogens, particularly effective against filamentous phytopathogenic fungi (Kawagoe et al., 2015; Li et al., 2016). These molecules consist of a cyclic heptapeptide linked to a β-amino fatty acid chain and they present different structural characteristics in terms of amino acid sequence and in the length and branching of their fatty acid chain (Zompra et al., 2022). Iturins are also involved in the disruption of fungal cell membranes, leading to cell lysis and subsequent inhibition of fungal growth by their ability to form ion-conducting pores on membranes of fungi (Li et al., 2016; Pandya et al., 2017; Zompra et al., 2022).

Fengycins are characterized by their amphiphilic nature and broad-spectrum antimicrobial activity, particularly against bacterial pathogens (Medeot et al., 2020; Rangarajan et al., 2015). These molecules consist of a β-hydroxy fatty acid chain attached to a decapeptide, forming a cyclic lactone ring (Aranda et al., 2005; Ongena and Jacques, 2008). Fengycins have been shown to insert into model biomembranes, creating permeabilization sites that disrupt the integrity of target cell membranes, leading to cell death (Medeot et al., 2020).

Overall, cyclic lipopeptides are primarily recognized for their amphiphilic nature, allowing them to easily integrate into cell plasma membranes. This integration leads to pore formation and membrane disruption, which amplifies their antimicrobial effects (Balleza et al., 2019). The lipid composition of the target organism plays a crucial role in this process, as it influences how these lipopeptides interact with the plasma membrane and determines the specificity of their antimicrobial activity (Patel et al., 2011; Wise et al., 2014; Fiedler et al., 2015; Balleza et al., 2019; Pinkas et al., 2020). Therefore, lipopeptides like fengycin and surfactin selectively target the membranes of pathogens, rather than the membranes of human cells, due to differences in lipid composition (Gilliard et al., 2024). Pathogen membranes often contain specific lipids like ergosterol and negatively charged phospholipids, which are the primary targets. Thus, lipopeptides interact with these lipids, causing permeabilization and destabilization of pathogen membranes, leading to their destruction (Balleza et al., 2019; Pinkas et al., 2020). In contrast, human cell membranes have a different lipid composition, including cholesterol and fewer negatively charged phospholipids, reducing the affinity of these lipopeptides for human membranes (Balleza et al., 2019). As a result, lipopeptides do not significantly alter human cell membranes at typical concentrations. This selectivity explains why lipopeptides can effectively control pathogens without posing significant toxicity risks to humans, making them safe for biocontrol applications (Gilliard et al., 2024).

In summary, surfactin, iturin, and fengycin are not considered significant risks to human health due to their low toxicity, biodegradability, and selective antimicrobial properties (Inès &

Dhouha, 2015). These naturally derived lipopeptides have been widely researched for their effectiveness in controlling plant pathogens without causing harm to humans (Álvarez et al., 2011; Li et al., 2019; Leconte et al., 2022; Gugel, 2024). There is no scientific evidence, from sources like Scopus or PubMed, indicating that these compounds are harmful, carcinogenic, mutagenic, or toxic to humans. In addition, as it has been mentioned, regulatory bodies such as the FDA classify *Bacillus* species that produce these lipopeptides as GRAS, while the EFSA includes *B. subtilis* in its QPS list, acknowledging the safety of these compounds.

The production of these lipopeptides is catalysed by non-ribosomal peptide synthetases (NRPSs), which are modular enzymes that synthesize important peptide products using a wide range of standard and non-proteinogenic amino acid substrates (Miller & Gulick, 2016). Each module contains multiple catalytic domains, with each module responsible for the incorporation of a single amino acid residue, as it is shown in Figure 3.2. This NRPSs allow for the biosynthesis of structurally diverse and biologically active molecules, highlighting their potential for diverse applications, ranging from agriculture to medicine and environmental remediation.

Regarding to the synthesis of surfactin, its production requires the *srfA* operon, the *sfp* gene, and two quorum-sensing systems. The master regulator *spo0A* is also essential for proper surfactin synthesis. Once produced, surfactin functions as a signaling molecule, activating the Spo0A gene, which subsequently controls cell differentiation (Rahman et al., 2021). Referring to iturins, the iturin A operon spans a region that is more than 38 kb long and is composed of four open reading frames, *ituD, ituA, ituB*, and *ituC* (Tsuge et al., 2001). For instance, the *ituD* gene encodes a putative malonyl coenzyme A transacylase, and its disruption leads to a mutated, inactive form of iturin A (Tsuge et al., 2001). Moreover, the *lpa-14* gene has been shown to be homologous to the *sfp* gene and it has been reported to be responsible for the biosynthesis of surfactin and iturin A in *B. subtilis* strain RB14 (Roongsawang et al., 2002). Finally, about the fengycin production, five fengycin synthetase genes, including *fenC, fenD, fenE, fenA,* and *fenB*, had been described (Lin et al., 1999; Steller et al., 1999). These enzymes activate all fengycin amino-acid components as aminoacyl adenylates or aminoacyl thioesters, activating each of them a different set of L-amino acids (Steller et al., 1999).

When discussing the genes involved in the synthesis of major secondary metabolites, it is important to note that having the genetic capacity to produce a particular compound does not necessarily guarantee its production. Thus, even if the genes responsible for the production are present, environmental signals, regulatory pathways, and post-translational modifications can influence gene activation, leading to the production of non-functional proteins or, in some cases, complete suppression of gene expression (Samuel Russell et al., 2023). Additionally, mutations in regulatory genes or within the biosynthetic gene cluster itself may prevent proper

folding or function of the enzymes involved, further disrupting the synthesis of the target compound (Lenzi et al., 2021; Samuel Russell et al., 2023).

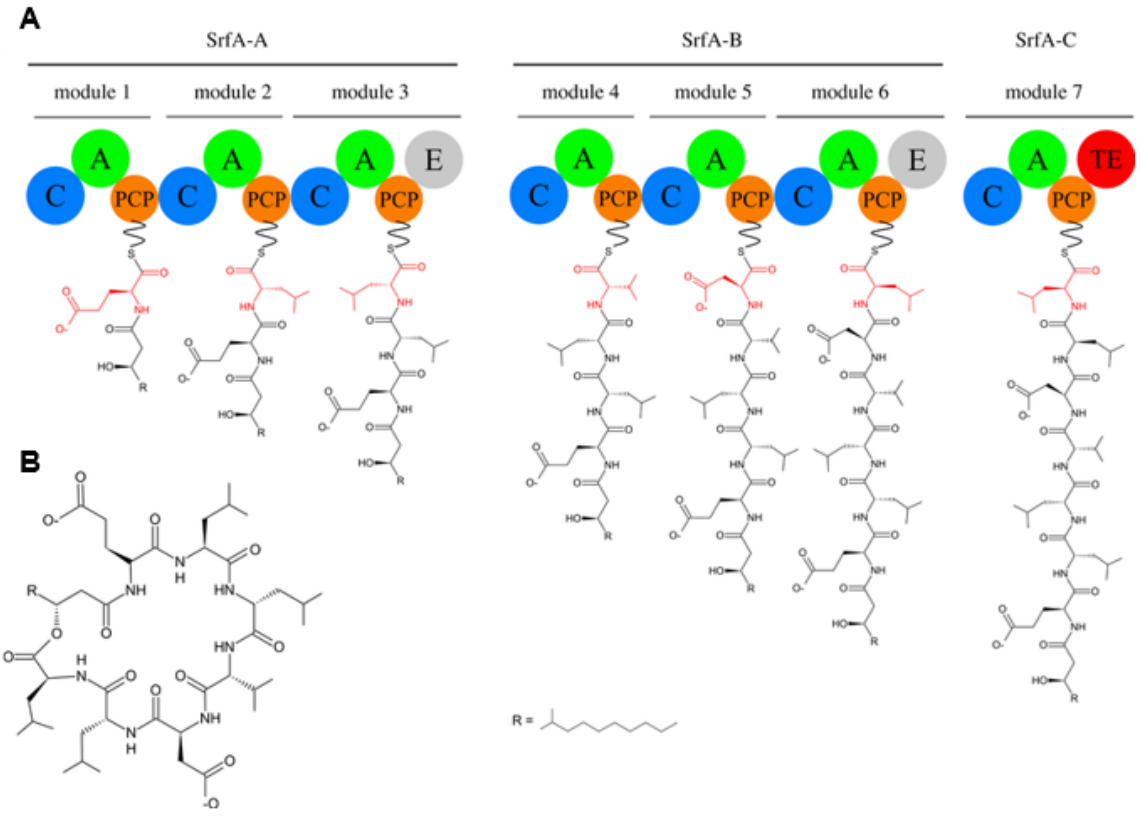

Figure 3.2. Organization of the surfactin NRPS. The surfactin non-ribosomal peptide synthetase (NRPS) is made up of three polypeptides: SrfA-A, SrfA-B, and SrfA-C, each containing one or more modules responsible for adding specific amino acids to the growing peptide chain. Module 1 initiates the process, module 7 terminates it, and the others function in elongation. Each module includes a non-catalytic PCP domain (orange) that holds the growing molecule, as well as catalytic domains: a condensation domain (C, blue) and an adenylation domain (A, green). Modules 3 and 6 also contain an epimerization domain (E, grey). The termination module includes a thioesterase domain (TE, red) that releases and cyclizes the final surfactin molecule. Image extracted from Bonhomme et al. (2021).

Production of other secondary metabolites. As it has been mentioned, *Bacillus* species are renowned for their ability to produce a wide range of biologically active secondary metabolites that can potentially inhibit the growth of plant pathogens (Rabbee et al., 2019). Some of the most important ones are presented in Figure 3.3. Among these secondary metabolites, bacillibactin stands out for being a catechol-based siderophore which plays a crucial role in iron acquisition and pathogen control, highlighting the multifaceted functions of these microbial metabolites (Miethke & Marahiel, 2007). Bacillaene is a linear polyketide with a conjugated hexene structure which exhibits bioactive characteristics that contribute to its role in inhibiting the growth of pathogenic microorganisms, making it a valuable asset in disease management, within other potential applications (Brudzynski, 2021; Miao et al., 2023). Finally, bacilysin is a dipeptide antibiotic composed of L-alanine and L-anticapsin also produced by certain strains

of *B. subtilis* (Abdulmalek & Yazgan-Karataş, 2023). It has been involved in plant growth promotion and biocontrol of plant diseases (Arguelles-Arias et al., 2009; Pérez et al., 2018).

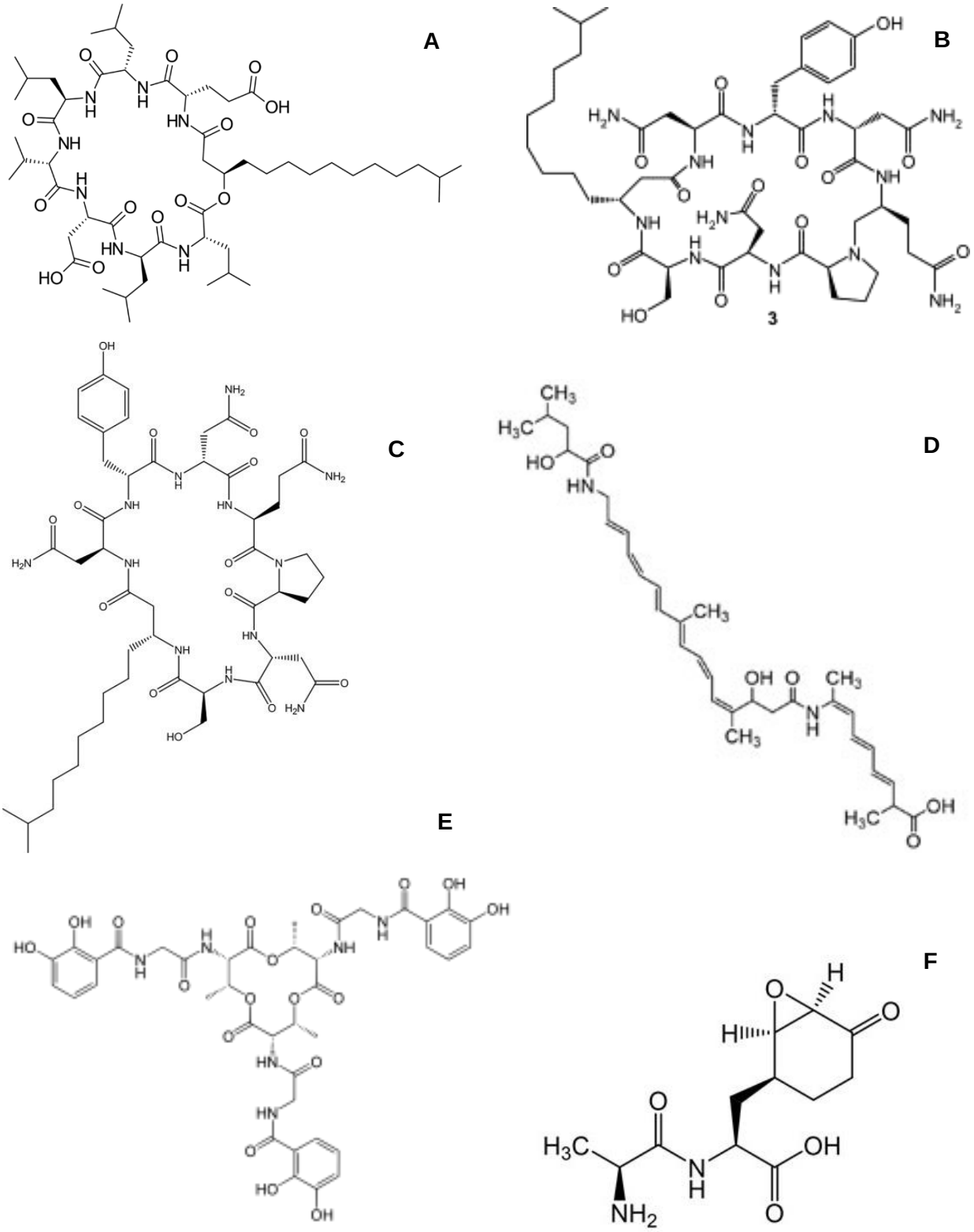

Figure 3.3. Molecular structure of some of the most typically produced secondary metabolites by *Bacillus* species, including **A**. Surfactin, **B.** Iturin, **C.** Fengycin, **D.** Bacillaene, **E.** Bacillibactin & **F.** Bacylisin.

OBJECTIVES

The main objective of this chapter was to conduct a WGS data analysis to stablish the safety profiles of [redacted] and [redacted], with focus on the detection of antimicrobial resistance genes, toxin producing regions or virulence factors and the secondary metabolites producing regions, with the corresponding phenotypical identification.

The specific objectives for this work were:

1. To assemble the genomes of the strains from the WGS data obtained.
2. To verify the taxonomical classification obtained with the 16S rRNA gene sequence to the taxonomical classification based on the WGS information of the mentioned bacterial strains.
3. To determine the phylogenetic relationships of these strains within the genus *Bacillus*, according to the WGS data.
4. To perform a functional annotation of the genes according to Gene Ontology (GO) and Cluster of Orthologous Groups (COG) classification.
5. To search for antimicrobial resistance genes, with focus with the ones linked to mobile genetic elements.
6. To determine the genetic capacity of producing secondary metabolites based on the WGS information.
7. To detect and quantify the most common lipopeptides *Bacillus* species produce, i.e., surfactins and iturins, by liquid chromatography coupled to mass spectrometry, using chemical standards.
8. To validate the chromatographic/spectrometric method through the determination of the accuracy (in terms of percent of recovery), the limit of detection (LOD) and the limit of quantitation (LOQ).
9. To detect other secondary metabolites for which the tested strains have the genetic capacity to produce according to the WGS data by liquid chromatography coupled to mass spectrometry.

MATERIALS AND METHODS

1. Whole Genome Sequencing and Bioinformatic analysis

Bacterial DNA extraction. The bacterial strains [redacted] were defrosted from -80 ºC and spread on Trypticasein Soy Agar (TSA, from Condalab, Spain) Petri dishes. After 48 h of incubation at 30 ºC, genomic DNA was extracted using E.Z.N.A.® Bacterial DNA Kit (Omega Bio-tek), following the fabricant's instructions. The quality of the DNAs was determined by 1%-agarose gel electrophoresis and by the NanoPhotometer™ (BioNova cientifica S.L.), which also served to determine the concentration of the DNAs obtained. Finally, the quality and the concentration of the DNA were verified again using the Qubit™ dsDNA Assay Kits (ThermoFisher, ref.: Q32851). Finally, the genomic DNAs were sent to Macrogen Inc. (Korea) to perform Whole Genome Sequencing using Illumina Sequencing by Synthesis (SBS) technology, which consisted of short-read sequencing, and the raw data was returned.

For the assembly of the genomic sequence, filtered data (forward and reverse) from the WGS was uploaded to the Galaxy server (https://usegalaxy.eu/), which contains various utilities to analyse this kind of data. The assembly was performed by using the Unicycler tool (Wick et al., 2017).

Taxonomic identification. A verification of the taxonomical identity of the main strains was performed using the EzBioCloud (https://www.ezbiocloud.net) Database. The species determination was verified by the average nucleotide identity or ANI value, which is a measure of nucleotide-level genomic similarity between the coding regions of two genomes (Arahal, 2014), with a proposed species boundary cut-off of 95-96% (Chun et al., 2018; EFSA 2021). The ANI values were measured using the ANI Calculator tool from EzBioCloud.

Phylogenetic trees. The genomic sequence data were submitted to the Type (Strain) Genome Server (TYGS) (https://tygs.dsmz.de) for a comprehensive taxonomic analysis based on whole-genome sequences (Meier-Kolthoff & Göker, 2019), with settings as default. The analysis made use of recently introduced methodological updates, and the necessary information was provided by TYGS's sister database, the List of Prokaryotic names with Standing in Nomenclature (LPSN, available at https://lpsn.dsmz.de) (Meier-Kolthoff et al., 2022). For the identification of closely related type strains, the given genomes were compared against the available type strain genomes in the TYGS database using the MASH algorithm, a rapid method for estimating intergenomic relatedness (Ondov et al., 2016). Subsequently, the type strains with the smallest MASH distances were selected for each user genome.

Precise distances were determined using the Genome BLAST Distance Phylogeny (GBDP) method, employing the 'coverage' algorithm and the d5 distance formula, which calculates genome-to-genome distances for species delimitation based on genome comparisons (Meier-Kolthoff et al., 2013). On the other hand, bootstrap scores, calculated from multiple resampled datasets, measure the confidence of branches in phylogenetic trees by representing the percentage of trees (built from each resampled dataset) supporting a particular branch (Efron, 1979; Felsenstein, 1985). Pseudo-bootstrap values improve this by considering the quality of each tree and how well it fits the resampled data (Makarenkov et al., 2010). Thus, the resulting intergenomic distances were used to construct a balanced minimum evolution tree with branch support, in which the branch lengths were scaled according to the GBDP distance formula d5, and the branch values represent GBDP pseudo-bootstrap support values greater than 60%, based on 100 replicates. (Lefort et al., 2015; Kreft et al., 2017).

Functional annotation and circular genome representation. A functional classification was performed by utilizing various functional gene categories identified using the EGGNOG-mapper v5.0 (Online Version -http://eggnog-mapper.embl.de/) (Cantalapiedra et al., 2021). The results of Coding DNA Sequence (CDS) prediction were analyzed using BLAST against widely used databases, including Gene Ontology (GO) (https://geneontology.org/) and the Cluster of Orthologous Groups (COGs) database from the NIH (https://www.ncbi.nlm.nih.gov/research/cog/). GO annotation provides a standardized framework for gene and gene product expressions across species (Huntley et al., 2015). COG annotation enables functional gene annotation by categorizing genes into clusters of orthologous groups (Cantalapiedra et al., 2021; Sunithakumari et al., 2024; Lee et al., 2024). Thus, genes were classified into various GO and COG categories, with a bar chart generated in SigmaPlot version 11.0 to visualize the distribution across these categories.

The circular genome representation was performed by CGView.js (Stothard & Wishart, 2005), which is the genome viewer of Proksee (https://proksee.ca/), an expert system for genome assembly, annotation and visualization. In the same Proksee platform, the genomes of [redacted] and [redacted] were passed through a set of tools provided by Proksee and represented in the figures obtained, including the annotation of the genome sequence with Prokka version 1.1.1. (Seemann, 2014), and the results from the Comprehensive Antibiotic Resistance Database (CARD) Resistance Gene Identifier (RGI) version 1.2.1. (Alcock et al., 2023). In this line, the mobileOG-db version 1.1.3 (Brown et al., 2022) tool was used to find MGEs. Moreover, the distribution of Contigs (Backbone), GC Content and GC Skew was also determined and represented.

Antimicrobial Resistance genes (AMR genes). Referring to the search for AMR genes, ResFinder-4.5.0 (http://genepi.food.dtu.dk/resfinder), from the Center for Genomic Epidemiology, was used for this purpose, according to Bortolaia et al., (2020) and Camacho et al. (2009).

In addition, the Resistance Genome identifier from the Comprehensive Antibiotic Resistance Database (https://card.mcmaster.ca/analyze/rgi) was also used to search for AMR genes in the WGS data. The sequence quality parameter was set as "high quality", which uses complete genomes, plasmids, or high-quality assemblies (includes contigs > 20,000 bp) and excludes prediction of partial genes.

Moreover, plasmidSPAdes (Vasilinetc et al., 2015; Antipov et al., 2016) was used to extract and assembly plasmids from WGS data, and also the MOB-Recon tool (Robertson & Nash, 2018) was used for type contigs (those that have been specifically identified as part of a particular plasmid or categorized based on the presence of key markers) and extract plasmid sequences. Both tools were used from the Galaxy server.

Secondary metabolite search. Afterwards, antiSMASH 7.0 (Blin et al., 2023) (https://antismash.secondarymetabolites.org/#!/start) was used to identify secondary metabolite producing regions in the genome, using detection strictness both "relaxed" and "strict".

2. Secondary metabolites production

A standard protocol based on chromatography coupled to mass spectrometry for bacterial metabolite production determination was conducted following the recommendations from Farzand et al. (2019). Thus, the secondary metabolites produced by strains [redacted] and [redacted] were phenotypically analysed and compared with the ones from *B. subtilis* strain QST 713 (Serenade®) which served as a positive control. The metabolites produced by this strain are published by Anastassiadou et al., (2021) in the EFSA Journal, including surfactin, iturin A, fengycin, bacillaene, difficidin, ericin A and ericin S.

Bacterial cultivation and metabolite recollection. The bacterial strains were cultivated in 100 mL of Landy medium (Farzand et al., 2019) at 30 ºC for 48 h in a rotary shaker at 200 rpm. The Landy medium consisted of 10 g/L of glucose, 5 g/L of L-monosodium glutamate, 0.5 g/L of $MgSO_4$, 0.78 g/L of KCl, 1 g/L of KH_2PO_4, 0.05 mg/L of $FeSO_4$, 5 mg/L $MnSO_4$, 0.16 mg/L of $CuSO_4$. All the compounds were dissolved in 1000 mL of distilled water and the pH was adjusted to 7.2 before autoclave. Once the 48 hours-incubation ended, the bacterial solutions were centrifuged at 10,000 × g at 4ºC for 30 min to obtain 100mL cell-free supernatant of each

strain. For a set of bacterial samples, the metabolite extraction protocol ended here, and the samples were filtered (through 0.2 µm filters) and stored at -20 ºC for further analysis (Protocol of samples directly resuspended from the Landy Medium = Protocol LM).

In contrast, another set of samples was further processed, in which the pH of the 100 mL cell-free supernatant was adjusted to 2 with H_2SO_4 and samples were kept overnight at 4 ºC (Protocol of samples Acidified and Precipitated = Protocol AP). After this second incubation, the precipitates were collected by centrifugation at 10,000 × g at 4 ºC for 20 min and were then dissolved in 5 mL of methanol (Ramarathnam et al., 2007). The extract was passed through 0.2 µm filters.

Two bacterial solutions were prepared separately for each strain to have independent replicates for the same bacteria and increase the reliability of the measurements.

Preparation of the standards. Iturin A (purity ≥ 95% from *Bacillus subtilis*, Ref. I1774), consisting of a mixture of the homologues variants (which share the same basic structure but differ in the length of the fatty acid chains), iturin A2 ($C_{48}H_{74}N_{12}O_{14}$ and m/z 1043.552 Da), iturin A4 ($C_{49}H_{76}N_{12}O_{14}$ and m/z 1057.5677 Da), iturin A6 ($C_{50}H_{78}N_{12}O_{14}$ and m/z 1071.5833 Da), and surfactin C (purity ≥ 98% from *Bacillus subtilis*, Ref. S3523) ($C_{53}H_{93}N_7O_{13}$ and m/z 1036.6904 Da) were purchased from Sigma-Aldrich® Lab & Production Materials, Spain. Formic acid (purity ≥ 99.7%), acetonitrile (HPLC Plus, ≥ 99.9%) and methanol (purity ≥ 99.8%) were purchased also from Sigma-Aldrich (Spain).

Individual stock solutions of the lipopeptides were prepared by dissolving each compound in methanol at a concentration of 1 ppm (1 mg/L). Then, a mixed solution of the standards was prepared at the same concentration of 1 ppm each. The calibration curve of the compounds was prepared by diluting a mixture of the standards solution in methanol, adjusting the concentrations to 0.1 ppm, 0.5 ppm, 1 ppm, 2.5 ppm and 5 ppm. All solutions were stored at − 20 °C.

Liquid Chromatography quadrupole time of flight mass spectrometry (LC-QTOF-MS/MS). The Agilent 6560 Ion Mobility QTOF LC/MS system, housed in the Chromatographic Services of the Scientific and Technological Centers of the University of Barcelona (CCiTUB) at the Parc Científic, was used to analyse the metabolites produced by the strains. Separations were carried out on a Acquity UPLC Peptide BEH C18 Column (2.1 x 100 mm, pore size of 130 Å and 1.7 µm particles). The injection volume was 2 µL and the flow rate was 0.4 mL/min, with a pressure of 460 bar. The mobile phase consisted of A) 0.1% formic acid (HCOOH) in water and B) 0.1% formic acid in acetonitrile (ACN). The gradient elution (t(min), %B) was performed as follows: (0, 5), (2, 5), (17, 95), (19, 95), (19.1, 5), (22, 5).

Mass spectrometry was carried out using electrospray source in positive ion mode (Farzand et al., 2019) in a range of mass-to-charge ratio (m/z) from 100 to 1,700. LC-MS modalities were applied to the selected ions, according to the conditions set during the analysis. These conditions were as follows; gas temperature 300 ºC, drying gas 5 L/min, Nebulizer 35 psi, sheath gas temperature 350 ºC, sheath gas flow 11 L/min, Vcap 3500 V and Nozzle voltage (Expt) 1000 V. Data acquisition and processing was performed using Agilent MassHunter Workstation Software programs (Agilent MassHunter Quantitative Analysis and Agilent MassHunter Qualitative Analysis 10.0). Statistical analysis was performed using the previous software to determine the linear relationships between the variables, including the coefficient of determination (R^2) and the equations of the regression lines.

Commercial standards were only available for iturin A and surfactin C. Thus, for the rest of secondary metabolites quantification was not possible. However, a tandem MS (MS/MS) was conducted to break down selected ions (precursor ions) into fragments (product ions) to reveal aspects of the chemical structure of the precursor ion and be able to putatively identify them. This technique was also conducted by using the same Agilent 6560 Ion Mobility QTOF LC/MS system, which allowed to measure at least 4 decimal places of the exact mass of the molecules sought. The “Exact Mass” and “Generate Formula” tools from the Agilent MassHunter Qualitative Analysis 10.0 software were utilized to generate molecular formulas from the detected spectrum peaks, enabling the assignment of compounds to the detected traces.

PubChem (https://pubchem.ncbi.nlm.nih.gov/), an open chemistry database of the National Institutes of Health (NIH), and ChemSpider (https://www.chemspider.com/), a free chemical structure database provided by the Royal Society of Chemistry (RSC) containing data on millions of compounds, including structures, properties, and links to scientific literature, were used to characterize the detected ions. Additionally, a comprehensive literature search was conducted to validate the results. The retention times (RTs) and mass-to-charge ratios (m/z) observed in the analysis were compared with those reported in the literature.

Validation of the method. To validate the analytical procedure for quantifying the potential presence of various secondary metabolites in the growth medium of strains [redacted] and [redacted], the harmonized tripartite guideline for the validation of analytical procedures (CPMP/ICH/381/95) was applied (Huber, 2003). This guideline was developed by the International Council for Harmonization (ICH) of Technical Requirements for Registration of Pharmaceuticals for Human Use.

For the **accuracy**, the samples were spiked with a known amount of chemical standards (2.5 ppm for samples processed with the Protocol AP and 1 ppm for the ones from the Protocol

LM) before processing and extracting the metabolites. The recovery was determined by comparing the response of these samples with the response of samples processed first and then spiked with the same known amount of standard.

The **detection limit (LOD)** was calculated in the matrix and in the solvent by comparing measured signals from a solution with 0.1 ppm of the standards surfactin C and iturin A variants with the signals corresponding to the baseline noise. A signal-to-noise ratio of 3:1 was used to estimate the detection limit.

The **quantitation limit (LOQ)** was calculated in the matrix and in the solvent by comparing measured signals from a solution with 0.1 ppm of the standards surfactin C and iturin A variants with the signals corresponding to the baseline noise. A signal-to-noise ratio of 10:1 was used to estimate the quantitation limit.

RESULTS

1. Whole Genome Sequencing and bioinformatics results

The WGS data was utilized to identify genes associated with pathogenicity and antimicrobial resistance of [redacted]. The preliminary sequencing results, provided confidentially by Bicontrol Technologies S.L., are not displayed in this PhD thesis. However, the key outcome of this preliminary analysis was that three out of the five strains—strains [redacted]—were eliminated from consideration due to regulatory challenges linked to their genomic profiles. Therefore, in this chapter, a comprehensive comparative analysis of [redacted] and [redacted] was specifically conducted.

Referring to the general description of the genomes, for strain [redacted], the raw data included [redacted]. In the case of strain [redacted], the raw data included [redacted]. The genome assembly performed using Unicycler produced [redacted].

Taxonomic identification. For [redacted], the top-hit strain was [redacted], with a similarity of 99.85%, a completeness of 100% and an ANI value of 98.6% when using the WGS data. For [redacted], the top-hit strain was [redacted], with a similarity of 99.93%, a completeness of 93.7% and

an ANI value of 98% when using the WGS data. Both ANI values are above the EFSA threshold of 95% (Chun et al., 2018; EFSA, 2021).

Phylogenetic trees for taxonomical classification. According to the TYGS, [redacted] was classified within the species [redacted]. As illustrated in Figure 3.4, the clustering analysis identified nine distinct species clusters, with strain [redacted] assigned to one of these. Moreover, the strain was placed within one of ten subspecies clusters.

Additional genomic characteristics were analysed, including the G+C content, which was approximately [redacted] across most strains. Genome sizes ranged from [redacted], while the number of predicted protein-coding genes varied between [redacted]. A detailed comparison of strain [redacted] with its closest match, [redacted], revealed genome sizes of [redacted] bp, and predicted protein counts of [redacted], respectively.

However, based on genome size and protein count, the strain most similar to strain [redacted] was [redacted], with a genome size of [redacted] predicted proteins.

Figure 3.4. Phylogenetic tree of [redacted] (in yellow) based on the WGS data by using the TYGS. The branch lengths are scaled in terms of GBDP distance formula d5. The numbers above branches (in blue) are GBDP pseudo-bootstrap support values > 60 % from 100 replications, with an average branch support of [redacted] The tree was rooted at the midpoint according to Farris (1972). The square columns refer to: column 1 = Species cluster; column 2 = Subspecies cluster; column 3 = Percent G+C; column 4 = Genome size (in bp) and column 5 = Protein count. Last two values represented according to the size of their respective squares.

On the other hand, the TYGS analysis identified strain [redacted] as belonging to the known species [redacted], with results presented in Figure 3.5. The clustering analysis yielded six distinct species clusters, and strain [redacted] was assigned to one of these. Additionally, the strain was classified within one of seven subspecies clusters.

The genomic analysis provided further details, including the G+C content, which ranged from [redacted]. Genome sizes across the strains varied between [redacted], while the number of predicted proteins ranged from [redacted]. A more detailed comparison of strain [redacted] with its closest relative, [redacted], revealed genome sizes of 4[redacted], with predicted protein counts of [redacted], respectively.

For strain [redacted], the most similar strains based on genome size and protein count were [redacted], with a genome size of [redacted] predicted proteins, and [redacted], with a genome size of [redacted] proteins.

Figure 3.5. Phylogenetic tree of [redacted] (in yellow) based on the WGS data by using the TYGS. The branch lengths are scaled in terms of GBDP distance formula d5. The numbers above branches (in blue) are GBDP pseudo-bootstrap support values > 60 % from 100 replications, with an average branch support of [redacted] The tree was rooted at the midpoint according to Farris (1972). The square columns refer to: column 1 = Species cluster; column 2 = Subspecies cluster; column 3 = Percent G+C; column 4 = Genome size (in bp) and column 5 = Protein count. Last two values represented according to the size of their respective squares.

Gene function analysis: GO and COG annotation. GO analysis was used to categorize genes into three main GO categories—biological process, cellular component, and molecular function—based on matches with known sequences. Figure 3.6 illustrates the classification of annotated genes from the WGS data of both strains within these categories, highlighting the most frequent GO terms in each. Notably, no significant differences were observed in gene distribution between the two strains.

The most represented pathways in the [redacted] category for both strains were [redacted], with gene counts ranging from [redacted]. In the [redacted] category, the [redacted] had the highest representation overall, with gene counts close to [redacted], and the [redacted] was also notably represented. Lastly, in the [redacted] category, [redacted] was the most represented pathway and the second most prominent overall.

Figure 3.6. Gene counts in the WGS of strains [redacted] (compact columns) and [redacted] (striped columns) distributed along the Gene Ontology (GO) terms grouped into the GO categories: Biological process (in purple), Cellular component (in green) and Molecular function (in red)

Referring to the COG classification, the Figure 3.7 shows the visual distribution of genes across different COG categories, providing a summarized representation of the functional classification of the bacterial genes. As it is clearly seen, most of the genes were classified in the S COG category, i. e., with an unknown function. After that, the great majority of the genes belonged to the [redacted]. The following more abundant category was the [redacted], closely followed by the [redacted]. Then, a great number of genes were count in both cases belonging to the categories [redacted]. Finally, many genes were also identified belonging to the [redacted]. Moreover, some other genes have been found in multi-letter COG categories (including two or three letters), indicating that the protein or gene belongs to multiple functional categories and reflecting the diverse functional roles that a single protein or gene might play within the cell.

Figure 3.7. Visual representation of the gene counts distributed along the Cluster of Ortologous Grups (COG) categories, presented in different colours, in the assembled WGS of strains [redacted] (compact columns) and [redacted] (striped columns).

Circular bacterial genome maps. In the case of the [redacted] (Figure 3.8), Prokka identified a total of [redacted] genes, consisting mostly of CDS and some tRNA sequences.

Additionally, [redacted] features associated with antibiotic resistance genes were detected using the CARD REGI, through a low-specificity and high-sensitivity detection approach. These weak hits included genes such as [redacted].

Furthermore, [redacted] features related to bacterial mobile genetic elements and phages were detected using mobileOG-db annotation, though these results also involved low-specificity and high-sensitivity detection.

Figure 3.8. CGView genome map of [redacted], using the Proksee Genome Analysis Sofware. From the outside to the inside, the first and ninth circles are the features detected with mobileOG-db annotation, in different colours, on the positive and negative chains, respectively; the second and eighth circles are the CARD RGI results (in orange) on the positive and negative chains, respectively; the third and the seventh circles are the coding sequences (CDSs), in black, on the positive and negative chains, respectively; the fourth circle correspond to the backbone of contigs, in grey; the fifth circle is the GC content, in blue; the sixth circle is the GC-skew value (in green for GC Skew+ and in purple for GC Skew-), and the innermost circle is the genome size indicator.

In the case of the [redacted] (Figure 3.9), [redacted] genes were identified by Prokka, also consisting mostly of CDS and some tRNA sequences.

Additionally, [redacted] features related to antibiotic resistance genes were detected using the CARD REGI database, with low-specificity and high-sensitivity. These weak hits included genes such as [redacted].

Furthermore, [redacted] features related to bacterial mobile genetic elements and phages were detected using mobileOG-db annotation, though these results also involved low-specificity and high-sensitivity detection.

Figure 3.9. CGView genome map of [redacted], using the Proksee Genome Analysis Sofware. From the outside to the inside, the first and ninth circles are the features detected with mobileOG-db annotation, in different colours, on the positive and negative chains, respectively; the second and eighth circles are the CARD RGI results (in orange) on the positive and negative chains, respectively; the third and the seventh circles are the coding sequences (CDSs), in black, on the positive and negative chains, respectively; the fourth circle correspond to the backbone of contigs, in grey; the fifth circle is the GC content, in blue; the sixth circle is the GC-skew value (in green for GC Skew+ and in purple for GC Skew-), and the innermost circle is the genome size indicator.

Assessment of potential antimicrobial resistance. According to the results obtained with ResFinder-4.5.0, in the case of [redacted] (Table 3.1), [redacted] AMR genes were found in its WGS data (with high-specificity and low-sensitivity detection), including [redacted].

Table 3.1. Antibiotic Resistant Genes of [redacted] found by using ResFinder-4.5.0, from the Center for Genomic Epidemiology.

Resistance gene	Identity	Phenotype	Accession number
[redacted]	[redacted]	[redacted]	[redacted]
[redacted]	[redacted]	[redacted]	[redacted]
[redacted]	[redacted]	[redacted]	[redacted]

On the other hand, according to the CARD-RGI results, a total of [redacted] different antibiotic resistance genes were found in the WGS data of strain [redacted]. However, since the thresholds set by EFSA (2021) are at least 80% identity and 70% coverage, only the detected genes exceeding these thresholds are shown (Table 3.2). Thus, the main antimicrobial resistance genes (i. e., the high-confidence annotations) included [redacted]. Other antibiotic resistance genes found with a % Identity between [redacted].

Table 3.2. Putative antimicrobial resistance genes found in the Whole Genome Sequence data of [redacted], by using the Resistance Genome identifier from the Comprehensive Antibiotic Resistance Database (https://card.mcmaster.ca/analyze/rgi). Only findings above the EFSA (2021) thresholds are presented. The detection criteria was "protein homolog model" and the RGI criteria used was "Strict" for all the hits.

ARO term	AMR gene family	Drug class	Resistance mechanism	Identity (%)	Length (%)
[redacted]	[redacted]	[redacted]	[redacted]	[redacted]	[redacted]
[redacted]	[redacted]	[redacted]	[redacted]	[redacted]	[redacted]

The ARO term refers to the name of the antibiotic resistance gene. The last two columns refer, respectively, to % Identity of matching region; % length of reference sequence. ab. = antibiotic. ANT(6) is a category of aminoglycoside O-nucleotidyltransferase enzymes with modification regiospecificity based at the 6-hydroxyl group of the respective antibiotic. **Note: tet(45) gene is also presented despites its % Identity is lower than 80%.*

In the case of [redacted], no AMR genes were found in its WGS data according to the results obtained with ResFinder-4.5.0. However, when using the Resistance Genome identifier, [redacted] antimicrobial resistance genes were found in its genome information, but only [redacted] of them exceeded the EFSA thresholds, which are shown in Table 3.3. These high confidence annotated genes included the [redacted]. Other antibiotic resistance genes found with a % Identity between [redacted].

Table 3.3. Putative antimicrobial resistance genes found in the Whole Genome Sequencing data of [redacted] by using the Resistance Genome identifier from the Comprehensive Antibiotic Resistance Database (https://card.mcmaster.ca/analyze/rgi). Only findings above the EFSA (2021) thresholds are presented. The detection criteria was "protein homolog model" and the RGI criteria used was "Strict" for all the hits.

ARO term	AMR gene family	Drug class	Resistance mechanism	Identity (%)	Length (%)
[redacted]					

The ARO term refers to the name of the antibiotic resistance gene. The last two columns refer, respectively, to % Identity of matching region; % length of reference sequence. *ab. = antibiotic.*

Referring to the search for plasmids in the WGS data of both strains, none was found neither by using plasmidSPAdes nor MOB-Recon.

Secondary metabolites search. AntiSMASH 7.0 was used for the search of the main secondary metabolites that both strains have the genetic potential to produce. Both strains have the genetic potential to produce almost the same secondary metabolites. Different genomic regions with potential to produce the enzymes (NRPSs and PKsS) involved in the synthesis of [redacted] were detected in the WGS data of both strains with a 100% of similarity (in green). A coding region for [redacted] was also detected with a 100% of similarity. In addition, a region that may code for genes responsible for the [redacted] synthesis, via NRPSs, was found with a [redacted] of similarity (in orange) in both strains.

In the case of strain [redacted] (Table 3.4), two genomic regions with the genetic potential for coding the NRPSs involved in the [redacted] production were found with a [redacted] of similarity (in red). Also, a coding region with the potential of producing [redacted] was detected with [redacted] of similarity (in orange). Finally, a region with [redacted] was also found. Moreover, other regions probably involved in secondary metabolite production were detected with very low percentages of similarity for the compounds [redacted] were identified (not shown in the Table).

Table 3.4. Coding regions of the principal secondary metabolites presumably produced by [redacted], by using antiSMASH 7.0 (both using detection strictness “relaxed” and “strict”) on the Whole Genome Sequencing data assembled with Unicycler. The colours from the column “Similarity” indicate high (green), medium (orange) and low (red) values of similarity.

Region	Most similar known cluster		Similarity (%)
[redacted]	[redacted]	[redacted]	53
[redacted]	[redacted]	[redacted]	100
[redacted]	subtilosin A	[redacted]	100
[redacted]	bacilysin	[redacted]	100
[redacted]	fengycin	[redacted]	73
[redacted]	bacillaene	[redacted]	100
[redacted]	surfactin	[redacted]	43
[redacted]	sporulation killing factor	[redacted]	100
[redacted]	surfactin	[redacted]	43

NRP = non-ribosomal peptide; RiPP = ribosomally synthesized, post-translationally modified peptides.

On the other hand, in the case of strain [redacted] (Table 3.5), a region with the genetic potential for coding the NRPSs involved in the [redacted] synthesis was also found with an [redacted] (in orange) of similarity, and a coding region implied in the synthesis of [redacted] was detected with [redacted] of similarity (in red). Furthermore, other regions involved in secondary metabolite production were detected with very low percentages of similarity for the compounds [redacted] (not shown in the Table).

Table 3.5. Coding regions of the principal secondary metabolites presumably produced by [redacted], by using antiSMASH 7.0 (both using detection strictness "relaxed" and "strict") on the Whole Genome Sequencing data assembled with Unicycler. The colours from the column "Similarity" indicate high (green), medium (orange) and low (red) values of similarity.

Region	Most similar known cluster		Similarity (%)
[redacted]	[redacted]	[redacted]	[redacted]
[redacted]	[redacted]	[redacted]	[redacted]
[redacted]	[redacted]	[redacted]	[redacted]
[redacted]	[redacted]	[redacted]	[redacted]
[redacted]	[redacted]	[redacted]	[redacted]
[redacted]	[redacted]	[redacted]	[redacted]
[redacted]	[redacted]	[redacted]	[redacted]

NRP = non-ribosomal peptide; RiPP = ribosomally synthesized, post-translationally modified peptides.

2. Secondary metabolites production

The secondary metabolites produced by strains [redacted] were analysed by LC-QTOF-MS/MS, considering the information about the secondary metabolites detected in the WGS data of both strains by using antiSMASH 7.0. These metabolites, which mostly coincided for both strains, included [redacted]. Iturin A was added in the analysis for being a typically produced lipopeptide by *Bacillus* species.

Validation of the method for the quantitative LC-QTOF-MS/MS analysis. The matrix used, consisting of the reagents alone from the Landy medium (blank of reagents), did not cause any ion suppression. As a result, very similar amounts of surfactin C and iturin A variants were detected whether they were dissolved in pure solvent (methanol) or in the matrix. The **Accuracy** was assessed by comparing the response of samples spiked with a known amount of standard before extraction to those spiked after extraction. As it is shown in Table 3.6, the metabolite extraction method was much less accurate when using the samples prepared with the Protocol AP than the ones from the Protocol LM, as the recovery values obtained were much lower, [redacted].

Table 3.6. Accuracy determination of molecular standards, expressed as recovery percentages, by comparing the chromatographic peak areas of samples spiked with a known amount of the standard (2.5 ppm in Protocol AP and 1 ppm in Protocol LM) and processed with the corresponding protocol, to those of samples processed first and then spiked with the same known amount of the standard.

Compound	Spiked and extracted	Extract and spiked	Recovery (%)
A. Protocol AP (acidified and precipitated samples)			
[redacted]			
B. Protocol LM (Landy medium samples)			
[redacted]			

The values provided represent the average of three separate measurements taken from different samples.

The **detection limit (LOD)** and **quantitation limit (LOQ)** in the matrix were determined by comparing the measured signals from a reagent blank sample spiked with 0.1 ppm of standards to the signals of the baseline noise. As shown in Table 3.7, the average signal-to-noise ratio for these samples spiked with 0.1 ppm of surfactin C was [redacted]. Thus, a signal-to-noise ratio of 3:1 corresponds to a LOD of [redacted] ppm (or µg/mL) for surfactin C in the matrix. Similarly, a signal-to-noise ratio of 10:1 corresponds to a LOQ of [redacted] ppm (or µg/mL). The LOD values for all compounds ranged from [redacted], and the LOQ values ranged from [redacted]. The lowest values were observed for surfactin C and iturin A2, while the highest were found for iturin A6 ([redacted]). The LOD and LOQ were also measured in pure solvent (methanol), but since the results were identical for each compound, these values are not necessary to display.

Table 3.7. Limit of detection (LOD) and limit of quantification (LOQ) of the method for surfactin C and iturins A quantification (in ppm or µg/mL), determined in the matrix by measuring the signal-to-noise (S/N) of samples spiked with 0.1 ppm of the reference standards.

Compound	S/N	LOD (µg/mL)	LOQ (µg/mL)
[redacted]			

The signal-to-noise (S/N) values represent the average of three separate measurements taken from different samples spiked with 0.1 ppm of the reference standards.

Secondary metabolite quantification with chemical standard (quantitative LC-QTOF-MS/MS analysis). Similar amounts of surfactin C and iturin A variants were detected in the two replicates of the same bacterial strain. Therefore, the average value for each strain is presented in Table 3.8, and the recovery percentages calculated for each compound are applied in the concentrations shown. For the samples processed using Protocol AP, only surfactin C was detected in strains [redacted] minutes. The amount of surfactin C detected in strain [redacted] was significantly lower than in strain [redacted], with values of [redacted], respectively. Iturins were either not detected or detected at negligible levels in the growth medium of both strains. In the case of strain QST 713, a larger amount of surfactin C was detected of [redacted] at the same RT. Iturin A variants were detected at concentrations of [redacted], respectively. In terms of nanograms of metabolite per cells of the initial growth media, surfactin C was found at [redacted] for each variant.

In contrast, for the samples processed using Protocol LM, all compounds were detected in the metabolite-producing media of all strains. Specifically, for strains [redacted], similar amounts of iturin A variants were detected at concentrations ranging from [redacted] approximately, with RTs of [redacted]. These values corresponded to concentrations ranging from [redacted] in the inicial growth medium. Regarding to surfactin C, strain [redacted] produced less than half the amount produced by strain [redacted], with concentrations of [redacted]. However, the corresponding concentrations per cell in the initial growth medium were very similar, as the initial cell concentration was also half in strain [redacted], resulting in values of [redacted]. In the case of strain QST 713, all metabolites were detected in considerably higher amounts at the same RTs, including [redacted]. These concentrations, respectively, corresponded to [redacted].

Table 3.8. Quantification of secondary metabolites (in µg/mL or ppm) from the initial bacterial solutions, considering the calculated percent recoveries, produced by [redacted], and *B. subtilis* strain QST 713. The analysis was performed using LC-QTOF-MS/MS with the standard molecules surfactin C and iturin A.

Sample	**Strain** [redacted]	**Strain** [redacted]	**Strain QST 713**	
A. Protocol AP (acidified and precipitated samples)				***RT (min)***
[redacted]				
[redacted]				
[redacted]				
[redacted]				
B. Protocol LM (Landy medium samples)				***RT (min)***
[redacted]				
[redacted]				
[redacted]				
[redacted]				

RT = Retention Time (average), in minutes. The values correspond to the average of the quantification obtained from the two replicates processed separately for each strain (1 & 2).

Secondary metabolite identification without standard (qualitative LC-QTOF-MS/MS analysis). For compounds where no reference standards were available for quantification, tandem MS (MS/MS) was performed for qualitative analysis. Since the mass spectrometry analysis covered a mass-to-charge ratio (m/z) range from 100 to 1,700, [redacted], with an m/z of [redacted], was excluded from the analysis.

Compounds such as [redacted] were putatively identified using literature references, PubChem and ChemSpider databases, and the "Exact mass" and "Generate formula" tools from the Agilent MassHunter Qualitative Analysis 10.0. Additionally, surfactin C and iturin A2 were included as control compounds for putative identification, since prior quantitative data provided a reference to validate the results of this qualitative analysis. Moreover, as strain QST 713 is known to produce surfactin, iturin A, fengycin, and bacillaene, it was used as a control measure throughout the analysis.

The results from the bacterial growth medium processed using the full extraction protocol (Protocol AP) are summarized in Table 3.9. For surfactin C, all detected molecules across the samples with [M + H]+ m/z values near [redacted] min (as referenced in the literature and from LC-MS quantitative analysis) were putatively identified as surfactin C. Accordingly, surfactin C was detected in the growth media of all strains, with m/z values ranging from [redacted]. The only exception was replicate 2 of strain [redacted], where the molecule detected at the expected

RT had an m/z of [redacted]. In all other cases, the calculated mass errors, ranging from [redacted], were sufficiently low to ensure reliable identification.

Regarding iturin A2, no molecules resembling this compound were detected in the samples from strains [redacted]. In contrast, m/z values very close to the literature value of 1043.552 Da were detected in the two replicates of strain QST 713 ([redacted]), at a RT of [redacted] min, which was very similar to the RT from the qualitative analysis of [redacted] min. Thus, the molecules detected in these samples were assigned as iturin A2, with calculated errors near zero.

Regarding [redacted], all three bacterial strains were able to produce it, as molecules with m/z values ranging from [redacted], matching the values reported in the literature (m/z [redacted]). Additionally, the calculated errors ranged from [redacted] ppm, supporting the accuracy of the identification. A similar result was observed for [redacted]. Its exact mass is [redacted] Da, and the detected m/z values, between [redacted], were very close to this value, with RTs between [redacted]. Moreover, the calculated errors were also low, ranging from [redacted] ppm.

Compounds similar to [redacted] were detected in the MS spectrum of all samples, but the calculated errors were too high for reliable compound identification, exceeding [redacted] in most cases. Additionally, compounds resembling [redacted] were found exclusively in strain QST 713-2, with an m/z value of [redacted], but the error was again too large to consider the result valid, of [redacted].

Table 3.9. Putative assignation of the secondary metabolites produced by [redacted] and *Bacillus subtilis* strain QST 713, by LC-QTOF-MS/MS, based on m/z values. The bacterial samples correspond to the ones obtained with Protocol AP.

Compound / Metric	**Strain** [redacted]	**Strain** [redacted]	**Strain** [redacted]	**Strain** [redacted]	**Strain QST 713-1**	**Strain QST 713-2**
[redacted]	RT					
	m/z					
	error					
[redacted]	RT					
	m/z					
	error					
[redacted]	RT					
	m/z					
	error					

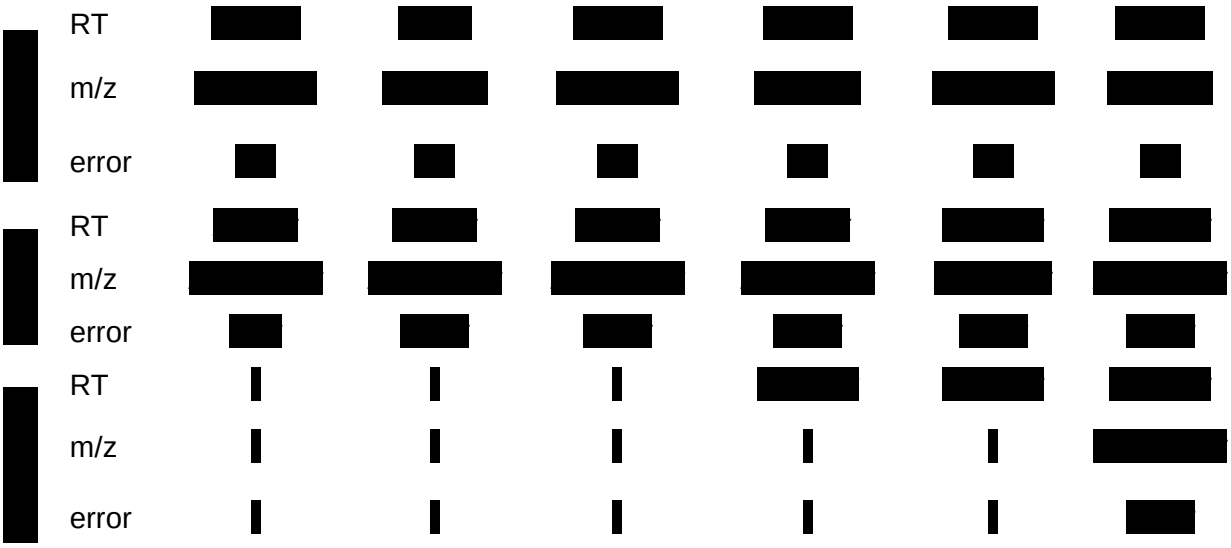

RT = Retention Time, in minutes; m/z ratio in Da; error in ppm. The asterisk (*) marks no reliable values.

For the samples processed using Protocol LM (Table 10), results were similar to those obtained with Protocol AP, particularly for surfactin C, [redacted], and [redacted]. Surfactin C was detected at an average RT of [redacted] min, with an m/z value of [redacted] and a low error of [redacted] ppm. The close match between these values and those from the quantitative analysis (RT of [redacted]) with similarly low errors allowed for the putative identification of these molecules as surfactin C in all samples. For iturin A2, compounds resembling this metabolite were identified across all samples at an average RT of [redacted] min, an m/z [redacted], and an average error of [redacted]. These values closely matched both the quantitative analysis (RT of [redacted]) and literature, confirming the assignment of these molecules as iturin A2.

[redacted] was found consistently across all samples with an average RT of [redacted] ppm. These values agreed with literature, supporting its assignment as [redacted]. Similarly, [redacted] was detected with an average m/z of [redacted] at [redacted] and an error of around [redacted], allowing for its putative identification in all samples. Additionally, in contrast to the results from Protocol AP, molecules resembling [redacted] were detected in all samples processed with Protocol LM. These molecules had an average RT of [redacted]—indicating a more reliable identification compared to previous analyses. As a result, these compounds were assigned to [redacted], which has an m/z of [redacted] according to the literature. Finally, although compounds resembling [redacted] were detected in all samples with m/z values close to the literature value of [redacted], the calculated errors were too high for a reliable identification, exceeding [redacted] ppm in most cases. Therefore, these compounds could not be confidently assigned to [redacted].

Table 10. Putative assignation of the secondary metabolites produced by [redacted] and *Bacillus subtilis* strain QST 713, by LC-QTOF-MS/MS, based on m/z values. The bacterial samples correspond to the ones obtained with Protocol LM.

Compound / Metric		**Strain [redacted]**	**Strain [redacted]**	**Strain [redacted]**	**Strain [redacted]**	**Strain QST 713-1**	**Strain QST 713-2**
[redacted]	RT	[redacted]	[redacted]	[redacted]	[redacted]	[redacted]	[redacted]
	m/z	[redacted]	[redacted]	[redacted]	[redacted]	[redacted]	[redacted]
	error	[redacted]	[redacted]	[redacted]	[redacted]	[redacted]	[redacted]
[redacted]	RT	[redacted]	[redacted]	[redacted]	[redacted]	[redacted]	[redacted]
	m/z	[redacted]	[redacted]	[redacted]	[redacted]	[redacted]	[redacted]
	error	[redacted]	[redacted]	[redacted]	[redacted]	[redacted]	[redacted]
[redacted]	RT	[redacted]	[redacted]	[redacted]	[redacted]	[redacted]	[redacted]
	m/z	[redacted]	[redacted]	[redacted]	[redacted]	[redacted]	[redacted]
	error	[redacted]	[redacted]	[redacted]	[redacted]	[redacted]	[redacted]
[redacted]	RT	[redacted]	[redacted]	[redacted]	[redacted]	[redacted]	[redacted]
	m/z	[redacted]	[redacted]	[redacted]	[redacted]	[redacted]	[redacted]
	error	[redacted]	[redacted]	[redacted]	[redacted]	[redacted]	[redacted]
[redacted]	RT	[redacted]	[redacted]	[redacted]	[redacted]	[redacted]	[redacted]
	m/z	[redacted]	[redacted]	[redacted]	[redacted]	[redacted]	[redacted]
	error	[redacted]	[redacted]	[redacted]	[redacted]	[redacted]	[redacted]
[redacted]	RT	[redacted]	[redacted]	[redacted]	[redacted]	[redacted]	[redacted]
	m/z	[redacted]	[redacted]	[redacted]	[redacted]	[redacted]	[redacted]
	error	[redacted]	[redacted]	[redacted]	[redacted]	[redacted]	[redacted]

RT = Retention Time, in minutes; m/z ratio in Da; error in ppm. The asterisk (*) marks no reliable values.

Furthermore, all the formulas generated with the Agilent software, as well as the calculated exact masses of the precursor adducts as [M + H]+ for each compound, coincided with those found in scientific literature. Specifically: [redacted]. Since [redacted] could not be confidently assigned to the detected molecules due to the high calculated errors, it was not possible to extract a reliable formula or exact mass using the Agilent software.

DISCUSSION

The current best practices typically involve combining both short- and long-read technologies to achieve a more accurate and complete genome assembly (van Dijk et al., 2023; Marx, 2023). However, the WSG-based bioinformatics analysis in this work relied solely on short-read sequencing technology, as it was intended as a preliminary study. Therefore, the resulting assembly for both strains showed a relatively high number of contigs, indicating that it may be fragmented or incomplete. This limitation suggests that the assembly could be further improved with the integration of long-read data, which would help to resolve repetitive regions and produce a more contiguous and reliable genome sequence.

Referring to the **taxonomic identification**, based on the evidence presented in the results section according to the WGS data, [redacted] is a member of the species [redacted] and is closely related to [redacted] type strain, with an ANI value over 98%. These results matched with the taxonomic identification performed in Chapter 1 by performing a BLAST in the NCBI using the 16S rRNA sequence. [redacted].

Referring to strain [redacted], based on the WGS data, this strain is a member of the species [redacted] and is closely related to [redacted] type strain, with an ANI value over 98%. In this case, the results of the taxonomic identification also coincided with the previous species assignation using the 16S rRNA gene sequence. [redacted]. On the other hand, strain [redacted] also showed an identity over 95% with [redacted], which was expected since [redacted].

Moreover, the **phylogenetic trees** constructed were consistent with the taxonomic assignments made using the 16S rRNA gene and the WGS data, as the closest strains identified in the trees matched those found in the BLAST search with the highest similarity scores. Additionally, these results align with phylogenetic relationships of *Bacillus* species widely reported in the literature (Adelskov & Patel, 2016; Patel & Gupta, 2020). Moreover, it is worth noting that most of the type strains appearing in both phylogenetic trees are shared between strains [redacted], indicating that these two strains are phylogenetically close to each other.

On the other hand, the results of the **GO analysis** are consistent with those reported by Li et al. (2020), where [redacted] was also the most abundant category, within which the five most frequent pathways identified were, in both studies, [redacted]. Additionally, in this work, the [redacted] were the most abundant pathways in the [redacted], while [redacted] were predominant in the [redacted] category. These findings also coincided with the annotations reported by Li et al. (2020).

On the other hand, regarding to the **COG classification**, from a total of gene counts higher than [redacted] in both cases, the great majority of them belonged to the [redacted], according with the Database of Clusters of Orthologous Genes (COGs), from the NIH. The following more abundant category was the [redacted]. The gene counts in genomes of strains [redacted] were very similar, which is also in accordance with scientific literature. For instance, in Li et al. (2020), a total of 3,046 genes were classified into COG categories, within which [redacted] were the most enriched COGs. In addition, in Liu et al. (2023), a total of 3,261 functional genes of *B. subtilis* RLI2019 were annotated based on the COG database, from which 1,277 genes were classified into the [redacted].

In the **circular genome maps,** gene annotation was performed using Prokka, identifying [redacted], respectively. In contrast, analysis of the genomic data by TYGS assigned [redacted] proteins to the CDS identified in each strain. It is essential to note that gene count and protein count are not identical and do not have to match, although they are closely related.

Gene count refers to the total number of genes in a genome, including both protein-coding genes (CDS) and non-coding RNA genes (like rRNA and tRNA), while protein count specifically refers to the number of unique proteins produced from CDS. In *Bacillus* species, the protein count can exceed the gene count due to factors like post-translational modifications (Macek et al., 2007), alternative protein isoforms, and secondary metabolite biosynthetic gene clusters, which allow a single gene to produce multiple proteins (Sansinenea & Ortiz, 2011). Additionally, evolutionary adaptations can lead to lineage-specific proteins that increase

diversity (Nikolaidis et al., 2022). Other reasons for a higher protein count include gene overlap, misannotation, or alternative start codons.

Furthermore, automated gene prediction tools such as Prokka or TYGS can sometimes over-predict coding regions, leading to the identification of more protein-coding genes than actually exist and increasing the protein count. A similar outcome was observed when using the CARD REGI tool within the Proksee platform, which, due to the low-specificity and high-sensitivity detection settings, identified [redacted] features related to antibiotic resistance genes in the assembled genomes of strains [redacted], respectively. However, a more accurate analysis of AMR genes, performed using more specific bioinformatic tools such as ResFinder-4.5.0 or the Resistance Genome Identifier directly from CARD and applying the “high-quality” parameter, yielded fewer gene assignments. This analysis excluded partial gene predictions and reduced the number of false positives, providing more reliable results.

Given that assessing **potential antimicrobial resistance** is a crucial factor in the registration and commercialization of microorganisms as PPPs—since they should not contribute to the pool of AMR genes or facilitate their spread—a more thorough analysis was conducted. It is important to note that particular attention is given to antimicrobials of high relevance for human and animal use, which the World Health Organization (WHO, 2019) classifies into three categories: Critically Important, Highly Important, and Important Antimicrobials. Also, while intrinsic AMR is not considered a safety concern (EFSA BIOHAZ Panel, 2023a), the presence of acquired resistance in a strain of a typically susceptible species is treated as a significant issue, warranting further investigation.

In this context, only AMR genes surpassing both the 80% identity and 70% coverage thresholds (EFSA, 2021) were considered in the analysis, as identified using ResFinder-4.5.0 and CARD-RGI with the "high-quality" parameter. This approach revealed that both studied strains carried some potential AMR genes initially detected by CARD-RGI on the Proksee platform. Specifically, in strain [redacted], genes that met the EFSA thresholds and were consistently identified by both ResFinder-4.5.0 and CARD-RGI included [redacted]. In strain [redacted], the genes [redacted] were confirmed. However, these genes were determined to be intrinsic to the species, with none associated with mobile genetic elements.

About the AMR genes found in the [redacted], the [redacted] gene encodes a [redacted]. The [redacted] gene

encodes a [redacted]. This gene is commonly found in *Bacillus amyloliquefaciens*. As the [redacted] gene is not present in most [redacted] genomes, it is recommended to carry out phenotypic test for tetracycline resistance (EFSA BIOHAZ Panel, 2023a).

The [redacted] gene encodes an [redacted]. This protein may confer resistance to several antibiotics, including the [redacted]. However, [redacted] gene is present in all of [redacted] strains and can be thus considered intrinsic.

Referring to the AMR genes detected in the genomes of both strains, the [redacted] gene, present also in the vast majority of [redacted] strains and can be thus considered intrinsic, encodes a [redacted]. In [redacted], but this reaction occurs inefficiently, resulting in an antibiotic-susceptible phenotype (Pawlowski et al., 2018). Lastly, the [redacted] genes encode components of a [redacted].

Moreover, verifying antimicrobial resistance through phenotypic testing is essential. Consequently, these analyses were conducted for both strains as part of project PLEC2021-007686. In summary, the results, provided confidentially by Biocontrol Technologies S.L., indicate that neither strain presents significant issues that would impede potential registration as PPPs.

As it has been mentioned, the principal problem of the AMR genes is whether they are linked to mobile genetic elements and therefore, these resistances could be transferred to other microorganisms in nature (EFSA BIOHAZ Panel, 2023a). Therefore, referring to the search for plasmids in the WGS data of the tested strains, none were found neither by using plasmidSPAdes (Galaxy Version 3.15.5+galaxy2) nor MOB-Recon (Galaxy Version 3.0.3+galaxy0). However, almost [redacted] features related to bacterial mobile genetic elements and phages were detected in both strains when using mobileOG-db annotation from Proksee, although these results involved again a low-specificity detection approach.

Notably, in *Bacillus* species, the presence of plasmids and MGEs varies widely depending on environmental and evolutionary factors. While many *Bacillus* strains harbour plasmids that confer adaptive advantages like antibiotic resistance or metabolic traits, some beneficial

strains may lack plasmids entirely. This absence is particularly common in non-pathogenic *Bacillus* strains from stable, low-stress environments where chromosomal stability is favoured, and the adaptive benefits of plasmids are less essential (Hafeez, 2024; Oyeniran & Oladunmoye, 2015). In fact, studies have shown that certain *Bacillus* strains prefer to integrate beneficial genes directly into their chromosomal DNA rather than maintain them on plasmids. For example, Li et al. (2020) found that *Bacillus* sp. S3 tended to incorporate MGEs into its chromosome, potentially enhancing genome stability. This tendency toward chromosomal integration may reduce the need for plasmid maintenance, especially in environments where plasmid-based traits like antibiotic resistance offer little advantage (Hafeez, 2024).

Thus, the presence of MGEs in *Bacillus* species is highly strain-specific and is generally more common in pathogenic or antibiotic-resistant strains. For example, *B. anthracis* is well-known for carrying virulence plasmids pXO1 and pXO2, which encode essential factors for its pathogenicity (Luna et al., 2006; Rood, 2014). Similarly, *B. cereus* can exhibit diverse plasmid profiles, with some strains harbouring virulence plasmids similar to those found in *B. anthracis*, while others lack them entirely (Klee et al., 2010; Pena-Gonzalez et al., 2018). This variability highlights considerable differences in plasmid content not only across species but also among strains within the same species, illustrating that plasmid presence is not universal, even within the same species (Bell et al., 2002; Ross et al., 2009). Overall, while plasmids offer advantages in specific contexts, their absence in certain beneficial *Bacillus* strains reflects adaptation to stable environments that prioritize chromosomal stability over rapid genetic shifts, underscoring the flexibility of *Bacillus* genomic architecture.

Regarding to the biocontrol features extracted from the WGS data, focusing on the **secondary metabolite production**, molecular studies on *Bacillus* revealed significant portions of the genomes dedicated to combat against plant pathogens. For instance, studies have shown that approximately 8.5% and 4% of the genomes of strains *B. amyloliquefaciens* FZB42 and *B. subtilis* 168, respectively, are dedicated to secondary metabolite production for this purpose (Raaijmakers & Mazzola, 2012). Therefore, a diverse array of *Bacillus* species has demonstrated antagonistic activity against various phytopathogens affecting agricultural crops such as maize, rice, and fruits (Wang et al., 2014; Li et al., 2015). In the case of *B. subtilis* strain QST 713, production of iturins, fengycins, surfactin, bacillaene, difficidin and ericins has been detected and may constitute part of the mode of action against pathogens (Anastassiadou et al., 2021).

Overall, genomic regions to produce [redacted] were identified in the WGS data of both strains. The different protocols for metabolite production (protocol AP and LM) conducted in this study revealed distinct differences in the

detection and quantification of compounds. Although the RTs obtained with both protocols were quite similar for all the compounds, the measured quantities differed a little due to the **accuracy** (or **recovery**) of the methods.

The recovery percentages from metabolite extraction using Protocol LM were significantly higher for all studied compounds compared to those achieved with Protocol AP. The low recoveries from Protocol AP indicated that it was unsuitable for extracting and quantifying the metabolites present in the growth medium, as only a minimal portion remained in the final solution prepared for LC-MS analysis. This outcome contrasted with Farzand et al. (2019), from which the protocol was originally derived.

Moreover, the recovery values for surfactin C were consistently higher than those for iturin A variants in both protocols, mostly in the Protocol AP. For instance, in Protocol AP, surfactin C had a recovery rate of only [redacted], while in the case of iturin A variants it was less than [redacted]. In contrast, Protocol LM achieved around [redacted] recovery for surfactin C, and between [redacted] for iturin A variants. Only the results from the Protocol LM aligned with those of Geissler et al. (2016), where the recovery rates for the model strain DSM 7T and strain DSM 23117 were 96.5% and 99.6% for surfactin, respectively, but only 68.6% and 71.6% for iturin A.

The limit of detection (LOD) and limit of quantitation (LOQ) were determined to **validate the method** for quantitative LC-QTOF-MS/MS analysis. For surfactin C, iturin A2, and iturin A4 were both less than [redacted], indicating that the method was sensitive enough to reliably detect and quantify concentrations above 0.1 ppm. In contrast, while the LOD of iturin A6 was almost [redacted] ppm ([redacted]), the LOQ was [redacted] ppm, meaning that concentrations between the [redacted] could be detected but not quantified accurately. Thus, only concentrations exceeding [redacted] could be accurately quantified for iturin A6.

In Geissler et al. (2016), the LOD for surfactin and iturin A was determined to be 16 ng/zone and 13 ng/zone, respectively, while the LOQ was calculated as 47 ng/zone for surfactin and 39 ng/zone for iturin A. Similarly, in our study, the LOD and LOQ values were found to be quite comparable to those reported by Geissler et al. (2016). For example, the LOD for surfactin C was [redacted].

The **quantitative LC-QTOF-MS/MS analysis** of secondary metabolite production using samples from protocol AP showed the lowest amount of surfactin C in the growth medium of strain [redacted]. Strain [redacted] and the positive control, QST 713, produced significantly higher amounts, at [redacted], respectively. No coding regions for iturins were identified in the genomic data of [redacted], and, as expected, no iturins were

detected in these strains when processed with protocol AP. In contrast, the positive control strain QST 713 produced high amounts of iturin A variants, including [redacted], in line with its genomic data. These findings are similar to those reported by Geissler et al. (2016), where, for the *Bacillus* strains DSM 10T, DSM 7T, and DSM 23117, the mean surfactin concentration was determined to be 54.9 µg/mL, 2.1 µg/mL, and 4.5 µg/mL, respectively, while iturin A was detected only in very small amounts or not at all.

In the samples processed using Protocol LM, a similar outcome was observed, but with higher quantities of metabolites for the strains tested. This is attributed to Protocol LM being more efficient in extracting and quantifying the metabolites, as reflected by the higher recovery percentages. Notably, iturin variants A2, A4, and A6 were detected in all three strains, with significantly higher concentrations found in strain QST 713. However, due to the presence of numerous compounds and reagents in the non-purified supernatant of the Landy medium, the interference and background noise were higher in this case.

Notably, the detection of iturin traces in bacterial culture broth via LC-MS, despite the absence of corresponding biosynthetic gene clusters in WGS data, is a known fact that can be attributed to several factors. One possibility is that limitations in genome annotation tools and databases might miss or misidentify biosynthetic gene clusters due to fragmented assembly, or because they encode unique (or poorly characterized) enzymes with limited homology to known proteins in reference databases (Medema et al., 2011). On the other hand, it is possible that the strain harbours cryptic or incomplete biosynthetic gene clusters that are not readily identifiable through standard genomic analysis but can still produce metabolites when environmental conditions are conducive (Adeniji et al., 2019). Regulatory mechanisms may influence the expression of these genes, resulting in the production of iturin in culture despite its absence in the genomic data (Kim et al., 2017; Deng et al., 2022).

Nevertheless, according to Tsuge et al. (2001), this unexpected detection of iturin traces could be attributed to alternative or homologous biosynthetic pathways that produce structurally similar compounds. In fact, bacteria are known to synthesize structurally similar compounds through variant metabolic routes, despite lacking the canonical biosynthetic genes associated with these metabolites. For instance, the *iturin A* operon in *Bacillus subtilis* RB14 can show structural similarities across different operons and strains, such as with the mycosubtilin operon (Tsuge et al., 2001). Although iturin A and mycosubtilin differ in specific amino acid arrangements, their high homology suggests that gene clusters might undergo domain swapping or horizontal gene transfer, leading to production of related compounds even if canonical pathways are absent (Tsuge et al., 2001). In this work, in fact, a genomic region with

the potential to produce [redacted] was detected in the WGS of strain [redacted] with a [redacted] of similarity.

Finally, the qualitative LC-QTOF-MS/MS analysis, performed for the less well-known secondary metabolites (no chemical standards available), allowed to characterize and confirm the identity of the detected compounds with greater accuracy. Since it is known that strain QST 713 produces surfactin, iturin A, fengycin, and bacillaene, the traces of these metabolites found in its growth medium could serve as a reference point for detecting, comparing and inferring the presence of these metabolites in the tested strains [redacted].

In this study, surfactin C was detected in all the samples from the Protocol AP, except from the case of strain [redacted], where the molecules detected could not be assigned to surfactin C. However, these values obtained in the other cases were quite close to the ones calculated with the software used ([redacted]) and to the m/z values from PubChem and literature (Geissler et al., 2016; Souza et al., 2018; Farzand et al., 2019). Moreover, surfactin C was also successfully assigned to the molecules detected in all the samples, with the RT, m/z values and calculated errors slightly lower than in the previous case. Regarding the other control compound iturin A2, the absence of a typical iturin A2 peak (m/z 1043.552) in strains [redacted] processed with Protocol AP aligns with the information obtained from the WGS data. However, for the same strains processed using Protocol LM, some molecules similar to iturin A2 were detected. However, it remains unclear whether these molecules can be definitively assigned to iturin A2, as mentioned. Overall, Iturin A2 was only conclusively identified in the samples from the control strain QST 713.

[redacted] was successfully assigned in all samples, with similar results obtained using both extraction protocols. The calculated errors from obtained data were very low in all the cases, being slightly lower with Protocol AP. These values coincided with the ones observed in PubChem and literature (Yang et al., 2015; Li et al., 2016; Souza et al., 2018; Farzand et al., 2019; Lin et al., 2020), where [redacted] was detected at m/z [redacted] with the precursor adduct [M + H]+. Moreover, [redacted] is one of the metabolites reported to be produced by strain QST 713, and therefore, considering this and the information from literature, the molecules found that resemble [redacted] can be presumptively identified as [redacted] with a high degree of confidence.

The calculated mass errors for [redacted] were notably low, particularly in the Protocol AP samples ([redacted]). These results align closely with those reported in PubChem and previous studies (Farzand et al., 2019; Su et al., 2020; Rabbee et al., 2023). Again, since [redacted] is one of the metabolites reported to be produced by strain QST 713, and also considering the

information from literature, the molecules found that resemble [redacted] can be potentially assigned to [redacted].

Molecules closely resembling [redacted] were detected in the growth media of all samples. However, in the samples from Protocol AP, the average m/z of [redacted] differed significantly from the reference [redacted] m/z value in the literature ([redacted]), resulting in a high error of [redacted] ppm, as calculated by the Agilent software, making accurate compound identification challenging. In contrast, samples from Protocol LM showed an average m/z of [redacted], with a much lower error of [redacted] ppm. This lower disagreement suggests that the detected molecules in Protocol LM could be putatively identified as [redacted], in line with values reported in PubChem and previous studies (Yang et al., 2015; Farzand et al., 2019).

Finally, [redacted] could not be definitively identified in any of the samples. In Protocol AP, only faint traces resembling [redacted] were detected in the growth medium of strain QST 713-2 ([redacted]), but with a high error of [redacted] ppm, making accurate assignment unreliable. Similarly, in Protocol LM, potential traces of [redacted] were found across all samples, but the average m/z ([redacted]) deviated significantly from the literature value ([redacted]), with an error of [redacted] ppm. These discrepancies hindered the conclusive identification of [redacted] in both protocols.

CONCLUSIONS

The main conclusion of this PhD chapter is that both *Bacillus* strains can be safely used as Plant Protection Products in agriculture. Genetic analysis showed they have typical *Bacillus* functions -including the ability to produce important antimicrobial compounds- and, while some antimicrobial resistance genes -typical from [redacted]- were found, they aren't linked to mobile genetic elements, meaning there's a low risk of transferring resistance to other organisms.

The principal conclusions extracted from this PhD chapter were:

1. Strain [redacted] was concluded to be a member of [redacted], while strain [redacted] resulted to belong to [redacted], both with an ANI value over 98% either by using the WGS information or the 16S rRNA gene sequence.
2. The genomes of both strains were assembled with Unicycler by using the WGS data obtained from Macrogen Inc.
3. Phylogenetic trees were constructed to determine relationships of the studied strains within the genus *Bacillus*, which results coincided with the ones determined by the taxonomical identification.

4. Regarding genome functional annotation, in both genomes, the highest gene counts were found in the GO category of [redacted]. With respect to the COG classification, most of the genes belonged to the [redacted].
5. [redacted] potential antimicrobial resistance genes ([redacted]) were found in the WGS data of strain [redacted], that are present in a majority of [redacted] genomes and are thus considered intrinsic. Those AMR genes were not associated with mobile genetic elements. On the other hand, strain [redacted] carries [redacted] potential antimicrobial resistance genes ([redacted]) above the EFSA thresholds, but none of them were associated with mobile genetic elements.
6. Different genomic regions with the capacity of producing [redacted] were identified in the WGS data of both strains, with a high percentage of similarity (between [redacted]).
7. Referring to the quantitative analysis via LC-QTOF-MS/MS using reference standards, high amounts of surfactin C were found in the metabolite producing medium of all the strains. In contrast, no or very low amounts of iturin A variants were detected in the samples. Only the positive control strain QST 713 was phenotypically confirmed as an iturin-producing strain. These results agreed with the WGS data.
8. Regarding to the validation of the LC-QTOF-MS/MS method, the recovery percentages obtained with Protocol LM were higher than the ones obtained with the Protocol AP for all secondary metabolites. Additionally, both LOD and LOQ for surfactin C, iturin A2, and iturin A4 was less than [redacted], indicating that the method was sensitive enough to reliably detect and quantify concentrations above 0.1 ppm. In contrast, while the LOD of iturin A6 was close to [redacted], the LOQ was higher ([redacted]), meaning that concentrations between [redacted] could be detected but not quantified accurately. Only concentrations of iturin A6 exceeding [redacted] could be quantified.
9. In the qualitative analysis via LC-QTOF-MS/MS, the secondary metabolites [redacted] were consistently detected in strains [redacted] and QST 713 using both metabolite extraction protocols. However, iturin A2 was only identified in strain QST 713 when using Protocol AP, and in all samples when using Protocol LM. Similarly, [redacted] could only be putatively detected in the samples processed with the protocol LM. Notably, despite the presence of genomic regions with the genetic potential to produce [redacted] in both strains, no evidence of this metabolite was observed in any sample.

Chapter 4. CHARACTERIZATION OF THE SELECTED ISOLATES: BIOFILMS

ABSTRACT

Bacillus species, particularly [redacted]*s* and close species, are known for their ability to form biofilms on plant surfaces, which enhance their persistence and efficacy as biocontrol agents in agricultural settings. This chapter investigates the biofilm formation capabilities of selected *Bacillus* strains ([redacted]) and their colonization and permanence on cucumber leaves (*Cucumis sativus*).

The biofilm formation process was studied through *in vitro* experiments using polystyrene plates and quantified by measuring Specific Biofilm Formation (SBF) values over time, where [redacted] demonstrated enhanced biofilm formation than [redacted]. The genetic basis for biofilm formation was explored through whole-genome sequencing and identification of key biofilm-related genes, including the [redacted]. On the other hand, the ecological characterization of these *Bacillus* strains involved monitoring their persistence on cucumber leaves under both controlled and outdoor conditions. Bacterial populations were assessed at various time points to determine their survival and colonization efficiency. Both *Bacillus* strains effectively colonized leaf surfaces. Although both performed similarly indoors (with lower populations than outdoors), [redacted] demonstrated greater resilience in outdoor conditions (under UV exposure), showing higher population stability compared to [redacted].

A detailed morphological analysis of the biofilms formed on leaf surfaces was conducted using Scanning Electron Microscopy (SEM). SEM revealed distinct differences in biofilm structure between the strains, with [redacted] forming more aggregated biofilms and [redacted] producing a more homogeneous, mucus-like biofilm. The interaction between these biofilms and plant pathogens, specifically *Pseudoperonospora cubensis* and *Podosphaera fusca*, was also examined. The results indicated that biofilm formation by *Bacillus* strains effectively inhibited pathogen colonization, particularly when applied as a preventive treatment.

The study concludes that biofilm formation is a critical factor in the effectiveness of *Bacillus* strains as biocontrol agents, with significant differences observed in the biofilm-forming abilities of the studied strains. [redacted] demonstrated superior biofilm formation and resilience on leaf surfaces, making it a promising candidate for biocontrol applications.

INTRODUCTION

1. Biofilms

Bacteria in nature often exist as members of structurally complex, surface-attached communities known as biofilms (Maddula et al., 2006). These biofilms typically consist of multiple layers of cells embedded in hydrated matrices and can form at nearly any solid-liquid or liquid-gas interface. The biofilm matrix slows the diffusion of small molecules in and out of the biofilm, creating an environment conducive to metabolic exchange (Kierek-Pearson and Karatan, 2005). In natural settings, biofilms may contain multiple species or strains coexisting, which can increase the chances for lateral gene transfer (Dahlberg et al., 1997; Roberts et al., 1999). Biofilm communities differ significantly from their surrounding environment and enable cells to perform functions not typically observed outside of the biofilm (Morris and Monier, 2003).

The biofilm's architecture is influenced by factors such as nutrient availability, quorum sensing, and the production of extracellular polysaccharides (Kierek-Pearson and Karatan, 2005; Maddula et al., 2006). Mature biofilms exhibit distinct gene expression patterns compared to individual bacterial cells. In this context, the formation of biofilms is hypothesized to create a "micro niche," a term first used by Costerton et al. (1994), which protects bacteria against various physical and chemical stresses, such as desiccation, UV radiation, antibiotics and detergents (Elkins et al., 1999; Davies et al., 2003; Mah et al., 2003).

Specifically referring to bacteria associated with plants, there are a wide range of interactions between them, including bacteria functioning as pathogens, commensals, or mutualists. These bacteria can form aggregated communities, or biofilms, on various plant surfaces such as leaves and roots, as well as within the intercellular spaces of plant tissues (Morris and Monier, 2003; Ramey et al., 2004; Danhorn and Fuqua, 2007).

Although the molecular mechanisms regulating the formation of biofilms may differ among species, its development is a well-organized process that follows defined steps (Maddula et al., 2006; Sauer et al., 2007). As it is shown in Figure 4.1, first include colony adhesion, with a reversible attachment which becomes irreversible (between 1 and 6 h approximately). The second step is the microcolony formation and maturation into three-dimensional structures with open channels (between 24 and 72 h approximately), followed by dispersion and propagation of the biofilm-forming cells and aggregates (Kierek-Pearson and Karatan, 2005; Sauer et al., 2007; Zhang et al., 2022).

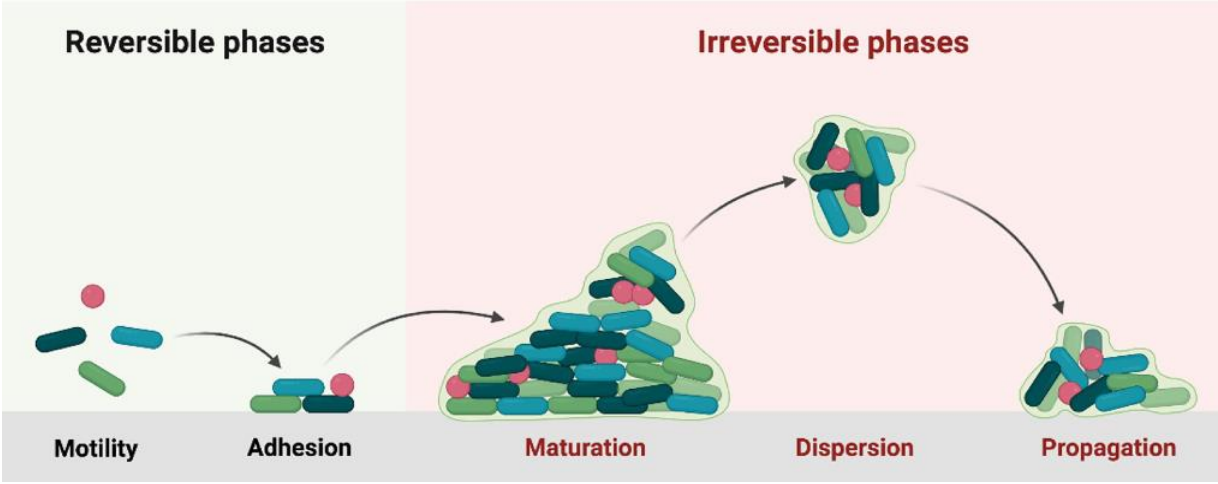

Figure 4.1. Typical cycle of biofilm formation. The stages of biofilm development, once bacterial cells have arrived on the surface, include a first adhesion with a reversible attachment to surface. Then, a microcolony is formed (with irreversible attachment to surface), which starts to mature in the form of a biofilm. Finally, the biofilm disperses and spreads, starting the cycle again. Image extracted from Zhang et al. (2022).

Biofilm formation in *Bacillus* species. The production of biofilms is a critical survival strategy that enhances *Bacillus'* resilience in various environments, including soil, water, and clinical settings. This phenomenon is particularly significant in *B. subtilis* and *B. cereus*, where biofilms contribute to their ability to colonize plant roots and pathogenicity, respectively, thereby influencing agricultural practices and food safety (Özdemir & Arslan, 2018; Yu et al., 2016).

In fact, the biocontrol efficacy of *Bacillus* spp. has mostly been linked to conserved genes mediating biofilm formation and to a great genomic and chemical diversity of secondary metabolites against plant pathogenic fungi (Chen et al., 2012). Studies have highlighted the ability of *Bacillus* isolates from natural environments to form stable biofilms and secrete surfactin upon root colonization and on plant surfaces, which collectively protect plants from pathogenic bacteria (Bais et al., 2004; Zeriouh et al., 2013). Moreover, species in the *B. subtilis* group can combat plant pathogens effectively due to the production of a wide variety of toxic substances and its multicellular behaviour (Nagorska et al., 2007). In addition, they have been shown to impact biotic stress in plants, decreasing disease incidence in various crops through induced systemic resistance (ISR) (Hashem & Tabassum, 2019).

Genes involved in the production of biofilms. The genetic basis of biofilm formation in *Bacillus* species is complex and involves multiple genes and regulatory pathways. Focusing on *B. subtilis* -which is commonly used as a model of biofilm formation (Beauregard et al., 2013; Mielich-Süss & Lopez, 2015)- it has been demonstrated that the extracellular matrix of its biofilms is mainly composed of an exopolysaccharide (EPS) component, synthesized by the 15-gene *epsA-O* operon, and the secreted protein TasA, which is a functional amyloid protein

encoded in the 3-gene operon *tapA-sipW-tasA* (Branda et al., 2006; Chu et al., 2008). Notably, these genes responsible for protein fibber and EPS production are kept inactive in actively growing, motile cells by the repressors SinR and AbrB (Elsholz et al., 2014). However, during biofilm formation, these repressors are lifted, allowing for high-level production of the protein and polysaccharide components of the extracellular matrix (Chu et al., 2006; Chai et al., 2008).

The exopolysaccharide (EPS) is a crucial carbohydrate component of the *B. subtilis* biofilm matrix, essential for maintaining biofilm architecture and function (Branda et al., 2006). EPS production involves a complex biosynthetic pathway encoded by a 15-gene operon, *epsABCDEFGHIJKLMNO* or *epsA-O* (Figure 4.2), which is similar to the N-glycosylation pathways found in other bacteria like *Campylobacter jejuni* (Arbour et al., 2023). The biosynthesis of EPS is regulated by several membrane-associated enzymes, including phosphoglycosyl transferases and glycosyltransferases. EpsL initiates the pathway by adding di-N-acetyl bacillosamine (diNAcBac) to a lipid carrier, and EpsD extends this structure by attaching N-acetyl glucosamine (GlcNAc). The EPS matrix promotes cell adhesion, provides structural integrity, and helps the biofilm resist mechanical forces, which are essential for the formation and stability of complex bacterial communities (Arbour et al., 2023).

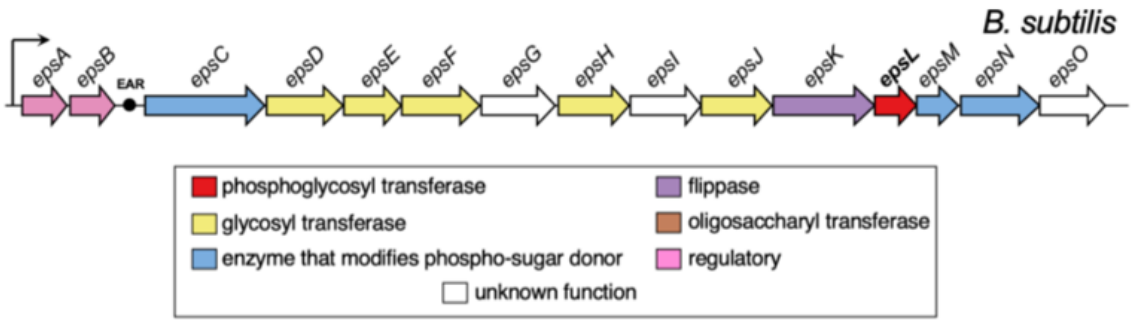

Figure 4.2. Chromosomal organization of the *epsA-O* operon genes involved in matrix synthesis in *B. subtilis*. Image extracted from Arbour et al. (2023).

On the other hand, TasA is the primary protein component of the biofilm extracellular matrix (Branda et al., 2006), where it forms amyloid fibbers that bind cells together within the biofilm, providing structural integrity and resilience against external stresses (Romero et al., 2010). It displays antibacterial activity against a range of both Gram-positive and Gram-negative bacteria (Stöver & Driks, 1999). In laboratory strains, TasA also plays a role in the proper assembly of the spore coat (Serrano et al., 1999). The regulation of its operon, i.e. the *tapA-sipW-tasA* operon, is influenced by various environmental signals, including the presence of surfactin, a signalling molecule that promotes biofilm development by inducing the expression of matrix genes (McLoon et al., 2011; Allard-Massicotte et al., 2016).

Additionally to the *tasA* gene, the *sipW* gene encodes Signal Peptidase I W, which is essential for cleaving the signal sequences of TasA and TapA (Chu et al., 2006; Romero et al., 2011). The *tapA* gene, in turn, encodes the anchoring/assembly protein for TasA, necessary for the proper anchoring and polymerization of TasA amyloid fibbers on the cell surface (Romero et al., 2011). TapA also serves as a minor structural component of TasA fibbers.

On the other hand, the *bslA* (or *yuaB*) gene also plays a crucial role in biofilm formation. It encodes a protein that self-polymerizes to form a protective layer on the biofilm surface, imparting hydrophobicity (Hobley et al., 2013; Liu et al., 2017). This layer is highly stable and withstands significant mechanical compression (Kobayashi & Iwano, 2012). BslA is essential for the development of complex colony architecture and may work synergistically with exopolysaccharides and TasA amyloid fibbers to support the assembly of the biofilm matrix (Ostrowski et al., 2011).

In addition to the *tasA* and *bslA* genes, the *bslB* gene, although less studied than the others, is also characteristic of *Bacillus* species. It plays a minor role in biofilm architecture and may contribute to surface hydrophobicity (Morris et al., 2017).

2. Leaf colonization and permanence

Bacillus species can effectively colonize the leaf surfaces of plants, establishing themselves in the phyllosphere, where they can exert beneficial effects on plant health and growth, and provide protection against pathogens, making them valuable in agricultural practices (Baard et al., 2023; Abdullahi et al., 2021; Bjelić et al., 2020). The ability of *Bacillus* species to persist on plant leaves is influenced by several factors, including the specific strains involved and environmental conditions such as moisture and surface type, which can significantly affect their survival and colonization efficiency (Cuyk et al., 2011).

Bacillus species have been isolated from various plants, indicating their adaptability and potential as beneficial microorganisms in diverse agricultural settings (Bjelić et al., 2020; Abdullahi et al., 2021; Tessema, 2023). For instance, *B. amyloliquefaciens* has been shown to reduce the incidence of diseases like citrus canker by promoting plant health and resilience (Qian et al., 2020). However, the survival of *Bacillus* species on plant leaves under outdoor conditions, particularly under UV exposure, poses significant challenges. Research indicates that UV radiation can adversely affect the viability of these bacteria, although some strains exhibit remarkable resilience. For example, some *B. thuringiensis* used as PPPs have been reported to persist on vegetation for extended periods, even in direct sunlight, highlighting the importance of strain selection for effective biocontrol applications (Cuyk et al., 2011).

The relationship between biofilm formation and the permanence of *Bacillus* species on plant leaves is a critical area of study, particularly in understanding how these bacteria can effectively colonize and persist in the phyllosphere. Thus, biofilms are essential for their survival and colonization on leaf surfaces. The biofilm matrix, composed of polysaccharides and proteins, not only facilitates adhesion but also protects the bacteria from adverse environmental conditions, thereby promoting their longevity on plant leaves (Tian et al., 2021; Baard et al., 2023). For instance, the production of surfactin by *B. subtilis* has been shown to enhance biofilm formation and surface colonization, which is crucial for their persistence on leaf surfaces (Tian et al., 2021). Moreover, the interaction between biofilm formation and environmental factors such as moisture and leaf wettability also play a significant role in the permanence of *Bacillus* species on leaves. Studies have shown that the wettability of leaf surfaces can influence the colonization efficiency of *Bacillus* species, with more hydrophilic surfaces promoting better adhesion and biofilm development (Cerón-Carpio et al., 2023).

In addition, when exposed to UV radiation, certain strains exhibit remarkable resilience to UV light, which is partly attributed to their biofilm-forming ability. The biofilm matrix can shield the bacterial cells from UV damage, allowing them to maintain their population levels on leaf surfaces even under harsh sunlight (Baard et al., 2023). This protective effect is crucial for their role as biocontrol agents, as it enables them to persist long enough to exert beneficial effects on plant health and to compete with pathogenic microorganisms (Baard et al., 2023).

Plant endophyte *Bacillus*. On the other hand, certain *Bacillus* species have the capacity to act as plant endophytes, i. e., microbes that reside within plant tissues without causing harm, and being able to confer numerous benefits to their host plants (Qiao et al., 2017; Albdaiwi et al., 2019). Research has shown that *Bacillus* species possess a range of mechanisms that contribute to their role as beneficial endophytes. These mechanisms include the production of phytohormones, such as auxins and gibberellins, as well as the secretion of enzymes that facilitate nutrient availability (Qiao et al., 2017; Kushwaha et al., 2021; Nithyapriya et al., 2021). Additionally, these bacteria can induce systemic resistance in plants, enabling them to better withstand biotic and abiotic stresses (Beneduzi et al., 2012; Manasa et al., 2021). Furthermore, studies have indicated that endophytic *Bacillus* strains can outcompete pathogenic microorganisms for colonization sites, thereby preventing infections (Olanrewaju et al., 2021). Therefore, the ability of *Bacillus* species to persist within plant tissues is also crucial for their effectiveness as biocontrol agents, being their resilience particularly important in agricultural settings, where plants are often exposed to various stressors (Adewale et al., 2015; Albdaiwi et al., 2019).

OBJECTIVES

The main objective of this chapter was to investigate and characterize the biofilm formation capabilities of selected *Bacillus* strains, [redacted] and [redacted], and to evaluate the role of biofilms in enhancing the colonization and persistence on plant leaves, to promote overall efficacy of these strains as biocontrol agents on plant surfaces against key plant pathogens.

The specific objectives were:

1. Quantify biofilm formation of strains [redacted] *in vitro*, by measuring the number of adherent cells present in 96-well polystyrene plates via measurements of the absorbance at 540 nm.
2. Study of the genes involved in the formation of biofilms which are present in the genomic data of strains [redacted].
3. Ecological characterization of strains [redacted], focused on their colonization and persistence on leaf surfaces, both indoors and outdoors, to assess the impact of environmental factors such as UV exposure and desiccation on bacterial survival.
4. Morphological characterization, determination of leaf surface colonization and biofilm formation patterns of strains [redacted] using Electron Microscopy, both *in vitro* and *in planta*, either independently or in combination with the plant pathogens *Pseudoperonospora cubensis* and *Podosphaera fusca*.

MATERIALS AND METHODS

Materials and growth/experimental conditions

The bacterial strains [redacted] and [redacted], stored at -80 ºC, were defrosted and spread on Trypticasein Soy Agar (TSA, from Condalab, Spain) Petri dishes to conduct the experiments.

The seeds of *Cucumis sativus* var. “Marketer” were provided by Semillas Fitó S.A. The plants were grown in an IBERCEX growth chamber (Ibercex-ASL. S.A., Madrid, Spain) during 3 weeks at 25ºC and 65% RH, with 16 h of light (white cool lamps with a mean PAR of 221 µmol m^{-2} s^{-1}) and 8 h of darkness.

The experimental conditions set for the studies with the cucumber downy mildew pathogen *Pseudoperonospora cubensis* were 19 ºC, a relative humidity (RH) around 90% and a cycle of 14h of light, inside plastic tunnels with a mean PAR of 180 µmol m^{-2} s^{-1}. On the other hand, the

studies performed with the cucurbit powdery mildew pathogen *Podosphaera fusca* were set at 25 ºC, a RH around 90% and a cycle of 16 h of light, inside plastic tunnels with a mean PAR of 205 µmol m^{-2} s^{-1}. Both pathogens were collected from infected cucumber plants grown in commercial greenhouses in Almería, between 2020 to 2023.

1. Biofilm formation on inert surfaces

Bacterial growth. Bacterial solutions were prepared by liquid culture in Luria Bertani (LB) broth (from Condalab, Spain), incubated at 30 ºC and 150 rpm during 24 h. Then, bacterial suspensions were centrifuged (4,000 g for 10 min) and pellets were suspended in sterile distilled water. The absorbance at 600nm (OD_{600}) of the solutions were read and concentrations were adjusted to 1 x 10^7 Colony Forming Units per mL (CFU/mL).

96-well polystyrene plates were used in the experiment, where a volume of 1.5 µL of each cell suspension was inoculated into 150 µL per well of two liquid media: LB and King's B (KB), according to Puopolo *et al.* (2014). In each plate, 40 wells were filled in with LB and 40 with KB. Bacterial strains were inoculated into half of the wells with each medium, leaving the rest of the wells as a negative control and stablishing 20 replicates per experimental condition. The plates were then incubated at 28 ºC during 0 h, 24 h, 48 h and 72 h. After the incubation, the final cell densities in each well were determined again by reading the OD_{600} through a xMARK™ Microplate Spectrophotometer (Bio-Rad) and using the Microplate Manager® Software (Bio-Rad).

Cellular staining and decolourization: adherent cells determination. To remove detached cells, the plate was turned over and gently tapped on absorbent paper. After fixing the remaining adhered bacterial cells to the plates for 20 minutes at 60 °C, 150 µL per well of 0.1% crystal violet solution was used for staining for 1 minute. Excess dye was removed by turning the plate over and two successive washes were done with 250 µL of distilled water per well. After that, adherent cells were decolorized with 200 µL per well of an acetone/ethanol (20%/80%) solution for 5 min to release the dye into the mixture (Puopolo *et al.*, 2014).

After that, 100 µL of each well solution was transferred, respectively, to the wells of a new 96-well polystyrene plate The amount of dye was quantified by reading the absorbance at 540 nm (OD_{540}), which is proportional to the density of adherent cells, by using the same xMark™ Microplate Spectrophotometer (Bio-Rad Laboratories, Inc.) and the Microplate Manager® 6 Software (Bio-Rad Laboratories, Inc.). Thus, the biofilm formation was determined at 0 h, 24 h, 48 h and 72 h. Per each well, OD_{540} values (adherent cells) were divided by OD_{600} values (bacterial growth) to calculate the Specific Biofilm Formation value (SBF). The experiments were repeated three different times per each bacterial strain and collecting time point.

2. Genes involved in the formation of biofilms

After defrosted, bacterial strains [redacted] were grown on TSA Petri dishes for 48 h at 30 ºC. Genomic DNAs were extracted using E.Z.N.A.® Bacterial DNA Kit (Omega Bio-tek), following the fabricant's instructions. The genomic DNAs were sent to Macrogen Inc. to perform the Whole Genome Sequencing, as explained in the previous chapter. The assembly was performed by Unicycler (https://github.com/rrwick/Unicycler) and the annotation of the genomes was conducted by Prokka (Galaxy Version 1.14.6 + galaxy1) (https://usegalaxy.org/root?tool_id=toolshed.g2.bx.psu.edu/repos/crs4/prokka/prokka/1.14.6+galaxy1). Data was returned and stored as Excel files, where the genes involved in the formation of biofilms were searched. The predicted Amino Acid (AA) sequences of the encoded proteins were analyzed using BLAST against UniProtKB/Swiss-Prot, the expertly curated segment of UniProtKB database (https://www.uniprot.org/). This process involved submitting the amino acid sequences to UniProtKB's BLAST tool (https://www.uniprot.org/blast) to identify and compare their similarity with sequences from other bacterial species.

Additionally, for genes without an attributed coding sequence, such as regulatory genes, a more targeted search was conducted by performing a BLAST analysis using the reference sequences of the corresponding genes from the NCBI database (https://www.ncbi.nlm.nih.gov/) within the genomic data of both strains. Specifically, the regulatory genes searched were the [redacted], both from the model type strain [redacted].

3. Ecological characterization: leaf colonization of the strains

Bacterial solutions of strains [redacted] were prepared as described previously, adjusted to 1 x 10^8 CFU/mL, and 1 mL was sprayed on the first fully expanded leaf of *Cucumis sativus* plants, maintained under controlled condition in the growth chamber. Leaf samples from the different plant treatments were collected at different times, corresponding to day 0 (or 2 h), day 1, day 3, day 6 and day 8 after the bacterial inoculation.

The treated leaves were collected and cut in 9 cm^2 pieces (3 cm wide × 3 cm long). Since the average area of the cucumber leaves used for the experiment was approximately 100 cm^2 and 1 mL was inoculated to the whole leaf, the final volume corresponding to the 9 cm^2 (~10 cm^2) of leaf pieces is approximately 0.1 mL, i.e. 1 x 10^7 CFU. The collected leaf pieces were then submerged in 10 mL of 9% saline solution and strongly vortexed for at least 1 min. Ten-fold dilutions were made for each bacterial solution until it could be spread on a TSA Petri dish and the number of colonies could be determined (in a range of 30 - 300 CFU).

The experiments were conducted three different times. In each experiment, 3 replicates were set per treatment and a total of 4 TSA Petri dishes were obtained through two sets of dilution tubes. The evolution of the CFU per cm^2 was analysed in each experiment at the given time points (days 0 or 2 h after inoculation, day 1, day 3, day 6 and day 8) and values represent the mean of all replicates for each strain and time point.

UV-survival assays. The same experiment was performed also outdoors. For this purpose, plants were progressively acclimatised: cucumber seeds were germinated in the growth chamber until the seedlings emerged, approximately a week after sowing. Then, the seedlings were transferred to a greenhouse for another week until the stage with the first two leaves quite developed. Finally, they were left outdoors during the period of the study, following the procedure explained above. The climatological data was extracted from Meteo.cat, Servei meteorològic de Catalunya, from the automatic station Barcelona – Zona Universitària (meteo.cat - https://www.meteo.cat/observacions/xema/dades?codi=X8).

Additionally, a set of plants inoculated with the same bacterial inoculum was set and studied under controlled condition in the growth chamber in order to stablish comparisons between the leaf populations found in both environments. Again, the experiments were conducted three different times and, in each experiment, 3 replicates were prepared per treatment and collecting point.

4. Statistical analysis

Data from all experiments were analysed using the Statistical Package for the Social Sciences (SPSS, IBM SPSS Statistics 25; SPSS Inc., Chicago, IL, United States). For each experimental condition—defined by bacterial strain and time point—the mean and Standard Error of the Mean (SEM) were calculated by averaging values across the three independent experiments. Comparisons were made between bacterial strains and with the respective controls across all specified time points. Statistical analysis was performed using one-way ANOVA and Tukey's post hoc test with a significance threshold of $p < 0.05$. Statistically distinct groups were denoted by different letters.

5. Scanning and Transmission Electron Microscopy

Preparation of the inoculums. Bacterial inoculums were prepared as explained above: strains were cultured in LB liquid media for 24 h with agitation, centrifuged (4000 g for 10 min) and adjust to 1×10^8 CFU/mL by reading the OD_{600}.

Both pathogens, *Pseudoperonospora cubensis* and *Podosphaera fusca*, were obtained from fresh infected cucumber leaves by gently scratching the surface of the leaf with a brush to obtain the sporangia or conidia, respectively, submerged in distilled water. The pathogens suspensions were observed in a Neubauer chamber under an optical microscope to adjust the concentration to 1 x 10^4 sporangia or conidia, respectively, per mL.

Chemical fixation for Transmission Electron Microscopy (TEM). The plant material consisted of 3-weeks old *Cucumis sativus* plants, inoculated with 1 x 10^4 sporangia/mL of the cucurbit downy mildew pathogen *P. cubensis.*

The leaf samples (only leaf 1) were collected at different days after the pathogen inoculation (dpi): at 0 dpi, 1 dpi, 3 dpi and 6 dpi, to qualitatively visualize the evolution of the pathogen once arrived at the plant. Two samples of 0.5 cm^2 from the infected plant material (with sporulation of the pathogen) were cut and put into a glass vial containing 1.5 mL of the fresh chemical fixer for TEM, which consisted of 2% paraformaldehyde and 2.5% glutaraldehyde in 0.1 M phosphate buffer. Two vials with 2 plant samples each were prepared and stores for maximum 2 days in the fridge at 4ºC.

After that, the vials were brought to the TEM-SEM Electron Microscopy Unit of the Scientific and Technological Centres (CCiTUB), University of Barcelona, for the pertinent sample preparation. Thus, samples were first incubated at 4°C for 30 minutes and an additional 4 h under vacuum. Following fixation, samples were washed at 4°C in the fixation buffer for 10 minutes, then rinsed four times for 10 minutes each in 0.1 M phosphate buffer (PB) at pH 7.4 at 4°C. Subsequently, a solution of 1% osmium tetroxide, 0.8% potassium ferrocyanide, and 0.1 M PB (pH 7.4) was added, and samples were incubated for 2.25 h at 4°C in the dark. Excess osmium was removed with four 10-minute washes in double-distilled water at 4°C. The samples were then dehydrated with a graded series of acetone and infiltrated with Spurr resin before polymerization. Ultrathin sections (60 nm) were prepared using a Leica UC7 ultramicrotome and stained with aqueous uranyl acetate and Reynolds lead citrate. Imaging was performed on a J1010 Transmission Electron Microscope (Jeol) equipped with an Orius CCD camera (Gatan) at an acceleration voltage of 80 kV.

Lyophilization for Sanning Electron Microscopy (SEM). *Cucumis sativus* plants were inoculated with one of the mentioned bacterial strains at a concentration of 1 x 10^8 cells/mL. In the cucumber downy mildew pathosystem, only preventive treatments with the *Bacillus* strains were studied, which consisted of treating the plants with the corresponding bacterial strain 24 h before inoculating the pathogen (at 1 x 10^4 sporangia/mL, as mentioned). On the other hand, in the pathosystem for cucurbit powdery mildew, against the pathogen *P. fusca*, both

preventive or curative treatments with the *Bacillus* strains were performed, which consisted of the inoculation of the plants 24 h before the pathogen inoculation or 5 days after the pathogen inoculation, respectively.

The inoculated leaves samples from the different plant treatments were collected at different times, corresponding to 0 dpi, 1 dpi, 3 dpi and 6 dpi. Two samples of approximately 0.5 cm^2 of plant material were cut and put into an empty Eppendorf. Two Eppendorfs were prepared and submerged in liquid nitrogen to freeze the plant material. Rapidly, the Eppendorfs were taken out and closed with parafilm with 3 little holes to allow the water to come out and they were lyophilized (-40 ºC into the void) for about 48 h.

The Eppendorfs were securely sealed and transported to the CCiTUB, at the Hospital Clínic. The samples were mounted on microscope holders using conductive adhesive discs (double carbon tape). They were then coated with a thin layer of carbon to enhance their electrical conductivity (Quorum Q150T Plus). Observations were conducted with the JEOL JSM-7001F equipment (Jeol, Japan) at 15 kV at the CCiTUB.

Bacterial strains fixed on poly-L-lysine coverslips. The bacterial strains were cultivated in LB liquid media during 48 h, as explained above, and the bacterial solutions were sent to the TEM-SEM CCiTUB to be processed. Very briefly, a drop of the sample was deposited on coverslips with poly-L-lysine (to ensure adhesion) and then they were fixed by a standard fixation protocol (washes, osmification, dehydration in ethanol, critical point drying, assembly and conductive coating). Finally, the samples were visualized by the JEOL JSM-7001F microscope at the CCiTUB.

RESULTS

1. Biofilm formation on inert surfaces

Data on the ability to produce biofilms on inert surfaces (polystyrene) for both *Bacillus* strains is showed on Figure 4.3. When comparing the two culture media, LB and KB, LB consistently supported the highest cell production across all time points (Figure 4.3A). After 72 h, strain [redacted] reached a final cell density (OD_{600}) of [redacted] in LB, while strain [redacted] achieved [redacted]. In contrast, KB medium resulted in significantly lower final cell densities, with final OD_{600} values of [redacted].

When comparing the two strains, no significant differences in cell density were observed in LB medium at 24 h. However, in KB medium, strain [redacted] showed a higher cell density (OD_{600} of [redacted]) compared to strain [redacted] (OD_{600} of [redacted]). Similar trends were observed at 48 and 72 h: in

LB medium, strain [redacted] exhibited significantly higher cell densities ([redacted], respectively) than strain [redacted] ([redacted], respectively). Conversely, in KB medium, strain [redacted] had lower cell densities ([redacted]) than strain [redacted] ([redacted]).

Regarding the number of adherent cells, measured by absorbance at 540 nm (Figure 4.3B), significant differences were observed at 24 h only between strain [redacted] grown in KB and strain [redacted] grown in LB, with OD_{540} values of [redacted], respectively. At 48 and 72 h, similar trends continued. Notably, significant differences were found for strain [redacted] between the two media, with OD_{540} values of approximately [redacted]. Additionally, strain [redacted] consistently showed significantly higher levels of adherent cells, with OD_{540} values ranging from [redacted] across the same time points.

The similarity in both OD_{600} and OD_{540} values observed at 48 and 72 h suggests that the growth curve begins to plateau at 48 h. This indicates that both cell densities and cell adhesion reach their stationary phase at this point, with minimal changes in growth or adhesion beyond 48 h.

The biofilm-forming ability is shown in Figure 4.3C. At 24 h, significant differences were only observed for strain [redacted] grown in LB medium, which had a significantly lower SBF value compared to all other conditions. Strain [redacted] in LB again showed the lowest SBF value ([redacted]) at 48 h, while its SBF value in KB, and those of strain [redacted] in LB, were around [redacted]. These values, in turn, were significantly lower than the SBF value for strain [redacted] grown in KB, which reached [redacted]. Significant differences were observed between all conditions at 72 h. SBF values ranged from the highest, observed in strain [redacted] ([redacted]), to the lowest in strain [redacted] ([redacted]).

Figure 4.3. Time course of cell adhesion by the two bacterial strains [redacted] (circles) and [redacted] (triangles) in two different liquid media, Luria-Bertani medium (black) and King's B medium (white), over 3 days. **A.** Bacterial growth measured as the bacterial cell density read at 600 nm (OD_{600}). **B.** Adherent cells determination by reading the absorbance at 540 nm (OD_{540}). **C.** Ability to produce biofilm in terms of Specific Biofilm Formation (SBF), calculated as the ratio of adherent cells (OD_{540}) to bacterial cell density (OD_{600}). The experiments were conducted three different times, with 20 replicates for each data point. The reported values represent the means of the data collected across all cases for the same strain and time point. The error bars represent the Standard Error of the Mean (SEM). The statistical analysis was conducted evaluating the differences between the bacterial strains and the culture media for each time point. Statistical differences are represented with letters, according to ANOVA and Tukey's test (p-value < 0.05).

2. Genes involved in the biofilm formation

In both strains [redacted], genes typically involved in biofilm formation in *Bacillus* species were identified via a BLAST search in the UniProtKB database to compare the similarity of the gene sequences with the reference type strain [redacted]. In all cases, the covery, the E-value and the percentage of identity were almost at the maximum score. Results are shown in Table 4.1. Notably, no differences were found in the genes involved in biofilm production between the two bacterial strains. However, the identity percentages for all predicted protein sequences were higher in strain [redacted], likely because the type strain [redacted] also belongs to [redacted].

Table 4.1. Genes involved in the formation of biofilms identified in the WGS data annotated with Prokka of the two bacterial strains [redacted] and [redacted].

gene	Uniprot entry	Identities [redacted]	Length (AAs) [redacted]	Identities [redacted]	Length (AAs) [redacted]
[redacted]					

BLAST searches were performed against the reference type strain [redacted]. The E-values are not shown because they were all 0 or very close to 0.

Additionally, a *misc_RNA* (miscellaneous RNA, with a potentially important but not clearly defined function within standard RNA classifications) was identified in both strains, with the predicted product being [redacted].

Moreover, a BLAST search within the genomes of the studied strains for sequences similar to the regulatory genes [redacted] from the type strain ([redacted]) revealed that the [redacted]. This suggests that the genes [redacted] may perform analogous roles to the [redacted] genes, potentially contributing to [redacted] in these strains. Specifically, in strain [redacted], the [redacted]. In strain

[redacted], the [redacted].

3. Ecological characterization: bacterial leaf colonization

Leaf populations in controlled conditions. The ability of the two strains to colonize and persist on leaf surfaces was determined and compared, as shown in Figure 4.4. At day 0 (2 h post-inoculation), no significant differences were observed in the cell populations of strains [redacted] and [redacted] on the leaves, as both strains started with similar inoculum concentrations: [redacted]. However, significant differences were found compared to the bacterial populations naturally present on the leaves, which were around 30 times lower ([redacted]) on the non-inoculated (control) plants.

By day 1, both strains showed significantly decreased cell populations than levels observed immediately after inoculation, with [redacted]. In this sense, significant differences were found between the two strains as well as when compared to the naturally occurring bacterial populations on the untreated control plants.

An interesting observation was made on day 3, when the bacterial population on the control plants began to increase, reaching [redacted]. Significant differences were also noted between the two inoculated strains at this time, with strain [redacted] having a significantly lower population ([redacted]) compared to strain [redacted]. However, none of them was significantly different compared to the untreated controls.

Nevertheless, cell populations of strains [redacted] remained relatively stable over the course of the 8-day analysis, with no significant differences observed between the strains nor the untreated controls at days 6 and 8. The final cell populations reached [redacted] for the untreated untrol plants.

Figure 4.4. Bacterial populations on cucumber leaves (*Cucumis sativus* var. Marketer) grown under controlled conditions (growth chamber). The circles represent strain [redacted], the triangles represent strain [redacted], and the squares represent the naturally occurring bacteria (NOB) on the untreated control plants. Data were collected at days 0 (or 2 h), 1, 3, 6, and 8 after bacterial inoculation. The experiments were performed three times and values are the mean of all replicates for each strain and time point. Error bars indicate the Standard Error of the Mean (SEM). Statistical analysis was performed on a daily basis to assess differences between bacterial strains, with significant differences indicated by different letters, according to ANOVA and Tukey's test (p-value < 0.05).

UV exposure and survival on leaves. The ambient conditions found outdoors during the week of the experiment are shown in Table 4.2.

Table 4.2. Climatological data extracted from Servei Meteorològic de Catalunya (Zona Universitària) of the weeks during which the UV-light exposure experiments were conducted.

Climatological data	**11/09 - 18/09/23**	**09/04 - 16/04/24**	**28/05 - 05/06/24**
Average temperature	24.1 °C	17.3 °C	20.5 °C
Average relative humidity	75.9 %	52.0 %	70.8 %
Accumulated precipitation	4.1 mm	0.0 mm	0.4 mm
Global solar radiation	16.7 MJ/m^2	23.8 MJ/m^2	27.3 MJ/m^2

The comparisons of naturally occurring bacterial populations and *Bacillus* strains [redacted] found outdoors and under controlled conditions are presented in Figure 4.5. The initial inoculum for each bacterial strain was the same in both environments, being [redacted]

[redacted]. The naturally occurring bacterial populations on leaves were around [redacted] under controlled conditions and [redacted] outdoors. The *Bacillus* strains behaved differently according to the environment, reaching the highest values with strain [redacted] under outdoors conditions ([redacted]). In contrast, strain [redacted] showed similar performance across both growth conditions, with lower leaf population levels compared to strain [redacted].

By day 1, similar cell populations were observed for strain [redacted] under controlled conditions and strain [redacted] outdoors, both around [redacted]. These populations were significantly higher than those of strain [redacted] under UV exposure and strain [redacted] under controlled conditions, which were approximately [redacted], as well as the naturally occurring bacteria on untreated plants in both environments.

At day 3, no significant differences were observed between the bacterial isolates and the untreated controls or environmental conditions. By day 6, however, significant differences appeared between the two strains when grown outdoors, with strain [redacted]. Significant differences were also observed between outdoor and controlled conditions, where both strains showed populations around [redacted]. In both cases, bacterial populations were significantly higher than the naturally occurring bacteria on the untreated plants from both environments.

At day 8, strain [redacted] showed no significant differences between conditions, maintaining populations around [redacted]. Conversely, strain [redacted] exhibited significantly higher populations in outdoor conditions ([redacted]) compared to under controlled conditions ([redacted]). Significant differences from untreated control plants in both environments were also evident at this time point.

Notably, in leaf samples where one of the strains was applied, naturally occurring bacterial populations were significantly reduced compared to those on untreated control plants, suggesting that the strains may also inhibit the growth of other bacteria.

Figure 4.5. Bacterial populations on cucumber leaves (*Cucumis sativus* var. Marketer) grown under protected conditions (growth chamber, in black) or outdoor conditions (UV exposure, in white). The circles represent strain [redacted], the triangles represent strain [redacted], and the squares represent the naturally occurring bacteria (NOB) on the untreated control plants. Data were collected at days 0 (or 2 h), 1, 3, 6, and 8 after bacterial inoculation. The experiments were performed three times and values are the mean of all replicates for each strain and time point. Error bars indicate the Standard Error of the Mean (SEM). Statistical analysis was performed on a daily basis to assess differences between bacterial strains and the growth conditions, with significant differences indicated by different letters, according to ANOVA and Tukey's test (p-value < 0.05).

4. Scanning & Transmission Electron Microscopy

***Pseudoperonospora cubensis*.** Regarding the lyophilized and coated leaf samples for SEM, the fresh and dry weights were measured to determine the minimum time needed to dry the piece of leaf completely. The results showed that 24 h of lyophilization were enough, since no differences were found in the dry weight at 24 and 48 h (Table 4.3).

Table 4.3. Fresh and dry weight of the different leaf samples lyophilized at -40 ºC into the void for 2 days.

Sample	Fresh weight (g)	Dry weight at 24h (g)	Dry weight at 48h (g)
1	0.0046	0.0007	0.0006
2	0.0058	0.0012	0.0012
3	0.0060	0.0012	0.0012

The SEM images from Figure 4.6 correspond to *P. cubensis* on *Cucumis sativus* plants, 12 days after pathogen inoculation. In images A and B, *P. cubensis* is seen emerging from the leaf stoma, the small openings on the leaf surface, in both early (A) and more advanced stages (B) of hyphal development. This emergence appears in a striking branched formation, resembling a flower structure, with each branching element set to grow and form the hyphae that will eventually colonize the leaf surface more extensively. In images C, D, E and F, it can be clearly seen that the pathogen has developed into a highly branched hyphal network that is actively producing sporangia, the spore-like structures that release zoospores critical for pathogen spread and infection. The SEM images capture the dense, intricate network of the pathogen, indicating a robust and well-established infection as it matures and new sporangia production is more prolific, setting the stage for further plant colonization.

Moreover, a transversal section of a cucumber leaf under TEM is shown in Figure 4.7. This series of TEM images provides a detailed view of the intracellular morphology of *P. cubensis* within the infected cucumber leaf. In image A, a plant stoma is shown transversally, where the guard cells and the stomatal pore are clearly observed, not yet colonized by the pathogen. The image B show a close-up, intracellular view of a guard cell, where various cytoplasmic structures and organelles are distinctly visible, offering a detailed illustration of its cellular organization. In image C and E, a transverse cut of the leaf reveals the pathogen confined to the most superficial layer, close to the external environment, suggesting its preference for occupying the substomatal cavity of the outermost leaf tissues. The pathogen adheres firmly to the outer epidermal cells, both externally and internally, indicating its capacity to penetrate and secure itself within the leaf tissue causing stomata closing. Finally, images D and F offer a closer look of the pathogen's attachment and interactions with the outer epidermal cells on the leaf’s underside. It is worth noting (image D) the notable thickness of the plant cell wall, as consequence of the presence of the pathogen. Figures D and F allow to observe the different sizes between the pathogen and the plant cell wall. Also, it is showed a detailed intracellular view of *P. cubensis*, where the pathogen's complex cytoplasmic structures and various organelles are visible, illustrating its cellular organization. The differences between the two cell types, i. e., the pathogen (oomycete) and plant cells can be clearly appreciated: the pathogen cells have a darker grey colour, a much denser cytoplasm and thinner walls compared to the plant cells.

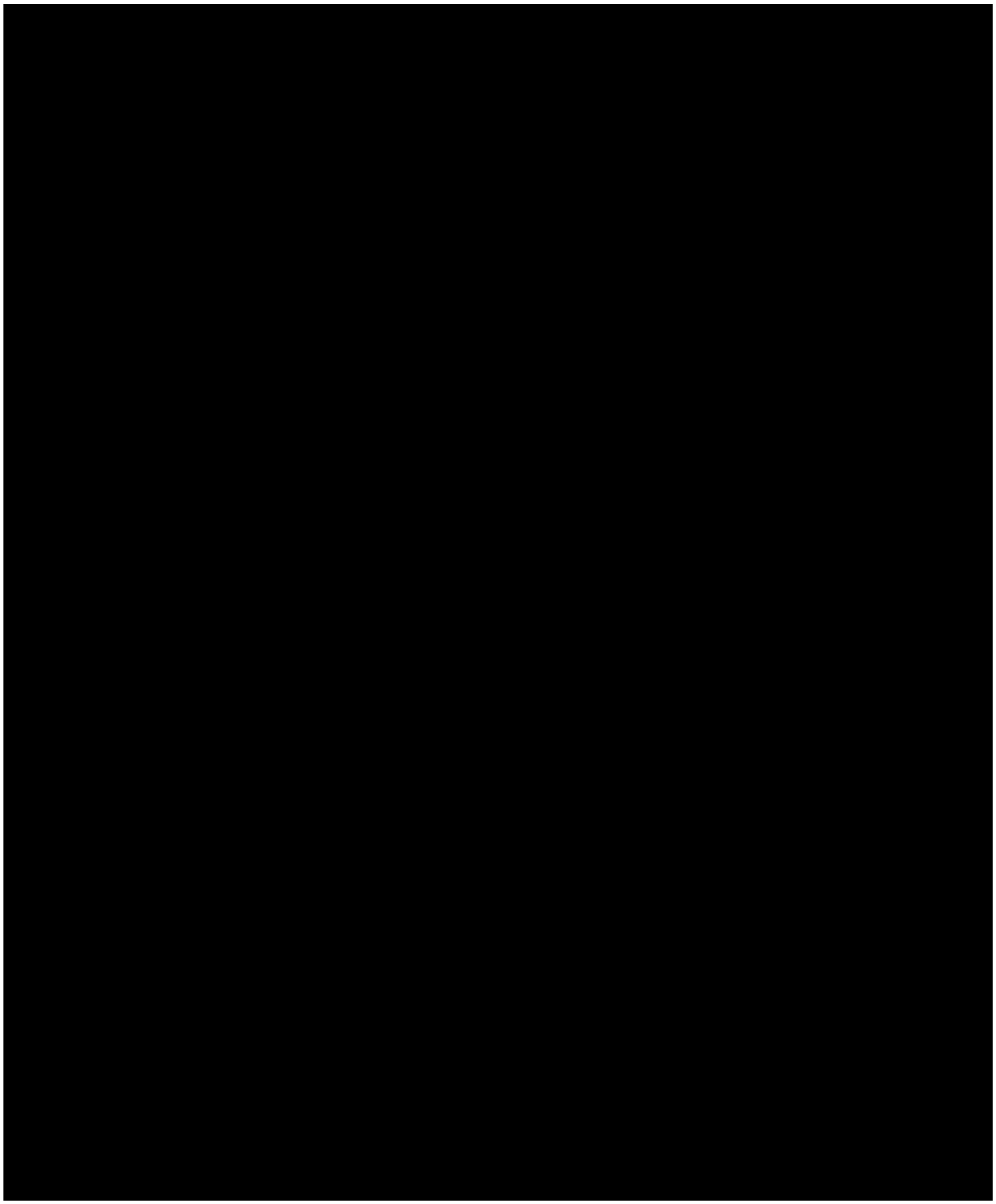

Figure 4.6. Morphology of *Pseudoperonospora cubensis* on the underside of *Cucumis sativus* var. "Marketer" leaves visualized using SEM, 12 days after inoculation. **A & B.** Sporangiophores emerging from a stoma. **C.** A mature sporangiophore emerging through a stoma. **D & E.** Sporangia attached to highly branched sporangiophores. **F.** Highly sporangia-producing sporangiophores wrapping around and ascending a trichome on the plant leaf.

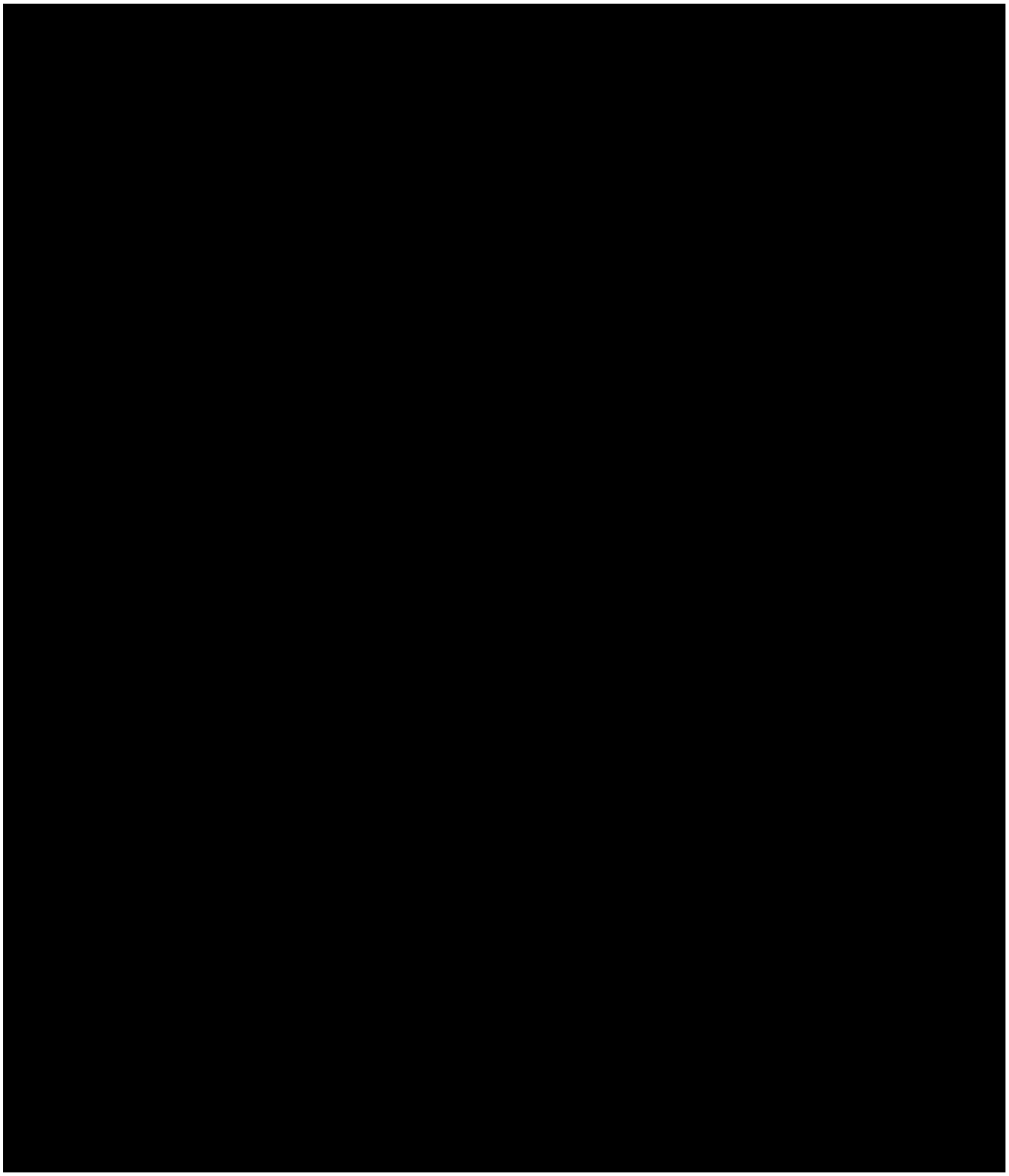

Figure 4.7. Transverse section of a *Cucumis sativus* var. "Marketer" leaf infected with *Pseudoperonospora cubensis*, visualized using TEM, 12 days after inoculation. **A & B.** Stoma shown transversally, where the guard cells and the stomatal pore are clearly observed. **C.** The outermost cell layers of the leaf show *P. cubensis* adhering to the epidermal cells, both externally and internally. **E.** Transverse section of the leaf reveals the pathogen localized in the most superficial region. **D & F.** Transversal section of *P. cubensis*, where a great variety of organelles and cytoplasmatic structures inside the pathogenic cells can be observed.

***Podosphaera fusca*: SEM of the lyophilized and coated leaf samples.** The SEM images from Figure 4.8 show the progressive infection by *P. fusca* on cucumber leaves, which were taken between 3 and 12 days after pathogen inoculation. In image A, the pathogen is present but has not yet formed a dense hyphal network, although some conidial chains can be already seen. In image B, several dehydrated conidia are clearly visible, likely remnants from the initial pathogen inoculation rather than newly produced conidia. In images C and D, there is an increase in hyphal development, as *P. fusca* expands its presence on the leaf surface, indicating an intermediate stage where the infection is more established but still in the growth phase. Notably, new conidia are beginning to form, arranged sequentially in a chain-like structure, each attached one by one. The images E, and F illustrate a dense and extensive network of hyphae covering much of the leaf surface, indicative of an advanced infection stage. By this time, *P. fusca* is well established, and the dense hyphal matrix (or mycelium) is likely producing conidia actively, contributing to further pathogen dispersal.

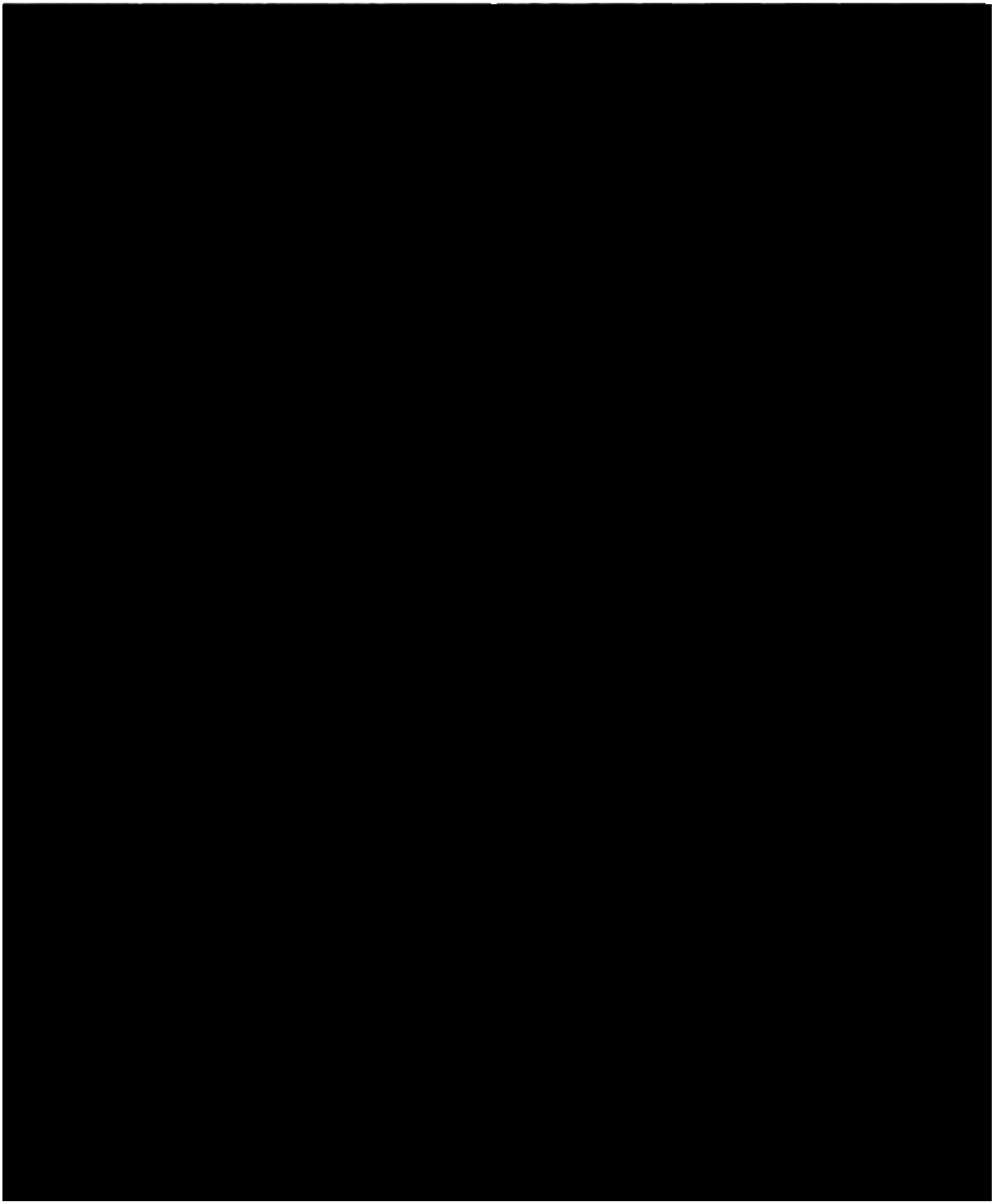

Figure 4.8. Morphology of *Podosphaera fusca* on the underside of *Cucumis sativus* var. "Marketer" leaves visualized using SEM. **A.** Early stage of pathogen infection. **B.** Several dehydrated conidia. **C & D.** Hyphal development as *P. fusca* expands its presence on the leaf surface, where new conidia are beginning to form, arranged sequentially in a chain-like structure. **E & F.** Dense and extensive network of hyphae (mycelium) covering much of the leaf surface.

Bacterial strains [redacted] and [redacted]. Figure 4.9 illustrates a morphological and behavioural comparison between [redacted] (images A & B) and [redacted] (images C & D) after 48 h of incubation on poly-L-lysine coverslips, which provides a controlled substrate to evaluate cell dimensions and morphological features. Individual cells (A & C) and initial cluster formations are visible (B & D).

Quantitative analysis based on 30 measurements of each strain highlights a slight but significant difference in cell dimensions. For [redacted], the average cell size is approximately [redacted]. In comparison, [redacted] measures slightly shorter in length, at an average [redacted], but is wider, with an average cell width [redacted]. Additionally, both strains display the characteristic rod-shaped morphology typical of the *Bacillus* genus, with cells appearing elongated and uniformly organized. The poly-L-lysine substrate enhances cell adherence, facilitating the formation of structured clusters that indicate early biofilm development. Notably, the cells of strain [redacted] seem to exhibit a higher level of organization compared to strain [redacted], aligning in pairs or forming chain-like structures.

The Figure 4.10 shows the colonization and growth behaviour of [redacted] on cucumber leaves over a six-day period, illustrating its interactions with the plant's surface. On day 1 (A and B), there is already evidence of increased bacterial clustering and early biofilm formation, suggesting that [redacted] has adhered and adapted extremely fast to the leaf environment and is beginning to establish a stable presence. By day 3 (C and D), a thick biofilm covers a large portion of the leaf surface, with a high density of bacterial cells clearly visible and distinguishable from one another. By day 6 (E and F), a well-defined biofilm is visible, with densely packed bacterial cells covering the leaf surface, predominantly clustering around the stomata. Thus, the formation of a dense biofilm is evident, containing small particles likely produced by the bacterial cells themselves to stabilize the biofilm matrix, as clearly seen in images B, D and F.

Similar to the previous figure, the images from Figure 4.11 document the colonization dynamics of [redacted] on cucumber leaves over a six-day period. On day 1 (A), [redacted] cells are sparsely present on the leaf surface, in a pattern that suggests initial attachment without substantial biofilm development. In contrast, in image B, some cells have already begun to form a biofilm and adhere to the leaf surface. By day 3 (C and D), the cells begin to form small clusters and some biofilms, indicating a transitional phase toward biofilm development as the bacteria adapt to the plant surface environment. Image D is showing a close-up view of a closed stoma slightly covered by the biofilm. Notably, the biofilm

margins are evident in images A and C, delineating areas with and without bacterial colonization. By day 6 (E and F), a more extensive biofilm has formed, with densely clustered cells covering the leaf surface, demonstrating the strain's capacity to establish a stable presence similar to that of [redacted]. In image F, the small particles likely produced by the bacterial cells to stabilize the biofilm matrix are also visible.

Figure 4.9. Comparative morphology and cell size analysis of [redacted] (**A & B)** and [redacted] (**C & D**) on poly-L-lysine coverslips after 48 h of incubation. Individual cells (A & C) and initial cluster formations (B & D) are visible.

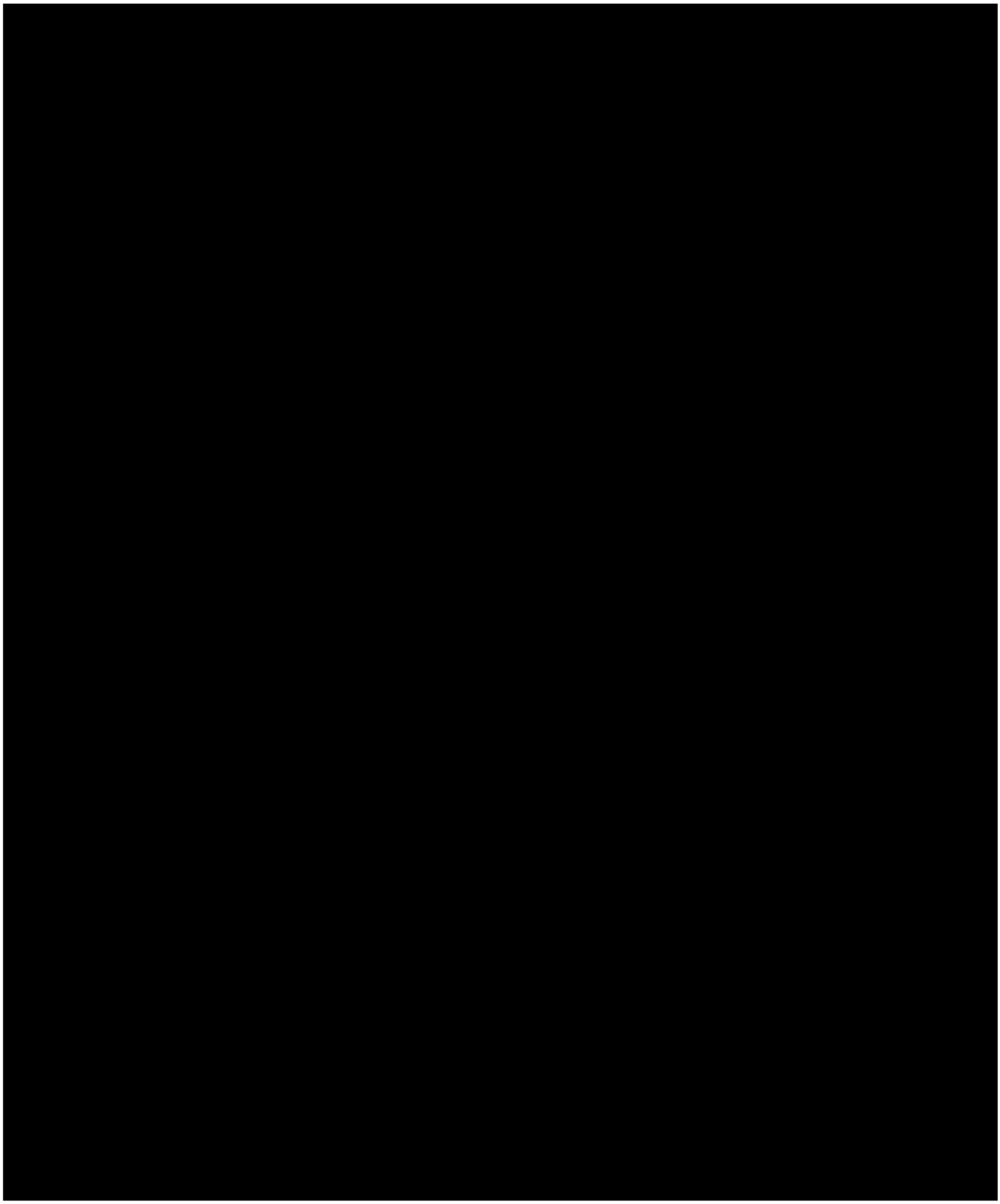

Figure 4.10. Morphological and behavioural characterization of [redacted] on the reverse of *Cucumis sativus* var. "Marketer" leaves collected on day 1 (A and B), day 3 (C and D), and day 6 (E and F). **A, C, & E.** Panoramic views of the bacterial biofilm. **B, D, & F.** Close-up views of the biofilm, where individual bacterial cells are visible.

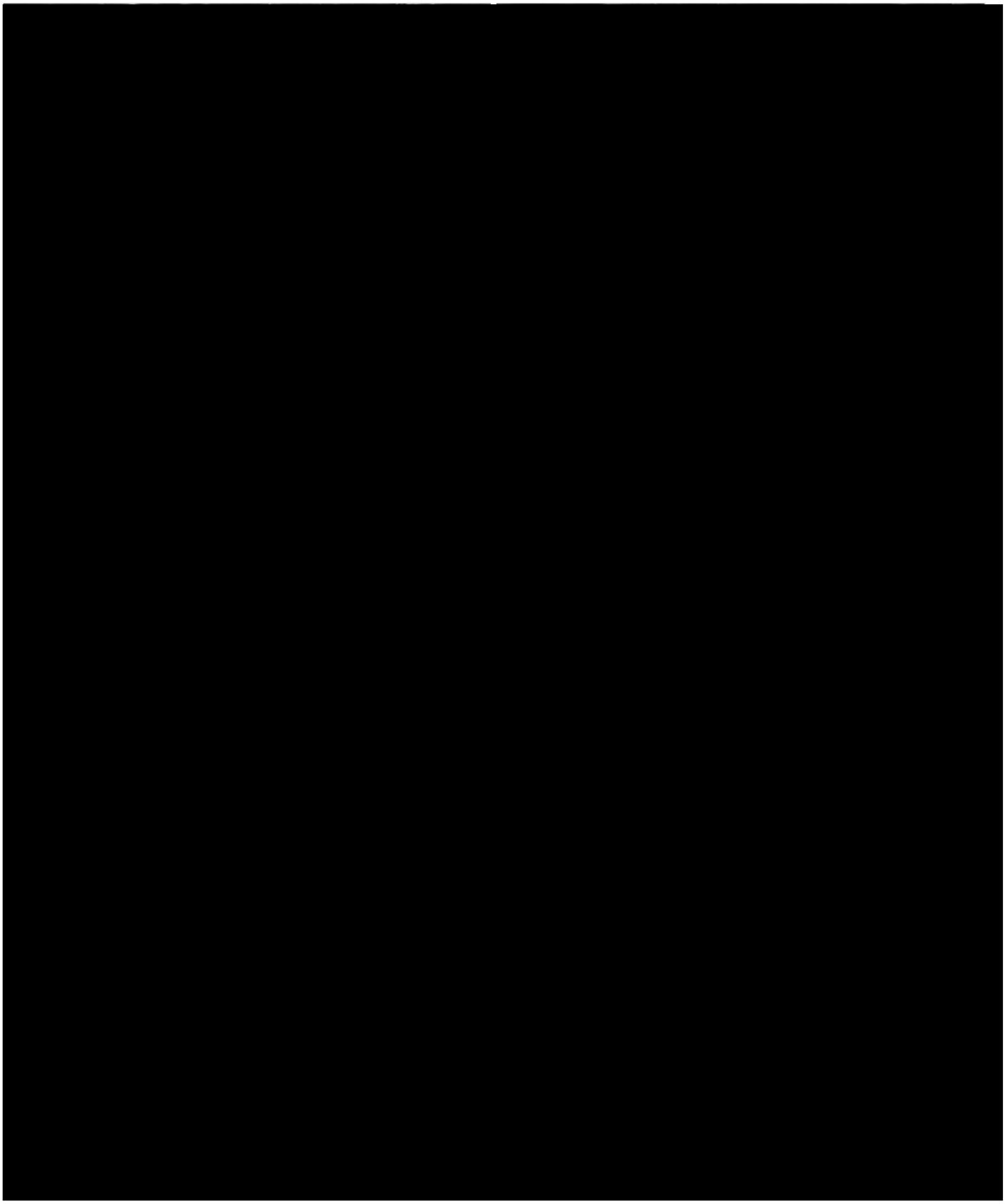

Figure 4.11. Morphological and behavioural characterization of [redacted] on the reverse of *Cucumis sativus* var. "Marketer" leaves collected on day 1 (A and B), day 3 (C and D), and day 6 (E and F). **A, C, & E.** Panoramic views of bacterial biofilm at progressively advanced stages of development. **B.** Biofilm partially covering a stoma. **D, & F.** Close-up views of the biofilm, where individual bacterial cells are visible.

Interactions: bacterial strains and *Pseudoperonospora cubensis.* Figure 4.12 shows the inoculation of strain [redacted] as a preventive treatment, already forming aggregates that cover portions of the leaf surface, along with *P. cubensis*, whose hyphal fragments and sporangia are visible in images C and E. By day 1 after bacterial application (A) -and shortly after pathogen inoculation-, strain [redacted] appears on parts of the leaf surface, with no noticeable pathogen development. By day 3 (B), strain [redacted] has expanded significantly, covering more extensive areas and surrounding several stomata. By day 6 (C, D, E, and F), the bacterial presence is substantial, with strain [redacted] forming dense biofilms across the leaf surface, potentially competing with *P. cubensis* for both space and nutrients. Images B and D display an open and closed stoma, respectively, each partially covered by bacterial structures, where individual bacterial cells and aggregates are distinctly visible.

Figure 4.13 illustrates the colonization dynamics of bacterial strain [redacted] when applied as a preventive treatment against *P. cubensis*. On day 3 (A and B), the images show the initial colonization pattern of strain [redacted] on the leaf surface. In image A, the biofilm is clearly distinguishable from the bare leaf surface. Notably, the stoma within the biofilm area is closed, while the stoma on the exposed leaf surface remains open, with a sporangiophore emerging from it, suggesting that even early biofilm formation may impede pathogen colonization. Uncolonized sporangiophores and sporangia are also visible in both images A and B. By day 6 (C, D, E, and F), strain [redacted] has developed a well-defined biofilm structure, densely covering the leaf surface and creating a substantial physical barrier against *P. cubensis*. This homogeneous, mucus-like biofilm is particularly visible in images C and E, indicating extensive coverage that may restrict pathogen access to the leaf tissue as strain [redacted] occupies available space effectively. Images D and F show stomata: in D, surrounded by bacterial aggregates, and in F, closed and thoroughly enveloped by the biofilm.

Summarizing, the preventive applications of both strains showed clear advantages in suppressing pathogen development. When applied preventively, both [redacted] and [redacted] had established biofilms that covered some portions of the leaf surface before pathogen inoculation, acting as a physical barrier against *P. cubensis*. For example, both strains covered the leaf surface effectively, with dense biofilm formation and bacterial cells surrounding stomata, a critical entry point for *P. cubensis*, before pathogens could grow and infect plant tissues. Thus, this extensive coverage likely inhibits pathogen attachment, germination, and further colonization by limiting pathogen access to the leaf surface.

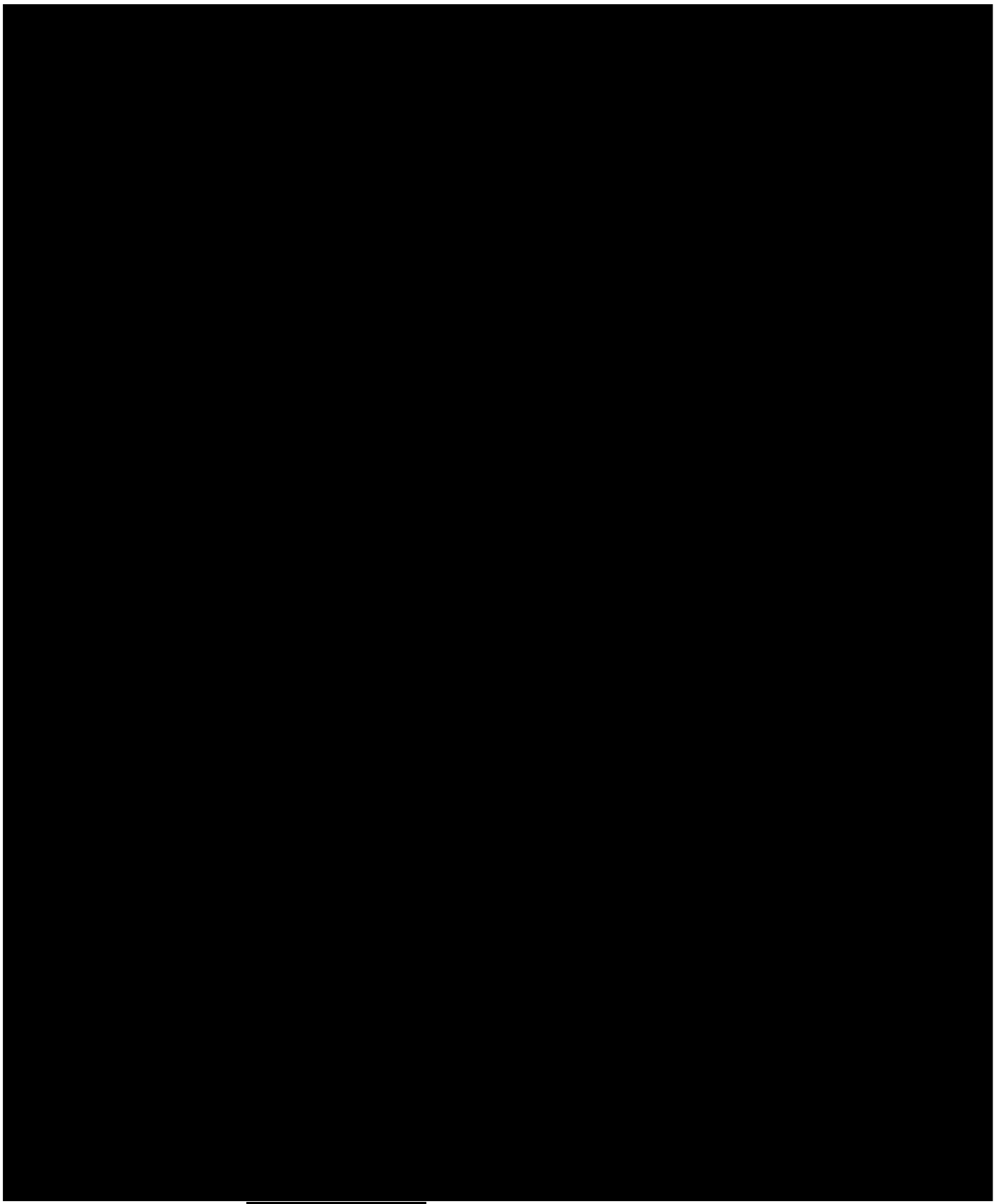

Figure 4.12. Inoculation of [redacted] as a preventive treatment and *Pseudoperonospora cubensis* on *Cucumis sativus* leaf surfaces. **A.** Day 1, showing initial colonization by strain [redacted]. **B.** Day 3, with expanded coverage by strain [redacted] surrounding stomata. **C, D, E, & F.** Day 6, demonstrating extensive biofilm formation by strain [redacted]. Images B and D show open and closed stomata, respectively, partially covered by bacterial cells and aggregates.

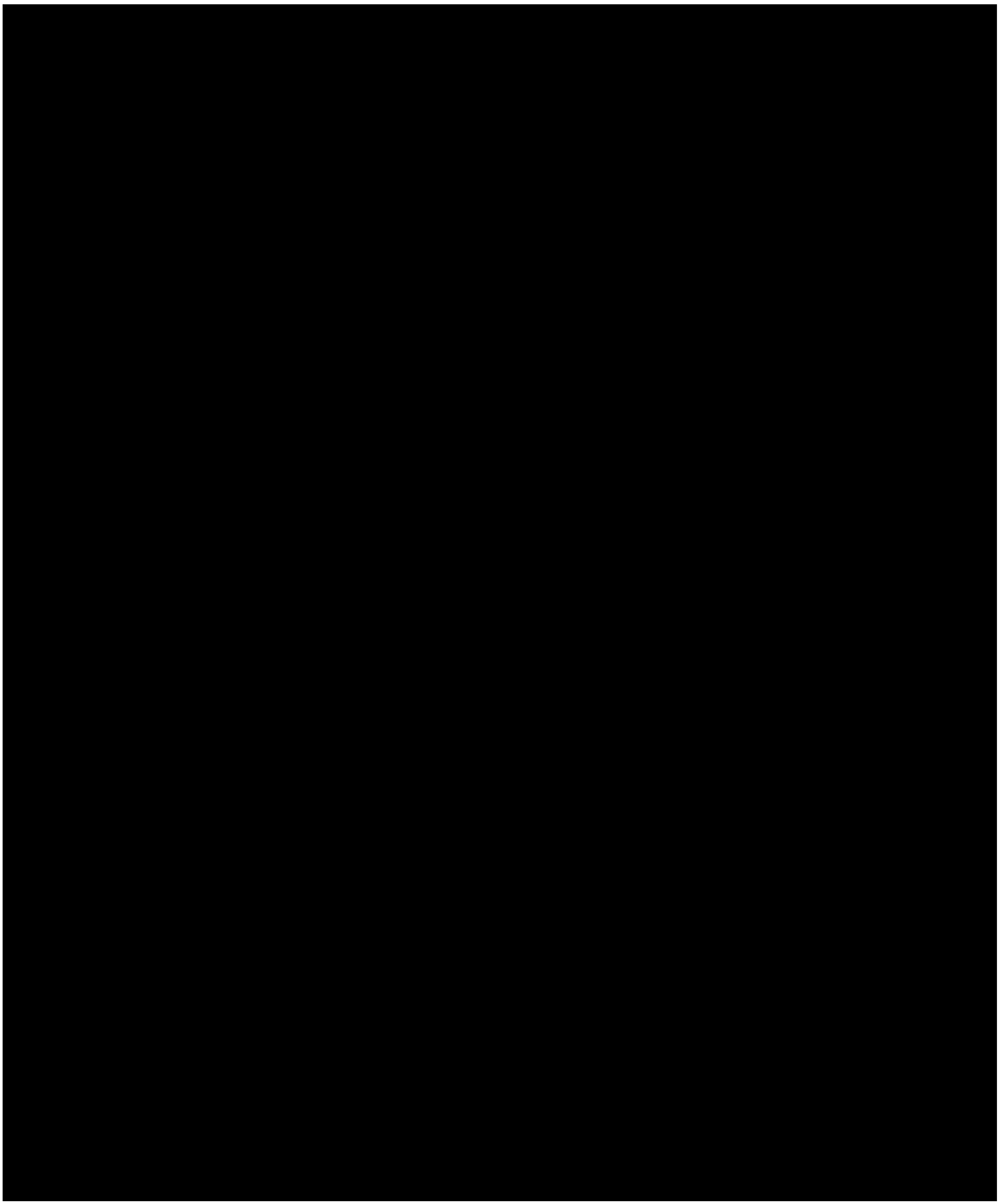

Figure 4.13. Inoculation of [redacted] as a preventive treatment and *Pseudoperonospora cubensis* on *Cucumis sativus* leaf surfaces. Day 3 (**A & B**): Initial biofilm formation of strain [redacted]. **C & E.** Dense, mucus-like biofilm, extensively covering the leaf surface. **D & F.** Stomata either surrounded by bacterial aggregates (D) or fully enclosed within the biofilm (F).

Interactions: bacterial strains against *Podosphaera fusca.* Figure 4.14 presents both preventive and curative applications of [redacted] against *P. fusca*. In the preventive treatment images (A and B), the initial establishment of strain [redacted] is visible (A). Notably, image B shows a dehydrated conidium partially covered by bacterial cells, indicating initial pathogen suppression by strain [redacted]. In the curative treatment images (C and D), taken one day post-bacterial application, strain [redacted] is seen in early stages of leaf colonization, with some pathogen conidiophores slightly covered by bacterial cells, suggesting limited immediate suppression of the pathogen. By day 3 post-application (E and F), however, strain [redacted] forms more substantial clusters and biofilms on infected leaf areas, conidiophores and conidia, gradually inhibiting pathogen progression.

Figure 4.15 shows both preventive and curative applications of [redacted] against *P. fusca*. In the preventive treatment images (A and B), leaf samples collected on day 3 (A) display both initial bacterial and pathogen colonization, while day 6 samples (B) reveal a more developed biofilm covering the leaf surface. In curative treatment images (C and D), taken one day post-application of strain [redacted], the bacteria are seen attaching to infected areas of the leaf, with visible *P. fusca* structures. Image E shows conidia arranged sequentially, forming a stick-like structure forming conidia in chains. Image F provides a close-up view of the biofilm, where individual bacterial cells and particles produced by them are clearly visible.

Summarizing, in preventive treatments, by day three post-application, both bacterial strains had developed dense biofilms that progressively encroached on pathogen-colonized areas, including conidiophores and conidia. On the other hand, when the strains were applied as curative treatments, they primarily targeted these existing fungal structures, with bacterial cells covering the hyphal fragments present at the time of inoculation. In fact, sporangiophores/conidiophores and sporangia/conidia enveloped by bacterial clusters or biofilms could be appreciated in the SEM images, exhibiting signs of dehydration and structural deterioration, which indicated that the bacterial strains were effectively impacting *P. cubensis* and *P. fusca*. Thus, curative applications resulted in targeted colonization around existing pathogen structures. However, the findings suggest that, while curative applications gradually inhibit pathogen spread, preventive treatments offer stronger pathogen suppression by establishing a protective bacterial presence before substantial pathogen colonization occurs, and also providing the benefits of the curative application. The consistent biocontrol effects observed in these images suggest an effective antagonistic relationship.

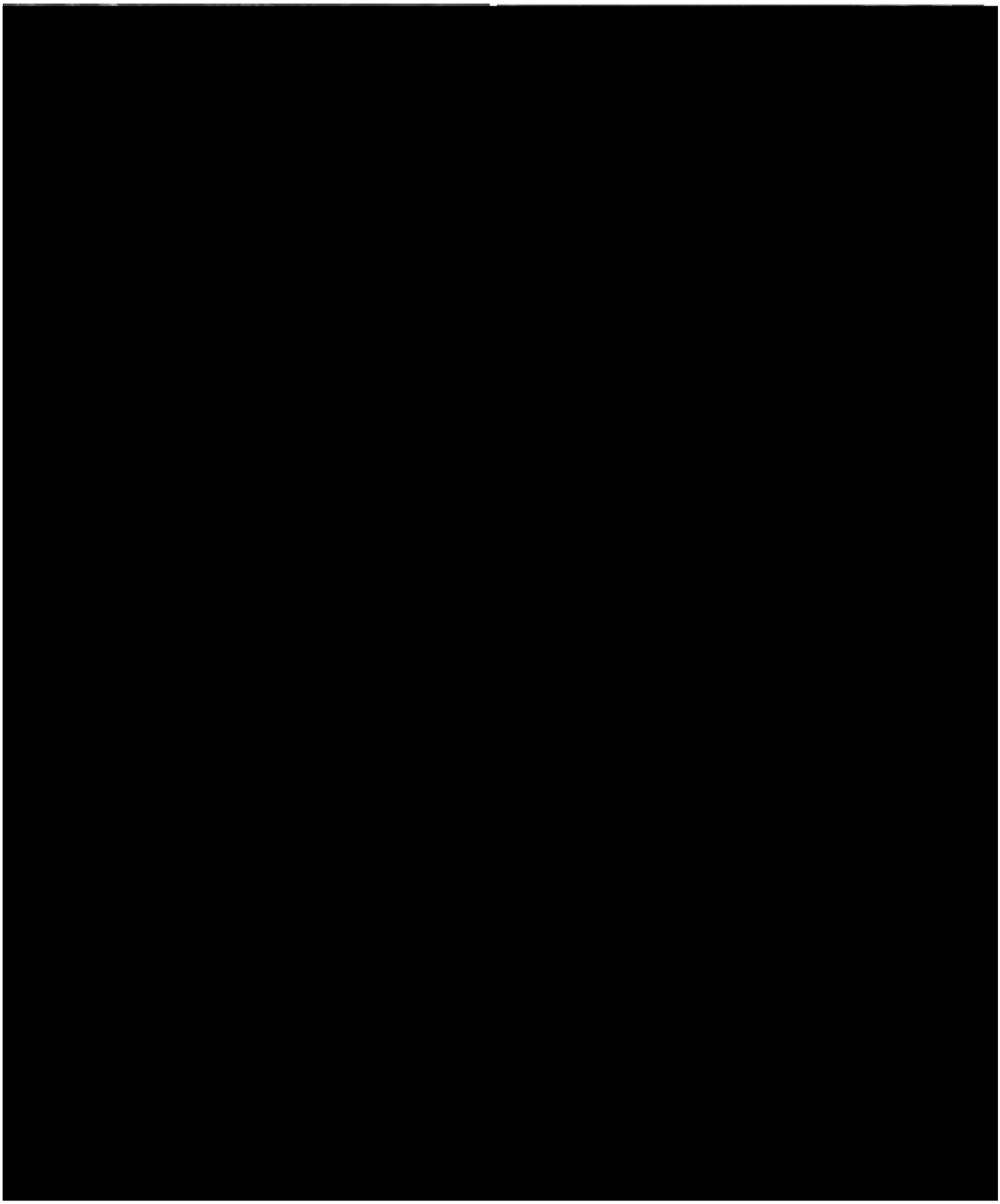

Figure 4.14. Preventive (A & B) and curative (C, D, E & F) applications of [redacted] against *Podosphaera fusca* on *Cucumis sativus* leaves. **A.** Initial bacterial establishment. **B.** Dehydrated conidium partially covered by bacterial cells. **C.** Early colonization stages of both strain [redacted] and *P. fusca*. **E.** Developed mycelium of *P. fusca*, already producing conidia. **D & F.** Biofilm clusters on leaf areas and conidia.

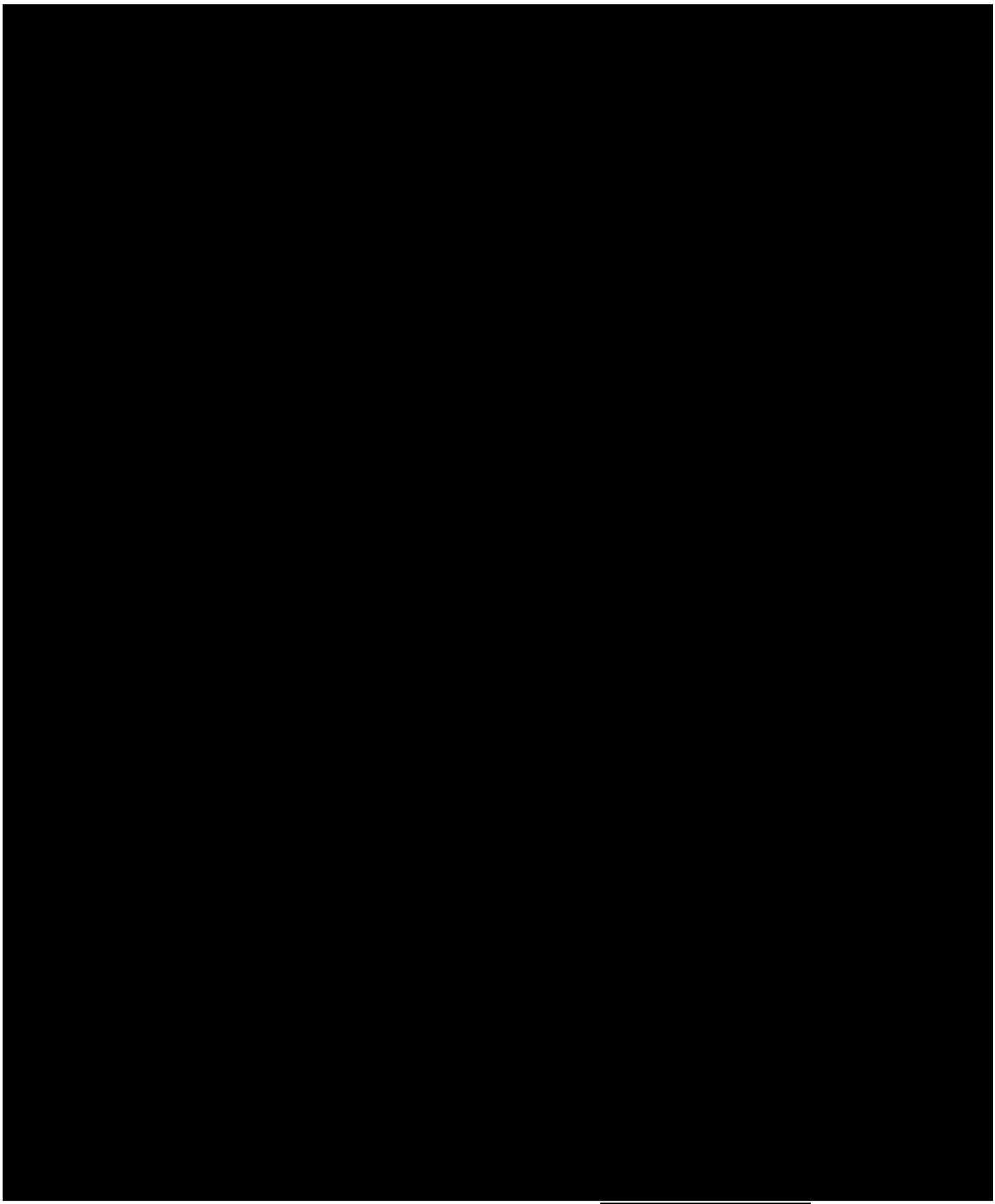

Figure 4.15. Preventive (A & B) and curative (C, D, E & F) applications of [redacted] against *Podosphaera fusca* on leaf surfaces. **A.** Initial *P. fusca* colonization. **B.** Developed biofilm covering the leaf surface. **C.** Pathogen mycelium covering the leaf surface, with some bacterial aggregates observed. **D & F.** Close-up of the biofilm. **E.** Higher magnification of conidia arranged sequentially in a stick-like formation.

DISCUSSION

In the context of the experiments analysing the **capacity to produce biofilms**, referring to the culture media, LB medium was found to be the one sustaining the highest cell production, reaching its peak at 72 h and with higher quantities in the case of strain [redacted] from 48 h. In contrast, KB medium was found to be the one sustaining the highest cell production in Puopolo et al. (2014), where they investigated the ability of *Lysobacter capsici* AZ78 to form biofilm on inert surfaces. However, the microbes from each assay were from different genus and this fact could be due to intrinsic differences within them.

Referring to the ability to form biofilm, assessed by SBF values, strain [redacted] demonstrated the highest biofilm production in KB medium. Biofilm formation for this strain began at 24 h, reaching its peak at 48 h, and then showed a slight decline. In contrast, Puopolo et al. (2014) reported that in KB medium, maximum SBF values were observed at 12 h, followed by a decrease. Strain [redacted] also produced biofilm in KB medium but in significantly lower amounts compared to strain [redacted].

In LB medium, strain [redacted] initiated biofilm production at 24 h, reaching its peak at 48 h and sustaining this level for at least 72 h. In contrast, Puopolo et al. (2014) reported that biofilm formation in LB medium did not begin until 48 h, with maximum production observed at 60 h. Similarly, strain [redacted] began biofilm production in LB medium at 48 h, though at significantly lower levels than both strain [redacted] and the strain described in Puopolo et al. (2014).

Respect to the **genes involved in the production of biofilms**, the genes [redacted] were found in the genomic information of both strains [redacted]. These genes are typically found in [redacted] and related species, since the extracellular matrix of [redacted] is mainly composed of exopolysaccharides, TasA (Branda et al., 2006) and BslA (Hobley et al., 2013), as it has been mentioned. Also, the presence of the [redacted] gene in biofilm-forming strains suggests that it may play a complementary role alongside TasA and BslA in maintaining the biofilm's architecture and functionality (Chen et al., 2012). Thus, these results are in accordance with the published data of strains [redacted], which exhibit robust biofilm formation due to the presence of the [redacted] (Belda et al., 2013; Kesel et al., 2016; Dergham et al., 2021).

On the other hand, the coding genes from the [redacted] were also identified in the genomic data of both strains (from [redacted]). These genes are crucial for producing the EPS component of the extracellular matrix during biofilm formation, as it has been mentioned (Elsholz et al., 2014; Arbour et al., 2023). Notably, the [redacted] gene was annotated in both strains

as a miscellaneous RNA, likely encoding the polysaccharide biosynthesis protein [redacted], which plays a crucial role in biofilm formation (Branda et al., 2004).

Furthermore, the regulatory [redacted]. This protein is essential for [redacted], likely facilitating the interaction between [redacted]. It is probably involved in the regulation of capsular polysaccharide biosynthesis (Mijakovic et al., 2003). Similarily, the [redacted], which likely encodes the putative [redacted]. In *Bacillus* species, [redacted]. This [redacted] phosphorylates and modulates proteins important for biofilm formation, contributing to biofilm structure by enhancing surface hydrophobicity, which aids in bacterial adhesion and stability on surfaces (Shi et al., 2014).

Here, it's important to note that since strain [redacted] and the type strain, [redacted], belong to the same species, the genes detected in strain [redacted] show higher identity percentages compared to those in strain [redacted]. In this context, the BLAST analysis conducted on strains [redacted] and [redacted] against the same type strain highlighted differences in their encoded proteins, reflected as differences in the AAs sequence (or percentage identity). Notably, extensive research has shown that protein functionality in *Bacillus* species is highly sensitive to even slight variations in amino acid sequences, which can affect structural conformation (critical for function), biomolecular interactions, and enzymatic activity (Bhalla et al., 2005; Yu et al., 2007; Agersø et al., 2019). Therefore, although no differences were found in biofilm-forming genes between both strains, these variations in protein composition may result in subtle functional differences, which could help explain the observed differences in formation capabilities and appearance of the biofilms produces by the two strains.

In summary, since strain [redacted] belongs to [redacted] and strain [redacted] is a closely related species ([redacted]), the presence of these characteristic [redacted] genes in their genomes was expected. Additionally, as both bacterial strains demonstrated biofilm-forming capabilities in previous phenotypic experiments, it was anticipated that some biofilm-associated genes would be detected in their genomes.

Regarding to the **leaf population studies**, the colonization and permanence of *Bacillus* species on plant leaves is a critical area of research, particularly in understanding their role in plant health and disease resistance. The first days following the bacterial inoculation are particularly significant, as this period encompasses the initial establishment of the bacterial population on the leaf surface and the onset of interactions with the plant host (Wagacha et al., 2010; Baard et al., 2023). Studies have shown that *Bacillus* populations can reach

substantial numbers within the first few days post-inoculation, often peaking around day 3 to 5 before stabilizing or declining (Seminara et al., 2012). This rapid growth is indicative of the species' ability to quickly colonize leaf surfaces, forming biofilms that can protect against pathogens and enhance plant health (Molina-Santiago et al., 2019). One week after inoculation, populations of *Bacillus* species can range from 1 x 10^6 to 1 x 10^8 CFU per gram of leaf tissue, depending on the inoculation method and environmental factors, although specific studies quantifying this range may vary (Molina-Santiago et al., 2019).

The significant population decrease for both strains [redacted] observed one day after inoculation could be attributed to loss during the inoculation process. This may have resulted from factors such as premature droplet fall, bacterial loss due to environmental exposure, or competition with naturally occurring bacteria. Thus, only a few cells were able to adhere well to the leaf surface and remain there. Nonetheless, once these bacterial cells had had enough time to efficiently attach, grow and form biofilms, they were able to maintain the populations stable along time.

Notably, the dense biofilms observed in the SEM images are an important consideration when studying bacterial populations on leaf surfaces. These biofilms may have limited the detachment of bacterial cells from the leaf surface under the mild agitation conditions used in the dilution plating protocol. As previously noted, biofilms can significantly enhance bacterial resilience and adherence to surfaces, making them more difficult to dislodge. As a result, many bacteria may have remained attached to the leaf surfaces and were not accurately quantified. To address this limitation and accurately quantify CFU/cm², future experiments should consider an alternative approach. Sonication or mechanical disruption helps detach biofilm-associated bacteria, with studies showing that sonication significantly aids CFU recovery (Herten et al., 2017; Wu et al., 2021). Also, the use of chemical agents, such as chlorhexidine, in other bacterial species have enhanced detachment depending on concentration and exposure time (Lee et al., 2016; Shin et al., 2022). Additionally, considering biofilm age is essential, as younger biofilms release more viable cells (Reynoso et al., 2019) than the mature biofilms observed in the SEM images from 3 to 6 days after the inoculation of the strains.

The differences between conducting experiments indoors versus outdoors can significantly impact the outcomes of leaf colonization studies, since outdoor experiments introduce a range of abiotic and biotic factors that can influence bacterial survival and colonization. The most frequently investigated limiting environmental factors for bacterial persistence in the phyllosphere are starvation, rainfall, temperature and humidity fluctuations and exposure to UV light irradiation (Wilson et al. 1999; Stockwell et al.2009; Singh et al., 2023). These factors may lead to a decline in bacterial populations over time, particularly if the inoculated strains

are not well-adapted to the specific conditions of the environment. In addition, studies have shown that host selection plays a crucial role in shaping the leaf microbiome, with certain plant species being more conducive to *Bacillus* colonization than others (Tariq et al., 2023).

Here, it is worth noting that strain [redacted]. Consequently, challenges with colonization and persistence on leaves might be anticipated when applying these bacteria directly on leaf surfaces outdoors. Nevertheless, both strains demonstrated the ability to colonize leaf surfaces outdoors, with strain [redacted] achieving higher populations than strain [redacted] by day 8, suggesting that [redacted] may be more adapted to environmental stressors like UV exposure and fluctuating humidity. Additionally, given that strain [redacted], it is possible that its cells could also [redacted], although this aspect was not investigated in this study.

Notably, differences were also found between the environmental conditions tested, and higher populations were found outdoors in the case of the two bacterial strains compared to indoors. This phenomenon could be related with the fact that outdoor conditions may also promote the establishment of *Bacillus* populations through natural selection processes that favour more resilient strains (Wagacha et al., 2010). Additionally, the interactions between *Bacillus* species and the plant host can differ significantly in controlled versus natural environments. In indoor experiments, the absence of competing flora and fauna may allow for more straightforward colonization patterns, while outdoor studies may reveal complex interactions that influence bacterial persistence.

Then after, all these results were finally confirmed by a qualitative analysis of the bacterial behaviour on the cucumber leaves by **Electron Microscopy**. Through SEM, infection structures such as sporangiophores or conidiophores could be observed in the case of downy and powdery mildew, respectively, allowing for detailed examination of the infection process (Thomas & Kropp, 2011). On the other hand, TEM facilitates the study of ultrastructural changes in plant tissues during pathogen invasion, which served to identify the stages of infection and morphological adaptations of both pathogen and host (Xu et al., 2021). For instance, in the TEM images from this work, the plant cell walls of the infected leaves with *P. cubensis* were significantly thicker in parts where the pathogen was close.

Additionally, SEM captures three-dimensional spatial relationships between pathogens and plant cells, offering insights into how pathogens navigate and adhere to host surfaces, thereby contributing to the development of targeted disease management strategies (Bushby et al., 2011). This capability is equally important in the study of microbial biofilms, such as those

formed by *Bacillus* species, to elucidate the intricate architecture of biofilms. Thus, SEM images of *Bacillus* biofilms typically reveal dense aggregations of bacterial cells embedded in a fibrous extracellular matrix, where the high magnification and depth of field allow the observation of the spatial arrangement of cells, the presence of spores, and the detailed structure of the matrix components (Malek, 2016; Gingichashvili et al., 2017; Catania, 2023).

Regarding to the SEM studies of *P. cubensis*, as it has been mentioned, the pathogen enters inside the leaf through stomata, both from the upper and lower surfaces of the leaves, in the form of zoospores. Once inside, these zoospores germinate, allowing the pathogen to grow and spread within the plant tissue (Lebeda & Cohen, 2010). After that, as it was clearly seen in the SEM images, the sporangiophores of the pathogen emerge through stomata, mostly from the lower surface of the leaves. This emergence appears shortly after inoculation, initially in small, localized areas of the leaf. Within a few days, however, the leaf surfaces are significantly covered with pathogen hyphae, and numerous sporangia are produced. Early symptoms of infection become visible around day six post-inoculation, intensifying daily as the infection progresses. Notably, as seen in the TEM images, *P. cubensis* remains closely attached to the epidermal cells on both the interior and exterior surfaces of the leaf, maintaining a tight association with these superficial cell layers.

A similar outcome was observed when referring to *P. fusca*. A few hyphal growths began to be seen from the very beginning, but it was not until around 6 days after its inoculation that pathogen began to form a dense and very brunched mycelium, and many conidia were produced. The growth and expansion of the hyphae are progressive. However, unlike the previous pathogen, the symptoms of *P. fusca* infection were not appreciated with the naked eye until well-passed the first week after its inoculation.

In the detailed analysis of *Bacillus* cell morphology and size on poly-L-lysine coverslips, the primary finding was that strain [redacted] appeared larger and thinner compared to strain [redacted]. According to the Bacterial Diversity Metadatabase (BacDive), managed and hosted by DSMZ (https://bacdive.dsmz.de/), [redacted] cells typically measure approximately [redacted], while [redacted] cells are approximately [redacted]. For [redacted], the observed average size was [redacted], closely matching the typical range. Similarly, [redacted] fit well within expected dimensions, with an average length of [redacted], confirming consistency with standard measurements for both *Bacillus* strains.

These dimensional differences highlight that while both strains belong to the *Bacillus* genus, their distinct ecological roles and environmental adaptations might influence their cell

morphology. [redacted], which can significantly impact its cellular structure. Studies have shown that [redacted], often exhibit shorter and wider cells compared to [redacted]. This morphological adaptation is likely a response to [redacted]

Regarding to the inoculation of the strains on leaves surfaces, the initial phase of reversible attachment of the individual cells (Vlamakis et al., 2013) could be observed in some images of samples collected at day 1 post bacterial inoculation. Once attached, the cells rapidly begin to proliferate and form microcolonies (microcolony formation), involving the production of the extracellular matrix (Sauer et al., 2007; Zhang et al., 2022), which was also clearly seen in some images collected at day 3 post bacterial inoculation. As the biofilm matures, it develops a more complex, three-dimensional architecture, often characterized by the formation of mushroom-shaped structures with channels that allow the distribution of nutrients and waste removal (Shemesh & Chai, 2013; Arnaouteli et al., 2021). These mature biofilms were observed in the case of both strains from day 3, being already very compact and evident on day 6 and 8 after inoculation. During this phase, *Bacillus* cells can differentiate into various cell types, including sporulating cells, which contribute to the biofilm's resilience (Vlamakis et al., 2013; Malek, 2016).

Additionally, the biofilm formation of [redacted] and [redacted] varied in density, structure, and spatial coverage, which may influence their ability to inhibit pathogen colonization. [redacted] displayed rapid colonization, forming dense biofilm clusters as early as day 1 post-inoculation. By day 6, strain [redacted] produced a well-structured biofilm that effectively covered the leaf surface, particularly around stomata, likely creating a physical barrier to pathogen ingress and depriving *P. cubensis* and *P. fusca* of access to essential resources. In contrast, [redacted] initially formed sparse clusters on day 1 but gradually expanded into a well-established biofilm by day 6. This progression highlights a slower but sustained colonization, suggesting that strain [redacted] may provide prolonged protection through its gradual occupation of available space and resources. Moreover, the mucus-like matrix surrounding strain [redacted] suggests a robust mechanism for maintaining biofilm integrity, which could be critical in competitive environments or under environmental stress, offering prolonged protective effects.

Moreover, the extracellular matrix particles observed in biofilms produced by both strains are notable, as they likely enhance biofilm stability and adherence to the leaf surface, an essential feature for withstanding environmental fluctuations and pathogen competition.

On the other hand, regarding to the inoculation experiments of bacterial strains and plant pathogens, when the bacterial strains were applied as preventive treatments to combat *P. cubensis*, clear distinctions were observed between leaf areas colonized by bacterial biofilms and those that were not. In areas lacking bacterial coverage, *P. cubensis* hyphae emerged readily through stomata and produced sporangia. In contrast, in areas densely colonized by bacterial biofilms, most stomata were covered and closed, effectively blocking pathogen entrance via zoospores, and also blocking sporangiophore emergence. Overall, the extensive biofilm formation by specific bacterial strains likely acts as a physical barrier against pathogens such as *P. cubensis,* or *P. fusca*, effectively restricting its growth and spread. This biofilm acts by limiting access to essential resources and space, which are critical for the pathogen's survival and proliferation (Fessia et al., 2022).

Additionally, in terms of plant-bacterial interactions, *Bacillus* strains can also serve as biocontrol agents by triggering plant immune responses. For example, García-Gutiérrez et al. (2013) showed that *Bacillus subtilis* UMAF6639 effectively controls *P. fusca* by activating plant defence pathways mediated by jasmonate and salicylic acid. Additionally, *Bacillus* species produce volatile organic compounds (VOCs) that have been shown to stimulate plant immune responses, adding another layer of protection against fungal infections (Soliman et al., 2022).

Regarding the pathogen and bacterial interactions, a key mechanism by which *Bacillus* strains inhibit plant pathogens is through lipopeptide secretion, specifically surfactins, iturins, and fengycins, widely documented in scientific literature. For example, Cawoy et al. (2014) and Zeriouh et al. (2011) noted that iturins and fengycins are crucial components of *Bacillus subtilis*' biocontrol efficacy, as these lipopeptides can disrupt the cellular integrity of various fungal phytopathogens. Consequently, as seen in the SEM images, the bacterial clusters and biofilms that reached and grew on pathogen surfaces likely impacted the pathogen strongly, with these compounds being secreted directly onto it. This proximity allows the lipopeptides to act effectively, disrupting the pathogen's cellular integrity and aiding in its inhibition.

Overall, the main outcome extracted from the images is to emphasize the importance of early biocontrol application for effective pathogen management, as preventive treatments resulted in more robust pathogen inhibition compared to curative applications. The ability of both strains to establish stable biofilms highlights their adaptability to the leaf surface environment, suggesting they could serve as long-term biocontrol agents with minimal need for reapplication. Furthermore, the strains’ targeted suppression of pathogen structures during curative treatments suggests a dual capability for preventive and reactive pathogen management, potentially extending their application to various stages of disease progression.

CONCLUSIONS

Both [redacted] and [redacted] demonstrate effective biofilm producing capabilities, with strain [redacted] showing superior biofilm density and resilience. Their biofilm-forming ability, supported by key genes, may enable them to inhibit pathogen growth and protect leaf surfaces.

The principal conclusions extracted from this PhD chapter were:

1. About the biofilm formation on inert surfaces, the study revealed differences in biofilm formation on inert surfaces (measured by SBF values) between [redacted] and [redacted]. Strain [redacted] showed the highest biofilm production in both KB and LB media, initiating biofilm formation early at 24 h and peaking at 48 h, with slightly different behaviours across media, performing better in KB. In contrast, strain [redacted] formed biofilm later and at significantly lower levels than strain [redacted].
2. The coding genes from the [redacted] genes were found in the genomic information of both strains [redacted], which are typically found in [redacted].
3. In leaf colonization experiments, both *Bacillus* strains effectively colonized leaf surfaces under both outdoor and controlled conditions. Although both performed similarly indoors (with lower populations than outdoors), [redacted] demonstrated greater resilience in outdoor conditions, showing higher population stability and enhanced biofilm formation compared to [redacted], though [redacted] also performed well. This resilience positions strain [redacted] as a strong candidate for biocontrol applications in field environments with UV exposure and fluctuating humidity. Its superior adherence and stable populations suggest strain [redacted] has strong potential for long-term colonization and effective pathogen suppression in outdoor crop protection.
4. Regarding to the Electron Microscopy analysis:
    a. SEM and TEM allowed detailed characterization of *Pseudoperonospora cubensis* and *Podosphaera fusca*, revealing their infection processes and evolution. It could be clearly observed that *P. cubensis* entered leaves through stomata, emerging as sporangiophores primarily on the lower leaf surface, while *P. fusca* developed dense mycelium and conidia mostly on the upper leaf surface.
    b. SEM images showed that strain [redacted], with larger and thinner cells, differed morphologically from strain [redacted], which formed denser, more uniform biofilms.

These differences reflect the strains' distinct ecological roles and environmental adaptations, with strain [redacted] displaying a more mucus-like matrix that may enhance biofilm resilience.

c. SEM images in the inoculation experiments of both the pathogens and the *Bacillus* strains demonstrated that biofilms formed by both bacterial strains potentially inhibit pathogen development. Preventive treatments allowed bacterial biofilms to cover leaf surfaces and stomata, blocking pathogen emergence and limiting nutrient access. Curative applications showed bacterial cells closely associated with pathogen structures, causing dehydration and deterioration, which highlights the biocontrol potential of both strains in managing *P. cubensis* and *P. fusca* infections.

GENERAL DISCUSSION AND MAIN CONCLUSIONS

GENERAL DISCUSSION

The general aim of this PhD thesis was to isolate microbial species, particularly *Bacillus* spp. and certain yeast-like fungi, as effective and safe biocontrol agents against the cucurbit downy mildew pathogen *Pseudoperonospora cubensis* and the cucurbit powdery mildew pathogen *Podosphaera fusca*. The research progressed through four main stages, including the isolation and screening of microbial strains, efficacy trials, security assessments, and the detailed characterization with focus on biofilm formation.

The first chapter focused on **isolating and screening microbial species** with potential biocontrol activity, according to literature, from a wide range of plant sources and locations. Particularly, the isolates were collected from downy and powdery mildew pustules on leaves of various plants exhibiting low disease severity. By focusing on downy and powdery mildew pustules as the source of isolates, the study aimed to increase the likelihood of discovering strains specifically adapted to the ecological niche of these pathogens (Köhl et al., 2019).

In the isolation of bacteria, almost 500 bacterial strains were obtained from approximately 200 leaf samples from various plant sources, and ultimately, around 150 bacilli were confirmed as Gram-positive. The first molecular identification of the isolates relied heavily on the [redacted] gene ([redacted]), followed by a taxonomic characterization through 16S rRNA sequencing. However, it was insufficient in some cases to distinguish some closely related species due to the low interspecific variability inherent in the gene (Zhao et al., 2020; Fox et al., 1992). As a result, more detailed genomic analyses were required for the final selection and precise identification of the most promising strains.

The bacterial isolation techniques used proved highly effective in obtaining a diverse collection of strains. Notably, the [redacted] method was particularly successful in identifying strains from the [redacted] group. This finding aligns with previous studies emphasizing the importance of [redacted] in plant health and disease resistance (Bacon & White, 2000; Khalaf and Raizada, 2018).

Regarding the fungal isolates, over 200 yeast-like fungi and hyphomycetes were obtained, indicating their common presence in powdery mildew pustules, existing as ungerminated spores, with the mildew acting as a spore trap, or they may actively grow within the pustules (Köhl et al., 2019). For fungal isolation, the protocol proposed by Köhl et al. (2019) was more effective than the one proposed by Urquhart et al. (1994) in isolating desired fungal species such as [redacted] and [redacted]. These fungi are known for their biocontrol potential, with [redacted] being particularly noted as an effective antagonist

against powdery mildew (Bélanger & Labbé, 2002). This highlights the potential role of these fungi as biocontrol agents within the complex microbial communities associated with mildew pustules.

Approximately 50% of the fungal isolates were selected for further analysis, where taxonomical identification using ITS1/ITS4 sequence data revealed significant diversity among the isolates, coinciding with findings in Köhl et al. (2019). Genus- or even species-level identification was crucial for assessing risks and excluding potential pathogens, with preliminary risk assessments guided by existing literature (Zinniel et al., 2002). Notably, around 10% of the isolates were identified as belonging to genera known for antagonizing powdery mildew, including [redacted] (Kiss, 2003).

However, differently from Köhl et al. (2019), where the selection criteria for cold tolerance, drought tolerance, and UV-B resistance were applied more stringently to reduce the number of isolates, in this PhD thesis, once the isolated strains were selected based on morphological and taxonomical features, the **efficacy trials against the plant diseases** of study were firstly conducted. The bioassays for antagonist screening were labour-intensive and variable, yet high disease pressure allowed for the exclusion of most non-antagonistic isolates. In this context, the efficacy trials conducted in Chapter 2 provided critical insights into the practical application of the previously selected *Bacillus* and yeast-like fungi strains and assessed their ability to combat against the plant pathogens *Pseudoperonospora cubensis* (downy mildew) and *Podosphaera fusca* (powdery mildew) on cucumber plants.

The principal outcome was that, in general terms, the effective bacterial strains coincided in both pathosystems, meaning that when a strain was efficient against one disease, it was also efficient against the other. Nonetheless, some strains were more effective in combating the specific disease they were isolated from, partially supporting the strategy of testing microbes against the diseases from which they were originally sourced, as suggested by Köhl et al. (2019). Overall, isolating microbial strains from infected tissues has demonstrated success as a biocontrol approach, as these strains can inhibit pathogens and enhance plant health, reinforcing the value of targeting pathogens within their ecological niches to maximize the efficacy (Maldonado-González et al., 2015; O'Brien, 2017; Araujo et al., 2020).

In cucurbit downy mildew (*P. cubensis*), approximately [redacted] of the isolates tested exhibited disease severities significantly lower than those in untreated control plants. This aligns with literature reporting a high proportion of *Bacillus* species isolated from natural environments that are effective in the biocontrol of plant diseases (Badia et al., 2011; Cawoy et al., 2011; Khalaf & Raizada, 2018; Pandin et al., 2018; Chen et al., 2019). Thus, only these most effective

isolates were selected for further evaluation, within which [redacted] was the most effective one, followed by [redacted]. Notably, the registered *B. subtilis* strain QST 713 from Serenade® Max was tested for comparison and resulted less effective than some of the newly identified strains.

Moreover, comparisons between isolates tested at the University of Barcelona and/or at the University of Sevilla indicated again that strains effective in one pathosystem were often effective in another. [redacted], tested first at Sevilla, performed well in both cucurbit and Solanaceae pathosystems, and against both downy and powdery mildews. Conversely, strains [redacted] tested first in Barcelona were also successful in Sevilla against both downy and powdery mildews. This fact, reinforce again the idea that when a strain was efficient against one disease, it may also be efficient against close related different pathogens that cause the same disease (downy and powdery mildews) for specific crops.

Additionally, strains [redacted] achieved significantly higher efficacy when treatments included metabolites produced during their growth, consistent with findings in the literature (Ongena & Jacques, 2008). However, strains [redacted] were effective enough against the downy mildew pathogen using only bacterial cells. This could be advantageous, as the effectiveness of these strains without added metabolites means that the final biocontrol product could rely solely on bacterial cells. This approach may simplify regulatory compliance according to Regulation (EC) No 1107/2009, which has streamlined requirements for products based solely on microbial active substances rather than products containing also metabolites.

Referring to the yeast-like fungi, they were less effective as preventive treatments against cucurbit downy mildew, which aligns with literature suggesting they are more effective, curatively, in superficial diseases like powdery mildew (Eken, 2004; Glawe, 2008; Khöl et al., 2019). Thus, in cucurbit powdery mildew, the fungal isolates [redacted] were quite effective in combating *P. fusca*, mostly when applied curatively. On the contrary, *Bacillus* strains showed higher efficacy as preventive treatments, also coinciding with literature. Among species tested, the most effective ones were the strains selected in the previous pathosystem. Strain [redacted] demonstrated the highest efficacy as a preventive treatment, while strain [redacted] excelled as a curative option. This could be attributed to its ability to rapidly colonize plant surfaces, as observed in the SEM characterization studies, and to produce bioactive compounds *in situ* that directly inhibit pathogen growth, as discussed by Kloepper et al. (2004). The ability of *Bacillus* strains to adapt to different application timings (preventive vs. curative) underscores their versatility as biocontrol agents. Both strains showed consistent disease reduction across varying severities, highlighting their robustness.

Relating the main results from Chapters 1 & 2, it is worth mentioning that most of the effective strains against downy and powdery mildew pathogens were isolated from [redacted]. In contrast, despite half of the bacterial isolates come from [redacted]—proved effective. [redacted], were also promising biocontrol agents. [redacted] are particularly effective, and in this study, strains [redacted] were highly successful against both downy and powdery mildews, echoing previous research on s[redacted].

In summary, five bacterial strains—[redacted]—were selected as promising biocontrol agents for further experimentation. Among the strains, strain [redacted] excelled for its broad-spectrum efficacy as a preventive treatment, showing potential for wider use in managing both downy and powdery mildews. The trains [redacted] were eliminated because of the regulatory challenges linked to their genomic profile. Therefore, in Chapters 3 & 4, a comprehensive comparative analysis of [redacted] and [redacted] was conducted in deepness, examining their genetic, phenotypic, and ecological characteristics to select one strain for patenting and registration as a novel biocontrol agent.

In Chapter 3, the genomic analyses provided foundational insights into the safety and efficacy of both strains. Strains [redacted] were finally confirmed as [redacted] and [redacted], respectively. Their intrinsic resistance profile, coupled with the absence of virulence factors and toxin-producing genes, established both strains as safe candidates for biocontrol applications under current regulatory standards. Additionally, both strains were found to produce key secondary metabolites, primarily lipopeptides, which are well-known for their biocontrol properties (Ongena & Jacques, 2008). Thus, [redacted] were putatively identified by LC-QTOF-MS/MS in the metabolite-producing medium of both strains, coinciding with literature (Yang et al., 2015; Geissler et al., 2016; Biniarz & Łukaszewicz, 2017; Souza et al., 2018; Farzand et al., 2019; Su et al., 2020; Allioui et al., 2021; Rabbee et al., 2023).

These findings align with those from the previous chapter. Although strains [redacted] were the most effective in combating downy and powdery mildew pathogens, for strain [redacted], the impact of its metabolites on disease severity was minimal, and in fact, the quantitative LC-QTOF-MS/MS analysis detected much lower quantities compared to strain [redacted]. Nevertheless, it is highly likely that strain [redacted] produces certain metabolites *in situ* to combat pathogens, as

mentioned and supported by numerous studies on [redacted] strains (Geissler et al., 2018; Farzand et al., 2019; Allioui et al., 2021). Similarly, while the metabolites of strain [redacted] had a more significant impact on disease reduction than those of strain [redacted], and the quantities detected were in fact higher, the effect was still not substantial.

Finally, in Chapter 4, additional studies were conducted to better understand the **key characteristics and capabilities** of the two selected strains, with focus on assessing their environmental adaptation. It is important to highlight that antagonistic bacteria used to control leaf or fruit diseases often encounter environmental challenges such as low temperatures and UV radiation (Köhl & Molhoek, 2001). This underscores again the importance of selecting antagonists from environments that match the intended application niche (Köhl et al., 2019).

One important factor investigated was their ability to form biofilms, which was first tested on inert surfaces using polystyrene plates, and absorbance measurements revealed that both strains initiated biofilm production 24 h after inoculation, reaching peak levels at 48 h. Strain [redacted] showed a higher efficiency in biofilm production compared to strain [redacted], indicating a greater ability to remain over time. Moreover, the presence of key biofilm-related genes typically found in [redacted], such as the [redacted], in the genomic information of both strains further supports their potential to form robust biofilms. These genes have been well-documented for their roles in biofilm formation (Branda et al., 2001; Kearns et al., 2005; Romero et al., 2010; Yannarell et al., 2019; Böhning et al., 2022).

Regarding to the leaf colonization studies, the results showed that both strains can colonize cucumber leaves effectively, indicating their capability to persist on plant surfaces. However, strain [redacted] displayed greater adaptability outdoors compared to strain [redacted]. Its higher population stability on leaf surfaces under UV exposure suggests that this strain can more effectively withstand environmental challenges. In fact, this finding aligns with previous studies indicating that [redacted], due to its [redacted], may be better equipped for use in variable or extreme conditions [redacted]

Additionally, the biofilm-forming abilities of these bacterial strains were visualized *in planta* using SEM, which showed that strain [redacted] produced more aggregated biofilms, whereas strain [redacted] formed more homogeneous, mucus-like structures. Both strains displayed small particles produced by the bacterial cells within the biofilm matrix, aligning with literature (Romero et al., 2010; Yannarell et al., 2019; Böhning et al., 2022). In this context, when the strains were applied alongside the pathogens, SEM images confirmed—consistent with the efficacy results

from Chapter 2—that preventive *Bacillus*-based treatments are more effective than curative ones. This emphasizes the importance of timing in biofilm establishment, which plays a crucial role in the effectiveness of *Bacillus*-based biocontrol products.

In summary, given that both strains demonstrated comparable safety profiles in genetic analysis and share foundational attributes that qualify them as effective biocontrol agents, the critical factors differentiating them for selection were their capacities for antimicrobial compound production and biofilm formation—both of which directly influence their efficacy as biocontrol agents. Strain [redacted] produced significantly higher quantities of surfactin C in growth media than strain [redacted], reaching levels comparable to the *B. subtilis* strain QST 713, the active ingredient in the commercial biocontrol product Serenade® Max. These findings aligned with the higher overall efficacy profile observed for this strain. Moreover, strain [redacted] also demonstrated superior biofilm-forming capabilities in both *in vitro* and in planta studies, where biofilms were found not only stable but also resilient under UV exposure in outdoor conditions.

In conclusion, a four-year screening program successfully identified 2 antagonists of cucurbit downy and powdery mildews, demonstrating the power of a stepwise approach in discovering new microbial biological control agents. Finally, the [redacted] was selected to be the active substance of the new biocontrol product being developed based on its efficacy and safety. Thus, with all this information in hand, a patent application for this microorganism as a biological control agent has been drafted and submitted.

Future studies will focus on the practical large-scale application of the product, including its industrial scaling in a factory, formulation and its use in real field and greenhouse conditions. Its efficacy will also be tested on new crops following the standards of Good Experimental Practice (GEP). In addition, throughout this year and 2025, various studies are planned to register strain [redacted] as a PPP in the European Union. These include toxicological tests (both with the active substance and the formulated product) and ecotoxicological tests on different organisms at varying doses, quality tests (contamination and colony-forming unit tests), and various physicochemical tests following Good Laboratory Practices (GLP) guidelines.

GENERAL CONCLUSIONS

This PhD thesis presents a thorough evaluation of the potential of [redacted] as a biocontrol agent against downy and powdery mildew pathogens, selected from a collection of over 700 isolates. The study highlights the importance of the proper strain selection in maximizing efficacy, with a focus on safety, environmental adaptability, and essential capabilities, such as biofilm-forming ability. The findings collectively contribute to the development of sustainable agricultural practices by demonstrating the potential of *Bacillus* spp. as effective and safe biocontrol agents, offering alternatives to chemical pesticides.

The main conclusions extracted from each PhD chapter are the ones as follows:

1. **Isolation and screening of microbial species.** The primary outcome of this chapter was the successful isolation of 724 microbial strains, from which 128 *Bacillus* strains and 11 yeast-like fungi strains were selected as potential biocontrol agents.
    a. The majority of [redacted] group species were isolated from plants in the [redacted], with the highest proportions coming from plants infected with [redacted].
    b. The [redacted] technique was identified as the most effective method for isolating these *Bacillus* species, [redacted].
    c. The selection process based on the internal portion of the [redacted] gene was successful in excluding undesired species.
    d. The isolation of fungal species was most successful from [redacted] for isolating the desired yeast-like fungi species.
2. **Efficacy trials of selected isolates.** The principal outcome of the second chapter was that [redacted] exhibited the highest overall efficacy against both cucurbit downy and powdery mildews ([redacted]), surpassing [redacted].
    a. In general, when a strain was effective against one disease, it also showed comparable efficacy against other pathogens causing similar diseases in different crops, as well as against the other disease within the same crop, with strain [redacted] showing the most promise for broader application.
    b. As a curative treatment for powdery mildew, strain [redacted] showed slightly higher efficacy than strain [redacted], with disease reductions of [redacted], respectively. However, the highest efficacy was observed with yeast strains [redacted]

[redacted], belonging to species [redacted], respectively, achieving around [redacted] disease reduction.

c. Both strains, [redacted], consistently achieved disease reductions between [redacted] across varying levels of disease severity in both cucurbit downy and powdery mildews, indicating robustness under different conditions.

d. In efficacy trials with the prototype formulations, strain [redacted] showed the best preventive results against cucurbit downy mildew, reducing disease severity by over [redacted], while strain [redacted] was more effective against cucurbit powdery mildew, achieving disease reductions around [redacted].

3. **Safety assessment of the selected isolates.** This PhD chapter's comprehensive analysis supports the safe use of [redacted] and [redacted] as Plant Protection Products in agriculture.

a. Genetic analysis confirmed both strains' identities with high Average Nucleotide Identity (ANI) values and revealed that both strains possessed genes for antimicrobial resistance that are considered intrinsic and not associated with mobile genetic elements, thereby posing minimal risk for resistance transfer.

b. The LC-QTOF-MS/MS analysis detected high levels of surfactin C, along with the presence of [redacted] in the culture medium of both strains. These findings align with the metabolites typically found in existing products based on *Bacillus* spp.

4. **Characterization of the selected isolates: biofilm formation.** [redacted] and [redacted] exhibit strong biofilm-forming capabilities, although strain [redacted] consistently demonstrates superior biofilm density, resilience, and environmental adaptability.

a. Strain [redacted] excelled in biofilm production on inert surfaces, achieving substantial biofilm density from 48 h onward.

b. The key biofilm-related genes, typically found in [redacted], were also detected in the genomic information of both strains, including the [redacted].

c. Both strains effectively established themselves on leaf surfaces under both indoor and outdoor conditions, but strain [redacted] exhibited greater resilience outdoors.

d. SEM images from inoculation experiments of either *Bacillus* strains with the pathogens (*Pseudoperonospora cubensis* and *Podosphaera fusca*) demonstrated that preventive treatments might enhance effectiveness.

REFERENCES

REFERENCES

Abdullahi, S., Muhammed, Y., Muhammad, A., Ahmed, J., & Shehu, D. (2021). Isolation and characterization of *Bacillus* spp. for plant growth promoting properties. *Acta Biologica Marisiensis*, *5*(2), 47-58. https://doi.org/10.2478/abmj-2022-0009

Abdulmalek, H. W., & Yazgan-Karataş, A. (2023). Improvement of Bacilysin production in *Bacillus subtilis* by CRISPR/Cas9-mediated editing of the 5'-untranslated region of the *bac* operon. *Journal of microbiology and biotechnology*, *33*(3), 410. https://doi.org/10.4014/jmb.2209.09035

Adelskov, J., & Patel, B. K. (2016). A molecular phylogenetic framework for *Bacillus subtilis* using genome sequences and its application to *Bacillus subtilis* subspecies *stecoris* strain D7XPN1, an isolate from a commercial food-waste degrading bioreactor. 3 *Biotech*, *6*(1), 96. https://doi.org/10.1007/s13205-016-0408-8

Adeniji, A. A., Aremu, O. S., & Babalola, O. O. (2019). Selecting lipopeptide-producing, *Fusarium*-suppressing *Bacillus* spp.: Metabolomic and genomic probing of *Bacillus velezensis* NWUMFkBS10. 5. *MicrobiologyOpen*, *8*(6), e00742. https://doi.org/10.1002/mbo3.742

Adewale, A., Kheng, G., Li, P., & Ting, A. (2015). Antimicrobial and enzymatic activities of endophytic bacteria isolated from *Mentha spicata* (mint). *Malaysian Journal of Microbiology 11,* 102-108. https://doi.org/10.21161/mjm.12014

Adhikari, B., Savory, E., Vaillancourt, B., Childs, K., Hamilton, J., Day, B., … & Buell, C. (2012). Expression profiling of *Cucumis sativus* in response to infection by *Pseudoperonospora cubensis*. *PloS one, 7*(4), e34954. https://doi.org/10.1371/journal.pone.0034954

Agersø, Y., Bjerre, K., Brockmann, E., Johansen, E., Nielsen, B., Siezen, R., … & Zeidan, A. (2019). Putative antibiotic resistance genes present in extant *Bacillus licheniformis* and *Bacillus paralicheniformis* strains are probably intrinsic and part of the ancient resistome. *Plos One, 14*(1), e0210363. https://doi.org/10.1371/journal.pone.0210363

Ahmed, N., Islam, M., Meah, M., & Hossain, M. (2013). Determination of races and biovars of *Ralstonia solanacearum* causing bacterial wilt disease of potato. *Journal of Agricultural Science*, *5*(6). https://doi.org/10.5539/jas.v5n6p86

Akai, S., Fukutomi, M., & Kunoh, H. (1968). An electron microscopic observation of conidium and hypha of Erysiphe *Graminis hordei*. *Mycopathologia et mycologia applicata*, *35*(3), 217-222. https://doi.org/10.1007/BF02050733

Alavilli, H., Lee, J., You, C., Yugandhar, P., Kim, H., Jain, A., … & Song, K. (2022). GWAS reveals a novel candidate gene *cmoap2/erf* in pumpkin (*Cucurbita moschata*) involved in resistance to powdery mildew. *International Journal of Molecular Sciences*, *23*(12), 6524. https://doi.org/10.3390/ijms23126524

[redacted]

Alcock, B. P., Huynh, W., Chalil, R., Smith, K. W., Raphenya, A. R., Wlodarski, M. A., ... & McArthur, A. G. (2023). CARD 2023: expanded curation, support for machine learning, and resistome prediction at the Comprehensive Antibiotic Resistance Database. *Nucleic acids research*, *51*(D1), D690-D699. https://doi.org/10.1093/nar/gkac920

Alhomaidi, E. (2024). Scanning electron microscopic exploration of intricate pollen morphology and antimicrobial potentials of gourd family. *Microscopy Research and Technique*, *87*(5), 999-1008. https://doi.org/10.1002/jemt.24485

Allard-Massicotte, R., Tessier, L., Lécuyer, F., Lakshmanan, V., Lucier, J., Garneau, D., … & Beauregard, P. (2016). *Bacillus subtilis* early colonization of *Arabidopsis thaliana* roots involves multiple chemotaxis receptors. *Microbiology*, *7*(6). https://doi.org/10.1128/mbio.01664-16

Al-Qaysi, S., Abdullah, N., Jaffer, M., & Abbas, Z. (2021). Biological control of phytopathogenic fungi by *Kluyveromyces marxianus* and *Torulaspora delbrueckii* isolated from iraqi date vinegar. *Journal of Pure and Applied Microbiology*, *15*(1), 300-311. https://doi.org/10.22207/jpam.15.1.23

Alvarez, F., Castro, M., Príncipe, A., Borioli, G., Fischer, S., Mori, G., & Jofré, E. (2012). The plant-associated *Bacillus amyloliquefaciens* strains $MEP_2$18 and $ARP_2$3 capable of producing the cyclic lipopeptides iturin or surfactin and fengycin are effective in biocontrol of *Sclerotinia* stem rot disease. *Journal of applied microbiology*, *112*(1), 159-174. https://doi.org/10.1111/j.1365-2672.2011.05182.x

REFERENCES

Anastassiadou, M., Arena, M., Auteri, D., Brancato, A., Bura, L., ... & Villamar-Bouza, L. (2021). Peer review of the pesticide risk assessment of the active substance *Bacillus amyloliquefaciens* strain QST 713 (formerly *Bacillus subtilis* strain QST 713). *EFSA Journal*, *19*(1). https://doi.org/10.2903/j.efsa.2021.6381

Andrews, J. H. (1992). Biological control in the phyllosphere. Annual review of *Phytopathology*, *30*(1), 603-635. https://www.annualreviews.org/content/journals/10.1146/annurev.py.30.090192.003131

Angelini, R., Pollastro, S., Rotondo, P., Laguardia, C., Abate, D., Rotolo, C., … & Faretra, F. (2019). Transcriptome sequence resource for the cucurbit powdery mildew pathogen *Podosphaera xanthii*. *Scientific Data, 6*(1). https://doi.org/10.1038/s41597-019-0107-5

Antipov, D., Hartwick, N., Shen, M., Raiko, M., Lapidus, A., & Pevzner, P. A. (2016). plasmidSPAdes: assembling plasmids from whole genome sequencing data. *Bioinformatics, 32*(22), 3380-3387. https://doi.org/10.1093/bioinformatics/btw493

Arahal, D. R. (2014). Whole-genome analyses: average nucleotide identity. In *Methods in microbiology* (Vol. 41, pp. 103-122). Academic Press. https://doi.org/10.1016/bs.mim.2014.07.002

Arbour, C. A., Nagar, R., Bernstein, H. M., Ghosh, S., Al-Sammarraie, Y., Dorfmueller, H. C., ... & Imperiali, B. (2023). Defining early steps in *Bacillus subtilis* biofilm biosynthesis. *Microbiology*, *14*(5), e00948-23. https://doi.org/10.1128/mbio.00948-23

Arguelles-Arias, A., Ongena, M., Halimi, B., Lara, Y., Brans, A., Joris, B., & Fickers, P. (2009). *Bacillus amyloliquefaciens* GA1 as a source of potent antibiotics and other secondary metabolites for biocontrol of plant pathogens. *Microbial cell factories*, *8*, 1-12. https://doi.org/10.1186/1475-2859-8-63

Arnaouteli, S., Bamford, N., Stanley-Wall, N., & Kovács, Á. (2021). *Bacillus subtilis* biofilm formation and social interactions. *Nature Reviews Microbiology*, *19*(9), 600-614. https://doi.org/10.1038/s41579-021-00540-9

Asci, S., Tangolar, S., Kazan, K., Özmen, C., Öktem, M., Kibar, U., … & Ergül, A. (2021). Evaluation of powdery mildew resistance of a diverse set of grape cultivars and testing the association between powdery mildew resistance and pr gene expression. *Turkish Journal of Agriculture and Forestry*, *45*(3), 273-284. https://doi.org/10.3906/tar-2009-109

Ash, C., Farrow, J. A., Dorsch, M., Stackebrandt, E., & Collins, M. D. (1991). Comparative analysis of *Bacillus anthracis, Bacillus cereus*, and related species on the basis of reverse transcriptase sequencing of 16S rRNA. *International Journal of Systematic and Evolutionary Microbiology*, *41*(3), 343-346. https://www.microbiologyresearch.org/content/journal/ijsem/10.1099/00207713-41-3-343

Ashe, S., Maji, U., Sen, R., Mohanty, S., & Maiti, N. (2013). Specific oligonucleotide primers for detection of endoglucanase positive *Bacillus subtilis* by PCR. 3 *Biotechnology*, *4*(5), 461-465. https://doi.org/10.1007/s13205-013-0177-6

Avis, T., Caron, S., Boekhout, T., Hamelin, R., & Bélanger, R. (2001). Molecular and physiological analysis of the powdery mildew antagonist *Pseudozyma flocculosa* and related fungi. *Phytopathology*, *91*(3), 249-254. https://doi.org/10.1094/phyto.2001.91.3.249

Baard, V., Bakare, O., Daniel, A., Nkomo, M., Gokul, A., Keyster, M., … & Klein, A. (2023). Biocontrol potential of *Bacillus subtilis* and *Bacillus tequilensis* against four *Fusarium* species. *Pathogens*, *12*(2), 254. https://doi.org/10.3390/pathogens12020254

Bahuguna, A., Joe, A. R., Kumar, V., Lee, J. S., Kim, S. Y., Moon, J. Y., ... & Kim, M. (2020). Study on the identification methods for effective microorganisms in commercially available organic agriculture materials. *Microorganisms*, *8(*10), 1568. https://doi.org/10.3390/microorganisms8101568

Balleza, D., Alessandrini, A., & Beltrán García, M. J. (2019). Role of lipid composition, physicochemical interactions, and membrane mechanics in the molecular actions of microbial cyclic lipopeptides. *The Journal of membrane biology, 252*(2), 131-157. https://doi.org/10.1007/s00232-019-00067-4

Beauregard, P. B., Chai, Y., Vlamakis, H., Losick, R., & Kolter, R. (2013). *Bacillus subtilis* biofilm induction by plant polysaccharides. *Proceedings of the National Academy of Sciences*, *110*(17), E1621-E1630. https://doi.org/10.1073/pnas.1218984110

Behary, N., Perwuelz, A., Campagne, C., Lecouturier, D., Dhulster, P., & Mamede, A. S. (2012). Adsorption of surfactin produced from *Bacillus subtilis* using nonwoven PET (polyethylene terephthalate) fibrous membranes functionalized with chitosan. *Colloids and Surfaces B: Biointerfaces*, *90,* 137-143. https://doi.org/10.1016/j.colsurfb.2011.10.009

REFERENCES

Belanger, R. R., & Labbe, C. (2002). Control of powdery mildews without chemicals: Prophylactic and biological alternatives for horticultural crops. In R. R. Belanger, W. R. Bushnell, A. J. Dik, & T. L. W. Carver (Eds.), *The powdery mildews: A comprehensive treatise* (pp. 256–267). APS Press.

Belda, E., Sekowska, A., Le Fèvre, F., Morgat, A., Mornico, D., Ouzounis, C., … & Danchin, A. (2013). An updated metabolic view of the *Bacillus subtilis* 168 genome. *Microbiology (Reading, England)*, *159*(Pt 4), 757–770. https://doi.org/10.1099/mic.0.064691-0

Bellón-Gómez, D., Vela-Corcía, D., Pérez-García, A., & Torés, J. (2014). Sensitivity of *Podosphaera xanthii* populations to anti-powdery-mildew fungicides in Spain. *Pest Management Science*, *71*(10), 1407-1413. https://doi.org/10.1002/ps.3943

Bell, C. A., Uhl, J. R., Hadfield, T. L., David, J. C., Meyer, R. F., Smith, T. F., & Cockerill III, F. R. (2002). Detection of *Bacillus anthracis* DNA by LightCycler PCR. *Journal of Clinical Microbiology*, *40*(8), 2897-2902. https://doi.org/10.1128/jcm.40.8.2897-2902.2002

Beneduzi, A., Ambrosini, A., & Passaglia, L. (2012). Plant growth-promoting rhizobacteria (PGPR): their potential as antagonists and biocontrol agents. *Genetics and Molecular Biology*, *35*(4 suppl 1), 1044-1051. https://doi.org/10.1590/s1415-47572012000600020

Benjamin, I., Kenigsbuch, D., Gal'perin, M., Abrameto, J., & Cohen, Y. (2009). Cisgenic melons over expressing glyoxylate-aminotransferase are resistant to downy mildew. *European Journal of Plant Pathology*, *125*(3), 355-365. https://doi.org/10.1007/s10658-009-9485-4

Berkeley, M. S., & Curtis, A. (1868). *Peronospora cubensis*. *Journal of the Linnean Society of Botany, 10*.

Bhalla, R., Dalal, M., Panguluri, S., Jagadish, B., Mandaokar, A., Singh, A., … & Kumar, P. (2005). Isolation, characterization and expression of a novel vegetative insecticidal protein gene of *Bacillus thuringiensis. Fems Microbiology Letters, 243*(2), 467-472. https://doi.org/10.1016/j.femsle.2005.01.011

Bhandari, V., Ahmod, N., Shah, H., & Gupta, R. (2013). Molecular signatures for *Bacillus* species: demarcation of the *Bacillus subtilis* and *Bacillus cereusclades* in molecular terms and proposal to limit the placement of new species into the genus *Bacillus*. *International Journal of Systematic and Evolutionary Microbiology, 63*(Pt_7), 2712-2726. https://doi.org/10.1099/ijs.0.048488-0

Bin Hafeez, A., Pełka, K., Worobo, R., & Szweda, P. (2024). *In silico* safety assessment of *Bacillus* isolated from polish bee pollen and bee bread as novel probiotic candidates. *International Journal of Molecular Sciences*, *25*(1), 666. https://doi.org/10.3390/ijms25010666

Bjelić, D., Marinković, J., & Balešević-Tubić, S. (2020). The significance of *Bacillus* spp. in disease suppression and growth promotion of field and vegetable crops. *Microorganisms*, *8*(7), 1037. https://doi.org/10.3390/microorganisms8071037

Blin, K., Shaw, S., Augustijn, H. E., Reitz, Z. L., Biermann, F., Alanjary, M., ... & Weber, T. (2023). antiSMASH 7.0: new and improved predictions for detection, regulation, chemical structures and visualisation. *Nucleic acids research*, *51*(W1), W46-W50. https://doi.org/10.1093/nar/gkad344

de Boer Sietske, A., & Diderichsen, B. (1991). On the safety of *Bacillus subtilis* and *B. amyloliquefaciens:* a review. *Applied microbiology and biotechnology*, *36,* 1-4.

Bonhomme, S., Dessen, A., & Macheboeuf, P. (2021). The inherent flexibility of type I non-ribosomal peptide synthetase multienzymes drives their catalytic activities. *Open Biology, 11*(5), 200386. https://doi.org/10.1098/rsob.200386

Borriss, R., Chen, X., Rueckert, C., Blom, J., Becker, A., Baumgarth, B., … & Klenk, H. (2011). Relationship of *Bacillus amyloliquefaciens* clades associated with strains DSM 7T and FZB42T: a proposal for *Bacillus amyloliquefaciens* subsp. *amyloliquefaciens* subsp. nov. and *Bacillus amyloliquefaciens* subsp. *plantarum* subsp. nov. based on complete genome sequence comparisons. *International Journal of Systematic and Evolutionary Microbiology*, *61*(8), 1786-1801. https://doi.org/10.1099/ijs.0.023267-0

Bortolaia, V., Kaas, R. S., Ruppe, E., Roberts, M. C., Schwarz, S., Cattoir, V., ... & Aarestrup, F. M. (2020). ResFinder 4.0 for predictions of phenotypes from genotypes. *Journal of Antimicrobial Chemotherapy*, *75*(12), 3491-3500. https://doi.org/10.1093/jac/dkaa345

Branda, S. S., Chu, F., Kearns, D. B., Losick, R., & Kolter, R. (2006). A major protein component of the *Bacillus subtilis* biofilm matrix. *Molecular microbiology, 59*(4), 1229-1238. https://doi.org/10.1111/j.1365-2958.2005.05020.x

Branda, S. S., González-Pastor, J. E., Dervyn, E., Ehrlich, S. D., Losick, R., & Kolter, R. (2004). Genes involved in formation of structured multicellular communities by *Bacillus subtilis*. *Journal of bacteriology*, *186*(12), 3970–3979. https://doi.org/10.1128/JB.186.12.3970-3979.2004

REFERENCES

Braun, U., Cook, T.A., Inman, A.J. and Shin, H.D. (2002) The taxonomy of powdery mildew fungi. In book: *The powdery mildews: a comprehrensive treatise*, pp. 13–55. Saint Paul, MN: APS Press.

Brito, I. L. (2021). Examining horizontal gene transfer in microbial communities. *Nature Reviews Microbiology, 19*(7), 442-453. https://doi.org/10.1038/s41579-021-00534-7

Brown, C. L., Mullet, J., Hindi, F., Stoll, J. E., Gupta, S., Choi, M., ... & Zhang, L. (2022). mobileOG-db: a manually curated database of protein families mediating the life cycle of bacterial mobile genetic elements. *Applied and environmental microbiology*, *88*(18), e00991-22. https://doi.org/10.1128/aem.00991-22

Brudzynski, K. (2021). Honey as an ecological reservoir of antibacterial compounds produced by antagonistic microbial interactions in plant nectars, honey and honeybee. *Antibiotics*, *10*(5), 551. https://doi.org/10.3390/antibiotics10050551

Bünemann, E., Schwenke, G., & Zwieten, L. (2006). Impact of agricultural inputs on soil organisms—a review. *Soil Research, 44*(4), 379. https://doi.org/10.1071/sr05125

Burandt, Q. (2023). Further limitations of synthetic fungicide use and expansion of organic agriculture in Europe will increase the environmental and health risks of chemical crop protection caused by copper-containing fungicides. *Environmental Toxicology and Chemistry*, *43*(1), 19-30. https://doi.org/10.1002/etc.5766

Byrne, J. M., Dianese, A. C., Ji, P., Campbell, H. L., Cuppels, D. A., Louws, F. J., ... & Wilson, M. (2005). Biological control of bacterial spot of tomato under field conditions at several locations in North America. *Biological Control, 32*(3), 408-418. https://doi.org/10.1016/j.biocontrol.2004.12.001

Camacho, C., Coulouris, G., Avagyan, V., Ma, N., Papadopoulos, J., Bealer, K., & Madden, T. L. (2009). BLAST+: architecture and applications*. BMC bioinformatics*, *10,* 1-9. https://doi.org/10.1186/1471-2105-10-421

Campana, R., Palma, F., & Sisti, M. (2022). Growth ability, carbon source utilization and biochemical features of the new specie *Zalaria obscura*. *World Journal of Microbiology and Biotechnology*, *38*(12). https://doi.org/10.1007/s11274-022-03417-y

Cantalapiedra, C. P., Hernández-Plaza, A., Letunic, I., Bork, P., & Huerta-Cepas, J. (2021). eggNOG-mapper v2: functional annotation, orthology assignments, and domain prediction at the metagenomic scale. *Molecular biology and evolution*, *38*(12), 5825-5829. https://doi.org/10.1093/molbev/msab293

Carlone, G., Valadez, M., & Pickett, M. (1982). Methods for distinguishing gram-positive from gram-negative bacteria. *Journal of Clinical Microbiology*, *16*(6), 1157-1159. https://doi.org/10.1128/jcm.16.6.1157-1159.1982

Catania, A. (2023). Evaluation of the biofilm-forming ability and molecular characterization of dairy *Bacillus* spp. isolates. *Frontiers in Cellular and Infection Microbiology, 13.* https://doi.org/10.3389/fcimb.2023.1229460

Cawoy, H., Debois, D., Franzil, L., Pauw, E., Thonart, P., & Ongena, M. (2014). Lipopeptides as main ingredients for inhibition of fungal phytopathogens by *Bacillus subtilis/amyloliquefaciens*. *Microbial Biotechnology, 8*(2), 281-295. https://doi.org/10.1111/1751-7915.12238

Cerón-Carpio, A., García, B., Guerrero-Analco, J., Pérez-Pérez, R., Sánchez-Coronado, M., Colín, P., … & Mehltreter, K. (2023). Impact of longevity and wettability of fern leaves on epiphyll colonization in a mexican lowland rainforest. *Journal of Vegetation Science*, *34*(3). https://doi.org/10.1111/jvs.13192

Chai, L., Romero, D., Kayatekin, C., Akabayov, B., Vlamakis, H., Losick, R., … & Kolter, R. (2013). Isolation, characterization, and aggregation of a structured bacterial matrix precursor. *Journal of Biological Chemistry*, *288*(24), 17559-17568. https://doi.org/10.1074/jbc.m113.453605

Chen, M., Wang, J., Liu, B., Zhu, Y., Xiao, R., Yang, W., … & Zheng, C. (2020). Biocontrol of tomato bacterial wilt by the new strain *Bacillus velezensis* FJAT-46737 and its lipopeptides*. BMC Microbiology*, *20*(1). https://doi.org/10.1186/s12866-020-01851-2

Chen, X., Zhang, Y., Fu, X., Li, Y., & Wang, Q. (2016). Isolation and characterization of *Bacillus amyloliquefaciens* PG12 for the biological control of apple ring rot. *Postharvest Biology and Technology, 115*, 113-121. https://doi.org/10.1016/j.postharvbio.2015.12.021

Chen, Y., Yan, F., Chai, Y., Liu, H., Kolter, R., Losick, R., … & Guo, J. (2012). Biocontrol of tomato wilt disease by *Bacillus subtilis* isolates from natural environments depends on conserved genes mediating biofilm formation. *Environmental Microbiology*, *15*(3), 848-864. https://doi.org/10.1111/j.1462-2920.2012.02860.x

Choi, Y.-J., Hong, S.-B., & Shin, H.-D. (2005). A re-consideration of *Pseudoperonospora cubensis* and *P. humuli* based on molecular and morphological data. *Mycological Research*, *109*(7), 841–848. doi:10.1017/S0953756205002534

REFERENCES

Choudhury, S. R., Traquair, J. A., & Jarvis, W. R. (1994). 4-methyl-7, 11-heptadecadienal and 4-methyl-7, 11-heptadecadienoic acid: New antibiotics from *Sporothrix flocculosa* and *Sporothrix rugulosa. Journal of natural products, 57*(6), 700-704. https://doi.org/10.1021/np50108a003

Chowdhury, S. P., Hartmann, A., Gao, X., & Borriss, R. (2015). Biocontrol mechanism by root-associated *Bacillus amyloliquefaciens* FZB42–a review. *Frontiers in microbiology, 6,* 137829. https://doi.org/10.3389/fmicb.2015.00780

Chu, F., Kearns, D. B., Branda, S. S., Kolter, R., & Losick, R. (2006). Targets of the master regulator of biofilm formation in *Bacillus subtilis*. *Molecular microbiology*, *59*(4), 1216–1228. https://doi.org/10.1111/j.1365-2958.2005.05019.x

Chu, F., Kearns, D. B., McLoon, A., Chai, Y., Kolter, R., & Losick, R. (2008). A novel regulatory protein governing biofilm formation in *Bacillus subtilis*. *Molecular microbiology*, *68*(5), 1117-1127. https://doi.org/10.1111/j.1365-2958.2008.06201.x

Chun, B. H., Kim, K. H., Jeong, S. E., & Jeon, C. O. (2019). Genomic and metabolic features of the *Bacillus amyloliquefaciens* group–*B. amyloliquefaciens, B. velezensis,* and *B. siamensis*–revealed by pan-genome analysis. *Food microbiology*, *77,* 146-157. https://doi.org/10.1016/j.fm.2018.09.001

Cohen, R., Burger, Y., & Katzir, N. (2004). Monitoring physiological races of *Podosphaera xanthii* (syn. *Sphaerotheca fuliginea*), the causal agent of powdery mildew in cucurbits: factors affecting race identification and the importance for research and commerce. *Phytoparasitica*, *32,* 174-183. https://doi.org/10.1007/BF02979784

Cohen, Y. (1981). Downy mildew of cucurbits. *The downy mildews*, 341-354.

Compant, S., Duffy, B., Nowak, J., Clément, C., & Barka, E. (2005). Use of plant growth-promoting bacteria for biocontrol of plant diseases: principles, mechanisms of action, and future prospects. *Applied and Environmental Microbiology, 71*(9), 4951-4959. https://doi.org/10.1128/aem.71.9.4951-4959.2005

Cuyk, S., Deshpande, A., Hollander, A., Duval, N., Ticknor, L., Layshock, J., … & Omberg, K. (2011). Persistence of *Bacillus thuringiensis* subsp. *kurstaki* in urban environments following spraying. *Applied and Environmental Microbiology*, *77*(22), 7954-7961. https://doi.org/10.1128/aem.05207-11

Daehre, K., Projahn, M., Friese, A., Semmler, T., Guenther, S., & Roesler, U. (2018). ESBL-producing *Klebsiella pneumoniae* in the broiler production chain and the first description of st3128. *Frontiers in Microbiology, 9*. https://doi.org/10.3389/fmicb.2018.02302

Darge, W. and Woldemariam, S. (2021). Botryosphaeria tree fungal pathogens and their diversity. *International Journal of Phytopathology*, *10*(1), 49-56. https://doi.org/10.33687/phytopath.010.01.3447

Deng, Q., Lin, H., Hua, M., Sun, L., Pu, Y., Liao, J., ... & Gooneratne, R. (2022). LC-MS and transcriptome analysis of Lipopeptide biosynthesis by Bacillus velezensis CMT-6 responding to dissolved oxygen. *Molecules*, *27*(20), 6822. https://doi.org/10.3390/molecules27206822

Dergham, Y., Sanchez-Vizuete, P., Coq, D., Deschamps, J., Bridier, A., Hamze, K., … & Briandet, R. (2021). Comparison of the genetic features involved in *Bacillus subtilis* biofilm formation using multi-culturing approaches. *Microorganisms*, *9*(3), 633. https://doi.org/10.3390/microorganisms9030633

Dick, M.W. (2001). The Peronosporomycetes. In: McLaughlin, D.J., McLaughlin, E.G., Lemke, P.A. (eds) *Systematics and Evolution. The Mycota*, vol 7A. Springer, Berlin, Heidelberg. https://doi.org/10.1007/978-3-662-10376-0_2

Dick, M. W. (2002). Towards and Understanding of the Evolution of the Downy Mildews. *Advances in downy mildew research*, 1-57.

van Dijk, E. L., Naquin, D., Gorrichon, K., Jaszczyszyn, Y., Ouazahrou, R., Thermes, C., & Hernandez, C. (2023). Genomics in the long-read sequencing era. *Trends in Genetics*, *39*(9), 649-671. https://doi.org/10.1016/j.tig.2023.04.006

Ding, X., Nie, W., Qian, T., He, L., Zhang, H., HaiJun, J., … & Yu, J. (2022). Low plant density improves fruit quality without affecting yield of cucumber in different cultivation periods in greenhouse. *Agronomy*, *12*(6), 1441. https://doi.org/10.3390/agronomy12061441

Drenker, C., Mazouar, D., Bücker, G., Weißhaupt, S., Wienke, E., Koch, E., … & Linkies, A. (2023). Characterization of a disease-suppressive isolate of *Lysobacter* enzymogenes with broad antagonistic activity against bacterial, oomycetal and fungal pathogens in different crops. *Plants*, *12*(3), 682. https://doi.org/10.3390/plants12030682

Droffner, M. and Yamamoto, N. (1985). Isolation of thermophilic mutants of *Bacillus subtilis* and *Bacillus pumilus* and transformation of the thermophilic trait to mesophilic strains. *Microbiology*, *131*(10), 2789-2794. https://doi.org/10.1099/00221287-131-10-2789

REFERENCES

Earl, A. M., Losick, R., & Kolter, R. (2008). Ecology and genomics of *Bacillus subtilis*. *Trends in microbiology, 16*(6), 269-275. https://doi.org/10.1016/j.tim.2008.03.004

Efron, B. (1992). Bootstrap methods: another look at the jackknife. In *Breakthroughs in statistics: Methodology and distribution* (pp. 569-593). New York, NY: Springer New York.

Eken, C. (2004). A review of biological control of rose powdery mildew (Sphaerotheca pannosa var. rosae) by fungal antagonists. In *I International Rose Hip Conference 690* (pp. 193-196). https://doi.org/10.17660/ActaHortic.2005.690.29

Elahie, M., Naeem, M., Bashir, T., Yasmin, H., Younas, M., Areeb, A., … & Qin, M. (2021). *Bacillus pumilus* induced tolerance of maize (*Zea mays* L.) against cadmium (cd) stress. https://doi.org/10.21203/rs.3.rs-567788/v1

[redacted]

Elsholz, A. K., Wacker, S. A., & Losick, R. (2014). Self-regulation of exopolysaccharide production in *Bacillus subtilis* by a tyrosine kinase. *Genes & development*, *28*(15), 1710–1720. https://doi.org/10.1101/gad.246397.114

Elsherbiny, E., Amin, B., Aleem, B., Kingsley, K., & Bennett, J. (2020). *Trichoderma* volatile organic compounds as a biofumigation tool against late blight pathogen *Phytophthora infestans* in postharvest potato tubers. *Journal of Agricultural and Food Chemistry, 68*(31), 8163-8171. https://doi.org/10.1021/acs.jafc.0c03150

European Commission (2011). Commission Regulation (EU) No 546/2011 of 10 June 2011 implementing Regulation (EC) No 1107/2009 of the European Parliament and of the Council as regards uniform principles for evaluation and authorisation of plant protection products, OJ L 155, 11.6.2011, p. 127–175.

European Commission (2013). Commission Regulation (EU) No 283/2013 of 1 March 2013 setting out the data requirements for active substances, in accordance with Regulation (EC) No 1107/2009 of the European Parliament and of the Council concerning the placing of plant protection products on the market, OJ L 93, 3.4.2013, p. 1–84.

European Commission (2020a). Guidance on the approval and low-risk criteria linked to “antimicrobial resistance" applicable to microorganisms used for plant protection in accordance with Regulation (EC) No 1107/2009, SANTE/2020/12260, 23 October 2020.

European Commission for Health and Food Safety Directorate-General (DG SANTE) 2020. Guidance on the approval and low-risk criteria linked to “antimicrobial resistance” applicable to microorganism used for plant protection in accordance with Regulation (EC) No 1107/2009. Available at: https://ec.europa.eu/food/system/files/2020-11/pesticides_ppp_app-proc_guide_180652_microorganism-amr_202011.pdf. Accessed: 30.12.2021.

European Commission. (2023). Guidance on the approval and low-risk criteria linked to “antimicrobial resistance" applicable to microorganisms used for plant protection in accordance with Regulation (EC) No 1107/2009. European Commission. /https://food.ec.europa.eu/system/files/2020-11/pesticides_ppp_app-proc_guide_180652_microorganism-amr_202011.pdf

European Food Safety Authority (EFSA), 2021. EFSA statement on the requirements for whole genome sequence analysis of microorganisms intentionally used in the food chain. *EFSA Journal*, *19*(7), 6506. https://doi.org/10.2903/.j.efsa.2021.6506.

Euzéby, J. (2009). List of prokaryotic names with standing in nomenclature. Retrieved from http://www. bacterio.cict.fr.

Fan, B., Blom, J., Klenk, H. P., & Borriss, R. (2017). *Bacillus amyloliquefaciens, Bacillus velezensis*, and *Bacillus siamensis* form an “operational group *B. amyloliquefaciens*” within the *B. subtilis* species complex. *Frontiers in microbiology*, *8*, 237721. https://doi.org/10.3389/fmicb.2017.00022

Fan, H., Ru, J., Zhang, Y., Wang, Q., & Li, Y. (2017). Fengycin produced by *Bacillus subtilis* 9407 plays a major role in the biocontrol of apple ring rot disease. *Microbiological Research*, 199, 89-97. https://doi.org/10.1016/j.micres.2017.03.004

Farris, J. S. (1972). Estimating phylogenetic trees from distance matrices. *The American Naturalist, 106*(951), 645-668.

Farzand, A., Moosa, A., Zubair, M., Khan, A. R., Hanif, A., Tahir, H. A. S., & Gao, X. (2019). Marker assisted detection and LC-MS analysis of antimicrobial compounds in different *Bacillus* strains and their antifungal effect on *Sclerotinia sclerotiorum. Biological Control*, *133*, 91-102. https://doi.org/10.1016/j.biocontrol.2019.03.014

Fawke, S., Doumane, M., & Schornack, S. (2015). Oomycete interactions with plants: infection strategies and resistance principles. *Microbiology and Molecular Biology Reviews*, *79*(3), 263-280. https://doi.org/10.1128/mmbr.00010-15

Felsenstein, J. (1985). Confidence limits on phylogenies: an approach using the bootstrap. *Evolution, 39*(4), 783-791. https://doi.org/10.1111/j.1558-5646.1985.tb00420.x

Feng, L., Li, D., Sun, X., Wang, G., & Li, M. (2016). *Bacillus cavernae* sp. nov. isolated from cave soil. *International Journal of Systematic and Evolutionary Microbiology*, *66*(2), 801-806. https://doi.org/10.1099/ijsem.0.000794

[redacted]

Fiedler, S., & Heerklotz, H. (2015). Vesicle leakage reflects the target selectivity of antimicrobial lipopeptides from Bacillus subtilis. *Biophysical Journal*, *109*(10), 2079-2089. https://doi.org/10.1016/j.bpj.2015.09.021

Fessia, A., Barra, P., Barros, G., & Nesci, A. (2022). Could *Bacillus* biofilms enhance the effectivity of biocontrol strategies in the phyllosphere?. *Journal of Applied Microbiology*, *133*(4), 2148-2166. https://doi.org/10.1111/jam.15596

Fox, G., Wisotzkey, J., & Jurtshuk, P. (1992). How close is close: 16s rRNA sequence identity may not be sufficient to guarantee species identity. *International Journal of Systematic Bacteriology*, *42*(1), 166-170. https://doi.org/10.1099/00207713-42-1-166

Fritze, D. (2004). Taxonomy of the genus *Bacillus* and related genera: the aerobic endospore-forming bacteria. *Phytopathology*, *94*(11), 1245-1248. https://doi.org/10.1094/PHYTO.2004.94.11.1245

Gafni, A., Calderón, C., Harris, R., Buxdorf, K., Dafa-Berger, A., Zeilinger-Reichert, E., … & Levy, M. (2015). Biological control of the cucurbit powdery mildew pathogen *Podosphaera xanthii* by means of the epiphytic fungus *Pseudozyma aphidis* and parasitism as a mode of action. *Frontiers in Plant Science, 6.* https://doi.org/10.3389/fpls.2015.00132

[redacted]

García-Gutiérrez, L., Romero, D., Zeriouh, H., Cazorla, F., Torés, J., Vicente, A., … & Pérez-García, A. (2012). Isolation and selection of plant growth-promoting rhizobacteria as inducers of systemic resistance in melon. *Plant and Soil*, *358*(1-2), 201-212. https://doi.org/10.1007/s11104-012-1173-z

García-Gutiérrez, L., Zeriouh, H., Romero, D., Cubero, J., Vicente, A., & Pérez-García, A. (2013). The antagonistic strain *Bacillus subtilis* UMAF6639 also confers protection to melon plants against cucurbit powdery mildew by activation of jasmonate- and salicylic acid-dependent defence responses. *Microbial Biotechnology, 6*(3), 264-274. https://doi.org/10.1111/1751-7915.12028

Gastélum, G., Torre, M., & Rocha, J. (2020). Rap protein paralogs of *Bacillus thuringiensis*: a multifunctional and redundant regulatory repertoire for the control of collective functions. *Journal of Bacteriology*, *202*(6). https://doi.org/10.1128/jb.00747-19

Geissler, M., Oellig, C., Moss, K., Schwack, W., Henkel, M., & Hausmann, R. (2016). High-performance thin-layer chromatography (HPTLC) for the simultaneous quantification of the cyclic lipopeptides Surfactin, Iturin A and Fengycin in culture samples of *Bacillus* species. *Journal of Chromatography B, 1044,* 214-224. https://doi.org/10.1016/j.jchromb.2016.11.013

[redacted]

Giacomelli, L. (2023). Simultaneous editing of two *dmr6* genes in grapevine results in reduced susceptibility to downy mildew. *Frontiers in Plant Science*, 14. https://doi.org/10.3389/fpls.2023.1242240

Gijzen, M. (2009). Runaway repeats force expansion of the *Phytophthora infestans* genome. *Genome Biology, 10*(10), 241. https://doi.org/10.1186/gb-2009-10-10-241

Gilliard, G., Demortier, T., Boubsi, F., Jijakli, M. H., Ongena, M., De Clerck, C., & Deleu, M. (2024). Deciphering the distinct biocontrol activities of lipopeptides fengycin and surfactin through their differential impact on lipid membranes. *Colloids and Surfaces B: Biointerfaces*, *239*, 113933. https://doi.org/10.1016/j.colsurfb.2024.113933

REFERENCES

Gingichashvili, S., Duanis-Assaf, D., Shemesh, M., Featherstone, J., Feuerstein, O., & Steinberg, D. (2017). *Bacillus subtilis* biofilm development – a computerized study of morphology and kinetics. *Frontiers in Microbiology*, *8.* https://doi.org/10.3389/fmicb.2017.02072

Glawe, D. A. (2003). First report of powdery mildew of *Nandina domestica* caused by *Microsphaera berberidis* (*Erysiphe berberidis*) in the Pacific Northwest. *Plant health progress*, *4*(1), 30. https://doi.org/10.1094/PHP-2003-1023-01-HN

Godebo, A., Wee, N., Yost, C., Walley, F., & Germida, J. (2022). A meta-analysis to determine the state of biological control of *Aphanomyces* root rot. *Frontiers in Molecular Biosciences*, *8*. https://doi.org/10.3389/fmolb.2021.777042

Göker, M., Voglmayr, H., Riethmüller, A., & Oberwinkler, F. (2007). How do obligate parasites evolve? A multi-gene phylogenetic analysis of downy mildews. *Fungal Genetics and Biology*, *44*(2), 105-122. https://doi.org/10.1016/j.fgb.2006.07.005

Gong, A. D., Li, H. P., Yuan, Q. S., Song, X. S., Yao, W., He, W. J., ... & Liao, Y. C. (2015). Antagonistic mechanism of iturin A and plipastatin A from *Bacillus amyloliquefaciens* S76-3 from wheat spikes against *Fusarium graminearum*. *PloS one*, *10*(2), e0116871. https://doi.org/10.1371/journal.pone.0116871

Green, J. R., Carver, T. L., & Gurr, S. J. (2002). The formation and function of infection and feeding structures. *The powdery mildews: a comprehensive treatise*, 66-82.

Guerra-Cantera, M. and Raymundo, A. (2005). Utilization of a polyphasic approach in the taxonomic reassessment of antibiotic- and enzyme-producing *Bacillus* spp. isolated from the Philippines. *World Journal of Microbiology and Biotechnology, 21*(5), 635-644. https://doi.org/10.1007/s11274-004-3567-4

Gugel, I. (2024). Fed-batch bioreactor cultivation of bacillus subtilis using vegetable juice as an alternative carbon source for lipopeptides production: a shift towards a circular bioeconomy. *Fermentation, 10*(6), 323. https://doi.org/10.3390/fermentation10060323

Guo, Q., Dong, W., Li, S., Lu, X., Wang, P., Zhang, X., ... & Ma, P. (2014). Fengycin produced by *Bacillus subtilis* NCD-2 plays a major role in biocontrol of cotton seedling damping-off disease*. Microbiological Research, 169*(7-8), 533-540. https://doi.org/10.1016/j.micres.2013.12.001

Guo, Q., Li, S., Dong, L., Su, Z., Wang, P., Liu, X., … & Ma, P. (2023). Screening biocontrol agents for cash crop *Fusarium* wilt based on fusaric acid tolerance and antagonistic activity against *Fusarium oxysporum. Toxins*, *15(*6), 381. https://doi.org/10.3390/toxins15060381

Gupta, R.S., Patel, S., Saini, N. & Chen, S., 2020. Robust demarcation of 17 distinct *Bacillus* species clades, proposed as novel *Bacillaceae* genera, by phylogenomics and comparative genomic analyses: description of *Robertmurraya kyonggiensis* sp. nov. and proposal for an emended genus *Bacillus* limiting it only to the members of the Subtilis and Cereus clades of species*. International Journal of Systematic and Evolutionary Microbiology*, *70(*11): 5753-5798. doi: 10.1099/ijsem.0.004475.

Hafez, Y., El-Nagar, A., Elzaawely, A., Kamel, S., & Maswada, H. (2018). Biological control of *Podosphaera xanthii* the causal agent of squash powdery mildew disease by upregulation of defense-related enzymes. *Egyptian Journal of Biological Pest Control, 28*(1). https://doi.org/10.1186/s41938-018-0058-8

Hajlaou, M. R., Traquair, J. A., Jarvis, W. R., & Bélanger, R. R. (1994). Antifungal activity of extracellular metabolites produced by *Sporothrix flocculosa*. *Biocontrol Science and Technology,* 4(2), 229-237. https://doi.org/10.1080/09583159409355331

Halebian, S., Harris, B., Finegold, S., & Rolfe, R. (1981). Rapid method that aids in distinguishing gram-positive from gram-negative anaerobic bacteria. *Journal of Clinical Microbiology*, *13*(3), 444-448. https://doi.org/10.1128/jcm.13.3.444-448.1981

Hall, T.A. 1999. BioEdit: a user-friendly biological sequence alignment editor and analysis program for Windows 95/98/NT. *Nucleic Acids Symposium Series*, *41,* 95-98.

Hammami, W., Castro, C., Rémus-Borel, W., Labbé, C., & Bélanger, R. (2011). Ecological basis of the interaction between *Pseudozyma flocculosa* and powdery mildew fungi. *Applied and Environmental Microbiology, 77(*3), 926-933. https://doi.org/10.1128/aem.01255-10

Hashem, A. and Tabassum, B. (2019). *Bacillus subtilis*: a plant-growth promoting rhizobacterium that also impacts biotic stress. *Saudi Journal of Biological Sciences, 26*(6), 1291-1297. https://doi.org/10.1016/j.sjbs.2019.05.004

Heo, J., Kim, J. S., Hong, S. B., Park, B. Y., Kim, S. J., & Kwon, S. W. (2019). Genetic marker gene, *recQ*, differentiating *Bacillus subtilis* and the closely related *Bacillus* species. *FEMS Microbiology Letters*, *366*(16), fnz172. https://doi.org/10.1093/femsle/fnz172

REFERENCES

Hernández, I., Gutiérrez, S., Ceballos, S., Palacios, F., Toffolatti, S., Maddalena, G., … & Tardáguila, J. (2022). Assessment of downy mildew in grapevine using computer vision and fuzzy logic. Development and validation of a new method. *OENO One, 56*(3), 41-53. https://doi.org/10.20870/oeno-one.2022.56.3.5359

Herten, M., Bisdas, T., Knaack, D., Becker, K., Osada, N., Torsello, G., … & Idelevich, E. (2017). Rapid *in vitro* quantification of *S. aureus* biofilms on vascular graft surfaces. *Frontiers in Microbiology, 8.* https://doi.org/10.3389/fmicb.2017.02333

Hobley, L., Ostrowski, A., Rao, F. V., Bromley, K. M., Porter, M., Prescott, A. R., ... & Stanley-Wall, N. R. (2013). BslA is a self-assembling bacterial hydrophobin that coats the *Bacillus subtilis* biofilm. *Proceedings of the National Academy of Sciences, 110*(33), 13600-13605. https://doi.org/10.1073/pnas.1306390110

Hong, D., Long, T., Tien, N., Hoa, D., Phan, T., & Tram, L. (2022). A multi locus sequence analysis scheme for phylogeny of the *Bacillus subtilis* species complex and its advantages over 16s rRNA genes. *Ho Chi Minh City Open University Journal of Science - Engineering and Technology*, *12*(2), 22-33. https://doi.org/10.46223/hcmcoujs.tech.en.12.2.2255.2022

Hossain, A., Hasan, R., Islam, M. M., Datta, J., Mahidul, M., & Masum, I. (2018). Elucidation of the antagonistic effect of *Bacillus* species against white mold fungus *Sclerotinia sclerotiorum. International Journal of Biosciences (Ijb), 13*(04), 195-207. https://doi.org/10.12692/ijb/13.4.195-207

Huber, L. (2003). Validation of analytical methods and processes. In *Pharmaceutical process validation* (pp. 550-567). CRC Press.

Huntley, R. P., Sawford, T., Mutowo-Meullenet, P., Shypitsyna, A., Bonilla, C., Martin, M. J., & O'Donovan, C. (2015). The GOA database: gene ontology annotation updates for 2015. *Nucleic acids research, 43*(D1), D1057-D1063. https://doi.org/10.1093/nar/gku1113

International Conference on Harmonisation (ICH). (2005). Validation of Analytical Procedures: Text and Methodology Q2(R1).

International Conference on Harmonization of Technical Requirements for Registration of Pharmaceuticals for Human Use (ICH) harmonized tripartite guideline for the validation of analytical procedures (CPMP/ICH/381/95). June 1995.

Inès, M., & Dhouha, G. (2015). Lipopeptide surfactants: production, recovery and pore forming capacity. *Peptides*, *71*, 100-112. https://doi.org/10.1016/j.peptides.2015.07.006

Iqbal, S., Ullah, N., & Janjua, H. (2021). *In vitro* evaluation and genome mining of *Bacillus subtilis* strain RS10 reveals its biocontrol and plant growth-promoting potential. *Agriculture*, *11*(12), 1273. https://doi.org/10.3390/agriculture11121273

Islam, M., Ali, M., Choi, S., Hyun, J., & Baek, K. (2019). Biocontrol of citrus canker disease caused by *Xanthomonas citri* subsp. *citri* using an endophytic *Bacillus thuringiensis. The Plant Pathology Journal, 35*(5), 486-497. https://doi.org/10.5423/ppj.oa.03.2019.0060

Jack, D. L., Storms, M. L., Tchieu, J. H., Paulsen, I. T., & Saier, M. H., Jr (2000). A broad-specificity multidrug efflux pump requiring a pair of homologous SMR-type proteins. *Journal of bacteriology*, *182*(8), 2311–2313. https://doi.org/10.1128/JB.182.8.2311-2313.2000

Jayadev, A. (2017). Activity screening and optimization of marine fungal strains for protease activity. *World Journal of Pharmacy and Pharmaceutical Sciences,* 1195-1201. https://doi.org/10.20959/wjpps20179-9984

Johnson, J., Spakowicz, D., Hong, B., Petersen, L., Demkowicz, P., Chen, L., … & Weinstock, G. (2019). Evaluation of 16s rRNA gene sequencing for species and strain-level microbiome analysis. *Nature Communications, 10*(1). https://doi.org/10.1038/s41467-019-13036-1

Johnson, M., Thatcher, E., & Cox, M. (1995). Techniques for controlling variability in gram staining of obligate anaerobes. *Journal of Clinical Microbiology, 33*(3), 755-758. https://doi.org/10.1128/jcm.33.3.755-758.1995

Juhas, M., Crook, D. W., & Hood, D. W. (2008). Type IV secretion systems: tools of bacterial horizontal gene transfer and virulence. *Cellular microbiology, 10*(12), 2377-2386. https://doi.org/10.1111/j.1462-5822.2008.01187.x

Júnior, A., Tränkner, M., Ribeiro, R., Tiedemann, A., & Amorim, L. (2020). Photosynthetic cost associated with induced defense to *Plasmopara viticola* in grapevine. *Frontiers in Plant Science, 11.* https://doi.org/10.3389/fpls.2020.00235

Junker, R., Loewel, C., Gross, R., Dötterl, S., Keller, A., & Blüthgen, N. (2011). Composition of epiphytic bacterial communities differs on petals and leaves. *Plant Biology*, *13*(6), 918-924. https://doi.org/10.1111/j.1438-8677.2011.00454.x

REFERENCES

Kamada, M., Hase, S., Fujii, K., Miyake, M., Sato, K., Kimura, K., & Sakakibara, Y. (2015). Whole-genome sequencing and comparative genome analysis of *Bacillus subtilis* strains isolated from non-salted fermented soybean foods. *PloS one, 10*(10), e0141369. https://doi.org/10.1371/journal.pone.0141369

Kanetis, L., Holmes, G., & Ojiambo, P. (2010). Survival of *Pseudoperonospora cubensis* sporangia exposed to solar radiation. *Plant Pathology*, *59*(2), 313-323. https://doi.org/10.1111/j.1365-3059.2009.02211.x

Karnwal, A., Shrivastava, S., Al-Tawaha, A., Kumar, G., Singh, R., Kumar, A., … & Malik, T. (2023). Microbial biosurfactant as an alternate to chemical surfactants for application in cosmetics industries in personal and skin care products: a critical review. *Biomed Research International, 2023,* 1-21. https://doi.org/10.1155/2023/2375223

Kawagoe, Y., Shiraishi, S., Kondo, H., Yamamoto, S., Aoki, Y., & Suzuki, S. (2015). Cyclic lipopeptide iturin A structure-dependently induces defence response in *Arabidopsis* plants by activating SA and JA signaling pathways. *Biochemical and Biophysical Research Communications*, *460*(4), 1015-1020. https://doi.org/10.1016/j.bbrc.2015.03.143

Kesel, S., Grumbein, S., Gümperlein, I., Tallawi, M., Marel, A., Lieleg, O., … & Opitz, M. (2016). Direct comparison of physical properties of *Bacillus subtilis* NCIB 3610 and B-1 biofilms. *Applied and Environmental Microbiology*, *82*(8), 2424-2432. https://doi.org/10.1128/aem.03957-15

Khalaf, E. M., & Raizada, M. N. (2018). Bacterial seed endophytes of domesticated cucurbits antagonize fungal and oomycete pathogens including powdery mildew. *Frontiers in microbiology*, *9,* 42. https://doi.org/10.3389/fmicb.2018.00042

Khudhair, A. (2023). The role of the relative humidity on the development of downy mildew infection of cucumber in the greenhouse in Baghdad. *Iop Conference Series Earth and Environmental Science*, *1252*(1), 012019. https://doi.org/10.1088/1755-1315/1252/1/012019

Kim, B., Chung, J., Kim, S., Jeong, H., Kang, S., Kwon, S., … & Kim, J. (2012). Genome sequence of the leaf-colonizing bacterium *Bacillus* sp. strain 5b6, isolated from a cherry tree. *Journal of Bacteriology, 194*(14), 3758-3759. https://doi.org/10.1128/jb.00682-12

Kim, M., Oh, H. S., Park, S. C., & Chun, J. (2014). Towards a taxonomic coherence between average nucleotide identity and 16S rRNA gene sequence similarity for species demarcation of prokaryotes. *International journal of systematic and evolutionary microbiology, 64*(Pt_2), 346-351. https://doi.org/10.1099/ijs.0.059774-0

Kim, S., Jung, M., Oh, E., Kim, T., & Kim, J. (2019). Mitochondrial genome of *Thepodosphaera xanthii:* a plant pathogen causes powdery mildew in cucurbits. *Mitochondrial DNA Part B, 4*(2), 4172-4173. https://doi.org/10.1080/23802359.2019.1618209

Kim, Y. T., Park, B. K., Kim, S. E., Lee, W. J., Moon, J. S., Cho, M. S., ... & Kim, S. U. (2017). Organization and characterization of genetic regions in *Bacillus subtilis* subsp. *krictiensis* ATCC55079 associated with the biosynthesis of iturin and surfactin compounds. *PLoS One*, *12*(12), e0188179. https://doi.org/10.1371/journal.pone.0188179

Kiss, L. (2003). A review of fungal antagonists of powdery mildews and their potential as biocontrol agents. *Pest Management Science: formerly Pesticide Science, 59*(4), 475-483. https://doi.org/10.1002/ps.689

Kiss, L. and Vaghefi, N. (2021). First report of powdery mildew of rainforest spinach (E*latostema reticulatum*), native to Australia, caused by *Podosphaera xanthii. Australasian Plant Disease Notes, 16*(1). https://doi.org/10.1007/s13314-021-00424-0

Kiss, L., Vaghefi, N., Bransgrove, K., Dearnaley, J., Takamatsu, S., Tan, Y., … & Braun, U. (2020). Australia: a continent without native powdery mildews? The first comprehensive catalog indicates recent introductions and multiple host range expansion events, and leads to the re-discovery of Salmonomyces as a new lineage of the Erysiphales. *Frontiers in Microbiology*, *11*. https://doi.org/10.3389/fmicb.2020.01571

Klecan, A. L., Hippe, S., & Somerville, S. C. (1990). Reduced growth of *Erysiphe graminis* f. sp. *hordei* induced by *Tilletiopsis pallescens*. *Phytopathology*, *80*(4), 325-331.

Klee, S. R., Brzuszkiewicz, E. B., Nattermann, H., Brüggemann, H., Dupke, S., Wollherr, A., ... & Liesegang, H. (2010). The genome of a Bacillus isolate causing anthrax in chimpanzees combines chromosomal properties of *B. cereus* with *B. anthracis* virulence plasmids. *PloS one*, *5*(7), e10986. https://doi.org/10.1371/journal.pone.0010986

Knight, B.C.J.G. and Proom, H. (1950) A comparative survey of the nutrition and physiology of mesophilic species in the genus *Bacillus*. J. gen. *Microbiology*. *4*, 508-538.

Knudsen, I. M., & Skou, J. P. (1993). The effectivity of *Tilletiopsis albescens* in biocontrol of powdery mildew. *Annals of applied biology*, *123*(1), 173-185.

Kobayashi, K. and Iwano, M. (2012). BslA (YuaB) forms a hydrophobic layer on the surface of *Bacillus subtilis* biofilms. *Molecular Microbiology, 85*(1), 51-66. https://doi.org/10.1111/j.1365-2958.2012.08094.x

Köhl, J., Goossen-van de Geijn, H., Groenenboom-de Haas, L., Henken, B., Hauschild, R., Hilscher, U., ... & Wikström, M. (2019). Stepwise screening of candidate antagonists for biological control of *Blumeria graminis* f. sp. tritici. *Biological Control, 136,* 104008. https://doi.org/10.1016/j.biocontrol.2019.104008

Koledenkova, K., Esmaeel, Q., Jacquard, C., Nowak, J., Clément, C., & Barka, E. (2022). *Plasmopara viticola* the causal agent of downy mildew of grapevine: from its taxonomy to disease management. *Frontiers in Microbiology, 13*. https://doi.org/10.3389/fmicb.2022.889472

Koneman, E. W., Allen, S. D., Janda, W. M., Schreckenberger, P. C., & Winn, W. C. (1997). Diagnostic microbiology. The nonfermentative gram-negative bacilli. Philedelphia: *Lippincott-Raven Publishers,* 253-320.

Koumoutsi, A., Chen, X. H., Henne, A., Liesegang, H., Hitzeroth, G., Franke, P., ... & Borriss, R. (2004). Structural and functional characterization of gene clusters directing nonribosomal synthesis of bioactive cyclic lipopeptides in *Bacillus amyloliquefaciens* strain FZB42. https://doi.org/10.1128/jb.186.4.1084-1096.2004

Koutsoumanis, K., Allende, A., Alvarez-Ordonez, A., Bolton, D., Bover-Cid, S., Chemaly, M., … & Herman, L. (2023b). Updated list of QPS-recommended biological agents for safety risk assessments carried out by EFSA. *Zenodo*. https://doi.org/10.5281/zenodo.1146566

Koutsoumanis, K., Allende, A., Alvarez-Ordóñez, A., Bolton, D., Bover-Cid, S., Chemaly, M., De Cesare, A., Hilbert, F., Lindqvist, R., Nauta, M., Nonno, R., Peixe, L., Ru, G., Simmons, M., Skandamis, P., Suffredini, E., Cocconcelli, P.S., Suarez, J.E., Fernández, N.E., Istace, F., Aguillera, J., Brozzi, R., Liébana, E., Guerra, B., Correia, S. & Herman, L. (2023a). Statement on how to interpret the QPS qualification on 'acquired antimicrobial resistance genes. *EFSA Journal*, *21*, 1–13. https://doi.org/10.2903/j.efsa.2023.8323

Kranz, J. (2003). *Comparative epidemiology of plant diseases* (pp. 585-590). New York: Springer.

Kreft, Ł., Botzki, A., Coppens, F., Vandepoele, K., & Van Bel, M. (2017). PhyD3: a phylogenetic tree viewer with extended phyloXML support for functional genomics data visualization. *Bioinformatics*, *33*(18), 2946-2947. https://doi.org/10.1093/bioinformatics/btx324

Krishnamurthi, S., Chakrabarti, T., & Stackebrandt, E. (2009). Re-examination of the taxonomic position of *Bacillus silvestris* Rheims et al. 1999 and proposal to transfer it to *Solibacillus* gen. nov. as *Solibacillus silvestris* comb. nov.. *International Journal of Systematic and Evolutionary Microbiology*, *59*(5), 1054-1058. https://doi.org/10.1099/ijs.0.65742-0

Kunova, A., Pizzatti, C., Saracchi, M., Pasquali, M., & Cortesi, P. (2021). Grapevine powdery mildew: fungicides for its management and advances in molecular detection of markers associated with resistance. *Microorganisms*, *9*(7), 1541. https://doi.org/10.3390/microorganisms9071541

Kushwaha, P., Srivastava, R., Pandiyan, K., Singh, A., Chakdar, H., Kashyap, P., … & Saxena, A. (2021). Enhancement in plant growth and zinc biofortification of chickpea (*Cicer arietinum* L.) by *Bacillus altitudinis. Journal of Soil Science and Plant Nutrition, 21*(2), 922-935. https://doi.org/10.1007/s42729-021-00411-5

Ladner, J. (2023). Towards a post-pandemic future for global pathogen genome sequencing. *PloS Biology, 21*(8), e3002225. https://doi.org/10.1371/journal.pbio.3002225

Lagesen, K., Hallin, P., Rødland, E. A., Stærfeldt, H. H., Rognes, T., & Ussery, D. W. (2007). RNAmmer: consistent and rapid annotation of ribosomal RNA genes. *Nucleic acids research, 35*(9), 3100-3108. https://doi.org/10.1093/nar/gkm160

Lamichhane, J., Osdaghi, E., Behlau, F., Köhl, J., Jones, J., & Aubertot, J. (2018). Thirteen decades of antimicrobial copper compounds applied in agriculture. A review. *Agronomy for Sustainable Development, 38*(3). https://doi.org/10.1007/s13593-018-0503-9

Law, J., Ser, H., Khan, T., Chuah, L., Pusparajah, P., Chan, K., … & Lee, L. (2017). The potential of Streptomyces as biocontrol agents against the rice blast fungus, *Magnaporthe oryzae* (P*yricularia oryzae)*. *Frontiers in Microbiology, 8*. https://doi.org/10.3389/fmicb.2017.00003

Lebeda, A. (1990). Biology and ecology of cucurbit downy mildew. *Cucurbit downy mildew,* 13-46.

Lebeda, A., & Cohen, Y. (2011). Cucurbit downy mildew (*Pseudoperonospora cubensis*)—biology, ecology, epidemiology, host-pathogen interaction and control. *European journal of plant pathology, 129,* 157-192. https://doi.org/10.1007/s10658-010-9658-1

Lebeda, A. & Mieslerová, B. (2010). Taxonomy, distribution and biology of lettuce powdery mildew *(Golovinomyces cichoracearum sensu stricto). Plant Pathology, 60*(3), 400-415. https://doi.org/10.1111/j.1365-3059.2010.02399.x

REFERENCES

Lebeda, A., & Schwinn, F. J. (1994). The downy mildews – an overview of recent research progress / Falscher Mehltau – Übersicht über neuere Forschungsresultate. *Zeitschrift Für Pflanzenkrankheiten Und Pflanzenschutz / Journal of Plant Diseases and Protection*, *101*(3), 225–254. http://www.jstor.org/stable/43386284

Lebeda, A., Křístková, E., Sedláková, B., Coffey, M., & McCreight, J. (2011). Gaps and perspectives of pathotype and race determination in *Golovinomyces cichoracearum* and *Podosphaera xanthii. Mycoscience*, *52(*3), 159-164. https://doi.org/10.47371/s10267-010-0098-8

Leconte, A., Tournant, L., Muchembled, J., Paucellier, J., Héquet, A., Deracinois, B., … & Coutte, F. (2022). Assessment of lipopeptide mixtures produced by *Bacillus subtilis* as biocontrol products against apple scab (*Venturia inaequalis*). *Microorganisms, 10*(9), 1810. https://doi.org/10.3390/microorganisms10091810

Lee, D., Jung, J., Yang, Y., Kim, J., Yi, H., & Jeon, J. (2016). The antibacterial activity of chlorhexidine digluconate against *Streptococcus* mutans biofilms follows sigmoidal patterns*. European Journal of Oral Sciences, 124*(5), 440-446. https://doi.org/10.1111/eos.12285

Lee, H., Lee, D. G., Jo, H., Heo, Y. M., Baek, C., Kim, H. B., ... & Han, K. (2024). Comparative whole genome analysis of face-derived *Streptococcus infantis* CX-4 unravels the functions related to skin barrier. *Genes & Genomics, 46*(4), 499-510. https://doi.org/10.1007/s13258-024-01495-w

Lefort, V., Desper, R., & Gascuel, O. (2015). FastME 2.0: a comprehensive, accurate, and fast distance-based phylogeny inference program. *Molecular biology and evolution, 32*(10), 2798-2800. https://doi.org/10.1093/molbev/msv150

Leguérinel, I., Couvert, O., & Mafart, P. (2006). Modelling the influence of the incubation temperature upon the estimated heat resistance of heated *Bacillus* spores. *Letters in Applied Microbiology, 43*(1), 17-21. https://doi.org/10.1111/j.1472-765x.2006.01921.x

Lemjiber, N., Naamani, K., Merieau, A., Dihazi, A., Zhar, N., Jediyi, H., & Boukerb, A. M. (2021). Identification and genomic characterization of pathogenic *Bacillus altitudinis* from common pear trees in Morocco. *Agronomy, 11*(7), 1344. https://doi.org/10.3390/agronomy11071344

Lenzi, M. H., Martins, W. M., Roch, M., Ramos, P. L., Sands, K., Cayô, R., ... & Gales, A. C. (2021). A new mutation in mgrb mediating polymyxin resistance in *Klebsiella variicola*. *International journal of antimicrobial agents, 58*(5), 106424. https://doi.org/10.1016/j.ijantimicag.2021.106424

Li, Y., Both, A., Wyenandt, C., Durner, E., & Heckman, J. (2019). Applying wollastonite to soil to adjust pH and suppress powdery mildew on pumpkin. *Horttechnology*, *29*(6), 811-820. https://doi.org/10.21273/horttech04391-19

Li, J., Gu, T., Li, L., Wu, X., Shen, L., Yu, R., ... & Zeng, W. (2020). Complete genome sequencing and comparative genomic analyses of *Bacillus* sp. S3, a novel hyper Sb (III)-oxidizing bacterium. *BMC microbiology*, *20*, 1-19. https://doi.org/10.1186/s12866-020-01737-3

Li, Y., Gu, Y., Li, J., Xu, M., Wei, Q., & Wang, Y. (2015). Biocontrol agent *Bacillus amyloliquefaciens* LJ02 induces systemic resistance against cucurbits powdery mildew. *Frontiers in Microbiology, 6*, 883. https://doi.org/10.3389/fmicb.2015.00883

Li, Y., Héloir, M., Zhang, X., Geissler, M., Trouvelot, S., Jacquens, L., … & Adrian, M. (2019). Surfactin and fengycin contribute to the protection of a *Bacillus subtilis* strain against grape downy mildew by both direct effect and defence stimulation. *Molecular Plant Pathology, 20*(8), 1037-1050. https://doi.org/10.1111/mpp.12809

Li, Y., Lei, L., Zheng, L., Xiao, X., Tang, H., & Luo, C. (2020). Genome sequencing of gut symbiotic *Bacillus velezensis* LC1 for bioethanol production from bamboo shoots. *Biotechnology for biofuels, 13*, 1-12. https://doi.org/10.1186/s13068-020-1671-9

Li, L., Wang, R., Liang, X., Gai, Y., Jiao, C., & Wang, M. (2023). Characterization of a *Bacillus velezensis* with antibacterial activity and its inhibitory effect on gray mold germ. *Agronomy, 13*(6), 1553. https://doi.org/10.3390/agronomy13061553

Li, X., Yanzhou, Z., Wei, Z., Zhang, G., Cai, Y., & Liao, X. (2016). Antifungal activity of isolated *Bacillus amyloliquefaciens* SYBC H47 for the biocontrol of peach gummosis. *PloS One, 11*(9), e0162125. https://doi.org/10.1371/journal.pone.0162125

Lin, T. P., Chen, C. L., Chang, L. K., Tschen, J. S. M., & Liu, S. T. (1999). Functional and transcriptional analyses of a fengycin synthetase gene, fenC, from *Bacillus subtilis. Journal of bacteriology, 181*(16), 5060-5067. https://doi.org/10.1128/JB.181.16.5060-5067.1999

Lin, Y. C., Chen, E. H. L., Chen, R. P. Y., Dunny, G. M., Hu, W. S., & Lee, K. T. (2021). Probiotic *Bacillus* affects *Enterococcus faecalis* antibiotic resistance transfer by interfering with pheromone signaling cascades. *Applied and environmental microbiology, 87*(13), e00442-21. https://doi.org/10.1128/AEM.00442-21

Lin, L. Z., Zheng, Q. W., Wei, T., Zhang, Z. Q., Zhao, C. F., Zhong, H., ... & Guo, L. Q. (2020). Isolation and characterization of fengycins produced by *Bacillus amyloliquefaciens* JFL21 and its broad-spectrum antimicrobial potential against multidrug-resistant foodborne pathogens. *Frontiers in microbiology, 11*, 579621. https://doi.org/10.3389/fmicb.2020.579621

Lindow, S. and Brandl, M. (2003). Microbiology of the phyllosphere. *Applied and Environmental Microbiology, 69*(4), 1875-1883. https://doi.org/10.1128/aem.69.4.1875-1883.2003

Liu, W., Li, S., Wang, Z., Yan, E. C. Y., & Leblanc, R. M. (2017). Characterization of Surface-Active Biofilm Protein BslA in Self-Assembling Langmuir Monolayer at the Air-Water Interface. *Langmuir: the ACS journal of surfaces and colloids*, *33*(30), 7548–7555. https://doi.org/10.1021/acs.langmuir.7b01739

Liu, J., Sun, Y., Liu, J., Wu, Y., Cao, C., Li, R., … & Jiang, J. (2020). *Saccharothrix deserti* sp. nov., an actinomycete isolated from desert soil. *International Journal of Systematic and Evolutionary Microbiology, 70*(3), 1882-1887. https://doi.org/10.1099/ijsem.0.003989

Liu, G., Zhang, K., Gong, H., Yang, K., Wang, X., Zhou, G., ... & Yang, Y. (2023). Whole Genome Sequencing and the lignocellulose degradation potential of *Bacillus subtilis* RLI2019 isolated from the intestine of termites. *Biotechnology for Biofuels and Bioproducts, 16*(1), 130.

Luna, V. A., King, D. S., Peak, K. K., Reeves, F., Heberlein-Larson, L., Veguilla, W., ... & Cattani, J. (2006). Bacillus anthracis virulent plasmid pX02 genes found in large plasmids of two other Bacillus species. *Journal of clinical microbiology*, *44*(7), 2367-2377. https://doi.org/10.1128/jcm.00154-06

Lv, J., Qi, J., Shi, Q., Shen, D., Zhang, S., Shao, G., ... & Huang, S. (2012). Genetic diversity and population structure of cucumber (*Cucumis sativus* L.). *PLoS ONE 7*(10): e46919. https://doi.org/10.1371/journal.pone.0046919

Macek, B., Mijakovic, I., Olsen, J. V., Gnad, F., Kumar, C., Jensen, P. R., & Mann, M. (2007). The serine/threonine/tyrosine phosphoproteome of the model bacterium *Bacillus subtilis. Molecular & Cellular Proteomics, 6*(4), 697-707. https://doi.org/10.1074/mcp.M600464-MCP200

Maddula, V. S. R. K., Zhang, Z., Pierson, E. A., & Pierson, L. (2006). Quorum sensing and phenazines are involved in biofilm formation by *Pseudomonas chlororaphis* (*aureofaciens*) strain 30-84. *Microbial ecology, 52*, 289-301. https://doi.org/10.1007/s00248-006-9064-6

Mahmood, T. (2022). Lipopeptides; powerful antifungal weapons produced by *Bacillus* species. *Plant Bulletin, 1*(1). https://doi.org/10.55627/pbulletin.001.01.0143

Makarenkov, V., Boc, A., Xie, J., Peres-Neto, P., Lapointe, F. J., & Legendre, P. (2010). Weighted bootstrapping: a correction method for assessing the robustness of phylogenetic trees. *BMC evolutionary biology, 10*, 1-16. https://doi.org/10.1186/1471-2148-10-250

Makky, E., Muharram, M., & Bayoumi, R. (2008). Identification of some *Bacillus* isolates producing exo-enzymes using Quantitative Real-Time Polymerase Chain Reaction (PCR). *Al-Azhar Bulletin of Science, 19*(Issue 1-C), 53-67. https://doi.org/10.21608/absb.2008.10501

Malek, F. (2016). Evaluation of a non-submerged cultivation assay combined to ESEM imaging for analysis of biofilms formed by dairy-associated sporeforming bacteria. *African Journal of Microbiology Research, 10*(32), 1263-1273. https://doi.org/10.5897/ajmr2016.8203

Manasa, M., Ravinder, P., Gopalakrishnan, S., Srinivas, V., Sayyed, R., Enshasy, H., … & Hameeda, B. (2021). Co-inoculation of *Bacillus* spp. for growth promotion and iron fortification in sorghum. *Sustainability, 13*(21), 12091. https://doi.org/10.3390/su132112091

Marine, S., Newark, M., Korir, R., & Everts, K. (2016). Evaluation of rotational biopesticide programs for disease management in organic cucurbit production. *Plant Disease, 100*(11), 2226-2233. https://doi.org/10.1094/pdis-02-16-0252-re

Marx, V. (2023). Method of the year: long-read sequencing. *Nature Methods*, *20*(1), 6-11. https://doi.org/10.1038/s41592-022-01759-x

Martin, M., & Gay, J. L. (1983). Ultrastructure of conidium development in *Erysiphe pisi. Canadian journal of botany, 61*(9), 2472-2495. https://doi.org/10.1139/b83-270

REFERENCES

Martínez-Cruz, J., Polonio, Á., Ruiz-Jiménez, L., Vielba-Fernández, A., Hierrezuelo, J., Romero, D., … & Pérez-García, A. (2022). Suppression of chitin-triggered immunity by a new fungal chitin-binding effector resulting from alternative splicing of a chitin deacetylase gene. *Journal of Fungi, 8*(10), 1022. https://doi.org/10.3390/jof8101022

Martínez-Cruz, J., Romero, D., Vicente, A., & Pérez-García, A. (2016). Transformation of the cucurbit powdery mildew pathogen *Podosphaera xanthii* by *Agrobacterium tumefaciens. New Phytologist, 213*(4), 1961-1973. https://doi.org/10.1111/nph.14297

Maugeri, T. L., Gugliandolo, C., Caccamo, D., Panico, A., Lama, L., Gambacorta, A., & Nicolaus, B. (2002). A halophilic thermotolerant *Bacillus* isolated from a marine hot spring able to produce a new exopolysaccharide. *Biotechnology Letters, 24*, 515-519. https://doi.org/10.1023/A:1014891431233

Maughan, H., & Van der Auwera, G. (2011). *Bacillus* taxonomy in the genomic era finds phenotypes to be essential though often misleading. *Infection, Genetics and Evolution, 11*(5), 789-797. https://doi.org/10.1016/j.meegid.2011.02.001

McInnes, R. S., McCallum, G. E., Lamberte, L. E., & van Schaik, W. (2020). Horizontal transfer of antibiotic resistance genes in the human gut microbiome. *Current opinion in Microbiology, 53*, 35-43. https://doi.org/10.1016/j.mib.2020.01.009

McLoon, A., Guttenplan, S., Kearns, D., Kolter, R., & Losick, R. (2011). Tracing the domestication of a biofilm-forming bacterium. *Journal of Bacteriology, 193*(8), 2027-2034. https://doi.org/10.1128/jb.01542-10

Medema, M. H., Blin, K., Cimermancic, P., De Jager, V., Zakrzewski, P., Fischbach, M. A., ... & Breitling, R. (2011). antiSMASH: rapid identification, annotation and analysis of secondary metabolite biosynthesis gene clusters in bacterial and fungal genome sequences. *Nucleic acids research*, *39*(suppl_2), W339-W346. https://doi.org/10.1093/nar/gkr466

Medeot, D., Fernandez, M., Morales, G., & Jofré, E. (2020). Fengycins from *Bacillus amyloliquefaciens* MEP218 exhibit antibacterial activity by producing alterations on the cell surface of the pathogens *Xanthomonas axonopodis* pv. *vesicatoria* and *Pseudomonas aeruginosa* PA01. *Frontiers in Microbiology, 10.* https://doi.org/10.3389/fmicb.2019.03107

Meena, K. R., & Kanwar, S. S. (2015). Lipopeptides as the antifungal and antibacterial agents: applications in food safety and therapeutics. *BioMed research international, 2015*. https://doi.org/10.1155/2015/473050

Meier-Kolthoff, J. P., & Göker, M. (2019). TYGS is an automated high-throughput platform for state-of-the-art genome-based taxonomy. *Nature communications, 10*(1), 2182. https://doi.org/10.1038/s41467-019-10210-3

Meier-Kolthoff, J. P., Auch, A. F., Klenk, H. P., & Göker, M. (2013). Genome sequence-based species delimitation with confidence intervals and improved distance functions. *BMC bioinformatics, 14*, 1-14. https://doi.org/10.1186/1471-2105-14-60

Meier-Kolthoff, J. P., Carbasse, J. S., Peinado-Olarte, R. L., & Göker, M. (2022). TYGS and LPSN: a database tandem for fast and reliable genome-based classification and nomenclature of prokaryotes. *Nucleic acids research, 50*(D1), D801-D807. https://doi.org/10.1093/nar/gkab902

Meier-Kolthoff, J. P., Hahnke, R. L., Petersen, J., Scheuner, C., Michael, V., Fiebig, A., ... & Klenk, H. P. (2014). Complete genome sequence of DSM 30083 T, the type strain (U5/41 T) of *Escherichia coli*, and a proposal for delineating subspecies in microbial taxonomy. *Standards in genomic sciences, 9,* 1-19. https://doi.org/10.1186/1944-3277-9-2

Miao, L. and Qian, P. (2005). Antagonistic antimicrobial activity of marine fungi and bacteria isolated from marine biofilm and seawaters of Hong Kong. *Aquatic Microbial Ecology, 38*, 231-238. https://doi.org/10.3354/ame038231

Miao, S., Liang, J., Xu, Y., Yu, G., & Shao, M. (2023). Bacillaene, sharp objects consist in the arsenal of antibiotics produced by *Bacillus. Journal of Cellular Physiology.* https://doi.org/10.1002/jcp.31228

Michereff, S. J., Noronha, M. A., Lima, G. S., Albert, Í. C., Melo, E. A., & Gusmão, L. O. (2009). Diagrammatic scale to assess downy mildew severity in melon. *Horticultura Brasileira, 27,* 76-79. https://doi.org/10.1590/S0102-05362009000100015

Mielich-Süss, B., & Lopez, D. (2015). Molecular mechanisms involved in *Bacillus subtilis* biofilm formation. *Environmental microbiology, 17*(3), 555-565. https://doi.org/10.1111/1462-2920.12527

Miethke, M. and Marahiel, M. (2007). Siderophore-based iron acquisition and pathogen control. *Microbiology and Molecular Biology Reviews, 71*(3), 413-451. https://doi.org/10.1128/mmbr.00012-07

REFERENCES

Miljaković, D., Marinković, J., & Balešević-Tubić, S. (2020). The significance of *Bacillus* spp. in disease suppression and growth promotion of field and vegetable crops. *Microorganisms, 8*(7), 1037. https://doi.org/10.3390/microorganisms8071037

Mijakovic, I., Poncet, S., Boël, G., Mazé, A., Gillet, S., Jamet, E., … & Deutscher, J. (2003). Transmembrane modulator-dependent bacterial tyrosine kinase activates UDP-glucose dehydrogenases. *The EMBO journal*, *22*(18), 4709–4718. https://doi.org/10.1093/emboj/cdg458

Miller, B. R., & Gulick, A. M. (2016). Structural biology of nonribosomal peptide synthetases. *Nonribosomal Peptide and Polyketide Biosynthesis: Methods and Protocols*, 3-29. https://doi.org/10.1007/978-1-4939-3375-4_1

Mims, C. W., Liljebjelke, K. A., & Richardson, E. A. (1995). Surface morphology, wall structure, and initial adhesion of conidia of the powdery mildew fungus *Uncinuliella australiana. Phytopathology, 85*(3), 352-358. https://doi.org/10.1094/Phyto-85-352

Molina-Santiago, C., Pearson, J., Navarro, Y., Berlanga-Clavero, M., Caraballo-Rodríguez, A., Petras, D., … & Romero, D. (2019). The extracellular matrix protects *Bacillus subtilis* colonies from *Pseudomonas* invasion and modulates plant co-colonization. *Nature Communications, 10*(1). https://doi.org/10.1038/s41467-019-09944-x

Mombert, P., Guijarro Díaz-Otero, B., & Alonso-Prados, J. L. (2022). Study of the different evaluation areas in the pesticide risk assessment process: Focus on pesticides based on microorganisms. *EFSA Journal, 20*, e200412. https://doi.org/10.2903/j.efsa.2022.e200412

Montazar, A., Cahn, M., & Putman, A. (2019). Research advances in adopting drip irrigation for california organic spinach: preliminary findings. *Agriculture, 9*(8), 177. https://doi.org/10.3390/agriculture9080177

Morikawa, M. (2006). Beneficial biofilm formation by industrial bacteria *Bacillus subtilis* and related species. *Journal of bioscience and bioengineering, 101*(1), 1-8. https://doi.org/10.1263/jbb.101.1

Morris, R. J., Schor, M., Gillespie, R. M. C., Ferreira, A. S., Baldauf, L., Earl, C., … & MacPhee, C. E. (2017). Natural variations in the biofilm-associated protein BslA from the genus *Bacillus*. *Scientific reports*, *7*(1), 6730. https://doi.org/10.1038/s41598-017-06786-9

Naegele, R., Quesada-Ocampo, L., Kurjan, J., Saude, C., & Hausbeck, M. (2016). Regional and temporal population structure of *Pseudoperonospora cubensis* in Michigan and Ontario. *Phytopathology, 106*(4), 372-379. https://doi.org/10.1094/phyto-02-15-0043-r

Nakamura, L., Roberts, M., & Cohan, F. (1999). Note: relationship of *Bacillus subtilis* clades associated with strains 168 and W23: a proposal for *Bacillus subtilis* subsp. *subtilis* subsp. nov. and *Bacillus subtilis* subsp. *spizizenii* subsp. nov.. *International Journal of Systematic and Evolutionary Microbiology, 49*(3), 1211-1215. https://doi.org/10.1099/00207713-49-3-1211

Neufeld, K. N., Keinath, A. P., & Ojiambo, P. S. (2017). A model to predict the risk of infection of cucumber by *Pseudoperonospora cubensis. Microbial risk analysis, 6*, 21-30. https://doi.org/10.1016/j.mran.2017.05.001

Neufeld, K., Isard, S., & Ojiambo, P. (2013). Relationship between disease severity and escape of *Pseudoperonospora cubensis* sporangia from a cucumber canopy during downy mildew epidemics. *Plant Pathology, 62*(6), 1366-1377. https://doi.org/10.1111/ppa.12040

Nikolaidis, M., Hesketh, A., Mossialos, D., Iliopoulos, I., Oliver, S. G., & Amoutzias, G. D. (2022). A comparative analysis of the core proteomes within and among the *Bacillus subtilis* and *Bacillus cereus* evolutionary groups reveals the patterns of lineage-and species-specific adaptations. *Microorganisms, 10*(9), 1720. https://doi.org/10.3390/microorganisms10091720

Nithyapriya, S., Sundaram, L., Sayyed, R., Reddy, M., Dailin, D., Enshasy, H., … & Herlambang, S. (2021). Production, purification, and characterization of bacillibactin siderophore of *Bacillus subtilis* and its application for improvement in plant growth and oil content in sesame. *Sustainability, 13*(10), 5394. https://doi.org/10.3390/su13105394

Nuñez-Palenius, H., Orosco-Alcalá, B., Espitia-Vázquez, I., Olalde-Portugal, V., Hoflack-Culebro, M., Ramírez-Santoyo, L., … & Valiente-Banuet, J. (2022). Biological control of downy mildew and yield enhancement of cucumber plants by *Trichoderma harzianum* and *Bacillus subtilis* (ehrenberg) under greenhouse conditions. *Horticulturae, 8*(12), 1133. https://doi.org/10.3390/horticulturae8121133

Nyland, G. (1950). The genus *Tilletiopsis. Mycologia, 42*(4), 487-496.

O'Brien, P. (2017). Biological control of plant diseases. *Australasian Plant Pathology, 46*(4), 293-304. https://doi.org/10.1007/s13313-017-0481-4

REFERENCES

OECD. (2018). Working document on the risk assessment of secondary metabolites of microbial biocontrol agents. *Series on Pesticides and Biocides, No. 98*. OECD Publishing. https://doi.org/10.1787/6ca93ea9-en

Ogbuji, N., Ataga, A., Tari-Ukuta, P., & Olisedeme, C. (2021). Molecular characterization of fungi associated with dump site soil. *Journal of Advances in Biology & Biotechnology,* 19-30. https://doi.org/10.9734/jabb/2021/v24i930239

Ojiambo, P., Gent, D., Quesada-Ocampo, L., Hausbeck, M., & Holmes, G. (2015). Epidemiology and population biology of *Pseudoperonospora cubensis*: a model system for management of downy mildews. *Annual Review of Phytopathology, 53*(1), 223-246. https://doi.org/10.1146/annurev-phyto-080614-120048

Ojwang, A., Ruiz, T., Bhattacharyya, S., Chatterjee, S., Ojiambo, P., & Gent, D. (2021). A general framework for spatio-temporal modeling of epidemics with multiple epicenters: application to an aerially dispersed plant pathogen. *Frontiers in Applied Mathematics and Statistics, 7*. https://doi.org/10.3389/fams.2021.721352

Oknin, H., Steinberg, D., & Shemesh, M. (2015). Magnesium ions mitigate biofilm formation of *Bacillus* species via downregulation of matrix genes expression. *Frontiers in Microbiology, 6*. https://doi.org/10.3389/fmicb.2015.00907

Okungbowa, F., Shittu, H., & Obiazikwor, H. (2019). Endophytic bacteria: hidden protective associates of plants against biotic and abiotic stresses. *Notulae Scientia Biologicae, 11*(2), 167-174. https://doi.org/10.15835/nsb11210423

Olanrewaju, O., Ayilara, M., & Babalola, O. (2021). Genome mining of three plant growth-promoting *Bacillus* species from maize rhizosphere. *Applied Biochemistry and Biotechnology, 193*(12), 3949-3969. https://doi.org/10.1007/s12010-021-03660-3

Ondov, B. D., Treangen, T. J., Melsted, P., Mallonee, A. B., Bergman, N. H., Koren, S., & Phillippy, A. M. (2016). Mash: fast genome and metagenome distance estimation using MinHash. *Genome biology, 17*, 1-14. https://doi.org/10.1186/s13059-016-0997-x

Ongena, M., & Jacques, P. (2008). *Bacillus* lipopeptides: versatile weapons for plant disease biocontrol. *Trends in microbiology, 16*(3), 115-125. https://doi.org/10.1016/j.tim.2007.12.009

Ongena, M., Jacques, P., Touré, Y., Destain, J., Jabrane, A., & Thonart, P. (2005). Involvement of fengycin-type lipopeptides in the multifaceted biocontrol potential of *Bacillus subtilis. Applied microbiology and biotechnology, 69*, 29-38. https://doi.org/10.1007/s00253-005-1940-3

Ostrowski, A., Mehert, A., Prescott, A., Kiley, T. B., & Stanley-Wall, N. R. (2011). YuaB functions synergistically with the exopolysaccharide and TasA amyloid fibers to allow biofilm formation by *Bacillus subtilis*. *Journal of bacteriology*, *193*(18), 4821–4831. https://doi.org/10.1128/JB.00223-11

Oyeniran, K. A., & Oladunmoye, M. K. (2015). Plasmid profiles of extremophiles associated with indigenous black soaps and functional groups present. https://doi.org/10.3923/mj.2015.76.84

Özdemir, F. and Arslan, S. (2018). Biofilm production and antimicrobial susceptibility profiles of *Bacillus* spp. from meats. *Sakarya University Journal of Science, 22*(6), 1674-1682. https://doi.org/10.16984/saufenbilder.395016

Palti, J., & Cohen, Y. (1980). Downy mildew of cucurbits (*Pseudoperonospora cubensis*): the fungus and its hosts, distribution, epidemiology and control. *Phytoparasitica, 8*, 109-147.

Pandya, U., Prakash, S., Shende, K., Dhuldhaj, U., & Saraf, M. (2017). Multifarious allelochemicals exhibiting antifungal activity from *Bacillus subtilis* MBCU5. *3 Biotech, 7*(3). https://doi.org/10.1007/s13205-017-0827-1

Park, J. H., Choi, Y., Choi, I., & Shin, H. (2023). First report of powdery mildew caused by *Golovinomyces ambrosiae* on *Leucanthemum vulgare* in Korea. *Plant Disease, 107*(3), 963. https://doi.org/10.1094/pdis-06-22-1472-pdn

Parte, A.C., Sardà Carbasse, J., Meier-Kolthoff, J.P., Reimer, L.C. and Göker, M. (2020). List of Prokaryotic names with Standing in Nomenclature (LPSN) moves to the DSMZ. *International Journal of Systematic and Evolutionary Microbiology, 70,* 5607-5612; DOI: 10.1099/ijsem.0.004332

Patel, S., & Gupta, R. S. (2020). A phylogenomic and comparative genomic framework for resolving the polyphyly of the genus *Bacillus*: Proposal for six new genera of *Bacillus* species, *Peribacillus* gen. nov., *Cytobacillus* gen. nov., *Mesobacillus* gen. nov., *Neobacillus* gen. nov., *Metabacillus* gen. nov. and *Alkalihalobacillus* gen. nov. *International journal of systematic and evolutionary microbiology, 70*(1), 406-438. https://doi.org/10.1099/ijsem.0.003775

Patel, H., Tscheka, C., Edwards, K., Karlsson, G., & Heerklotz, H. (2011). All-or-none membrane permeabilization by fengycin-type lipopeptides from *Bacillus subtilis* QST713. *Biochimica et Biophysica Acta (BBA)-Biomembranes*, *1808*(8), 2000-2008. https://doi.org/10.1016/j.bbamem.2011.04.016

REFERENCES

Paudel, Y., Lin, C., Shen, Z., & Qin, W. (2015). Characterization of pectin depolymerising exo polygalacturonase by *Bacillus* sp. HD2 isolated from the gut of *Apis mellifera* L.. *Microbiology Discovery, 3*(1), 2. https://doi.org/10.7243/2052-6180-3-2

Paulitz, T. C., & Bélanger, R. R. (2001). Biological control in greenhouse systems. *Annual review of phytopathology, 39*(1), 103-133. https://doi.org/10.1146/annurev.phyto.39.1.103

Pena-Gonzalez, A., Rodriguez-R, L. M., Marston, C. K., Gee, J. E., Gulvik, C. A., Kolton, C. B., ... & Konstantinidis, K. T. (2018). Genomic characterization and copy number variation of *Bacillus anthracis* plasmids pXO1 and pXO2 in a historical collection of 412 strains. *Msystems*, *3*(4), 10-1128. https://doi.org/10.1128/mSystems.00122-18

Perazzolli, M., Moretto, M., Fontana, P., Ferrarini, A., Velasco, R., Moser, C., … & Pertot, I. (2012). Downy mildew resistance induced by *Trichoderma harzianum* T39 in susceptible grapevines partially mimics transcriptional changes of resistant genotypes. *BMC Genomics, 13*(1), 660. https://doi.org/10.1186/1471-2164-13-660

Pérez, R., Zendo, T., & Sonomoto, K. (2018). Circular and leaderless bacteriocins: biosynthesis, mode of action, applications, and prospects. *Frontiers in Microbiology, 9*. https://doi.org/10.3389/fmicb.2018.02085

Pérez-García, A., Romero, D., Fernandez-Ortuño, D., López-Ruiz, F., De Vicente, A., & Tores, J. A. (2009). The powdery mildew fungus *Podosphaera fusca* (synonym *Podosphaera xanthii*), a constant threat to cucurbits. *Molecular plant pathology, 10*(2), 153-160. https://doi.org/10.1111/j.1364-3703.2008.00527.x

Petrillo, C., Castaldi, S., Lanzilli, M., Selci, M., Cordone, A., Giovannelli, D., … & Isticato, R. (2021). Genomic and physiological characterization of new plant growth promoting bacilli isolated from salt-pans. https://doi.org/10.1101/2021.05.17.444429

Pietrzak, U. and McPhail, D. (2004). Copper accumulation, distribution and fractionation in vineyard soils of Victoria, Australia. *Geoderma, 122*(2-4), 151-166. https://doi.org/10.1016/j.geoderma.2004.01.005

Pinkas, D., Fišer, R., Kozlík, P., Dolejšová, T., Hryzáková, K., Konopásek, I., & Mikušová, G. (2020). *Bacillus subtilis* cardiolipin protects its own membrane against surfactin-induced permeabilization. *Biochimica et Biophysica Acta (BBA)-Biomembranes*, *1862*(10), 183405. https://doi.org/10.1016/j.bbamem.2020.183405

Polesani, M., Bortesi, L., Ferrarini, A., Zamboni, A., Fasoli, M., Zadra, C., … & Polverari, A. (2010). General and species-specific transcriptional responses to downy mildew infection in a susceptible (*Vitis vinifera*) and a resistant (*V. riparia*) grapevine species. *BMC Genomics, 11*(1). https://doi.org/10.1186/1471-2164-11-117

Polonio, Á., Fernández-Ortuño, D., Vicente, A., & Pérez-García, A. (2021). A haustorial-expressed lytic polysaccharide monooxygenase from the cucurbit powdery mildew pathogen *Podosphaera xanthii* contributes to the suppression of chitin-triggered immunity. *Molecular Plant Pathology, 22*(5), 580-601. https://doi.org/10.1111/mpp.13045

Polonio, Á., Pineda, M., Bautista, R., Martínez-Cruz, J., Pérez-Bueno, M., Barón, M., … & Pérez-García, A. (2019). RNA-seq analysis and fluorescence imaging of melon powdery mildew disease reveal an orchestrated reprogramming of host physiology. *Scientific Reports, 9*(1). https://doi.org/10.1038/s41598-019-44443-5

Polonio, Á., Seoane, P., Claros, M., & Pérez-García, A. (2019). The haustorial transcriptome of the cucurbit pathogen *Podosphaera xanthii* reveals new insights into the biotrophy and pathogenesis of powdery mildew fungi. *BMC Genomics, 20*(1). https://doi.org/10.1186/s12864-019-5938-0

Pramanik, D., Shelake, R., Park, J., Kim, M., Hwang, I., Park, Y., … & Kim, J. (2021). CRISPR/Cas9-mediated generation of pathogen-resistant tomato against *tomato yellow leaf curl virus* and powdery mildew. *International Journal of Molecular Sciences, 22*(4), 1878. https://doi.org/10.3390/ijms22041878

Punina, N. V., Makridakis, N. M., Remnev, M. A., & Topunov, A. F. (2015). Whole-genome sequencing targets drug-resistant bacterial infections. *Human genomics, 9,* 1-20. https://doi.org/10.1186/s40246-015-0037-z

Puopolo, G., Giovannini, O., & Pertot, I. (2014). *Lysobacter capsici* AZ78 can be combined with copper to effectively control *Plasmopara viticola* on grapevine. *Microbiological Research, 169*(7-8), 633-642. https://doi.org/10.1016/j.micres.2013.09.013

Qian, J., Zhang, T., Tang, S., Zhou, L., Li, K., Xue-qin, F., … & Yu, S. (2020). Biocontrol of *Citrus canker* with endophyte *Bacillus amyloliquefaciens* QC-Y. *Plant Protection Science, 57*(1), 1-13. https://doi.org/10.17221/62/2020-pps

Qiao, J., Wu, H., Huo, R., Gao, X., & Borriss, R. (2014). Stimulation of plant growth and biocontrol by *Bacillus amyloliquefaciens* subsp. *plantarum* FZB42 engineered for improved action. *Chemical and Biological Technologies in Agriculture, 1*(1). https://doi.org/10.1186/s40538-014-0012-2

REFERENCES

Qiao, J., Yu, X., Liang, X., Liu, Y., Borriss, R., & Liu, Y. (2017). Addition of plant-growth-promoting *Bacillus subtilis* PTS-394 on tomato rhizosphere has no durable impact on composition of root microbiome. *BMC Microbiology, 17*(1). https://doi.org/10.1186/s12866-017-1039-x

Qin, H., & Driks, A. (2013). Contrasting evolutionary patterns of spore coat proteins in two *Bacillus* species groups are linked to a difference in cellular structure. *BMC evolutionary biology, 13,* 1-12. https://doi.org/10.1186/1471-2148-13-261

Raaijmakers, J. M., & Mazzola, M. (2012). Diversity and natural functions of antibiotics produced by beneficial and plant pathogenic bacteria. *Annual review of phytopathology, 50*, 403-424. https://doi.org/10.1146/annurev-phyto-081211-172908

Rabbee, M. F., Ali, M. S., Choi, J., Hwang, B. S., Jeong, S. C., & Baek, K. H. (2019). *Bacillus velezensis*: a valuable member of bioactive molecules within plant microbiomes. *Molecules, 24*(6), 1046. https://doi.org/10.3390/molecules24061046

Rabbee, M. F., & Baek, K. H. (2023). Detection of Antagonistic Compounds Synthesized by *Bacillus velezensis* against *Xanthomonas citri* subsp. *citri* by Metabolome and RNA Sequencing. *Microorganisms, 11*(6), 1523. https://doi.org/10.3390/microorganisms11061523

Rabha, M., Das, D., Konwar, T., Acharjee, S., & Sarmah, B. K. (2023). Whole genome sequencing of a novel *Bacillus thuringiensis* isolated from Assam soil. *BMC microbiology, 23*(1), 91. https://doi.org/10.1186/s12866-023-02780-y

Rahman, F. B., Sarkar, B., Moni, R., & Rahman, M. S. (2021). Molecular genetics of surfactin and its effects on different sub-populations of *Bacillus subtilis. Biotechnology Reports, 32*, e00686. https://doi.org/10.1016/j.btre.2021.e00686

Raja, H., Miller, A., Pearce, C., & Oberlies, N. (2017). Fungal identification using molecular tools: a primer for the natural products research community. *Journal of Natural Products, 80*(3), 756-770. https://doi.org/10.1021/acs.jnatprod.6b01085

Rangarajan, V., Dhanarajan, G., & Sen, R. (2015). Bioprocess design for selective enhancement of fengycin production by a marine isolate *Bacillus megaterium*. *Biochemical engineering journal, 99*, 147-155. https://doi.org/10.1016/j.bej.2015.03.016

Resti, Z., Liswarni, Y., & MARTINIUS, M. (2020). Endophytic bacterial consortia as biological control of bacterial leaf blight and plant growth promoter of rice (*Oryza sativa* L.). *Journal of Applied Agricultural Science and Technology, 4*(2), 134-145. https://doi.org/10.32530/jaast.v4i2.146

Reynoso, E., Ferreyra, D., Durantini, E., & Spesia, M. (2019). Photodynamic inactivation to prevent and disrupt *Staphylococcus aureus* biofilm under different media conditions. *Photodermatology Photoimmunology & Photomedicine, 35*(5), 322-331. https://doi.org/10.1111/phpp.12477

Richter, M., & Rosselló-Móra, R. (2009). Shifting the genomic gold standard for the prokaryotic species definition. *Proceedings of the National Academy of Sciences, 106*(45), 19126-19131. https://doi.org/10.1073/pnas.0906412106

Rijavec, M., Budič, M., Mrak, P., Müller-Premru, M., Podlesek, Z., & Žgur-Bertok, D. (2007). Prevalence of cole1-like plasmids and colicin k production among uropathogenic *Escherichia coli* strains and quantification of inhibitory activity of colicin k. *Applied and Environmental Microbiology, 73*(3), 1029-1032. https://doi.org/10.1128/aem.01780-06

Roberts, M. C. (2005). Update on acquired tetracycline resistance genes. *FEMS microbiology letters*, *245*(2), 195-203. https://doi.org/10.1016/j.femsle.2005.02.034

Roberts Jr, D. R., Mims, C. W., & Fuller, M. S. (1996). Ultrastructure of the ungerminated conidium of *Blumeria graminis* f. sp. *hordei. Canadian journal of botany, 74*(2), 231-237. https://doi.org/10.1139/b96-030

Robertson, J., & Nash, J. H. (2018). MOB-suite: software tools for clustering, reconstruction and typing of plasmids from draft assemblies. *Microbial genomics, 4*(8), e000206. https://doi.org/10.1099/mgen.0.000206

Rohayati, R., Yuana, R., Yuningsih, W., Yolanda, P., Nugroho, A., & Istiqomah, D. (2023). Pesticide degrading ability of indigenous-bacteria from contaminated cropland in Kersana, Brebes Regency, Indonesia., 284-293. https://doi.org/10.2991/978-94-6463-128-9_29

Romero, D., Aguilar, C., Losick, R., & Kolter, R. (2010). Amyloid fibers provide structural integrity to *Bacillus subtilis* biofilms. *Proceedings of the National Academy of Sciences, 107*(5), 2230-2234. https://doi.org/10.1073/pnas.0910560107

REFERENCES

Romero, D., Pérez-García, A., Rivera, M., De Cazorla, F. M., & Vicente, A. (2004). Isolation and evaluation of antagonistic bacteria towards the cucurbit powdery mildew fungus *Podosphaera fusca. Applied Microbiology and Biotechnology, 64*(2), 263-269. https://doi.org/10.1007/s00253-003-1439-8

Romero, D., De Vicente, A., Rakotoaly, R. H., Dufour, S. E., Veening, J. W., Arrebola, E., ... & Pérez-García, A. (2007). The iturin and fengycin families of lipopeptides are key factors in antagonism of *Bacillus subtilis* toward *Podosphaera fusca. Molecular Plant-Microbe Interactions, 20*(4), 430-440. https://doi.org/10.1094/MPMI-20-4-0430

Romero, D., De Vicente, A., Zeriouh, H., Cazorla, F. M., Fernández-Ortuño, D., Torés, J. A., & Pérez-García, A. (2007). Evaluation of biological control agents for managing cucurbit powdery mildew on greenhouse-grown melon. *Plant Pathology, 56*(6), 976-986. https://doi.org/10.1111/j.1365-3059.2007.01684.x

Romero, D., Vlamakis, H., Losick, R., & Kolter, R. (2011). An accessory protein required for anchoring and assembly of amyloid fibres in *B. subtilis* biofilms. *Molecular microbiology*, *80*(5), 1155–1168. https://doi.org/10.1111/j.1365-2958.2011.07653.x

Rood, J. I. (2004). Virulence plasmids of spore-forming bacteria. *Plasmid biology*, 413-422. https://doi.org/10.1128/9781555817732.ch19

Rooney, A. P., Price, N. P., Ehrhardt, C., Swezey, J. L., & Bannan, J. D. (2009). Phylogeny and molecular taxonomy of the *Bacillus subtilis* species complex and description of *Bacillus subtilis* subsp. *inaquosorum* subsp. nov. *International journal of systematic and evolutionary microbiology, 59*(10), 2429-2436. https://doi.org/10.1099/ijs.0.009126-0

[redacted]

Ross, C. L., Thomason, K. S., & Koehler, T. M. (2009). An extracytoplasmic function sigma factor controls β-lactamase gene expression in *Bacillus anthracis* and other *Bacillus cereus* group species. *Journal of bacteriology*, *191*(21), 6683-6693. https://doi.org/10.1128/JB.00792-09

Rsaliyev, A., Amirkhanova, N., Rametov, N., Pahratdinova, Z., Ojiambo, P., & Lebeda, A. (2018). *Pseudoperonospora cubensis* virulence and pathotype structure in Kazakhstan. *Plant Pathology, 67*(9), 1924-1935. https://doi.org/10.1111/ppa.12890

Ruiz-García, C., Béjar, V., Martínez-Checa, F., Llamas, I., & Quesada, E. (2005). *Bacillus velezensis* sp. nov., a surfactant-producing bacterium isolated from the river vélez in Málaga, southern Spain. *International Journal of Systematic and Evolutionary Microbiology, 55*(1), 191-195. https://doi.org/10.1099/ijs.0.63310-0

[redacted]

Samuel Russell, P. P., Alaeen, S., & Pogorelov, T. V. (2023). In-cell dynamics: the next focus of all-atom simulations. *The Journal of Physical Chemistry B, 127*(46), 9863-9872. https://doi.org/10.1021/acs.jpcb.3c05166

Sansinenea, E., & Ortiz, A. (2011). Secondary metabolites of soil *Bacillus* spp. *Biotechnology letters, 33,* 1523-1538. https://doi.org/10.1007/s10529-011-0617-5

Savory, E. A., Adhikari, B. N., Hamilton, J. P., Vaillancourt, B., Buell, C. R., & Day, B. (2012). mRNA-Seq analysis of the *Pseudoperonospora cubensis* transcriptome during cucumber (*Cucumis sativus* L.) infection. *PloS One, 7*(4), e35796. https://doi.org/10.1371/journal.pone.0035796

Schaefer, H. and Renner, S. (2011). Phylogenetic relationships in the order Cucurbitales and a new classification of the gourd family (Cucurbitaceae). *Taxon, 60*(1), 122-138. https://doi.org/10.1002/tax.601011

Schoch, C., Seifert, K., Huhndorf, S., Robert, V., Spouge, J., Lévesque, C., … & Schindel, D. (2012). Nuclear ribosomal Internal Transcribed Spacer (ITS) region as a universal dna barcode marker for fungi. *Proceedings of the National Academy of Sciences, 109*(16), 6241-6246. https://doi.org/10.1073/pnas.1117018109

Seemann, T. (2014). Prokka: rapid prokaryotic genome annotation. *Bioinformatics, 30*(14), 2068-2069. https://doi.org/10.1093/bioinformatics/btu153

Seminara, A., Angelini, T., Wilking, J., Vlamakis, H., Ebrahim, S., Kolter, R., … & Brenner, M. (2012). Osmotic spreading of *Bacillus subtilis* biofilms driven by an extracellular matrix. *Proceedings of the National Academy of Sciences, 109*(4), 1116-1121. https://doi.org/10.1073/pnas.1109261108

REFERENCES

Serrano, M., Zilhão, R., Ricca, E., Ozin, A. J., Moran, C. P., Jr, & Henriques, A. O. (1999). A *Bacillus subtilis* secreted protein with a role in endospore coat assembly and function. *Journal of bacteriology, 181*(12), 3632–3643. https://doi.org/10.1128/JB.181.12.3632-3643.1999

Seydlová, G. and Svobodová, J. (2008). Review of surfactin chemical properties and the potential biomedical applications. *Open Medicine, 3*(2), 123-133. https://doi.org/10.2478/s11536-008-0002-5

Shafi, J., Tian, H., & Ji, M. (2017). *Bacillus* species as versatile weapons for plant pathogens: a review. *Biotechnology & Biotechnological Equipment, 31*(3), 446-459. https://doi.org/10.1080/13102818.2017.1286950

Shemesh, M. and Chai, Y. (2013). A combination of glycerol and manganese promotes biofilm formation in *Bacillus subtilis* via histidine kinase kind signaling. *Journal of Bacteriology, 195*(12), 2747-2754. https://doi.org/10.1128/jb.00028-13

Shi, L., Pigeonneau, N., Ventroux, M., Derouiche, A., Bidnenko, V., Mijakovic, I., & Noirot-Gros, M. F. (2014). Protein-tyrosine phosphorylation interaction network in *Bacillus subtilis* reveals new substrates, kinase activators and kinase cross-talk. *Frontiers in microbiology*, *5*, 538. https://doi.org/10.3389/fmicb.2014.00538

Shin, Y., Park, H., Lee, J., & Lee, S. (2022). Recovery of streptococcus mutans biofilm after photodynamic therapy with erythrosine and led light source. *The Journal of the Korean Academy of Pedtatric Dentistry, 49*(2), 149-157. https://doi.org/10.5933/jkapd.2022.49.2.149

Singh, A., Gupta, V. K., Kumar, A., Singh, V. K., & Nayakwadi, S. (2013). 16S rRNA and omp31 gene based molecular characterization of field strains of *B. melitensis* from aborted foetus of goats in India. *The Scientific World Journal, 2013*(1), 160376. https://doi.org/10.1002/sae2.12043

Singh, P., Egidi, E., Macdonald, C., & Singh, B. (2023). Host selection has a stronger impact on leaf microbiome assembly compared to land-management practices. *Journal of Sustainable Agriculture and Environment, 2*(2), 99-111. https://doi.org/10.1002/sae2.12043

Sipiczki, M., & Kajdacsi, E. (2009). *Jaminaea angkorensis* gen. nov., sp. nov., a novel anamorphic fungus containing an S943 nuclear small-subunit rRNA group IB intron represents a basal branch of Microstromatales. *International Journal of Systematic and Evolutionary Microbiology, 59*(4), 914-920. https://doi.org/10.1099/ijs.0.003939-0

[redacted]

Słomnicka, R., Olczak-Woltman, H., Oskiera, M., Schollenberger, M., Niemirowicz-Szczytt, K., & Bartoszewski, G. (2017). Genome analysis of *Pseudomonas syringae* pv. *lachrymans* strain 814/98 indicates diversity within the pathovar. *European Journal of Plant Pathology, 151*(3), 663-676. https://doi.org/10.1007/s10658-017-1401-8

Soliman, S. A., Khaleil, M. M., & Metwally, R. A. (2022). Evaluation of the antifungal activity of *Bacillus amyloliquefaciens* and *B. velezensis* and characterization of the bioactive secondary metabolites produced against plant pathogenic fungi. *Biology*, *11*(10), 1390. https://doi.org/10.3390/biology11101390

Sornchuer, P., Saninjuk, K., Prathaphan, P., Tiengtip, R., & Wattanaphansak, S. (2022). Antimicrobial susceptibility profile and whole-genome analysis of a strong biofilm-forming *Bacillus* sp. B87 strain isolated from food. *Microorganisms, 10*(2), 252. https://doi.org/10.3390/microorganisms10020252

de Souza, C. G., Martins, F. I. C. C., Zocolo, G. J., Figueiredo, J. E. F., Canuto, K. M., & de Brito, E. S. (2018). Simultaneous quantification of lipopeptide isoforms by UPLC-MS in the fermentation broth from *Bacillus subtilis* CNPMS22. *Analytical and bioanalytical chemistry*, *410,* 6827-6836. https://doi.org/10.1007/s00216-018-1326-7

Stackebrandt, E., & Goebel, B. M. (1994). Taxonomic note: a place for DNA-DNA reassociation and 16S rRNA sequence analysis in the present species definition in bacteriology. *International journal of systematic and evolutionary microbiology, 44(*4), 846-849. https://doi.org/10.1099/00207713-44-4-846

Steller, S., Vollenbroich, D., Leenders, F., Stein, T., Conrad, B., Hofemeister, J., ... & Vater, J. (1999). Structural and functional organization of the fengycin synthetase multienzyme system from *Bacillus subtilis* B213 and A1/3. *Chemistry & biology, 6*(1), 31-41. https://doi.org/10.1016/S1074-5521(99)80025-5

Stockwell, V. O., Hockett, K., & Loper, J. E. (2009). Role of RpoS in stress tolerance and environmental fitness of the phyllosphere bacterium *Pseudomonas fluorescens* strain 122. *Phytopathology, 99*(6), 689-695. https://doi.org/10.1094/PHYTO-99-6-0689

Stothard, P., & Wishart, D. S. (2005). Circular genome visualization and exploration using CGView. *Bioinformatics, 21*(4), 537-539. https://doi.org/10.1093/bioinformatics/bti054

REFERENCES

Stöver, A. G., & Driks, A. (1999). Secretion, localization, and antibacterial activity of TasA, a *Bacillus subtilis* spore-associated protein. *Journal of bacteriology*, *181*(5), 1664–1672. https://doi.org/10.1128/JB.181.5.1664-1672.1999

Suárez-Contreras, L. and Yañez-Meneses, L. (2020). 16S rRNA as an applied tool in the molecular characterization of genera and species of bacteria. *Respuestas, 25*(1), 127-137. https://doi.org/10.22463/0122820x.2430

Sun, M., Meng, X., Peng, T., & Hu, X. (2022). Effect of *Bacillus methylotrophicus* on tomato plug seedling. *Horticulturae, 8*(10), 947. https://doi.org/10.3390/horticulturae8100947

Sun, Q., Cao, H., Zhou, Y., Wang, X., Jiang, H., Gong, L., ... & Rong, R. (2016). Qualitative and quantitative analysis of the chemical constituents in Mahuang-Fuzi-Xixin decoction based on high performance liquid chromatography combined with time-of-flight mass spectrometry and triple quadrupole mass spectrometers. *Biomedical Chromatography, 30*(11), 1820-1834. https://doi.org/10.1002/bmc.3778

Sunithakumari, V. S., Menon, R. R., Suresh, G. G., Krishnan, R., & Rameshkumar, N. (2024). Characterization of a novel root-associated diazotrophic rare PGPR taxa, *Aquabacter pokkalii* sp. nov., isolated from pokkali rice: new insights into the plant-associated lifestyle and brackish adaptation. *BMC genomics, 25*(1), 424.

Tanaka, K., Fukuda, M., Amaki, Y., Sakaguchi, T., Inai, K., Ishihara, A., … & Nakajima, H. (2017). Importance of prumycin produced by *Bacillus amyloliquefaciens* SD-32 in biocontrol against cucumber powdery mildew disease. *Pest Management Science, 73*(12), 2419-2428. https://doi.org/10.1002/ps.4630

Tariq, S., Bano, A., & Khan, N. (2023). Comparative analysis of various strains of plant growth promoting rhizobacteria on the physiology of garlic (*Allium sativum*). *Natural Science, 15*(03), 79-90.

Taylor, J. W., Jacobson, D. J., Kroken, S., Kasuga, T., Geiser, D. M., Hibbett, D. S., & Fisher, M. C. (2000). Phylogenetic species recognition and species concepts in fungi. *Fungal genetics and biology*, *31*(1), 21-32. https://doi.org/10.1006/fgbi.2000.1228

Tejera-Hernández, B., Rojas-Badía, M. M., & Heydrich-Pérez, M. (2011). Potencialidades del género *Bacillus* en la promoción del crecimiento vegetal y el control biológico de hongos fitopatógenos. *Revista CENIC. Ciencias Biológicas, 42*(3), 131-138.

Tesfagiorgis, H. B., & Laing, M. D. (2010). Isolation and in vitro screening of potential biocontrol agents against powdery mildew of zucchini caused by *Podosphaera xanthii. South African Journal of Plant and Soil, 27*(2), 179-186. https://doi.org/10.1080/02571862.2010.10639990

Tessema, H. (2023). Assessment of the natural prevalence of *Bacillus* isolates on faba bean (*V. faba* L) leaves and identification of the potential Antagonistic species for the management of Ascochyta blight in Northwestern Ethiopia.

Thambugala, K., Daranagama, D., Phillips, A., Kannangara, S., & Promputtha, I. (2020). Fungi vs. fungi in biocontrol: an overview of fungal antagonists applied against fungal plant pathogens. *Frontiers in Cellular and Infection Microbiology, 10*. https://doi.org/10.3389/fcimb.2020.604923

Thennarasu, S., Lee, D. K., Poon, A., Kawulka, K. E., Vederas, J. C., & Ramamoorthy, A. (2005). Membrane permeabilization, orientation, and antimicrobial mechanism of subtilosin A. *Chemistry and physics of lipids, 137*(1-2), 38-51. https://doi.org/10.1016/j.chemphyslip.2005.06.002

Thomas, C. E., Cohen, Y., Jourdain, E. L., & Eyal, H. (1987). Use of reaction types to identify downy mildew resistance in muskmelons. *HortScience, 22*(4), 638-640. https://doi.org/10.21273/HORTSCI.22.4.638

Thomas, C. M., & Nielsen, K. M. (2005). Mechanisms of, and barriers to, horizontal gene transfer between bacteria. *Nature reviews microbiology*, *3*(9), 711-721. https://doi.org/10.1038/nrmicro1234

[redacted]

Tian, T., Sun, B., Shi, H., Gao, T., He, Y., Li, Y., … & Chai, Y. (2021). Sucrose triggers a novel signaling cascade promoting *Bacillus subtilis* rhizosphere colonization. *The Isme Journal, 15*(9), 2723-2737. https://doi.org/10.1038/s41396-021-00966-2

[redacted]

Tonelli, M., Magallanes-Noguera, C., & Fabra, A. (2017). Symbiotic performance and induction of systemic resistance against *Cercospora sojina* in soybean plants co-inoculated with *Bacillus* sp. CHEP5 and *Bradyrhizobium japonicum* E109. *Archives of Microbiology, 199*(9), 1283-1291. https://doi.org/10.1007/s00203-017-1401-2

Toubal, S., Bouchenak, O., Elhaddad, D., Yahiaoui, K., Boumaza, S., & Karim, A. (2018). Maldi-TOF MS detection of endophytic bacteria associated with great nettle (*Urtica dioica* L.), grown in Algeria. *Polish Journal of Microbiology, 67*(1), 67-72. https://doi.org/10.5604/01.3001.0011.6145

Tsuge, K., Akiyama, T., & Shoda, M. (2001). Cloning, sequencing, and characterization of the iturin A operon. *Journal of bacteriology*, *183*(21), 6265-6273. https://doi.org/10.1128/JB.183.21.6265-6273.2001

Urquhart, E. J., Menzies, J. G., & Punja, Z. K. (1994). Growth and biological control activity of *Tilletiopsis* species against powdery mildew (*Sphaerotheca fuliginea*) on greenhouse cucumber. *Phytopathology, 84*(4), 341-351. https://doi.org/10.1094/Phyto-84-341

del Valle, E. E., Frizzo, L. S., Malmierca, M., Zbrun, M. V., Lax, P., & Doucet, M. E. (2016). Biological control of *Alphitobius diaperinus* with *Steinernema rarum* CUL and *Heterorhabditis bacteriophora* SMC and feasibility of application in rice hull. *Journal of Pest Science*, *89*, 161-170. https://doi.org/10.1007/s10340-015-0664-2

Vasilinetc, I., Prjibelski, A. D., Gurevich, A., Korobeynikov, A., & Pevzner, P. A. (2015). Assembling short reads from jumping libraries with large insert sizes. *Bioinformatics, 31*(20), 3262-3268. https://doi.org/10.1093/bioinformatics/btv374

Ventosa, A., Garcia, M. T., Kamekura, M., Onishi, H., & Ruiz-Berraquero, F. (1989). *Bacillus halophilus* sp. nov., a moderately halophilic *Bacillus* species. *Systematic and Applied Microbiology, 12*(2), 162-166. https://doi.org/10.1016/S0723-2020(89)80075-4

de Vienne, D.M. (2016). Lifemap: exploring the entire Tree of Life. *PLOS Biology 14*(12): e2001624. https://doi.org/10.1371/journal.pbio.2001624.

Vlamakis, H., Chai, Y., Beauregard, P., Losick, R., & Kolter, R. (2013). Sticking together: building a biofilm the *Bacillus subtilis* way. *Nature Reviews Microbiology, 11*(3), 157-168. https://doi.org/10.1038/nrmicro2960

Voglmayr, H. (2003). Phylogenetic relationships of *Peronospora* and related genera based on nuclear ribosomal ITS sequences. *Mycological Research, 107*(10), 1132-1142. https://doi.org/10.1017/S0953756203008438

Voglmayr, H. (2008). Progress and challenges in systematics of downy mildews and white blister rusts: new insights from genes and morphology. *The Downy Mildews-Genetics, Molecular Biology and Control*, 3-18. https://doi.org/10.1007/978-1-4020-8973-2_2

Vogt, C., Schraner, E., Aguilar, C., & Eichwald, C. (2016). Heterologous expression of antigenic peptides in bacillus subtilis biofilms. *Microbial Cell Factories, 15*(1). https://doi.org/10.1186/s12934-016-0532-5

Wagacha, J., Muthomi, J., Mutitu, E., & Mwaura, F. (2010). Control of bean rust using antibiotics produced by *Bacillus* and *Streptomyces* species - translocation and persistence in snap beans. *Journal of Applied Sciences and Environmental Management, 11*(2). https://doi.org/10.4314/jasem.v11i2.55023

Wang, N., Wang, L., Zhu, K., Hou, S., Chen, L., Mi, D., … & Guo, J. (2019). Plant root exudates are involved in *Bacillus cereus* AR156 mediated biocontrol against *Ralstonia solanacearum. Frontiers in Microbiology, 10*. https://doi.org/10.3389/fmicb.2019.00098

Wang, X., Wang, L., Wang, J., Jin, P., Liu, H., & Zheng, Y. (2014). *Bacillus cereus* AR156-induced resistance to *Colletotrichum acutatum* is associated with priming of defense responses in loquat fruit. *PloS One, 9*(11), e112494. https://doi.org/10.1371/journal.pone.0112494

Wang, Y., Zhao, Q., Sun, Z., Li, Y., He, H., Zhang, Y., ... & Zheng, H. (2022). Whole-genome analysis revealed the growth-promoting mechanism of endophytic bacterial strain Q2H1 in potato plants. *Frontiers in Microbiology, 13,* 1035901. https://doi.org/10.3389/fmicb.2022.1035901

Wattiau, P., Renard, M. E., Ledent, P., Debois, V., Blackman, G., & Agathos, S. (2001). A PCR test to identify *Bacillus subtilis* and closely related species and its application to the monitoring of wastewater biotreatment. *Applied microbiology and biotechnology, 56,* 816-819. https://doi.org/10.1007/s002530100720

Weßling, R., Schmidt, S. M., Micali, C., Knaust, F., Reinhardt, R., Neumann, U., … & Panstruga, R. (2012). Transcriptome analysis of enriched *Golovinomyces orontii* haustoria by deep 454 pyrosequencing. *Fungal Genetics and Biology, 49*(6), 470-482. https://doi.org/10.1016/j.fgb.2012.04.001

REFERENCES

White, T. J., Bruns, T., Lee, S. J. W. T., & Taylor, J. (1990). Amplification and direct sequencing of fungal ribosomal RNA genes for phylogenetics. *PCR protocols: a guide to methods and applications, 18*(1), 315-322.

WHO, 2019. Critically important antimicrobials for human medicine, 6th revision. Geneva: World Health Organization. https://www.who.int/foodsafety/publications/antimicrobials-sixth/en/.

Wick, R. R., Judd, L. M., Gorrie, C. L., & Holt, K. E. (2017). Unicycler: resolving bacterial genome assemblies from short and long sequencing reads. *PLoS computational biology, 13*(6), e1005595. https://doi.org/10.1371/journal.pcbi.1005595

Wilson, M., Hirano, S. S., & Lindow, S. E. (1999). Location and survival of leaf-associated bacteria in relation to pathogenicity and potential for growth within the leaf. *Applied and Environmental Microbiology, 65*(4), 1435-1443.

Wise, C., Falardeau, J., Hagberg, I., & Avis, T. J. (2014). Cellular lipid composition affects sensitivity of plant pathogens to fengycin, an antifungal compound produced by *Bacillus subtilis* strain CU12. *Phytopathology*, *104*(10), 1036-1041. https://doi.org/10.1094/PHYTO-02-14-0046-R

Wu, X., Shi, X., Chen, M., Zhang, C., Zhang, X., & Zhu, J. (2021). Direct-contact low-frequency ultrasound and pulse lavage eradicates biofilms on implant materials *in vitro. Evidence-Based Complementary and Alternative Medicine,* 1-5. https://doi.org/10.1155/2021/1562605

[redacted]

[redacted]

Xiang, M., Kang, Q., & Zhang, D. (2020). Advances on systems metabolic engineering of *Bacillus subtilis* as a chassis cell. *Synthetic and systems biotechnology, 5*(4), 245-251. https://doi.org/10.1016/j.synbio.2020.10.005

Yan, F., Yu, Y., Gozzi, K., Chen, Y., Guo, J., & Chai, Y. (2017). Genome-wide investigation of biofilm formation in *Bacillus cereus. Applied and Environmental Microbiology, 83*(13). https://doi.org/10.1128/aem.00561-17

Yang, H., Li, X., Li, X., Yu, H., & Shen, Z. (2015). Identification of lipopeptide isoforms by MALDI-TOF-MS/MS based on the simultaneous purification of iturin, fengycin, and surfactin by RP-HPLC. *Analytical and Bioanalytical Chemistry, 407*, 2529-2542. https://doi.org/10.1007/s00216-015-8495-4

Yang, L., Chen, H., Yan, W., Huang, S., Cheng, D., Xu, H., & Zhang, Z. (2022). A pH-and redox-stimulated responsive hollow mesoporous silica for triggered delivery of fungicides to control downy mildew of Luffa cylindrica. *Pest Management Science*, *78*(8), 3365-3375. https://doi.org/10.1002/ps.6992

Yang, W., Yan, H., Dong, G., Li, Z., Jiang, C., Gu, D., ... & Luo, Y. (2022). Comparative transcriptomics reveal different genetic adaptations of biofilm formation in *Bacillus subtilis* isolate 1JN2 in response to Cd^{2+} treatment. *Frontiers in Microbiology, 13*, 1002482. https://doi.org/10.3389/fmicb.2022.1002482

Yeh, Y., Wu, T., Wen, H., Jair, H., Lee, M., & Kirschner, R. (2020). Host plants of the powdery mildew fungus *Podosphaera xanthii* in Taiwan. *Tropical Plant Pathology, 46*(1),44-61. https://doi.org/10.1007/s40858-020-00393-2

Yeturi, S. and Velazhahan, R. (2016). Biological control of downy mildew of maize caused by *Peronosclerospora sorghi* under environmentally controlled conditions. *Journal of Applied and Natural Science, 8*(1), 279-283. https://doi.org/10.31018/jans.v8i1.786

Yılmaz, S., Idris, A., Ayvaz, A., Çetin, A., Ulgen, F., Çetın, M., … & Hassan, M. (2021). New insights into molecular basis identification of three novel strains of the *Bacillus subtilis* group produce cry proteins isolated from soil samples in Adana, Turkey. *bioRxiv*, 2021-12. https://doi.org/10.1101/2021.12.24.474129

Yoon, S. H., Ha, S. M., Lim, J., Kwon, S., & Chun, J. (2017). A large-scale evaluation of algorithms to calculate average nucleotide identity. *Antonie Van Leeuwenhoek, 110*, 1281-1286. https://doi.org/10.1007/s10482-017-0844-4

Yu, X., Huang, T., Huang, Z., Powell, C., & Guan, X. (2007). Expression and characterization of inha gene from *Bacillus thuringiensis* 8010. *World Journal of Microbiology and Biotechnology, 23*(11), 1621-1625. https://doi.org/10.1007/s11274-007-9408-5

Yu, G. Y., Sinclair, J. B., Hartman, G. L., & Bertagnolli, B. L. (2002). Production of iturin A by *Bacillus amyloliquefaciens* suppressing *Rhizoctonia solani. Soil Biology and Biochemistry, 34*(7), 955-963. https://doi.org/10.1016/S0038-0717(02)00027-5

Yu, Y., Yan, F., Chen, Y., Jin, C., Guo, J., & Chai, Y. (2016). Poly-γ-glutamic acids contribute to biofilm formation and plant root colonization in selected environmental isolates of *Bacillus subtilis. Frontiers in Microbiology, 7.* https://doi.org/10.3389/fmicb.2016.01811

[redacted]

Zeriouh, H., Romero, D., García-Gutiérrez, L., Cazorla, F., Vicente, A., & Pérez-García, A. (2011). The iturin-like lipopeptides are essential components in the biological control arsenal of *Bacillus subtilis* against bacterial diseases of cucurbits. *Molecular Plant-Microbe Interactions, 24(*12), 1540-1552. https://doi.org/10.1094/mpmi-06-11-0162

Zhang, M., Han, W., Gu, J., Qiu, C., Jiang, Q., Dong, J., ... & Li, F. (2022). Recent advances on the regulation of bacterial biofilm formation by herbal medicines. *Frontiers in Microbiology, 13*, 1039297. https://doi.org/10.3389/fmicb.2022.1039297

Zhang, K., Hu, Y., Yang, D., Yan, C., Li, N., Li, Z., … & Li, J. (2022). Genome-wide identification of gasa gene family in ten Cucurbitaceae species and expression analysis in cucumber. *Agronomy, 12*(8), 1978. https://doi.org/10.3390/agronomy12081978

Zhang, Z., Nonomura, T., Appiano, M., Pavan, S., Matsuda, Y., Toyoda, H., … & Bai, Y. (2013). Loss of function in mlo orthologs reduces susceptibility of pepper and tomato to powdery mildew disease caused by *Leveillula taurica*. *Plos One, 8*(7), e70723. https://doi.org/10.1371/journal.pone.0070723

Zhang, D., Spadaro, D., Garibaldi, A., & Gullino, M. (2010). Efficacy of the antagonist *Aureobasidium pullulans* PL5 against postharvest pathogens of peach, apple and plum and its modes of action. *Biological Control, 54*(3), 172-180. https://doi.org/10.1016/j.biocontrol.2010.05.003

Zhang, D., Wu, S., Li, N., Gao, J., Liu, S., Zhu, S., … & Kuai, B. (2022). Chemical induction of leaf senescence and powdery mildew resistance involves ethylene-mediated chlorophyll degradation and ros metabolism in cucumber. *Horticulture Research, 9.* https://doi.org/10.1093/hr/uhac101

Zhang, Q., Zhang, G., Li, D., & Ding, Z. (2019). Characterization and discrimination of microbial community and co-occurrence patterns in fresh and strong flavor style flue-cured tobacco leaves. *Microbiologyopen, 9*(2). https://doi.org/10.1002/mbo3.965

Zhang, T., Zhang, X. X., & Ye, L. (2011). Plasmid metagenome reveals high levels of antibiotic resistance genes and mobile genetic elements in activated sludge. *PloS one, 6*(10), e26041. https://doi.org/10.1371/journal.pone.0026041

Zhao, P., Xu, L., Zhang, A., Zhu, B., & Shao, Z. (2020). Evolutionary analysis of gyrA gene from *Neisseria meningitidis* bacterial strains of clonal complex 4821 collected in China between 1978 and 2016. *BMC Microbiology, 20*(1). https://doi.org/10.1186/s12866-020-01751-5

Zhao, W., Li, A., Zhou, B., Zhang, J., & Wu, W. (2022). Antifungal activity of l-azetidine-2-carboxylic acid isolated from *Disporopsis aspera* rhizomes against *Podosphaera xanthii. Pest Management Science, 78*(5), 1946-1952. https://doi.org/10.1002/ps.6812

Zhao, Y., Selvaraj, J. N., Xing, F., Zhou, L., Wang, Y., Song, H., ... & Liu, Y. (2014). Antagonistic action of *Bacillus subtilis* strain SG6 on *Fusarium graminearum. PloS one, 9*(3), e92486. https://doi.org/10.1371/journal.pone.0092486

Zheng, L., Gu, C., Cao, J., Li, S. M., Wang, G., Luo, Y. M., & Guo, J. H. (2018). Selecting bacterial antagonists for cucurbit downy mildew and developing an effective application method. *Plant disease, 102*(3), 628-639. https://doi.org/10.1094/PDIS-06-17-0838-RE

Zhou, Z., Wan, D., Zhou, J., Zhang, Y., & Wang, R. (2023). Self-assembly of surfactin-like polymer in solution by the dissipative particle dynamics method. *Polymer International, 72*(6), 545-551. https://doi.org/10.1002/pi.6503

Zitter, T. A., Hopkins, D. L., & Thomas, C. E. (1996). Compendium of cucurbit diseases. *The American Phytopathological Society.*

Zompra, A., Chasapi, S., Twigg, M., Sałek, K., Anestopoulos, I., Galanis, A., … & Spyroulias, G. (2022). Multi-method biophysical analysis in discovery, identification, and in-depth characterization of surface-active compounds. *Frontiers in Marine Science, 9*. https://doi.org/10.3389/fmars.2022.1023287

The assistance of OpenAI's ChatGPT was used to improve the clarity and coherence of the English language in this thesis. All intellectual content, ideas, and research remain my own, and the AI's role was limited to language refinement.